CHAPTER 4

SYNTHESIS, IDENTIFICATION AND QUANTIFICATION OF NOVEL HUMAN LENS METABOLITES

The overall aims of this chapter were to investigate human lenses for the presence of novel human lens metabolites of Kyn and 3OHKyn, and, if present, to quantify their levels in normal and cataractous human lenses.

4.1 Introduction

The human lens contains a range of UV filter compounds that absorb at ~360 nm. Based on RP-HPLC analysis of human lens extracts there are still a number of unidentified UV filter compounds. Due to their specific protective role and possible involvement in ARN cataract formation it is crucial to understand the types of UV filters and their metabolites present in the human lens.

Previous studies in our laboratory have shown that 3OHKG, Kyn and 3OHKyn undergo non-enzymatic deamination at physiological pH to form α,β-unsaturated carbonyl compounds.[100,117] *In vivo*, deaminated 3OHKG (23) undergoes covalent binding (Michael addition) with thiol nucleophiles (GSH) or reduction by NAD(P)H to give GSH-3OHKG and AHBG, respectively (Scheme 4.1).[85,86] *In vitro* studies have also shown that in the lens deaminated Kyn (51) readily reacts with GSH to give GSH-Kyn, while deaminated Kyn (51) and deaminated 3OHKyn (52) can also be reduced by NAD(P)H to give 4-(2-aminophenyl)-4-oxobutanoic acid (AHA) and 4-(2-amino-3-hydroxyphenyl)-4-oxobutanoic acid (AHB), respectively.[117] In the absence of NAD(P)H or GSH, deaminated Kyn, 3OHKyn and 3OHKG undergo slow intramolecular Michael addition *in vitro* to give kynurenine yellow (Kyn yellow), 3-hydroxykynurenine yellow (3OHKyn yellow) and 3-hydroxykunurenine-*O*-β-D-glucoside yellow (3OHKG yellow), respectively (Scheme 4.1).[117]

Despite the similar structures and reactivities of Kyn and 3OHKyn to 3OHKG, no previous studies have examined human lenses for the presence of metabolites derived from deaminated Kyn or 3OHKyn. Therefore, the aims of this chapter were to i) synthesise the reduced compounds of Kyn and 3OHKyn (AHA and AHB), the GSH adducts, GSH-Kyn and

glutathionyl-3-hydroxykynurenine (GSH-3OHKyn), and the cyclised compounds, Kyn yellow and 3OHKyn yellow, ii) examine normal and cataractous lenses for their presence, and if present, iii) identify, and iv) quantify them (**Part A**). An additional aim was to characterise, synthesise and quantify an unknown lens metabolite seen by RP-HPLC of EtOH lens extracts (**Part B**).

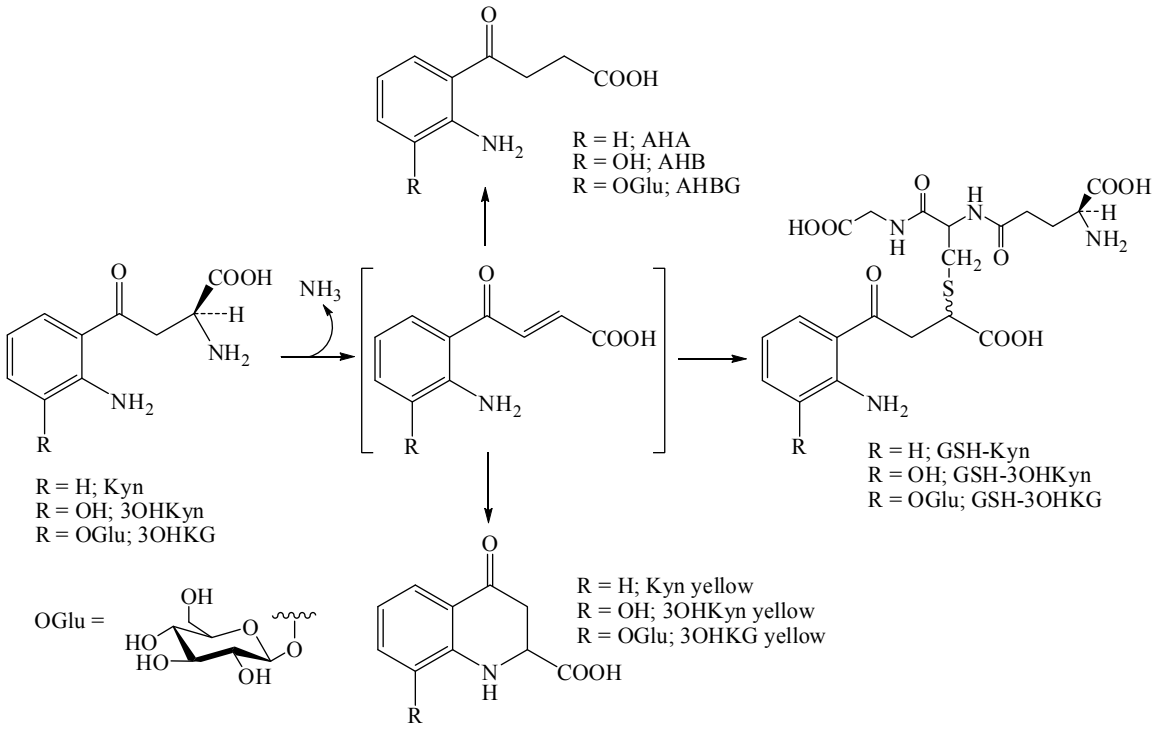

Scheme 4.1: Proposed *in vivo* degradation pathways of the human lens UV filters Kyn, 3OHKyn and 3OHKG.

4.2 Results and Discussion

Part A

Synthesis of 4-(2-aminophenyl)-4-oxobutanoic acid (AHA)

The synthesis of AHA was reported after the course of our work, however no spectral data were provided.[337] Rossi *et al.*[337] synthesised AHA in two steps from commercially available indole-3-propionic acid (53) in an overall yield of 55%. (Scheme 4.2) The first step involved oxidative opening of the five-membered hetero-ring of the indole nucleus by sodium periodate to give butyric acid (54). The *N*-formyl group was subsequently removed by acid hydrolysis to yield AHA.

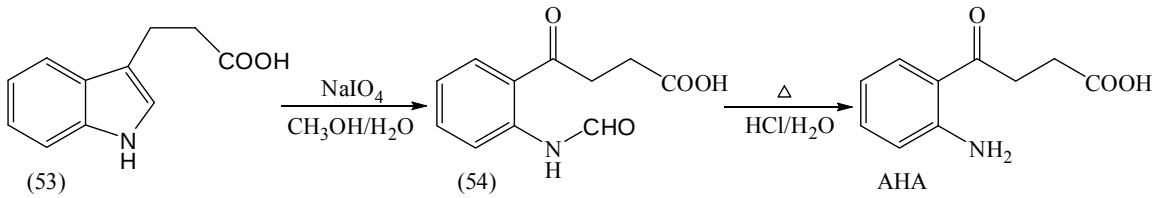

Scheme 4.2: Synthesis of AHA by Rossi *et al.*[337]

For this study, the synthesis of AHA was anticipated to occur *via* condensation of glyoxylic acid monohydrate with commercially available 2-nitroacetophenone (55), in a similar manner to that described in Chapter 2 for the synthesis of the acrylic acid (7), followed by reduction. The proposed reaction pathway for the synthesis of AHA is given in Scheme 4.3.

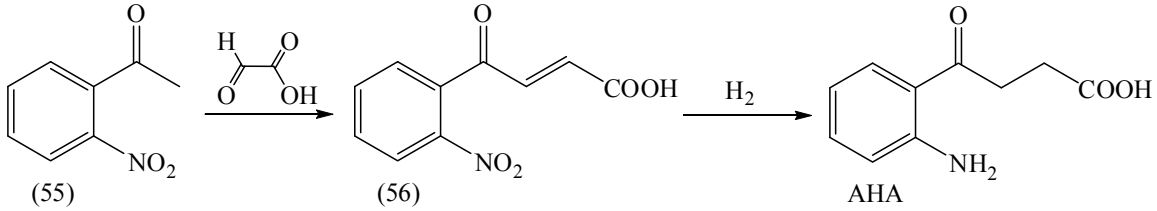

Scheme 4.3: Proposed synthetic pathway towards AHA.

4.2.1 Synthesis of 4-(2-nitrophenyl)-4-oxobut-2-enoic acid (56)

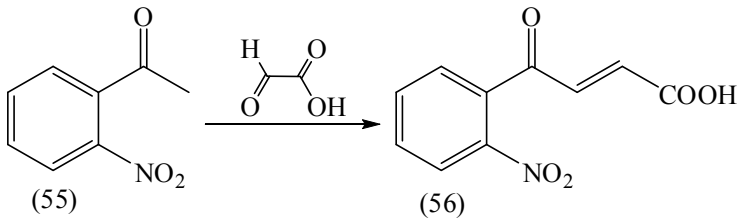

4.2.1.1 Method 1 and 2

Following the optimised method of Bianchi *et al.*[276] for the formation of the acrylic acid (7), as described in Chapter 2, the synthesis of the acrylic acid (56) was attempted. Thus, 2-nitroacetophenone (55) (mp 23-27°C, bp 159°C) and glyoxylic acid monohydrate (mp 49-52°C, bp 100°C, 10 mol equivalents) were mixed and melted at 60°C. The reaction temperature was increased to 110°C and the thick yellow mixture was placed under vacuum (~20 mBa) for ~13 h. A small scale (~20 mg) condensation reaction was also investigated at 90°C, however it resulted in a significantly longer reaction time (> 24 h). TLC revealed a brown baseline spot, most likely due to decomposition of glyoxylic acid monohydrate. A separate incubation of glyoxylic acid under the given reaction conditions confirmed that a brown baseline material on TLC was originating from glyoxylic acid. Therefore, one separate

addition (~1 mol equivalent) of this reactant was made after 5 h. In addition, glyoxylic acid monohydrate boils at 100°C, thus some losses were expected due to evaporation. TLC revealed formation of the acrylic acid (56) as the major reaction product and a minor unknown spot below the acrylic acid. Similarly to the acrylic acid (7) (Chapter 2), to isolate the product, the reaction mixture was initially cooled to RT, dissolved in brine, extracted with DCM and purified by normal phase column chromatography (Method 1). This resulted in moderate yields of the desired material (~27%). Therefore, in subsequent experiments the hot reaction mixture was adsorbed onto normal phase silica, followed by normal phase column chromatography purification (Method 2). This gave an improved yield of 45%.

For both methods a melting point of 171-172°C (lit.[276] 169-171°C) was obtained, indicating that the product was obtained in high purity. The ^{1}H NMR spectrum showed a distinct *trans*-configuration of the olefinic protons on the side chain with a coupling constant of 16.1 Hz. ES-MS displayed a molecular ion at *m/z* 222 ($M+H^{+}$), consistent with the molecular mass of 221 Da for the acrylic acid (56).

4.2.1.2 Method 3

Following the success of application of microwave chemistry for the synthesis of the acrylic acid (7) (Chapter 2), 2-nitroacetophenone (55) and glyoxylic acid monohydrate (10 mol equivalents) were mixed and placed into the cavity of a focused microwave reactor (CEM Discover) at 110°C. A controlled heating system was employed in conjunction with the rapid cooling system, maintaining the temperature at 110 ± 1°C. A power of ~50 W was used during the reaction and the pressure was kept to a minimum (< 5 psi). Approximately 1 mol equivalent of glyoxylic acid monohydrate was added after 20 and 40 min. After 60 min, TLC showed the desired product to be the major compound. Additionally, a brown baseline material originating from the decomposition of glyoxylic acid and a minor unknown spot below the acrylic acid (56) were observed. The brown viscous reaction mixture was adsorbed onto normal phase silica and purified by normal phase column chromatography. This gave the acrylic acid (56) in 54% yield as a white solid. Use of the microwave resulted in an improvement in reaction time, from 14 h to 60 min, and reaction yields, from 45% to 54%, when compared to Method 2.

4.2.2 Synthesis of 4-(2-aminophenyl)-4-oxobutanoic acid (AHA)

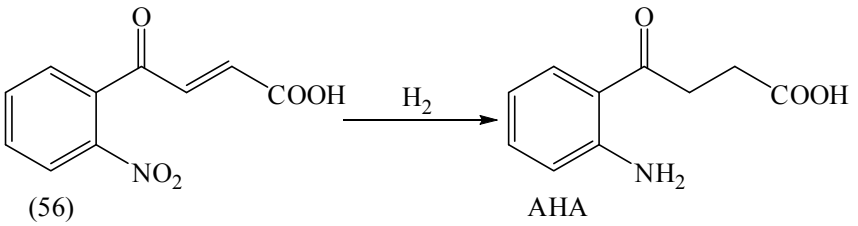

4.2.2.1 Method 1

Reduction of the double bond and the nitro group of the acrylic acid (56) was conducted in EtOAc with ~0.2% AcOH at ~1 mg/mL under an atmosphere of H_2 (1 atm) in the presence of PtO_2 at RT in the dark. PtO_2 was chosen as it was readily available at the time of the synthesis. AcOH was employed to protonate the newly formed amine group and decrease its ability to undergo Michael addition to form Kyn yellow or a Kyn-like dimer (Scheme 4.4). The dilute conditions were also used to decrease formation of the dimer.

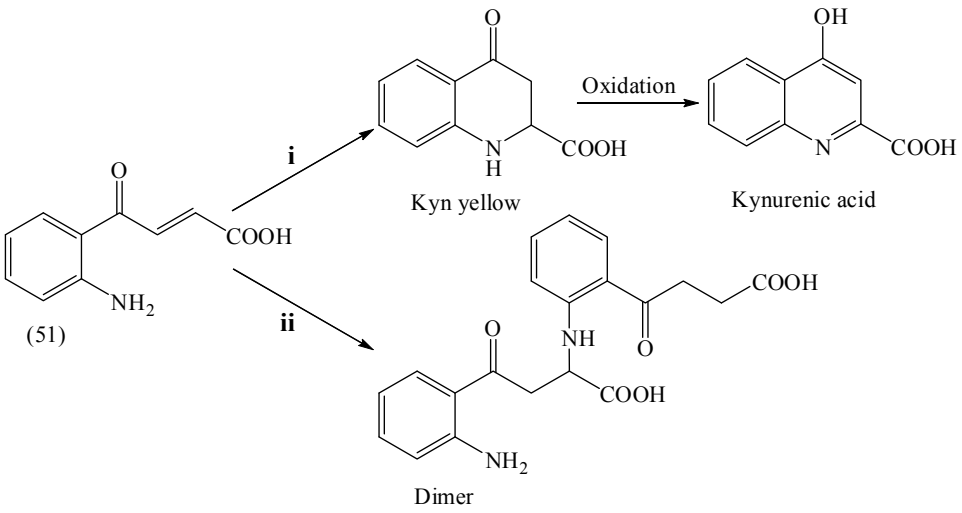

Scheme 4.4: Proposed pathways leading to **i**) intra- and **ii**) intermolecular Michael adducts in the synthesis of AHA.

Soon after commencement of the reaction, TLC and LC-MS analysis of the yellow solution revealed formation of AHA as the major product, along with multiple spots (> 3) of higher polarity. After 22 h, the starting material was consumed. The yellow solution was filtered through a plug of celite and the solvent removed under vacuum. The crude AHA was partially purified by a C18 reversed phase Sep-Pak column. Fractions containing AHA were pooled and after lyophilisation purified by RP-HPLC to afford AHA in 41% yield as an off-white solid. The formation of multiple compounds, seen both by TLC and LC-MS of the crude

reaction mixture, accounted for the moderate yield of the desired product. LC-MS analysis of the crude reaction mixture revealed a small quantity of kynurenic acid (*m/z* 190 ($M+H^+$)). This compound arises from the oxidation of Kyn yellow in the presence of oxygen or UV light.[117] Other fractions containing side products were also collected, but upon drying changed in colour from yellow to brown. This suggested decomposition. In addition, LC-MS showed formation of additional compounds after drying. Therefore, none of these side products were identified.

The aromatic region of the ^1H NMR spectrum of AHA revealed four adjacent aromatic resonances. The chemical shifts and coupling patterns of the aromatic protons were similar to the aromatic protons of Kyn.[18] Two isolated triplets at δ 2.65 and 3.25, consistent with the CH_2-CH_2 side chain, were also observed.[85,262] The ES-MS/MS spectrum (positive mode) of AHA showed a molecular ion at *m/z* 194 ($M+H^+$) and major fragment ions at *m/z* 176 and *m/z* 148, indicative of loss of water and formic acid, respectively. In PBS at pH 7.0, AHA showed absorption maxima at 254 and 365 nm and maximum fluorescence at λ_{ex} 346 and λ_{em} 480 nm.

4.2.2.2 Method 2

Due to obtaining only moderate yields of AHA by the method described above, an alternative hydrogenation method using conditions more likely to fully protonate the amine group once formed was investigated. Hydrogenation of nitro groups to stable amine hydrochloride salts is known to occur efficiently with H_2 and a catalyst in the presence of dilute aqueous HCl. For example, Moriya *et al*.[338] reported hydrogenation of 6-nitro-D-tryptophan in aqueous HCl and MeOH under an atmosphere of H_2 (1 atm) in the presence of Pd/C. This yielded 6-amino-D-tryptophan hydrochloride salt in 91% yield. Initially a stability trial was performed by separately suspending the acrylic acid (56) in a solution of dilute HCl (7 mol equivalents) in ~30% aqueous MeOH for 24 h at RT in the dark. TLC and ^1H NMR showed that no change occurred, illustrating that the Cl^- and MeOH had not acted as nucleophiles, leaving the double bond intact. Therefore, a solution of the acrylic acid (56) was treated as above in the presence of H_2 (1 atm) and Pd/C at RT in the dark. After 1 h, TLC revealed formation of AHA as the major product and faint multiple unknown spots of higher and lower polarity. After 3 h, the starting material was consumed and the yellow solution was filtered through a plug of celite. The pH was adjusted to ~6 by 1 M NaOH and lyophilised. The yellow solid was purified by RP-HPLC to afford AHA in 28% yield as an off-white solid. The formation of side products

at a level similar to the previous method was surprising and suggests that the side products were not solely due to Michael addition. The identification of the side products was not conducted.

4.2.2.3 Method 3

The hydrogenation condition described above was repeated in aqueous HCl (7.5 mol equivalents) in the absence of MeOH at RT in the dark. The addition of MeOH did not seem to be necessary as the acrylic acid (56) dissolved within 10 min. After 1 h, TLC analysis revealed formation of faint multiple spots of similar polarity to that described in Method 2, along with AHA as the major product. After 1.5 h, TLC showed the complete disappearance of the starting material, and the yellow solution was worked up and purified, as described in Method 2, to yield AHA in 34% yield as an off-white solid. As the higher yields of AHA were obtained using the optimised conditions described in Method 1, this was regarded as the optimal method.

4.2.3 Synthesis of 4-(2-amino-3-hydroxyphenyl)-4-oxobutanoic acid (AHB)

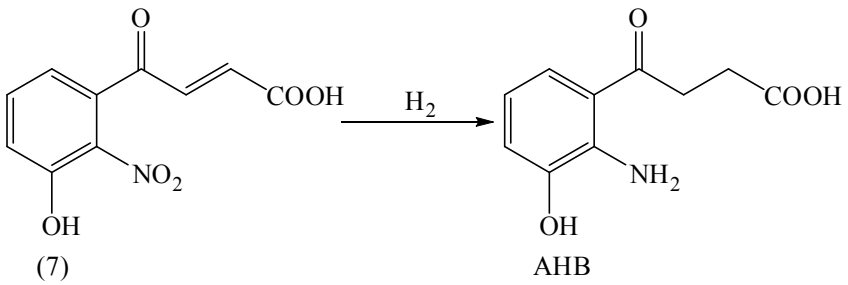

(7) AHB

In a similar manner to the synthesis of AHA, the synthesis of AHB from the acrylic acid (7) was investigated. The synthesis of the acrylic acid is described in Chapter 2. It was achieved in two steps from commercially available 3-hydroxyacetophenone (8) in an overall yield of ~18%. The first step involved nitration of 3-hydroxyacetophenone by copper nitrate and acetic anhydride in AcOH to yield 3-hydroxy-2-nitroacetophenone (9). 3-Hydroxy-2-nitroacetophenone was subsequently condensed with glyoxylic acid monohydrate under microwave conditions to afford the acrylic acid (7).

4.2.3.1 Method 1

Following Method 1 for the synthesis of AHA, the acrylic acid (7) was dissolved in EtOAc and AcOH (~0.2 %) at ~1 mg/mL and hydrogenated under an atmosphere of H_2 (1 atm) in the presence of PtO_2 at RT in the dark. For similar reasons to the AHA synthesis, AcOH was employed to assist protonation of the amine group and prevent intra- and intermolecular Michael addition reactions. After 1 and 2 h, TLC and LC-MS analysis of the yellow solution revealed AHB as the major product. Faint but multiple side products of higher polarity were also observed. After 3 h, the starting material was completely consumed and the yellow solution was worked up and purified, as described for AHA, to afford AHB in 47% yield as a light brown solid. The aromatic region of the ^{1}H NMR spectrum of AHB revealed three adjacent aromatic resonances at δ 7.82, 7.25 and 6.57. Chemical shifts and coupling patterns of the aromatic protons were similar to the aromatic ring of 3OHKyn.[202] Two isolated triplets at δ 3.26 and 2.66, consistent with the CH_2-CH_2 side chain, were also observed.[85,262] The ES-MS/MS spectrum (positive mode) of AHB showed a molecular ion at *m/z* 210 ($M+H^+$) with accompanying fragment ions at *m/z* 192 due to loss of water and *m/z* 164 due to loss of formic acid. In PBS at pH 7.0, AHB showed absorption maxima at 267 and 369 nm and maximum fluorescence at λ_{ex} 346 and λ_{em} 435 nm.

In addition to AHB, a red solid was collected by RP-HPLC in 6% yield as the second major compound detected at 360 nm. The ES-MS/MS spectrum (positive mode) of the red solid showed a molecular ion at *m/z* 206 ($M+H^+$), which is consistent with the molecular mass of the ring closed and aromatised compound xanthurenic acid. Further fragmentation of the molecular ion showed fragment ions at *m/z* 188, *m/z* 160 and *m/z* 132. These are consistent with loss of water and two successive losses of CO, respectively. The spectrum also showed loss of CO_2 from the molecular ion to give an ion at *m/z* 162, which provided further evidence for the presence of a carboxylic function in the molecule. Using the same conditions, the ES-MS/MS spectrum (positive mode) of an authentic sample of xanthurenic acid revealed a molecular ion at *m/z* 206 ($M+H^+$) with accompanying fragment ions at *m/z* 178 due to CO loss, *m/z* 160 due to formic acid loss and *m/z* 132 due to formic acid and CO loss. This showed inconsistencies between the fragmentation patterns of the red solid and xanthurenic acid. Further identification of the red solid was conducted by ^{1}H NMR. The aromatic region revealed three adjacent aromatic resonances at δ 7.07, 7.0 and 6.82, and one isolated singlet at δ 5.96 with an integration of 1H. The coupling patterns of the aromatic protons were similar to AHB, while the singlet at δ 5.96 was indicative of a non-aromatic but highly deshielded

proton. This also agreed with the ES-MS/MS data that the red compound was not xanthurenic acid. The red solid in PBS (pH 7.0) showed absorbance maxima at 266 and 489 nm, and maximum fluorescence at λ_{ex} 395 and λ_{em} 520 nm, while xanthurenic acid under the same conditions showed absorbance maxima at 244 and 344 nm, and maximum fluorescence at λ_{ex} 340 and λ_{em} 455 nm. From the physical and spectral data, the unknown product was identified as the 4-keto tautomer of xanthurenic acid (57) (Scheme 4.5). Support for this comes from the finding that kynurenic acid can exist as its 4-keto tautomer and that this is the preferred form in polar solvents.[339,340] This may explain why only the 4-keto tautomer of xanthurenic acid (57) was isolated in this study, as only polar solvents were used in either purification (*e.g.* aqueous CH_3CN) or characterisation (*e.g.* MeOD). The ES-MS/MS fragmentation pattern of the 4-keto tautomer of kynurenic acid showed similarities with the 4-keto tautomer of xanthurenic acid isolated in this study.[340,341,342-344] The other minor reaction side products were not identified.

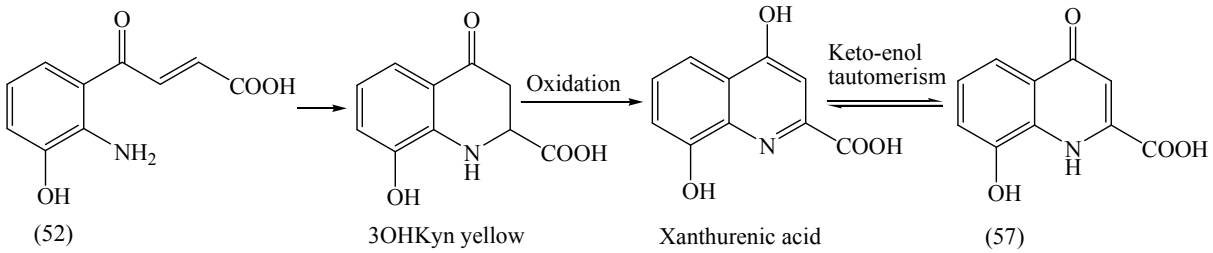

Scheme 4.5: Proposed pathways leading to intramolecular Michael adducts in the synthesis of AHB. The tautomeric forms of xanthurenic acid.

4.2.3.2 Method 2

For similar reasons to those described for the AHA synthesis (Method 3), hydrogenation of the acrylic acid (7) was investigated in dilute aqueous HCl (7.8 mol equivalents). Initially, a stability trial was performed by suspending the acrylic acid in dilute HCl for 24 h. TLC and ^{1}H NMR showed that no change occurred. Thus, a mixture of the acrylic acid (7) and aqueous HCl was placed under an atmosphere of H_2 (1 atm) in the presence of Pd/C at RT in the dark. After 10 min, TLC revealed AHB as the major product, with faint but multiple side products and some starting material. After ~50 min, the acrylic acid (7) was not observed by TLC, therefore the yellow solution was worked up and purified, as described for AHA (Method 3), to afford AHB in 38% yield as a light brown solid. The identification of the side products was not conducted. As the higher yields of AHB were obtained using the conditions described in Method 1, this was regarded as the best method for the synthesis of AHB.

4.2.4 Synthesis of glutathionyl-kynurenine (GSH-Kyn) and glutathionyl-3-hydroxykynurenine (GSH-3OHKyn)

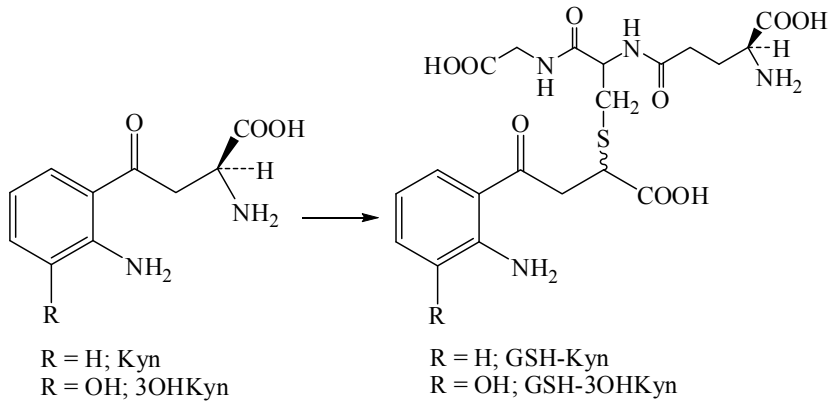

R = H; Kyn
R = OH; 3OHKyn

R = H; GSH-Kyn
R = OH; GSH-3OHKyn

In a similar manner to the reported synthesis of GSH-3OHKG from 3OHKG,[86] the synthesis of GSH-Kyn and GSH-3OHKyn from Kyn and 3OHKyn, respectively, were conducted under basic conditions in the presence of GSH. The reaction is known to proceed through deamination of the amino acid side chain, which is then readily attacked, *via* Michael addition, by the thiol group of GSH (Scheme 4.6).[18,86,117,345] Thus, Kyn and 3OHKyn were separately dissolved in argon-gassed (~20 min) Na_2CO_3-$NaHCO_3$ buffer at pH 9.5 in the presence of 3.6-5 mol equivalents of GSH. The two yellow solutions were incubated at 37°C in the dark. After 24 h, TLC of each reaction mixture revealed two major compounds, the GSH adducts and the starting materials. Due to the known ready oxidation of GSH to GSSG, even in the presence of trace amounts of oxygen, additional GSH (1 mol equivalent) was added to both reaction mixtures after 24 h and the pH was readjusted to ~9.5 with 1 M NaOH. After 72 h, in addition to the GSH adducts and the small quantities of the starting materials, TLC of both of the reactions revealed formation of at least two unknown side products. Therefore, the yellow solutions were separately acidified to pH 2 by dropwise addition of 25% aqueous HCl and lyophilised. The crude solids were purified by RP-HPLC to afford diastereomeric mixtures (~1:1) of GSH-Kyn in 51% yield and GSH-3OHKyn in 44% yield, respectively. Trace quantities of Kyn and 3OHKyn were observed by RP-HPLC, however they were not collected.

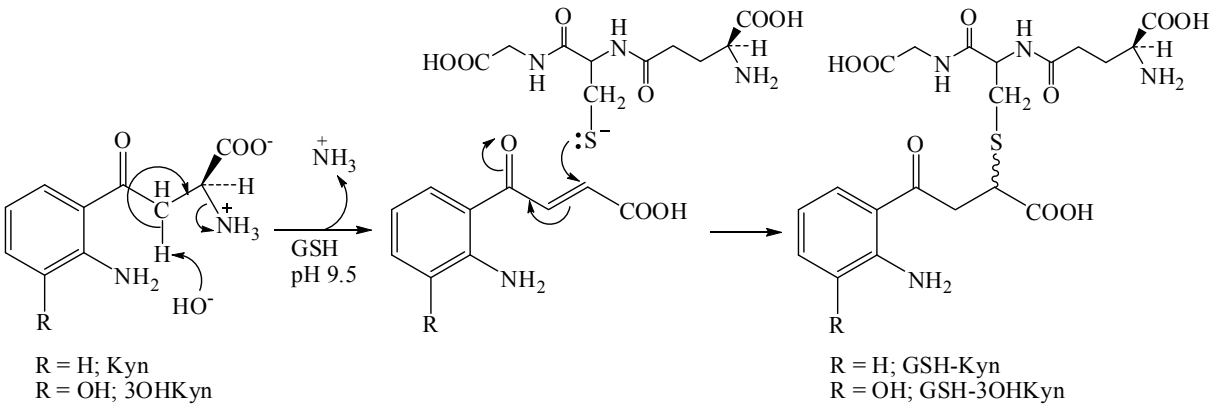

Scheme 4.6: Formation of GSH-Kyn and GSH-3OHKyn under basic conditions.

The aromatic region of the ^{1}H NMR spectrum of GSH-Kyn revealed four adjacent aromatic resonances, while GSH-3OHKyn showed three adjacent aromatic resonances. The chemical shifts and coupling patterns of the GSH-Kyn and GSH-3OHKyn aromatic protons were consistent with the aromatic ring of Kyn[18] and 3OHKyn,[20,202] respectively. The aliphatic side chains of GSH-Kyn and GSH-3OHKyn contained characteristic signals for a CH_2-CH moiety with diastereotopic methylene protons at δ ~3.3 and ~3.5 and a methine proton at δ ~3.8.[18] The distinctive deshielded diastereotopic protons are indicative of covalent attachment of the cysteine of GSH at C-2 of the Kyn and 3OHKyn side chain.[18,86] Further analysis of GSH-Kyn and GSH-3OHKyn by COSY, HSQC and HMBC confirmed that the GSH moiety was intact and chemical shifts and coupling constants agreed with the literature.[86,346] ES-MS/MS (positive mode) of GSH-Kyn and GSH-3OHKyn showed the presence of a molecular ion at *m/z* 499 ($M+H^+$) and *m/z* 515 ($M+H^+$), respectively, and fragment ions at *m/z* 481, *m/z* 424, *m/z* 370 and *m/z* 192 for GSH-Kyn, and *m/z* 497, *m/z* 440, *m/z* 386 and *m/z* 208 for GSH-3OHKyn. These are indicative of loss of water, glycine, glutamic acid and GSH, respectively. These were similar to the fragmentation pattern observed in the mass spectrum of GSH-3OHKG.[86]

4.2.5 Synthesis of Kyn yellow and 3OHKyn yellow

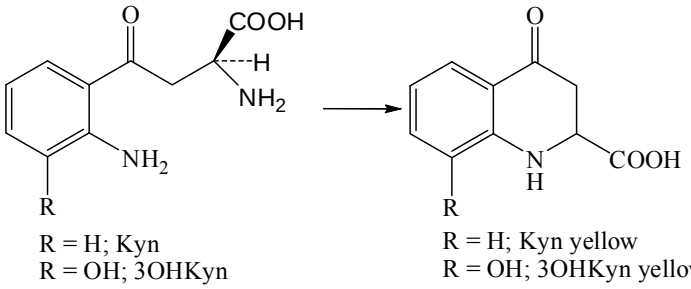

4.2.5.1 Method 1

3OHKyn yellow has been extracted as a pigment from the wings and bodies of the Ithomid and Heliconian butterflies.[347] Kyn yellow and 3OHKyn yellow have also been previously synthesised by Tokuyama *et al.*[336,348] from Kyn and 3OHKyn, respectively, under refluxing basic conditions. These products arise *via* intramolecular Michael addition of the *ortho* amino group of the aromatic ring onto the activated alkene of deaminated Kyn and 3OHKyn (Scheme 4.7).[101]

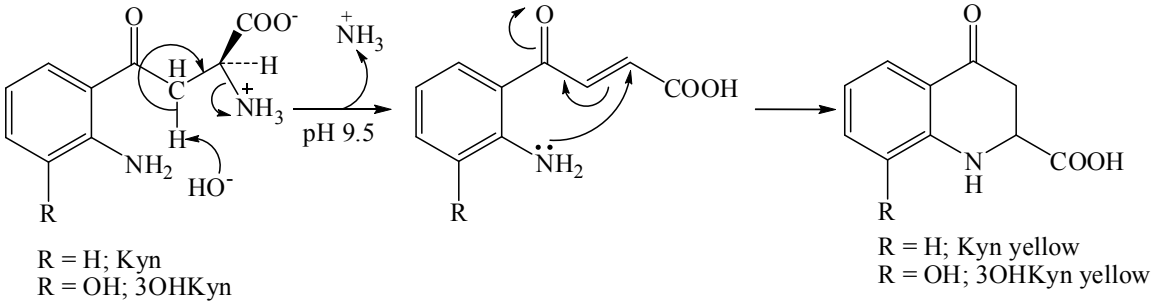

Scheme 4.7: Formation of Kyn yellow and 3OHKyn yellow under basic conditions.

Following the method of Tokuyama *et al.*,[348] Kyn and 3OHKyn were separately dissolved in $NaHCO_3$ (~0.5 M) at pH ~9 and refluxed under argon in the dark. The reactions were conducted under argon to prevent oxidation of the cyclised products to kynurenic acid or xanthurenic acid for the Kyn and 3OHKyn reactions, respectively (Scheme 4.8). The bright orange solutions gradually faded to a dull orange colour until the starting material was used up (20 h), as seen by TLC. In addition to the desired products, TLC revealed at least 3 other products of similar polarity and lower intensity when visualised at 365 nm. Both reactions were cooled to RT and the pH adjusted to ~14 by dropwise addition of 1 M NaOH. Both basic solutions were extracted with diethyl ether to remove 2-aminoacetophenone and 3-hydroxy-2-aminoacetophenone for the Kyn and 3OHKyn reactions, respectively. These side products are reported to be formed due to base catalysed reverse aldol reactions.[348] Not being the desired products, the organic layers likely to contain 2-aminoacetophenone and 3-hydroxy-2-aminoacetophenone, as determined by TLC, were discarded. The remaining basic aqueous layers were acidified to pH 2 *via* dropwise addition of 10% aqueous HCl and reextracted with diethyl ether to obtain Kyn yellow and 3OHKyn yellow. TLC of the aqueous layers showed complete extraction of the desired products. The organic layers were washed with water, dried with $MgSO_4$ and evaporated to dryness under reduced pressure. The orange residues were further purified by RP-HPLC to afford Kyn yellow in 26% yield and 3OHKyn yellow in 22%

yield. In addition to Kyn yellow, only trace amounts of kynurenic acid (*m/z* 190 ($M+H^+$)) and deaminated Kyn (*m/z* 192 ($M+H^+$)) were observed by LC-MS for the Kyn reaction, while in addition to 3OHKyn yellow, deaminated 3OHKyn (*m/z* 208 ($M+H^+$)) in 13% yield and xanthurenic acid (*m/z* 206 ($M+H^+$)) in trace amounts were isolated from the 3OHKyn reaction. As the reactions were conducted under anaerobic conditions, it is likely that kynurenic acid and xanthurenic acid were formed during the work up steps.

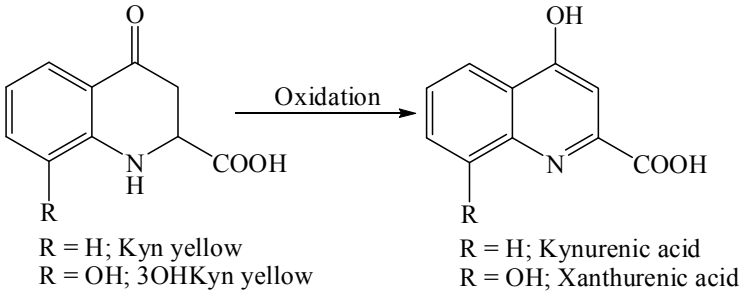

Scheme 4.8: Oxidation of Kyn yellow and 3OHKyn yellow to kynurenic acid and xanthurenic acid, respectively.

The ^{1}H NMR spectra of Kyn yellow and 3OHKyn yellow revealed the presence of four and three adjacent aromatic protons, respectively. Three additional protons from the methylene (δ 2.80-2.93) and methine (δ 4.20-4.35) groups were seen in both compounds. ES-MS/MS (positive mode) of Kyn yellow showed a molecular ion at *m/z* 192 ($M+H^+$) and major fragment ions at *m/z* 174 and *m/z* 146. These are consistent with loss of water and formic acid, respectively. Using the same conditions, the mass spectrum of 3OHKyn yellow revealed a molecular ion at *m/z* 208 ($M+H^+$), with accompanying fragment ions at *m/z* 190, *m/z* 162 and *m/z* 148 due to water, formic acid, and water and formic acid loss, respectively. The spectral data were in agreement with the literature.[336,347]

4.2.5.2 Alternative methods

As Tokuyama *et al.'s* method[348] resulted in only moderate yields of the desired products and a number of side materials, including the base-induced cleavage products, 2-aminoacetophenone and 3-hydroxy-2-aminoacetophenone, for the Kyn and 3OHKyn reactions, respectively, alternative methods were investigated.

4.2.5.2.1 Method 2

Bunce *et al.*[349] have reported the use of iron powder in refluxing glacial AcOH for the selective reduction of nitroarenes in the presence of an α,β-unsaturated ester and their subsequent intramolecular Michael addition to give aryl fused nitrogen heterocycles in high yields (Scheme 4.9). Iron has been found to be an extremely mild reagent that permits reduction of nitroarenes bearing carbonyl containing group with no reduction or degradation of the unsaturated side chain.[349]

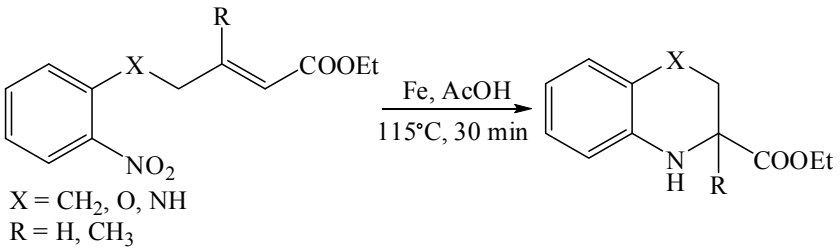

Scheme 4.9: Ring closure by tandem reduction-Michael addition by Bunce *et al.*[349]

A small scale reaction (20 mg) was therefore trialled on the acrylic acid (7) in refluxing glacial AcOH and iron powder under argon. After 20 and 45 min, TLC analysis revealed AHB as the major product and multiple side products of lower intensity to AHB at 365 nm detection. After 1 h, the starting material was consumed. The reaction mixture was cooled and filtered to remove the catalyst. The pH of the yellow solution was made basic (pH ~12) to assist organic solubility of the amine, and extracted with EtOAc. The aqueous layer was acidified to pH ~2 by 10% aqueous HCl (v/v) and extracted with EtOAc. LC-MS analysis revealed AHB (*m/z* 210 ($M+H^+$)) as a major reaction product in the acidic extract, while the basic extract showed multiple unknown side products of similar polarity and absorbance to those formed by Method 1 in the synthesis of AHB. LC-MS of the remaining aqueous layer showed complete extraction of the products. The desired cyclised product was not observed, possibly due to protonation of the amine group under the acidic conditions, although this seemed not to be an issue in the literature.[349] Further purification of the products was not attempted.

4.2.5.2.2 Method 3

It has been reported that selective reduction of nitro groups over double bonds can be achieved by tin(II) chloride dihydrate ($SnCl_2 \cdot 2H_2O$).[350-352] Thus, it was anticipated that the

treatment of the acrylic acid (7) with $SnCl_2 \cdot 2H_2O$ would selectively reduce the nitro group to the amine. Subsequent cyclisation in refluxing base (pH ~9) *via* intramolecular Michael addition would result in 3OHKyn yellow. The proposed two step pathway is given below (Scheme 4.10).

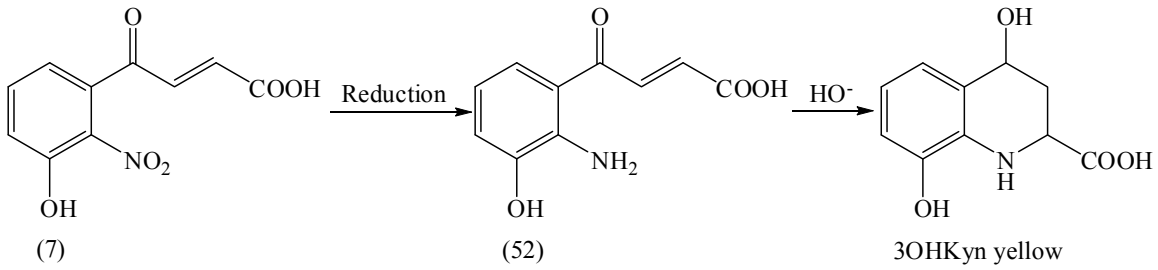

(7) (52) 3OHKyn yellow

Scheme 4.10: Proposed pathway for synthesis of 3OHKyn yellow from the acrylic acid (7).

A small scale reaction (30 mg) was trialled on the acrylic acid (7) in EtOAc with $SnCl_2 \cdot 2H_2O$ at RT under argon in the dark. Almost immediately, TLC revealed formation of AHB with faint but multiple side products. After 12 h, the starting material was consumed, and the orange solution was basified to pH ~9 with 0.5 M $NaHCO_3$ and extracted with EtOAc. The aqueous layer was filtered, acidified to pH 2 with 10% aqueous HCl (v/v) and extracted with EtOAc. The organic layers were washed with cold water and the solvent removed under reduced pressure. The crude orange residue obtained upon extraction of the acidic aqueous layer was analysed by LC-MS and showed AHB (*m/z* 210 ($M+H^+$)) as the major product. In contrast to the literature, this suggests that $SnCl_2 \cdot 2H_2O$ resulted in simultaneous reduction of the nitro group and the double bond of the acrylic acid (7). Only trace quantities of the reduced acrylic acid (52) (*m/z* 208 ($M+H^+$)) were observed. The basic organic extract showed unidentifiable side products. Further purification and characterisation of the products was not attempted.

As the $SnCl_2 \cdot 2H_2O$ (Method 3) conditions resulted in simultaneous reduction of the nitro group and the double bond, the reduced acrylic acid (52) was not obtained in sufficient quantities. As a result, the proposed cyclisation of the reduced acrylic acid (52) in base was not performed. The method of Tokuyama *et al.*[348] was therefore the method of choice for the synthesis of Kyn yellow and 3OHKyn yellow.

4.2.6 Identification of the proposed metabolites in human lenses

To determine the presence of the proposed metabolites in human lenses, eight normal human lenses ranging in age from 24 to 88 and two cataractous lenses of ages 60 and 70 were examined. Extraction, RP-HPLC and MS analysis of the human lenses were performed by Dr Peter Hains (Save Sight Institute, Sydney, NSW).

The nuclear and cortical regions were separately treated with 80% EtOH (v/v) to allow extraction of kynurenine-based metabolites.[353] The first EtOH extraction was performed with absolute EtOH rather than aqueous EtOH, as lenses are ~60% water.[354,355] The subsequent extraction was performed with 80% aqueous EtOH (v/v). RP-HPLC analysis was consistent with previous studies, showing the presence of the major UV filters 3OHKG, AHBG, Kyn, GSH-3OHKG and AHBDG at 360 nm.[39] A typical lens profile is shown in Figure 4.1. 3OHKyn was not detected in the investigated lenses. This may be due to the instability of 3OHKyn under experimental conditions or upon storage, as it is an *o*-aminophenol and can readily oxidise.[119,204,205] RP-HPLC elution times of the proposed lens metabolites were determined using synthetic standards. The elution times are indicated in Figure 4.1 (regions 6-9). In addition, a distinct doublet was eluted at the retention time of ~31 min (peak X, Figure 4.1). The identity and quantification of the compound responsible for this peak is discussed in Part B of this chapter.

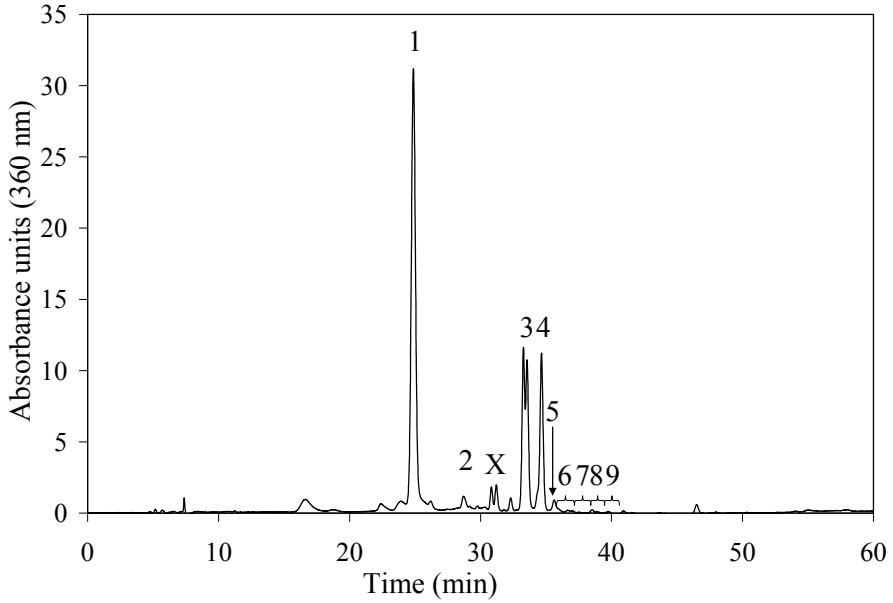

Figure 4.1: RP-HPLC profile of the UV filter extract from a normal lens nucleus (88 years old). Detection was at 360 nm in Absorbance units (arbitrary units). 3OHKG (1); Kyn (2); GSH-3OHKG (3); AHBG (4) and AHBDG (5). "X" represents an unknown compound shown as a double peak on the RP-HPLC trace. Expected elution times of AHB and GSH-3OHKyn (6), AHA and GSH-Kyn (7), 3OHKyn yellow (8) and Kyn yellow (9).

The extracted UV filters from both the nuclear and cortical sections of each lens were analysed by RP-HPLC. The major UV filters were quantified by RP-HPLC using standard curves of the synthetic samples. A standard curve of synthetic 3OHKG was used for the quantification of 3OHKG and GSH-3OHKG, commercially available Kyn was used for the quantification of Kyn and synthetic AHBG was used for the quantification of AHBG. Nuclear and cortical concentrations of 3OHKG and AHBG were found to be 0.1-3.6 nmol/mg lens (dry mass), while Kyn, GSH-3OHKG and AHBDG were found in 0-580 pmol/mg lens (dry mass) (Table 4.1, A and B). A marked decline in the levels of 3OHKG, Kyn, AHBG and AHBDG was noted after the seventh decade of life, whilst the levels of GSH-3OHKG were generally higher after middle age. These findings are consistent with previous studies.[39]

Table 4.1: Quantification of lens compounds in nuclei of normal and cataractous lenses (**A**) and cortices of normal lenses (**B**). Quantities are given in pmol/mg lens (dry mass).

A

Nucleus Age	**3OHKG**[b]	**AHBG**[b]	**Kyn**[b]	**GSH-3OHKG**[b]	**AHBDG**[b]	**AHA**[a]	**AHB**[a]	**GSH-Kyn**[a]
24	3600	692	586	0.00	176.74	4.00	2.67	1.80
27	3630	690	385	50.4	92.27	4.39	5.97	1.05
42	1840	408	135	39.5	55.11	0.86	1.14	0.63
47	2560	897	261	282	90.98	1.87	5.20	4.76
65	2220	527	188	562	79.54	1.83	2.40	28.0
66	658	268	73.1	89.9	36.82	1.37	0.69	3.09
83	426	72.0	61.4	41.1	19.66	0.70	0.00	2.00
88	452	127	14.9	210	13.02	0.32	0.63	7.60
60[c]	N/D	N/D	N/D	N/D	N/D	1.83	0.99	0.11
70[c]	N/D	N/D	N/D	N/D	N/D	1.21	1.31	0.10

B

Cortex Age	**3OHKG**[b]	**AHBG**[b]	**Kyn**[b]	**GSH-3OHKG**[b]	**AHBDG**[b]	**AHA**[a]	**AHB**[a]	**GSH-Kyn**[a]
24	3100	558	317	0.00	59.18	2.24	1.76	0.34
27	2300	328	226	14.2	55.89	1.39	0.79	0.30
42	1500	365	114	27.5	43.21	8.20	6.04	2.21
47	3850	891	361	56.9	144.99	2.82	3.03	1.23
65	1900	407	177	173	70.99	1.40	2.79	18.4
66	1490	311	80.3	71.7	53.24	1.14	1.11	2.36
83	732	147	93.8	44.8	23.13	0.85	0.58	0.52
88	418	90.7	10.8	48.5	12.01	0.21	0.37	2.58

[a] determined by LC-MS
[b] determined by RP-HPLC
[c] cataractous lenses
N/D, not determined

The RP-HPLC absorbance traces of both normal and cataractous lenses did not show distinct peaks for any of the proposed lens metabolites (Figure 4.1). Therefore, the eluents from the RP-HPLC regions corresponding to the retention times of the synthetic compounds were collected. The collected fractions were concentrated, analysed by ES-MS/MS, and subsequently quantified by LC-MS using the standard addition method.[356] The standard addition method is based on LC-MS analysis of the extract solution followed by analysis of the spiked extract with a known quantity of a standard. The amount of the measured compound in the extract is calculated following the procedure: $X = SI_x / (I_s - I_x)$, where X is the unknown amount of the measured compound in the extract solution, S is the amount of the spiked compound in the extract solution, I_x is the signal intensity of the measured compound in the extract solution and I_s is the signal intensity of the compound in the spiked extract solution.

MS analyses and spiking experiments with the authentic synthetic standards confirmed the presence of the reduced compounds AHA and AHB and the GSH adduct of Kyn, GSH-Kyn. The intramolecular Michael adducts Kyn yellow and 3OHKyn yellow and the GSH adduct of 3OHKyn, GSH-3OHKyn, were not detected in any of the lenses. This suggests that, if present, they would be in very low levels (the estimated MS sensitivity was ~50 fmol). Taylor *et al.*[101] have investigated decomposition rates of the major UV filters at pH 7.0. They concluded that the deaminated UV filters cyclise very slowly to the yellow compounds and were more prone to react with lens components, such as GSH,[117] Cys, proteins[18,19] or NAD(P)H,[357] than to undergo intramolecular Michael addition. Therefore, the absence of Kyn yellow and 3OHKyn yellow in the investigated lenses was not unexpected. Furthermore, 3OHKyn was not detected in the investigated lenses in this study, and as a result it was not surprising GSH-3OHKyn and consequently 3OHKyn yellow were undetected.

The concentrations of AHA, AHB and GSH-Kyn were determined using the standard addition method with the authentic synthetic standards. AHA and AHB were present in both the nucleus and cortex of all normal human lenses in 0-8.2 pmol/mg lens (dry mass) (Table 4.1, A and B). Similarly to the lenticular levels of AHBG,[39] AHA and AHB did not show any clear age correlation in the first 4 decades, however a steady decrease in AHA and AHB concentrations was observed after ~40 years of age in both the nucleus and cortex. This is in accordance with the decline of their metabolic precursors Kyn and 3OHKyn (Table 4.1, A and B).[39] Interestingly, while AHBG is typically present at 20-40% of the levels of 3OHKG in normal human lenses, AHA was only present at 0.5-2% of the levels of Kyn.[39] Levels of

AHB could not be correlated to levels of its precursor since 3OHKyn was not detected in the investigated lenses.

The concentration of GSH-Kyn was found to be low (0.3-28 pmol/mg lens (dry mass)) in both the nucleus and cortex (Table 4.1, A and B). Even though no clear age-related correlation was seen for the concentrations of GSH-Kyn, the normal nuclear concentration of GSH-Kyn was generally higher than in the cortex of the same lens. This was consistent with GSH-3OHKG, which has been shown in this and related studies to generally be present in higher levels in the lens nucleus than cortex.[39]

Due to the mode of cataractous lens removal in extracapsular cataract extraction (the cortex was not collected), only the nuclear concentrations of AHA, AHB and GSH-Kyn could be obtained for these lenses. The concentrations were found to be similar to those in the normal nucleus (Table 4.1, A). GSH-3OHKyn, Kyn yellow and 3OHKy yellow were not detected.

4.2.7 Stability of the novel lens metabolites

The finding of the novel lens metabolites in only low pmol levels, particularly the reduced compound AHA and GSH-Kyn (both derived from Kyn), was surprising, given the much greater concentrations of AHBG and GSH-3OHKG typically present in lenses relative to their precursor (3OHKG). 3OHKG has been shown to deaminate faster (~70% after 7 days) at pH 7.0 than Kyn (~58% after 7 days),[101] but the difference was not significant enough to account for the lower levels of AHA and GSH-Kyn. The stabilities of AHA, AHB and GSH-Kyn were therefore examined under the extraction conditions (80% aqueous EtOH (v/v), used to recover the UV filters from the human lenses) and RP-HPLC conditions (H_2O/0.01% TFA (v/v), used to analyse the extracts). The stabilities were also examined under conditions that were aimed at mimicking the low oxygen[358] and high antioxidant content of younger lenses,[123] and the oxygen rich and typically antioxidant depleted environment of older lenses.[39,66,122,123] In addition, the stability of GSH-3OHKyn was investigated to confirm if the lack of its precursor (3OHKyn) or stability of GSH-3OHKyn may have contributed to its absence from the investigated lenses. All analyses were conducted in triplicate and the results are presented as an average ± SD.

Initially, the efficiency of the 80% aqueous EtOH extraction process was examined by separately mixing known quantities (500 pmol/mg protein) of Kyn, 3OHKyn, 3OHKG AHA,

AHB, GSH-Kyn and GSH-3OHKyn in the presence of bovine lens proteins (BLP), extracting with 80% EtOH, quantifying the UV filters and their metabolites by RP-HPLC. BLP were used as a model for human lens proteins, since bovine lenses lack human UV filter compounds.[80] Recovery was 57-79% (Table 4.2). This was lower than the 97% previously reported for Kyn extracted from normal human lens proteins.[40] No other peaks were detected by RP-HPLC. AHA, AHB, GSH-Kyn and GSH-3OHKyn were stable for 24 h in the extraction solvent and for up to 5 h in the RP-HPLC solvent at 37ºC. This confirms that the low concentrations measured for AHA, AHB and GSH-Kyn, and the lack of detection of GSH-3OHKyn, were representative of the concentrations in the investigated lenses, and not due to significant loss or breakdown during extraction and analysis of the lens extracts.

Table 4.2: Extraction efficiency of UV filters and their metabolites from BLP. Analyses were performed in duplicate.

Lens compound	Extraction efficiency (%)
Kyn	74.2, 74.8
3OHKyn	62.4, 64.6
3OHKG	59.8, 60.2
AHA	56.2, 56.8
AHB	61.7, 63.7
GSH-Kyn	72.9, 75.3
GSH-3OHKyn	77.7, 80.9

To mimic the oxygen rich environment of older lenses, AHA, AHB, GSH-Kyn and GSH-3OHKyn were incubated with chelex-treated phosphate buffered saline (PBS) at pH 7.0, *i.e.* physiological pH conditions in the presence of atmospheric oxygen at 37ºC. Chelex is an ion exchange resin, which chelates polyvalent metal ions. It has been added to the buffer to prevent metal catalysed reactions such as Fenton reactions.[359] AHA proved to be stable under these conditions for > 200 h (0.42 ± 0.04 mM AHA at 0 h and 0.42 ± 0.05 mM AHA at 215 h). This suggests that formation of AHA may protect the lens from modification due to its greater stability compared to its precursor (Kyn).[117] By contrast, under the same conditions the initially colourless AHB incubation mixtures became yellow/tanned over time (Figure 4.2), exhibiting absorbance maxima at 240 and 420 nm, which are characteristic absorption peaks of xanthommatin-like compounds (Section 1.6.1).[207,360,361] RP-HPLC analysis of the AHB incubation solutions revealed steady decomposition of AHB, resulting in its total disappearance after 7 days of incubation (Figure 4.3).

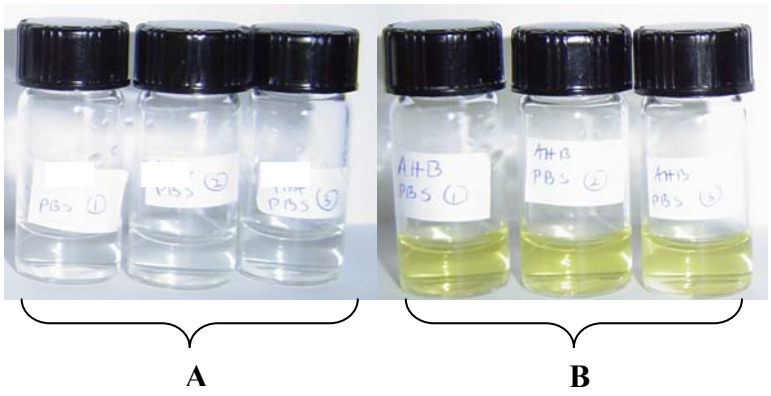

Figure 4.2: The colour of solutions of AHB in PBS (pH 7.0) at 37°C at time 0 h (**A**) and after 200 h (**B**) under aerobic conditions.

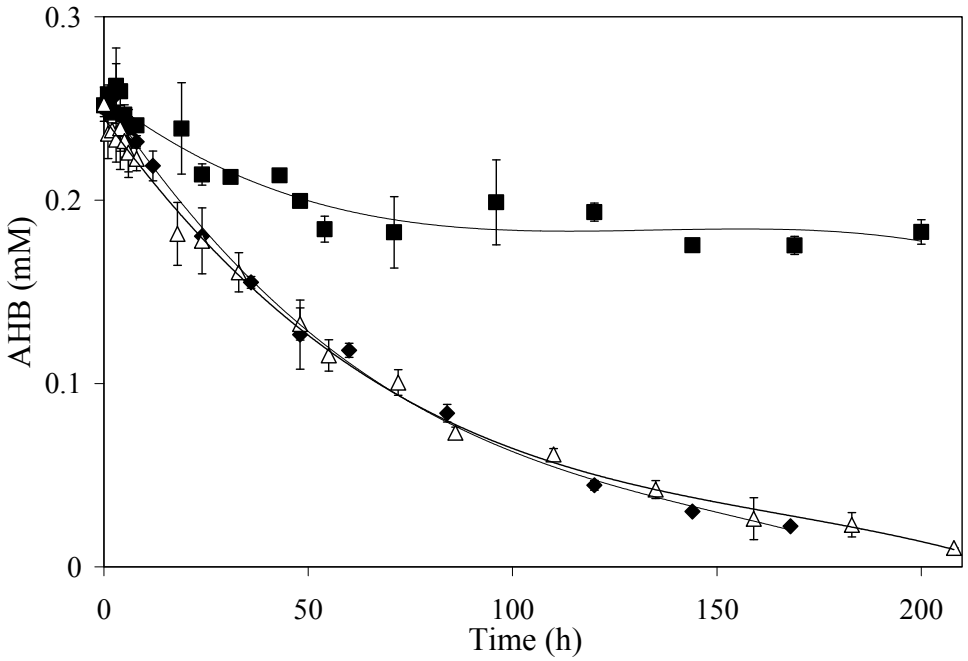

Figure 4.3: AHB (0.25 mM) was incubated in PBS (pH 7.0) in the presence of atmospheric oxygen (♦), in oxygen free PBS (pH 7.0) in the presence of BHT (0.1 mM) (Δ) and in oxygen free PBS (pH 7.0) in the presence of ascorbic acid (2.0 mM) and BHT (0.1 mM) (■). Aliquots of the reaction mixtures were taken at the indicated time points and analysed by RP-HPLC. Detection was at 254 nm.

The decomposition of AHB was accompanied by generation of high molecular mass compounds of 398 Da (λ_{max} 265/295/395), 412 Da (λ_{max} 251/315) and 413 Da (λ_{max} 243/296), as predominantly less polar peaks, which were probably dimeric aggregates arising from oxidation of this *o*-aminophenol.[204,205,211,360,362] Possible structures for these three compounds are shown in Scheme 4.11 and Scheme 4.12. A proposed mechanism for AHB oxidation *via* quinone imine formation and formation of the dimeric oxidation product of molecular mass of 412 Da is shown in Scheme 4.11.[201,209,360,362] The compound of molecular mass 413 Da could be formed by a similar mechanism to that for the compound of molecular mass 412 Da, with

the quinone derived from hydrolysis of the quinone imine. A similar compound is known to be formed *via* oxidation of 3-hydroxyanthralinic acid.[363-365]

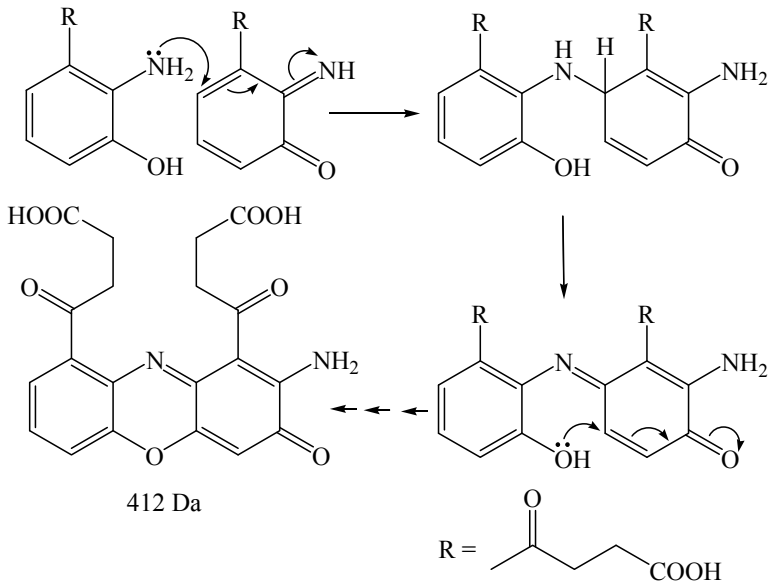

Scheme 4.11: Proposed mechanism for the oxidation of AHB at pH 7.0 (PBS) under aerobic conditions and formation of the oxidation product of molecular mass of 412 Da.[201,209,362]

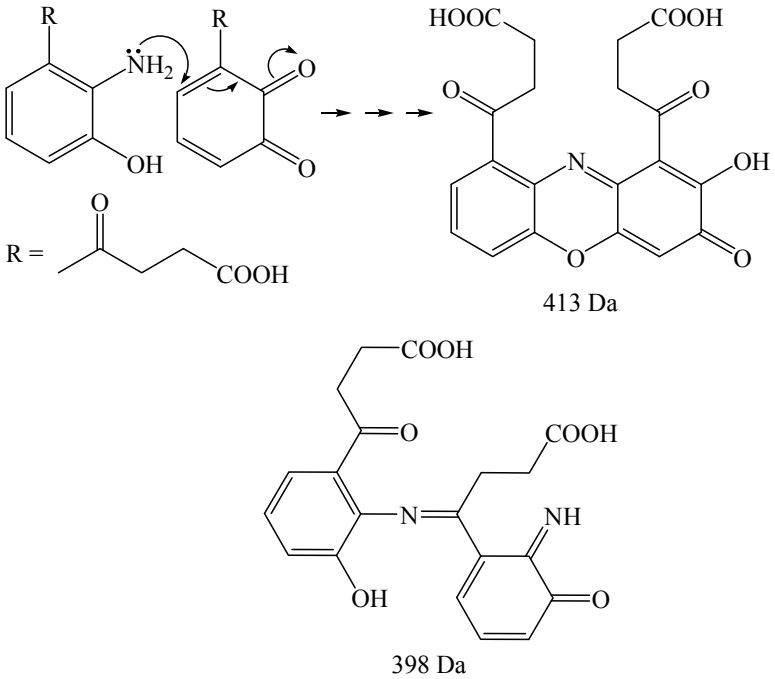

Scheme 4.12: Proposed decomposition products of AHB at pH 7.0 (PBS) under aerobic conditions.

In order to examine the stability of AHB in an environment resembling a healthy lens, it was incubated with argon-degassed (5 cycles of freeze-thaw) chelex-treated PBS (pH 7.0) in the presence of the radical scavenger butylated hydroxytoluene (BHT). BHT is known to act by donating a hydrogen atom to free radicals, such as $HO^{\cdot}$, $ROO^{\cdot}$ and to a lesser extent $O_2^{\cdot-}$,

thereby preventing oxidation reactions induced by these species.[366,367] It is structurally related to the major lipophilic antioxidant α-tocopherol.[368,369] RP-HPLC analysis of the AHB incubation solutions revealed similar decomposition (~96% decomposition after 208 h) to the stability of AHB under the aerobic conditions described above (Figure 4.3). It was therefore clear that the presence of BHT alone was insufficient to stabilise AHB. This is possibly due to rapid consumption of BHT by free radicals resulting in the formation of resonance stabilised phenoxyl radicals (BHT$^{\cdot}$) that subsequently undergo termination reactions and become inactive, *e.g.* BHT$^{\cdot}$ + BHT$^{\cdot}$ → BHT:BHT or BHT$^{\cdot}$ + ROO$^{\cdot}$ → ROO:BHT).[368] Similar free radical scavenging properties have been described for α-tocopherol.[369]

Incubation of AHB, as above, with the addition of the potent radical scavenger ascorbic acid, gave significantly greater stability of AHB. This suggests that BHT and ascorbic acid may act in concert, *i.e.* BHT, as the primary antioxidant, gets oxidised to a radical, which can then be repaired by ascorbic acid *via* donation of an electron. A similar synergistic interaction has been reported for ascorbic acid and α-tocopherol.[368] In the presence of these two agents only ~27% of AHB was decomposed after 9 days of incubation (Figure 4.3). The effect of ascorbic acid alone on AHB stability was not examined in this study. Overall these results suggest that AHB is likely to be unstable in the oxidising environment of the cataractous lens and that the degradation of this compound may contribute to lens colouration and ARN cataract formation.

GSH-Kyn decreased in concentration by 60-64% under the incubation conditions in PBS at pH 7.0, independent of the level of oxygen (Figure 4.4). Similarly to GSH-Kyn, a significant decrease in GSH-3OHKyn concentration was noted both in the aerobic (74% loss) and anaerobic conditions (80% loss) (Figure 4.5). The breakdown products were identified by LC-MS and UV-vis absorbance as the α,β-unsaturated ketones (*via* elimination of GSH) and intramolecular Michael adducts, Kyn yellow and 3OHKyn yellow. Similar instability of Kyn and 3OHKyn was observed by Taylor *et al.*[101] The dynamic nature of GSH adduct formation and breakdown suggests that the GSH adducts may delay binding of deaminated 3OHKG (23), deaminated Kyn (51) and deaminated 3OHKyn (52) to lens proteins in younger lenses that have high levels of GSH (~4.5-6 mM), but to a lesser degree in aged (~1-3 mM) lenses.[39]

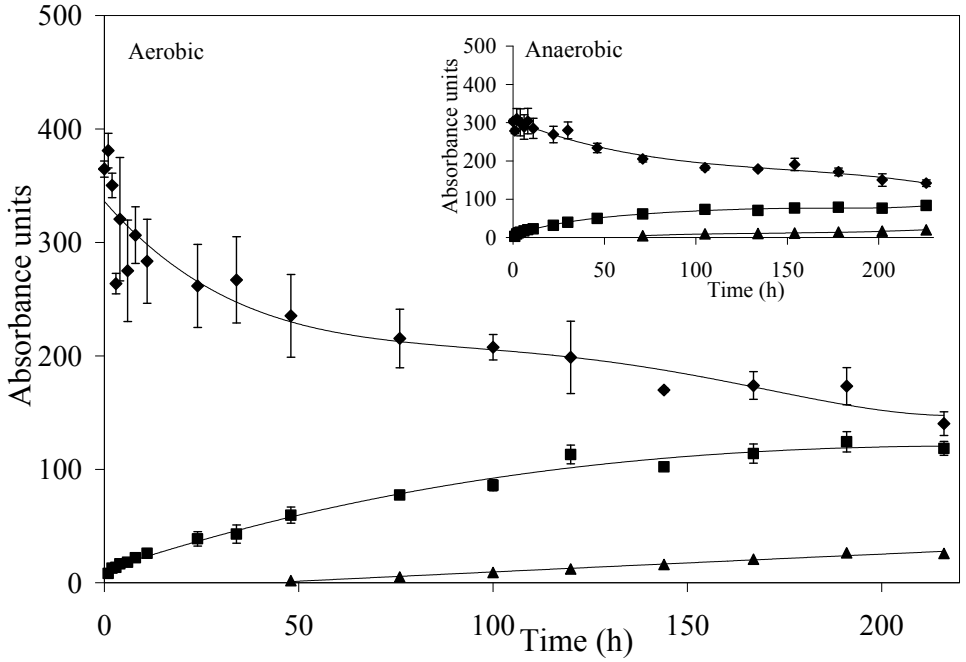

Figure 4.4: GSH-Kyn (0.40 mM) was incubated in PBS (pH 7.0) in the presence of atmospheric oxygen or in oxygen free PBS (pH 7.0) in the presence of ascorbic acid (0.2 mM) and BHT (0.1 mM). Aliquots of the reaction mixtures were taken at the indicated time points and analysed by RP-HPLC. Detection was at 254 nm. GSH-Kyn (♦); deaminated Kyn (■); Kyn yellow (▲).

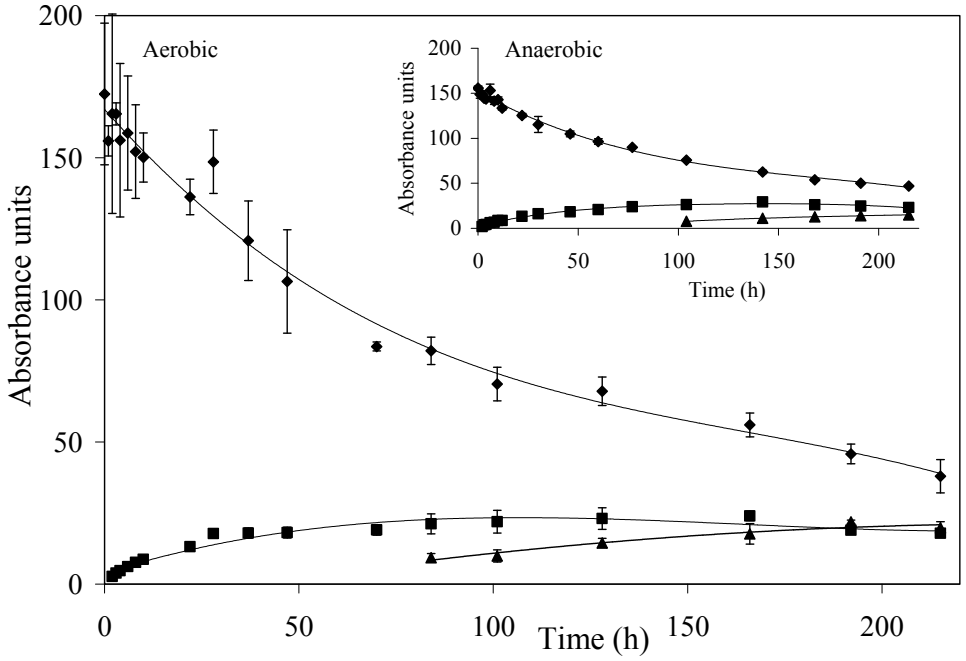

Figure 4.5: GSH-3OHKyn (0.10 mM) was incubated in PBS (pH 7.0) in the presence of atmospheric oxygen or in oxygen free PBS (pH 7.0) in the presence of ascorbic acid (2.0 mM) and BHT (0.1 mM). Aliquots of the reaction mixtures were taken at the indicated time points and analysed by RP-HPLC. Detection was at 254 nm. GSH-3OHKyn (♦); deaminated 3OHKyn (■); 3OHKyn yellow (▲).

Part B

4.2.8 Identification of cysteinyl-3-hydroxykynurenine-*O*-β-D-glucoside (Cys-3OHKG)

As shown in Figure 4.1, the RP-HPLC trace of UV filters isolated from an EtOH extract of human lenses showed an unknown compound that eluted as a double peak at the retention time of ~31 min (peak X, Figure 4.1). Both peaks were analysed by ES-MS and ES-MS/MS by Dr Peter Hains (Save Sight Institute, Sydney, NSW). A major molecular ion at *m/z* 491.13 ($M+H^+$), correlating to a mass of 490.13 Da, was detected. The ES-MS/MS data suggested the identity of the compound as cysteinyl-3-hydroxykynurenine-*O*-β-D-glucoside (Cys-3OHKG). This preliminary identification was from neutral losses of 162 Da (glucose), 109 Da (*o*-aminophenol), 98 Da (deaminated 3OHKG), 121 Da (Cys) and 18 Da (water). All other major ions observed in the mass spectrum were accounted for by loss of various combinations of these fragments. Analysis of both nuclear and cortical lens extracts showed essentially identical RP-HPLC profiles.

4.2.9 Synthesis and identification of cysteinyl-3-hydroxykynurenine-*O*-β-D-glucoside (Cys-3OHKG)

In order to confirm the identity of this unknown compound as Cys-3OHKG, the synthesis of an authentic standard was conducted. Two synthetic routes were considered. The first route was by incubating Cys with 3OHKG under basic conditions, similar to the synthesis of the GSH adducts (GSH-3OHKG, GSH-Kyn and GSH-3OHKyn).[86] The second route was based on cysteination of the double bond of the methyl ester glucoside (11) (Chapter 2), followed by reduction of the amine group and deprotection of the ester and acetyl moieties (Scheme 4.13). The first route was based on use of synthetic 3OHKG that also had to be used in reasonable amounts for studies described in Chapter 5 and 6. It was therefore decided to proceed with the second proposed synthetic pathway. The second route was seen as a good option due to the high reactivity of the double bond (as seen in Chapter 2 and Part A of Chapter 4).

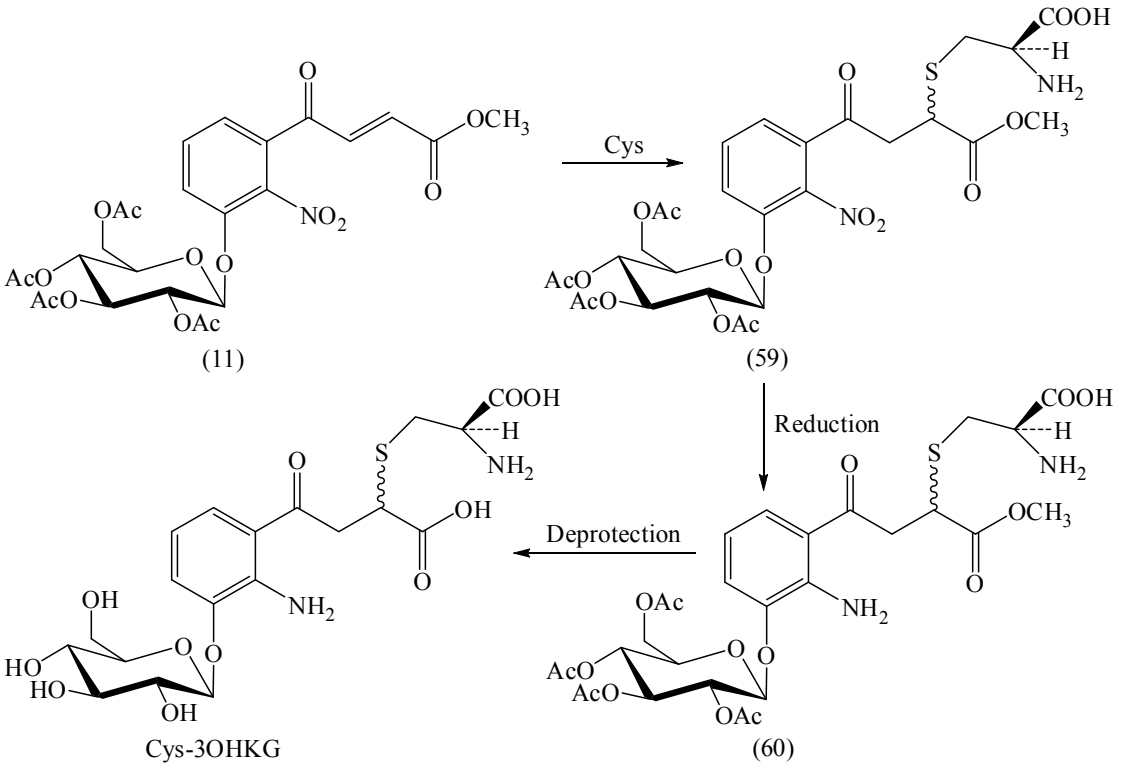

Scheme 4.13: Proposed synthetic pathway towards Cys-3OHKG.

4.2.9.1 Synthesis of Cys-3OHKG - Method 1

4.2.9.1.1 Synthesis of methyl 2-cysteinyl-4-(2-nitro-3-((2,3,4,5-tetra-*O*-acetyl-β-D-glucopyranosyl)oxyphenyl)-4-oxobutanoate (59)

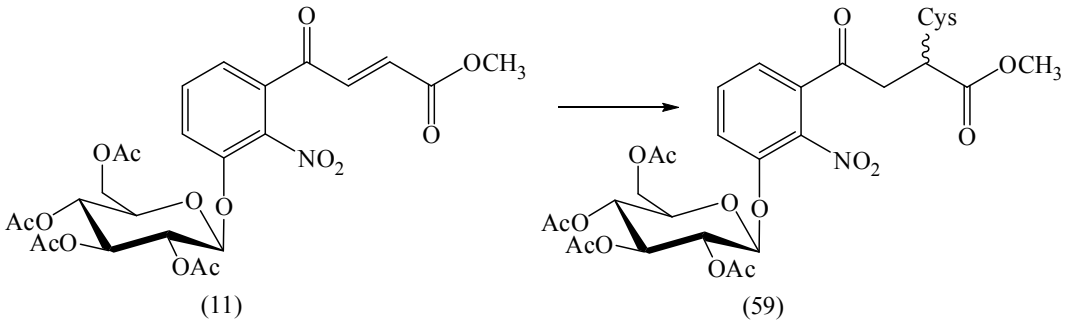

Following literature procedures for the cysteination of α,β-unsaturated acids, lactones and esters,[370-372] 1.2 mol equivalents of Cys was reacted with the methyl ester glucoside (11) in 50% aqueous CH_3CN at RT under argon. Clean and rapid cysteination of the methyl ester glucoside (11) was observed by normal phase TLC. After 30 min, the starting material was consumed and the white suspension was evaporated to yield the crude Cys adduct (59). Purification of the Cys adduct (59), to eliminate excess Cys and cystine (Cys is known to oxidise even in the presence of trace amounts of oxygen[373,374]), proved to be challenging by a

C18 reversed-phase Sep-Pak column as a rapid elimination of Cys and regeneration of the starting material occurred.[371,375] As a result, the crude product was carried through to the next step without purification. ES-MS/MS (positive mode) of the crude product showed a molecular ion at *m/z* 703 ($M+H^+$), as expected for the Cys adduct (59), and fragment ions at *m/z* 582 and *m/z* 373 due to loss of Cys and loss of $Glu(OAc)_4$, respectively. Further identification by ^1H NMR was not conducted.

4.2.9.1.2 Synthesis of methyl 2-cysteinyl-4-(2-amino-3-((2,3,4,5-tetra-*O*-acetyl-β-D-glucopyranosyl)oxyphenyl)-4-oxobutanoate (60)

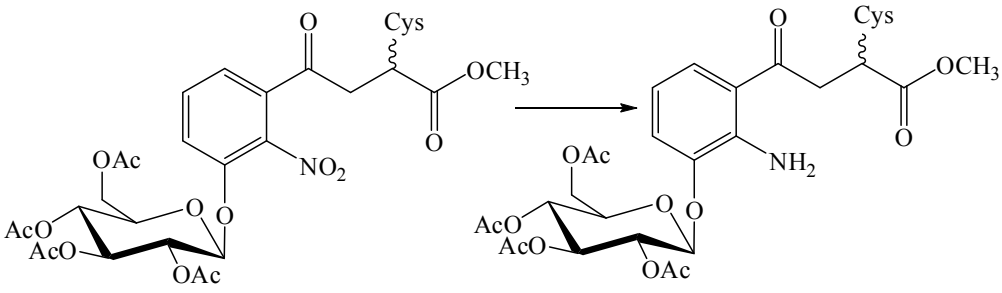

Initially, hydrogenation of the crude Cys adduct (59) was attempted under an atmosphere of H_2 (1 atm) in the presence of Pd/C as a catalyst. TLC and LC-MS analysis revealed more than five unknown products and no desired product. This was most likely due to the known poisoning effect of thiol groups and the sulfur atom towards noble metals.[376-378] Honma *et al.*[379] reported catalytic reduction of aliphatic nitro Cys derivatives by 1-7 wt % Pt on active carbon in the presence of formic acid, acetic acid and propionic acid at 30-70°C. Due to the known instability of the glucose moiety under acidic conditions, this method was not considered as an option.

Clavier *et al.*[380] reported use of sodium dithionite ($Na_2S_2O_4$) in 50% aqueous MeOH for the reduction of the aromatic nitro group of mercaptoquinoline based compounds (*e.g.* 5,7-dinitroquinoline-8-thiol). In addition to being non-toxic and an inexpensive reducing agent, use of $Na_2S_2O_4$ has been reported to give high yields of the reduced products.[380] Therefore, the Cys adduct (59) was dissolved in 50% aqueous MeOH at RT under argon. To prevent decysteination of the Cys adduct, 1 mol equivalent of Cys was added to the reaction mixture.[371,375] $Na_2S_2O_4$ (10 mol equivalents) was added in portions to the white suspension during the first hour. Due to possible Cys oxidation,[373,374] ~0.5 mol equivalents of Cys was added after 30 and 60 min. Disappearance of the Cys adduct (59) and generation of three new products was observed by normal phase TLC. After 2 h, the starting material was consumed

and the white suspension was evaporated. The white solid was dissolved in CH_3CN and filtered to remove $Na_2S_2O_4$ and excess Cys or cystine. After lyophilisation, the pale yellow solid was purified by RP-HPLC to afford the reduced Cys adduct (60) in 38% yield as a white solid. ES-MS/MS (positive mode) showed a molecular ion at *m/z* 673 ($M+H^+$) and fragment ions at *m/z* 655, *m/z* 552 and *m/z* 325 due to loss of water, loss of Cys and loss of the $OGlu(OAc)_4$, respectively. Further characterisation by ^1H NMR and identification of the side products was not conducted.

4.2.9.1.3 Synthesis of cysteinyl-3-hydroxykynurenine-*O*-β-D-glucoside (Cys-3OHKG)

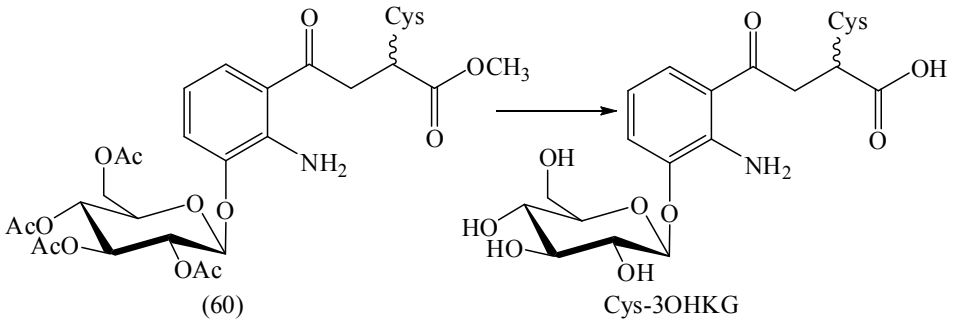

Deprotection of the acetyl and ester groups of the reduced Cys adduct (60) was trialled by using a modified procedure of Manthey *et al.*[262] (Chapter 2) in aqueous NaOH at pH ~12.5 under argon. Cys is known to be prone to elimination,[371,374,375] therefore ~2 mol equivalents of Cys were added to the reaction mixture in portions over 1.5 h. The progress of the reaction was monitored by normal and reversed phase TLC. This revealed a complex reaction mixture. After 2 h, TLC showed complete disappearance of the starting material. The pale yellow suspension was therefore acidified to pH 6 by 1 M AcOH. LC-MS showed more than six undesired and unknown products. The desired product was not observed, possibly suggesting instability of the reduced Cys adduct (60) under the given experimental conditions. As seen by TLC and LC-MS, control experiments of the nitro Cys adduct (59), under the above described basic conditions, resulted in formation of multiple products (~5) after 2 h. One of the medium sized peaks on LC-MS (360 nm) showed a molecular ion at *m/z* 400 ($M+H^+$), which is the expected mass for product that had undergone Cys elimination and deprotection of the ester and acetyl moieties. Other products could not be identified. It was, therefore, not surprising to observe decomposition of the reduced Cys adduct (60) under the given conditions.

4.2.9.2 Synthesis and stability of cysteinyl-4-oxo-4-phenylbutanoic acid (Cys-BAA)

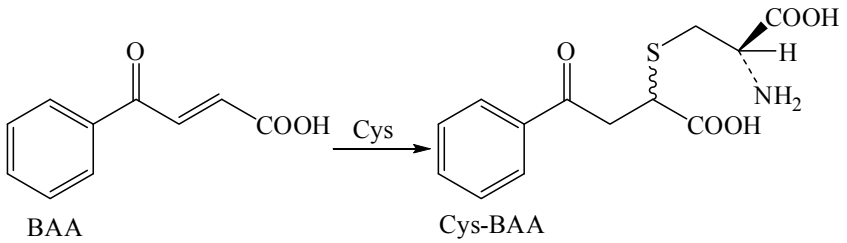

To further investigate the stability of the Cys adduct (59), a simple model compound, cysteinyl-4-oxo-4-phenylbutanoic acid (Cys-BAA), was synthesised. A mixture of β-benzoylacrylic acid (BAA) and 1.2 mol equivalents of Cys in 50% aqueous CH_3CN was stirred at RT in the dark under argon.[372] Clean and rapid cysteination was observed by normal and reversed phase TLC. After 30 min, TLC showed no starting material and the white suspension was evaporated to dryness to yield crude Cys-BAA as a white solid. The product was used without further purification. The aromatic region of the ^1H NMR spectrum revealed five adjacent aromatic resonances with chemical shifts and coupling patterns similar to the aromatic ring of BAA. The aliphatic side chain contained characteristic signals for a CH_2-CH moiety similar to the GSH adducts of Kyn and 3OHKyn.[18,20] The chemical shifts of the methylene (δ 3.52 and 3.70) and methine (δ 3.85) protons were consistent with the literature for related adducts.[18,20] ES-MS/MS (positive mode) showed a molecular ion at *m/z* 298 ($M+H^+$) and fragment ions at *m/z* 280, *m/z* 252, *m/z* 209 and *m/z* 177 due to loss of water, loss of formic acid, two successive losses of CO_2H and loss of Cys, respectively.

The stability of Cys-BAA was investigated over a range of pH values from pH 2.5 to pH 12.5 over 25 h. This range of pH conditions was chosen to better understand the stability of Cys adducts, including under the reaction conditions (*e.g.* deprotection (~pH 12.5)) and purification conditions (*e.g.* RP-HPLC purification (~pH 2-3)). The argon-gassed (~20 min) solutions were incubated at 25°C in the dark. Single aliquots were taken from each solution and analysed by RP-HPLC (Figure 4.6). Cys-BAA proved to be stable under acidic conditions (pH 2.5 and 4.0), while rapid decysteination was observed for physiological pH (pH 7.2, 97% loss after 25 h) and pH 12.5 (100% loss after 4 h). An excess of cysteine (~0.15 mol equivalents) at pH 12.5 did not result in an increase in the stability of Cys-BAA. It was then not surprising that Cys-3OHKG was not isolated upon deprotection of the reduced Cys adduct (60) under the basic conditions. Incubation of Cys-BAA at pH 7.2 resulted in decysteination and recovery of BAA, while at pH 12.5, both in the presence and absence of an excess of Cys, it resulted in formation of multiple peaks (~ 5). These peaks could not be identified by LC-

MS as they showed multiple ions. At pH 9.5, however, Cys-BAA showed greater stability than at pH 7.2 and 12.5, with 50% decomposition during a period of 25 h. In addition to Cys-BAA (*m/z* 298 ($M+H^+$)) and BAA (*m/z* 177 ($M+H^+$)), LC-MS analysis (positive mode) of the mixture at pH 9.5 after 25 h of incubation revealed a molecular ion at *m/z* 474 ($M+H^+$), suggesting formation of the dimer (61) (Figure 4.7).

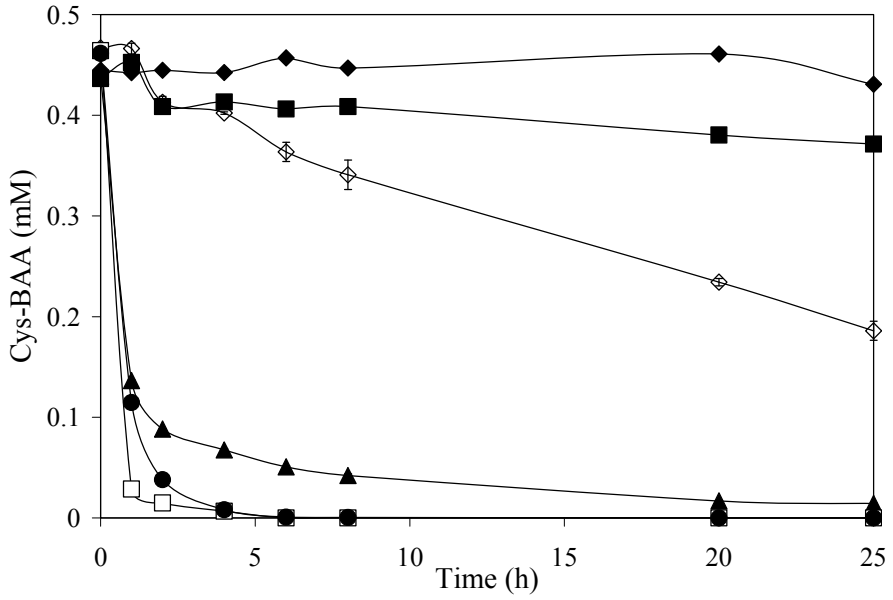

Figure 4.6: Stability of Cys-BAA at pH 2.5 (♦), 4.0 (■), 7.2 (▲), 9.5 (◊), 12.5 (□) and 12.5 (excess of Cys, 0.15 mol equivalents; ●) for 25 h.

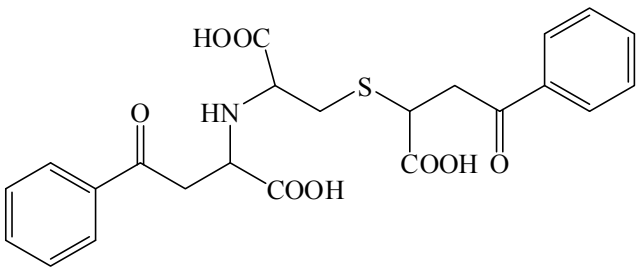

(61) *m/z* 474 ($M+H^+$)

Figure 4.7: Proposed dimeric structure (*m/z* 474 ($M+H^+$)) formed following incubation of Cys-BAA at pH 9.5 for 25 h.

4.2.9.3 Synthesis of Cys-3OHKG - Method 2

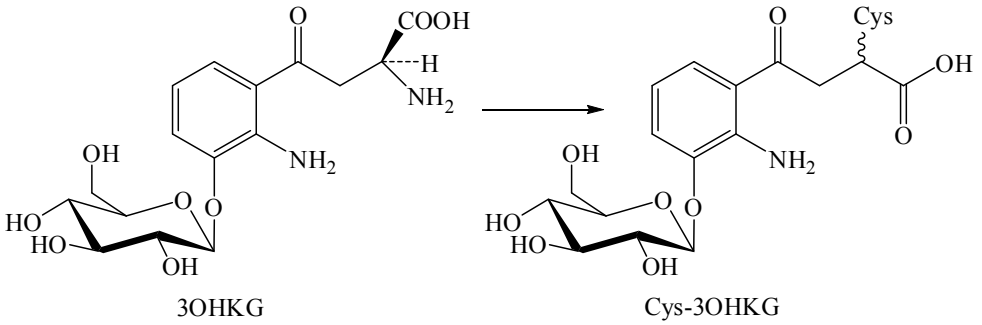

Due to the obvious base instability of the reduced Cys adduct (60) and the known acid instability of the glucose moiety, it was evident that removal of the acetyl and ester moieties would be challenging. Therefore, the synthesis of Cys-3OHKG from 3OHKG was investigated, using a similar deamination and Michael addition method to that of the GSH adducts.[86] While this may not be the most economic route, due to the time constraints and the small quantity of Cys-3OHKG required for this study, this was regarded as an appropriate approach. 3OHKG was dissolved in argon-gassed (~20 min) Na_2CO_3-$NaHCO_3$ buffer at pH 9.2 in the presence of ~11 mol equivalents of Cys in the dark at 37°C. The progress of the reaction was monitored by normal phase TLC. This revealed the formation of one product. Due to the expected Cys oxidation, and to ensure a good yield of Cys-3OHKG, ~11 mol equivalents of Cys were added after 24 and 48 h. After 72 h, TLC, detected at 365 nm, showed the starting material and the product both of similar intensities. As the reaction did not appear to be progressing further, the light yellow solution was therefore acidified to pH 6.5 by dropwise addition of 1 M AcOH and lyophilised. The crude pale yellow solid was purified by RP-HPLC to afford, in addition to the recovered starting material (3OHKG) in 35% yield, a pale yellow solid as a diastereoisomeric mixture (~1:1). This product had a similar retention time to the unknown compound isolated from the human lenses.

^{1}H NMR of the yellow solid revealed three aromatic protons and six protons from the glucose moiety consistent with those present in 3OHKG (Sections 2.2.6 and 2.2.8). The anomeric carbon appeared at 101.9 ppm and the anomeric proton appeared as a doublet at 4.94 ppm with a coupling constant of 7.4 Hz. This was indicative of a β-configuration. The side chain displayed a distinctive CH_2-CH moiety, assigned by the combination of DEPT (90 and 45) and HSQC. Chemical shifts at δ 3.60-3.45 and δ 3.75 were assigned to the methylene protons at C-3 and the methine proton at C-2, respectively. Further analysis of the yellow solid by COSY, HSQC and HMBC confirmed the Cys moiety was intact, displaying the methine

proton at δ 3.93 and methylene protons at δ 3.32-3.08. The chemical shifts and coupling constants were similar to literature reports of Cys-Kyn and Cys-3OHKyn adducts.[18,20]

ES-MS/MS (positive mode) showed a molecular ion at *m/z* 491 ($M+H^+$), as expected for Cys-3OHKG, and fragment ions at *m/z* 473, *m/z* 370 and *m/z* 311 due to loss of water, loss of Cys and loss of OGlu, respectively (Figure 4.8, B). This was identical to the ES-MS/MS spectrum of the compound isolated from the human lenses (Figure 4.8, A).

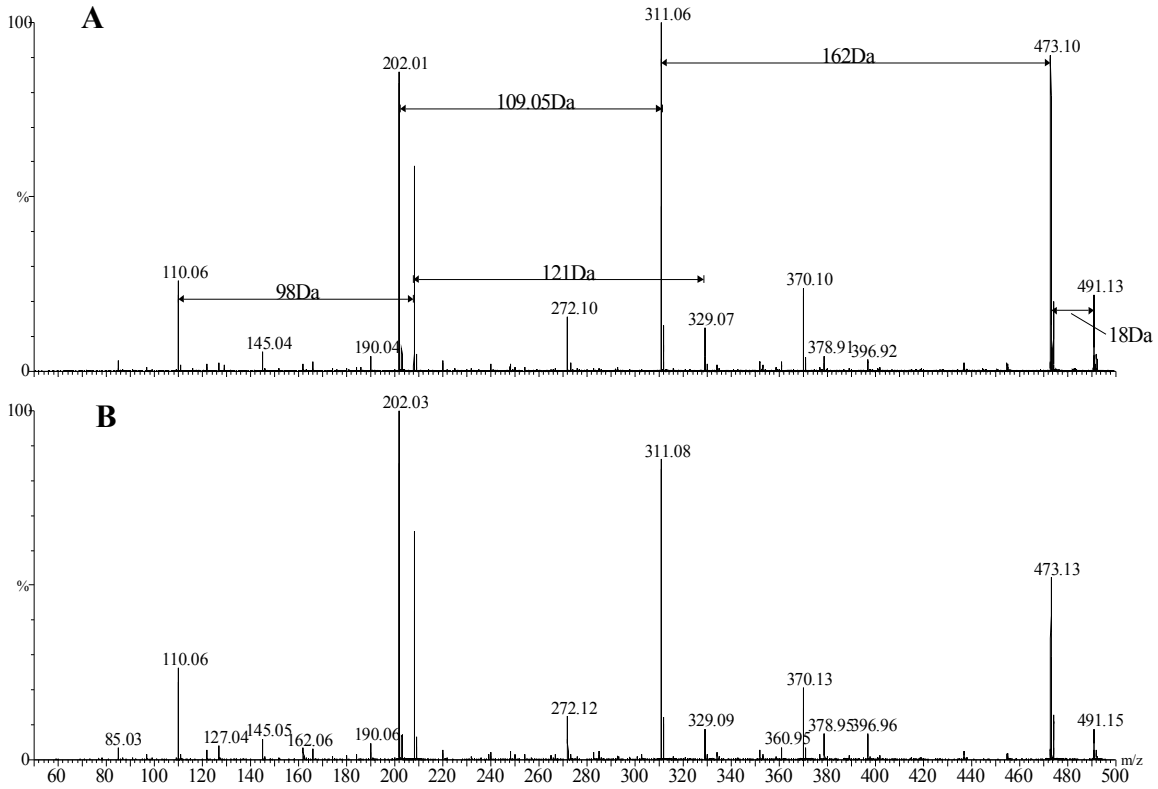

Figure 4.8: ES-MS/MS of compound (X) isolated from human lenses (**A**) and synthetic Cys-3OHKG (**B**) in positive ion mode. Mass differences between major ions are indicated in Daltons (Da).

The synthetic Cys-3OHKG and the unknown compound isolated from the human lenses displayed identical UV-vis profiles with absorption maxima at 262 and 365 nm in PBS at pH 7.0. The synthetic Cys-3OHKG was also found to be fluorescent, showing a maximum λ_{ex} at 337 nm and maximum λ_{em} at 438 nm. These spectral characteristics of Cys-3OHKG are similar to those determined for the major UV filters under the same conditions, *i.e.* 3OHKG: λ_{max} 263 and 365 nm and maximum fluorescence at λ_{ex} 360 / λ_{em} 500 nm; AHBG at λ_{max} 259 and 358 nm and maximum fluorescence at λ_{ex} 357 / λ_{em} 495 nm; Kyn λ_{max} at 257 and 359 nm and maximum fluorescence at λ_{ex} 355 / λ_{em} 485 nm; 3OHKyn λ_{max} at 268 and 370 nm and λ_{ex} 370 / λ_{em} 460 nm. This experimental data is consistent with the literature.[85,86,336,381,382] In

addition, the synthetic Cys-3OHKG and the lens compound coeluted on RP-HPLC, confirming the identity of unknown human lens compound as Cys-3OHKG.

It was not surprising to find Cys-3OHKG in the lenses as free Cys is found in the cortex and nucleus of human lenses, ranging from 160 nmol/g of protein (wet mass) at infancy to approximately 27 nmol/g of protein (wet mass) after the 6-7th decade of life. Cys concentrations are higher in the nucleus compared to the cortex and Cys is known to be involved in thiolation of lens proteins and in the biosynthesis of GSH.[187] Cys-3OHKG is presumably formed in the lens by the addition of free Cys to the deaminated product of 3OHKG in a manner analogous to that for the formation of the GSH adducts of 3OHKG, Kyn and 3OHKyn.[86]

4.2.9.4 Quantification of Cys-3OHKG in human lenses

The amount of Cys-3OHKG extracted from the normal human lenses of different ages was determined from the area under the RP-HPLC curve at 360 nm, by comparison with a standard curve constructed using the synthetic compound. Cys-3OHKG was not detected in the lens nucleus until the 5th decade (the age at which Cys was found to decrease substantially) and was absent in the cortex until the 7th decade (Figure 4.9).[121] The earlier detection of Cys-3OHKG in the nucleus was consistent with the onset of the barrier to diffusion that appears in human lenses after middle age.[115,116]

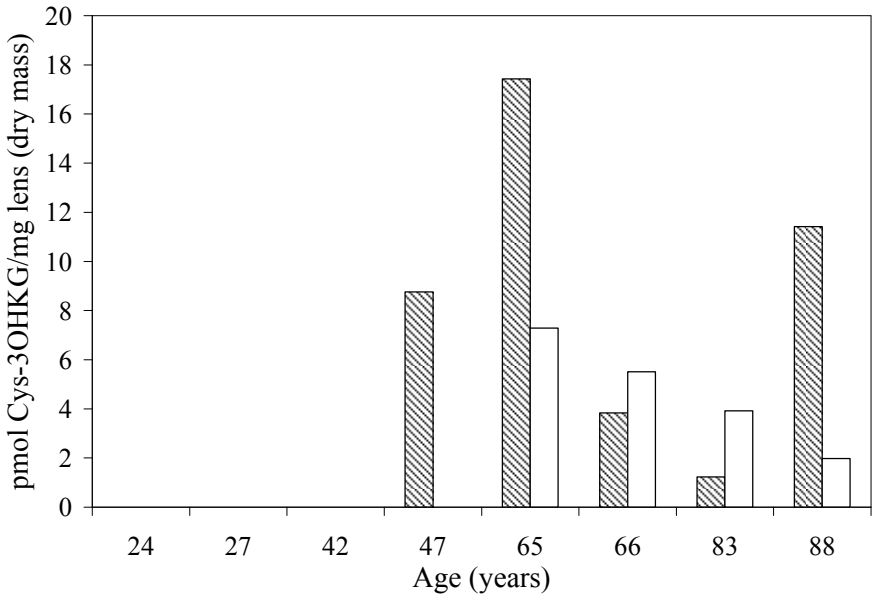

Figure 4.9: Quantification of Cys-3OHKG in normal human lenses. Cys-3OHKG was quantified in the nucleus (shaded) and cortex (unshaded) of normal human lenses.

Bova *et al.*[39] found that the concentration of 3OHKG, and other major UV filters, decreased linearly with age. In this study, however, Cys-3OHKG did not show a clear age related correlation in the nucleus, whereas, the concentration of cortical Cys-3OHKG did show signs of decreasing relative to age. Given the lack of a clear relationship between the nuclear levels of Cys-3OHKG and age, it appears that the formation of Cys-3OHKG is not solely influenced by the concentration of free Cys or 3OHKG. This is shown by a plot of Cys-3OHKG versus 3OHKG, where there is no correlation between the concentration of these compounds in the nucleus or cortex of human lenses (Figure 4.10). By comparison, a plot of nuclear levels of Cys-3OHKG versus GSH-3OHKG, shows a strong correlation (R^2 = 0.9105), indicating any deaminated 3OHKG is likely to react competitively with GSH or Cys (Figure 4.11). This relationship also holds for cortical levels of each compound, albeit at a lower correlation (R^2 = 0.7033) (Figure 4.11). One factor that may explain a lack of a clear correlation between Cys-3OHKG levels and age is the pronounced instability of Cys-3OHKG (discussed in Section 4.2.9.5).

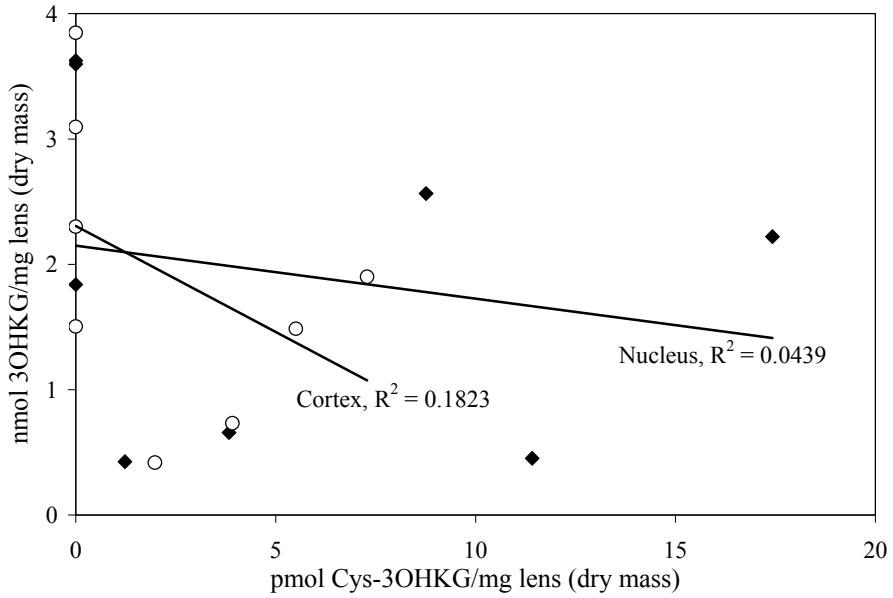

Figure 4.10: Linear regression plot of the nuclear (◆, R^2 = 0.0439) and cortical (○, R^2 = 0.1823) concentration of Cys-3OHKG versus 3OHKG in normal human lenses. The quantity of each compound was determined by comparison to a standard curve.

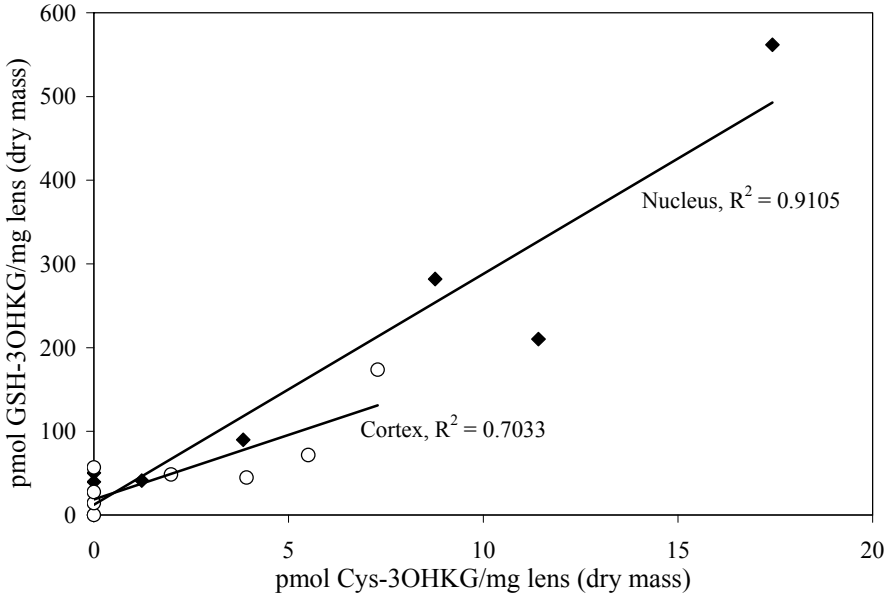

Figure 4.11: Linear regression plot of the nuclear (◆, R^2 = 0.9105) and cortical (○, R^2 = 0.7033) concentration of Cys-3OHKG versus GSH-3OHKG in normal human lenses. The quantity of each compound was determined by comparison to a standard curve.

UV filters were additionally extracted from 15 individual cataractous lenses, and a pool of 10 dark cataractous lenses, and analysed by RP-HPLC. Fractions were collected around the known retention time of Cys-3OHKG and analysed by ES-MS. There was no evidence of Cys-3OHKG in any of the fractions collected from these pooled or individual lenses. This suggested either that the concentration of free Cys or 3OHKG had decreased to a level where Cys-3OHKG cannot form, or it is formed in quantities below the detection limit of the instrumentation used in this study. The estimated MS sensitivity was ~50 fmol.

4.2.9.5 Stability of Cys-3OHKG

Given the fact that Cys-3OHKG was found in low pmol levels per mg lens (dry mass), the stability of Cys-3OHKG was investigated in argon-gassed (~20 min) PBS (pH 7.0) in the dark at 37°C. Triplicate aliquots were taken at intervals over a period of 240 h and analysed by RP-HPLC. Cys-3OHKG was found to rapidly decompose, with Cys-3OHKG decreasing to ~30% after only 2 h of incubation and totally decomposing after 8 h (Figure 4.12). Concomitantly, the formation of another compound was observed at the same wavelength. This instability of Cys-3OHKG may explain the fact that it was present in low pmol levels in normal lenses and absent in cataractous lenses. It was also very unlikely that free Cys was available in the nuclei of cataractous lenses. The nuclei of advanced nuclear cataractous lenses are in an oxidising environment, therefore it would be surprising to have reduced Cys available for reaction.[11]

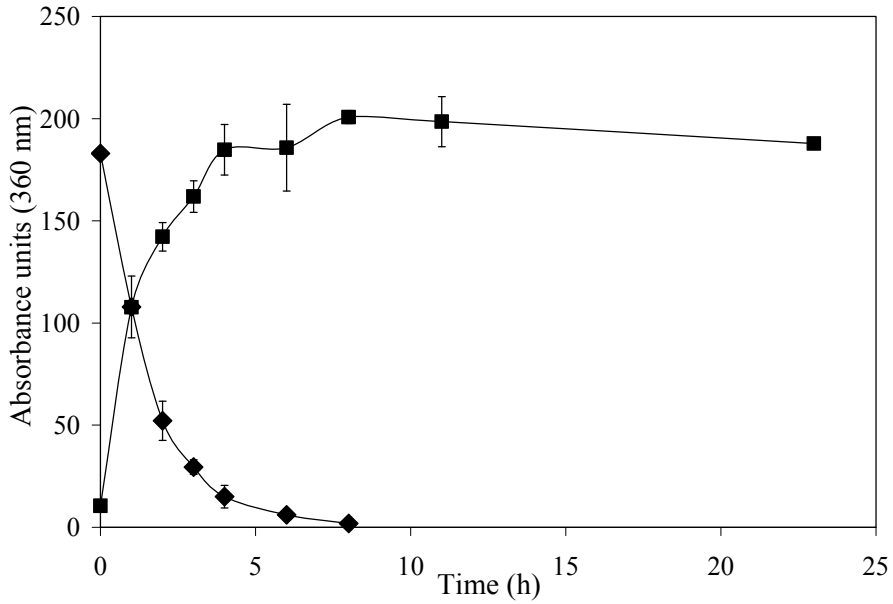

Figure 4.12: Cys-3OHKG (0.2 mM) was incubated in argon-gassed PBS (pH 7.0). Aliquots of the reaction mixtures were taken at the indicated time points and analysed by RP-HPLC. Detection was at 360 nm. Cys-3OHKG (♦); deaminated 3OHKG (■).

This stability of Cys-3OHKG was comparable to the stability of Cys-BAA at pH 7.2 at 25°C (Figure 4.6). Decomposition of Cys-3OHKG was, however, more rapid than that reported for Cys-Kyn (4.2 mM) and Cys-3OHKyn (0.2 mM) under similar conditions.[175,383] Cys-Kyn showed ~50% decomposition after 24 h and ~74% after 100 h, while Cys-3OHKyn decomposed nearly 100% after 24 h of incubation either in the presence or absence of oxygen.[175,383]

As determined by LC-MS, the major product formed as a result of the decomposition of Cys-3OHKG within the first 24 h was decysteinated 3OHKG (23) (*m/z* 370 ($M+H^+$), λ_{max} 283/411 nm) (Figure 4.13). After 24 h, decysteinated 3OHKG started to decompose to 3OHKG yellow (*m/z* 370 ($M+H^+$), λ_{max} 270/378 nm), which is formed by cyclisation of decysteinated 3OHKG.[101] After 240 h, 3OHKG yellow represented approximately one third of the total decysteinated 3OHKG. As 3OHKG yellow closely eluted with the decysteinated 3OHKG on RP-HPLC, the ratio of these two compounds could not be accurately determined.

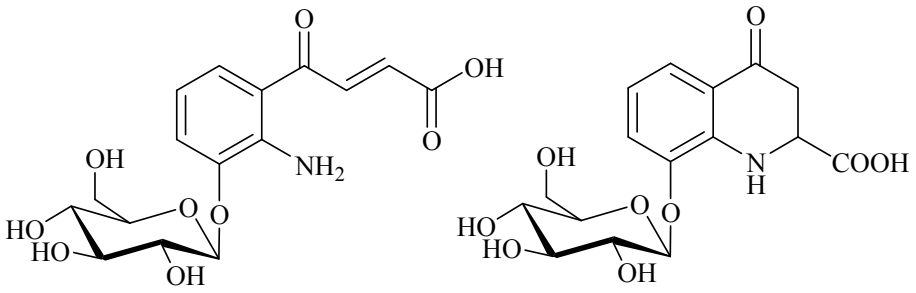

Decysteinated 3OHKG (23) 3OHKG yellow

Figure 4.13: Chemical structures of the decysteinated 3OHKG (23) and 3OHKG yellow.

4.3 Conclusions

This study describes the identification and quantification of four novel human lens metabolites, AHA, AHB, GSH-Kyn and Cys-3OHKG. Other proposed lens metabolites, GSH-3OHKyn, Kyn yellow and 3OHKyn yellow, were not found in the investigated human lenses. The spectral characteristics of these novel metabolites suggest that they may have the capability to act as UV filters and protect the lens from UV-induced photo-damage.

The lens metabolites were identified *via* total synthesis and spectral analysis. AHA was synthesised by condensing 2-nitroacetophenone (55) and glyoxylic acid monohydrate under microwave conditions to yield the acrylic acid (56). The acrylic acid (56) was further reduced to give AHA in an overall yield of 22% from 2-nitroacetophenone (2 steps). Similarly to the synthesis of AHA, AHB was synthesised from the acrylic acid (7), *via* reduction, to afford AHB in an overall yield of 5% from 3-hydroxyacetophenone (3 steps). The GSH adducts (GSH-Kyn and GSH-3OHKyn) and intramolecular Michael adducts (Kyn yellow and 3OHKyn yellow) were synthesised from commercially available Kyn and 3OHKyn in 44-51 and 22-26% yield, respectively. Cys-3OHKG was synthesised from 3OHKG under similar conditions to the synthesis of the GSH adducts. This resulted in Cys-3OHKG in 36% yield from 3OHKG (1 step).

AHA, AHB and GSH-Kyn were isolated in low pmol/mg lens (dry mass) levels in normal and cataractous lenses of all ages, while Cys-3OHKG was found only in low pmol/mg lens (dry mass) levels in normal lenses after the 5th decade of life. The stability of AHA, AHB, GSH-Kyn and GSH-3OHKyn under extraction and RP-HPLC conditions confirmed that the low concentrations measured for AHA, AHB and GSH-Kyn, and the lack of detection of GSH-3OHKyn, were not due to significant loss or breakdown during extraction and analysis of the

lens extracts and were representative of the concentrations in the investigated lenses. In addition, AHA was found to be very stable under conditions mimicking the lens environment. This suggested that formation of AHA may protect the lens from modifications due to its greater stability compared to its precursor (Kyn). In contrast, AHB, GSH-Kyn, GSH-3OHKyn and Cys-3OHKG were not stable under physiological conditions. In particular, AHB was unstable under aerobic conditions and produced yellow/tanned products that may contribute to lens colouration observed during lens aging and ARN cataract.

4.4 Experimental

4.4.1 General experimental

Acetonitrile (CH_3CN) was of HPLC grade (Ajax Chemicals, NSW, Australia). All other organic solvents were AR grade and distilled prior to use. DL-Kynurenine sulphate salt (≥ 95%), 3-hydroxy-DL-kynurenine (3OHKyn), 2-nitroacetophenone (55, 95%), GSH (99%), L-cysteine (Cys), tin(II) chloride dihydrate ($SnCl_2{\cdot}2H_2O$), PtO_2 (Pt 81-83%), Pd/C (10 wt % on activated carbon) and trifluoroacetic acid (TFA) (> 99%) were from Sigma-Aldrich. Glacial acetic acid (AcOH) (> 99.9%), sodium dithionite ($Na_2S_2O_4$) and ascorbic acid (99.7%) were purchased from BDH. Chelex resin (100-200 mesh) was purchased from BioRad and butylated hydroxytoluene (BHT) from CalBiochem. CD_3OD (99.8%), D_2O (99.9%) and acetone-*d*6 (99.9%) were from Cambridge Isotope Laboratories. β-Benzoylacrylic acid (BAA) was from Acros Organics. Dulbelcco's phosphate-buffered saline (PBS), without calcium and magnesium, consisted of KCl (2.7 mM), KH_2PO_4 (1.4 mM), NaCl (137 mM), Na_2HPO_4 (7.68 mM).[257] Pre-washed chelex resin was added to the PBS buffer (~2 g/L) and left for 24 h prior to use. The pH was adjusted to 7.0 with 1 M NaOH. Milli-Q® H_2O (purified to 18.2 MΩ cm^{-2}) was used in all aqueous preparations. Normal human lenses were obtained post-mortem from donor eyes at the Sydney Eye Bank (Sydney, Australia) and cataractous lenses were obtained from K.T. Seth Eye Hospital (Rajkot, Gujarat, India) with ethical approval from the University of Wollongong Human Ethics Committee (HE99/001). After removal, lenses were immediately placed into sterile plastic screw-capped vials and kept at -80°C until analysed. Thin-layer chromatography (TLC) plates were of normal phase 60 F_{254} and reversed phase 18 F_{254} (Merck, Germany). Normal phase TLC plates were developed using the mobile phase of *n*-butanol/AcOH/H_2O (12:3:5 BAW, v/v), where indicated. TLC plates were visualised under UV light (254 and 365 nm) and ninhydrin (ninhydrin [0.2%, w/v]

in *n*-butanol [94.8%, v/v] and AcOH [5%, v/v]),[288] where indicated. C18 reversed phase Sep-Pak® cartridges were purchased from Waters. Normal phase silica gel (230-400 mesh) was from Merck (Germany). Melting points were determined on a SMP 10 Stuart scientific (UK) apparatus and are uncorrected. Infrared spectra were recorded on a PerkinElmer Paragon 1000 PC FT-IR spectrometer. A Labconco FreeZone 12 plus freeze drier (0.04 mBa, -80°C) from Crown Scientific was used for aqueous lyophilisation. Microwave assisted aldol condensation reactions were conducted in a focused microwave reactor (CEM Discover) at ~50 W and < 5 psi. Other aldol condensation reactions were conducted in a 12 place head carousel reactor station from Radley Discovery Technologies. A vacuum pump used for reactions under vacuum and evaporation of organic solvents was of ~20 mBar.

4.4.2 UV-visible absorbance and fluorescence spectrometric measurements

See Section 2.4.2 for details.

4.4.3 Reversed phase-high performance liquid chromatography (RP-HPLC)

RP-HPLC was performed on a Shimadzu HPLC equipped with LC-10ADvp pumps, a SIL-10Avp autoinjector, DGU-12A degasser and SPD-M10Avp diode array detector. Detection was at 254 and 360 nm. The analytical separations were performed on a Phenomenex (Luna, 100 Å, 5 μm, 4.6 x 250 mm, C18) column fitted with a Phenomenex (Synergy Fusion, 100 Å, 4 μm, 2 x 4 mm, C18) guard column, unless otherwise stated, while preparative purifications were performed on a Phenomenex (Luna, 100 Å, 10 μm, 15 x 250 mm, C18) column fitted with a Phenomenex (Synergy Fusion, 100 Å, 4 μm, 10 x 10 mm, C18) guard column. The following mobile phase system; buffer A (H_2O/0.05% TFA, v/v) and buffer B (80% CH_3CN/0.05% TFA, v/v) and the flow rate 1 mL/min for analytical and 7 mL/min for preparative separations were kept constant. Standard curves and stability analyses for AHA, AHB, GSH-Kyn and GSH-3OHKyn were performed with a mobile phase gradient as follows: 0-3 min (20% buffer B), 3-15 min (20-90% buffer B), 15-18 min (90% buffer B), 18-22 min (90-20% buffer B) and 22-28 min (20% buffer B). Preparative separations of AHA and AHB were performed with a mobile phase gradient as follows: 0-10 min (10% buffer B), 10-40 min (10-70% buffer B), 40-50 min (70% buffer B), 50-55 min (70-10% buffer B) and 55-65 min (10% buffer B). Preparative separations of GSH-Kyn and GSH-3OHKyn were performed with a mobile phase gradient as follows: 0-10 min (5% buffer B), 10-40 min (5-55% buffer

B), 40-45 min (55% buffer B), 45-50 min (55-5% buffer B) and 50-60 min (5% buffer B). Preparative separations of Kyn yellow and 3OHKyn yellow were performed with a mobile phase gradient as follows: 0-10 min (20% buffer B), 10-30 min (20-80% buffer B), 30-35 min (80% buffer B), 35-40 min (80-20% buffer B) and 40-50 min (20% buffer B). Standard curve and stability analyses of Cys-3OHKG were performed with a mobile phase gradient as follows: 0-4 min (5% buffer B), 4-12 min (5-80% buffer B), 12-15 min (80% buffer B), 15-18 min (80-5% buffer B) and 18-26 min (5% buffer B). Preparative separation of Cys-3OHKG was conducted with a mobile phase gradient as follows: 0-10 min (5% buffer B), 10-30 min (5-70% buffer B), 30-35 min (70% buffer B), 35-40 min (70-5% buffer B) and 40-50 min (5% buffer B). Standard curves and stability analyses of Cys-BAA were performed with a mobile phase gradient as follows: 0-3 min (10% buffer B), 3-15 min (10-90% buffer B), 15-20 min (90% buffer B), 20-24 min (90-10% buffer B) and 24-30 min (10% buffer B).

4.4.4 Liquid chromatography-mass spectrometry (LC-MS)

See Section 2.4.4 for details.

4.4.5 Nuclear magnetic resonance (NMR) spectroscopy

See Section 2.4.5 for details.

4.4.6 Mass spectrometry (MS)

For details on ES-MS and ES-MS/MS see Section 2.4.6. High resolution mass spectrometry (HR-MS) was performed on a Q-TOF Ultima with lock spray. Leucine-encephalin (555.2692 Da) was used as the reference compound.

4.4.7 Synthesis of 4-(2-nitrophenyl)-4-oxobut-2-enoic acid (56)

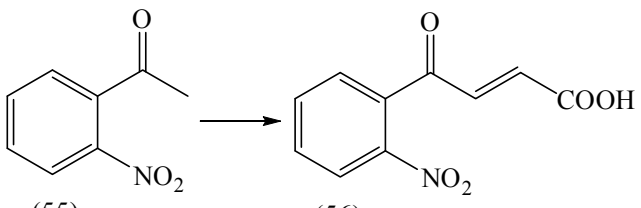

(55) (56)

4.4.7.1 Method 1 (modified method of Bianchi *et al*.[276])

2-Nitroacetophenone (55) (0.50 mL, 3.0 mmol) was combined with melted glyoxylic acid monohydrate (2.78 g, 30.2 mmol) at 60°C. The temperature was increased to 110°C and the yellow thick reaction mixture was left under vacuum (~20 mBar). The reaction progress was monitored by TLC (EtOAc/1% AcOH, v/v). After 5 h another portion of glyoxylic acid monohydrate (0.20 g, 2.17 mmol) was added. After 14 h in total, the brown viscous reaction mixture was set aside to cool to RT, dissolved in brine and extracted with DCM (6-7 x 200-300 mL). The organic layer was dried with $MgSO_4$ and evaporated to ~50 mL under reduced pressure. The brown-yellow solution was mixed with normal phase silica (~5 g) and evaporated to dryness. The crude mixture was purified by normal phase chromatography (DCM/1% AcOH, v/v) to yield 4-(2-nitrophenyl)-4-oxobut-2-enoic acid (0.18 g, 27%, R_f 0.46 (EtOAc/1% AcOH, v/v), mp 171-172°C (lit.[276] 170-173°C)) as a white solid.

4-(2-Nitrophenyl)-4-oxobut-2-enoic acid (56): ν_{max}(KBr disc) 3500-2300 (br, OH, with C-H superimposed), 1707 (C=O), 1679 (C=O), 1519 (NO_2), 1343 (NO_2), 1317, 1297 (C-O), 740 (out-of-plane aromatic C-H bend) cm^{-1}; ^{1}H NMR δ (acetone-d_6) 8.25 (1H, d, *J* 8.0, ArH-3), 7.95 (1H, ddd, *J* 1.1, 7.5, 7.5, ArH-5), 7.85 (1H, ddd, *J* 1.3, 7.5, 8.0, ArH-4), 7.69 (1H, dd, *J* 1.3, 7.5, ArH-6), 7.26 (1H, d, *J* 16.1, H-3), 6.45 (1H, dd, *J* 16.1, H-2); ^{13}C NMR δ (acetone-d_6) 192.8 (CO-4), 166.2 (CO-1), 147.6 (ArC-2), 139.9 (C-3), 135.8 (ArC-1), 135.5 (ArC-5), 134.4 (C-2), 132.5 (ArC-4), 129.8 (ArC-6), 125.4 (ArC-3); ES-MS *m/z* 222 ($M+H^+$, 89%).

4.4.7.2 Method 2 (modified method of Bianchi *et al*.[276])

2-Nitroacetophenone (55) (0.50 mL, 3.0 mmol) was combined with melted glyoxylic acid monohydrate (2.78 g, 30.2 mmol) at 60°C. The temperature was increased to 110°C and the yellow thick reaction mixture was left under vacuum (~20 mBar). The reaction progress was monitored by TLC, as described above. After 5 h another portion of glyoxylic acid monohydrate (0.20 g, 2.2 mmol) was added. After 14 h, the brown viscous reaction mixture was mixed with normal phase silica (~5 g) and set aside to cool to RT. The mixture was purified by normal phase chromatography (DCM/1% AcOH, v/v) to yield 4-(2-nitrophenyl)-4-oxobut-2-enoic acid (0.30 g, 45%, R_f 0.46 (EtOAc/1% AcOH, v/v)) as a white solid. ^{1}H NMR, ^{13}C NMR, ES-MS and mp were consistent with the literature and above.[276]

4.4.7.3 Method 3 (modified method of Bianchi *et al*.[276])

2-Nitroacetophenone (55) (0.30 mL, 1.8 mmol) was mixed with glyoxylic acid monohydrate (1.65 mg, 18.1 mmol) and placed into the cavity of a focused microwave reactor (CEM Discover) at 110°C. The reaction progress was monitored by TLC, as described above. Glyoxylic acid monohydrate (100 mg, 1.10 mmol) was added at 20 and 40 min. After 60 min the brown viscous reaction mixture was mixed with normal phase silica gel (~3 g) and left aside to cool to RT. The crude solid was purified by normal phase chromatography (DCM/1% AcOH, v/v) to obtain 4-(2-nitrophenyl)-4-oxobut-2-enoic acid (216 mg, 53.8%, R_f 0.46 (EtOAc/1% AcOH, v/v)) as a white solid. ^{1}H NMR, ^{13}C NMR, ES-MS and mp were consistent with the literature and above.[276]

4.4.8 Synthesis of 4-(2-aminophenyl)-4-oxobutanoic acid (AHA)

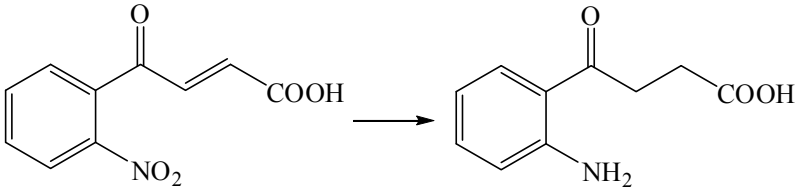

(56) AHA

4.4.8.1 Method 1

A solution of 4-(2-nitrophenyl)-4-oxobut-2-enoic acid (56) (255 mg, 1.15 mmol), EtOAc (280 mL) and AcOH (450 µL) was treated with H_2 gas (1 atm) in the presence of PtO_2 (15 mg, 0.06 mmol) at RT in the dark for 22 h. TLC analysis of normal (BAW and EtOAc/1% AcOH, v/v) and reversed (20% CH_3CN/H_2O, v/v) phase revealed multiple spots including AHA, visualising by UV light and ninhydrin. The yellow reaction mixture was gravity filtered through a plug of celite and the solvent removed under vacuum. Crude AHA was dissolved in 10% aqueous CH_3CN (v/v) and loaded onto a preconditioned C18 reversed phase Sep-Pak column and eluted with an increasing gradient of aqueous CH_3CN (10 to 40%, v/v). The fractions containing the product were pooled and lyophilised to yield AHA in ~80-85% purity. Further purification was achieved by preparative RP-HPLC. The fraction containing AHA was collected and lyophilised to yield an off-white solid (43 mg, 41%, R_f 0.88 (BAW), R_f 0.64 (EtOAc/1% AcOH, v/v), R_f 0.37 (20% CH_3CN/H_2O, v/v), mp 92-94°C).

4-(2-Aminophenyl)-4-oxobutanoic acid (AHA): $M+H^+$, 194.0823. Calculated for $C_{10}H_{12}NO_3$: $M+H^+$, 194.0817; ν_{max}(KBr disc) 3486 (NH_2), 3338 (NH_2), 3300–2300 (br, OH, with C-H superimposed), 1709 (C=O), 1650 (C=O), 763 (out-of-plane aromatic C-H bend) cm^{-1}; ^1H NMR δ (CD_3OD) 7.82 (1H, dd, *J* 1.5, 8.2, ArH-6), 7.25 (1H, ddd, *J* 1.5, 7.0, 8.0, ArH-4), 6.75 (1H, dd, *J* 1.0, 8.0, ArH-3), 6.65 (1H, ddd, *J* 1.0, 7.0, 8.2, ArH-5), 3.25 (2H, t, *J* 6.4, H-2), 2.65 (2H, t, *J* 6.4, H-3); ^{13}C NMR δ (CD_3OD) 201.7 (CO-4), 177.0 (CO-1), 152.1 (ArC-2), 135.3 (ArC-4), 132.0 (ArC-6), 118.6 (ArC-1), 118.4 (ArC-3), 116.4 (ArC-5), 35.7 (C-2), 29.1 (C-3); ES-MS/MS *m/z* 194.1 ($M+H^+$, 37%), 176.1 ($M+H^+$ - H_2O, 100%), 148.0 ($M+H^+$ - HCOOH, 62%), 130.1 (37%), 94.0 (34%). λ_{max} 254 and 365 nm and maximum fluorescence at λ_{ex} 346 / λ_{em} 480 nm.

4.4.8.2 Method 2 (modified method of Moriya *et al.*[338])

4-(2-Nitrophenyl)-4-oxobut-2-enoic acid (56) (21.7 mg, 0.10 mmol) was dissolved in MeOH (0.38 mL). After 10 min, aqueous HCl (1.0 mL (2.2%, v/v), 0.71 mmol) and Pd/C (~4 mg) were added and the reaction mixture was treated with H_2 gas (1 atm) at RT in the dark for 3 h. The progress of the reaction was monitored by TLC, as described in Method 1, to reveal multiple spots including AHA. The reaction mixture was filtered through a plug of celite and the pH adjusted to ~6 by dropwise addition of 1 M NaOH. The yellow solution was lyophilised and the yellow solid purified by RP-HPLC to afford AHA (5.3 mg, 28%, R_f 0.88 (BAW), R_f 0.64 (EtOAc/1% AcOH, v/v)) as an off-white solid. ^1H NMR, ^{13}C NMR, ES-MS/MS, mp, absorbance and fluorescence were consistent with above.

4.4.8.3 Method 3 (modified method of Moriya *et al.*[338])

A solution of 4-(2-nitrophenyl)-4-oxobut-2-enoic acid (56) (20.9 mg, 0.10 mmol) and aqueous HCl (1.0 mL (2.2%, v/v), 0.71 mmol) was treated with H_2 gas (1 atm) in the presence of Pd/C (~4 mg) at RT in the dark for 1.5 h. The progress of the reaction was monitored by TLC as described above to reveal multiple spots including AHA. The yellow solution was worked up and purified, as described in Method 2, to afford AHA (6.2 mg, 34%, R_f 0.88 (BAW), R_f 0.64 (EtOAc/1% AcOH, v/v)) as an off-white solid. ^1H NMR, ^{13}C NMR, ES-MS/MS, mp, absorbance and fluorescence were consistent with above.

4.4.9 Synthesis of 4-(2-amino-3-hydroxyphenyl)-4-oxobutanoic acid (AHB)

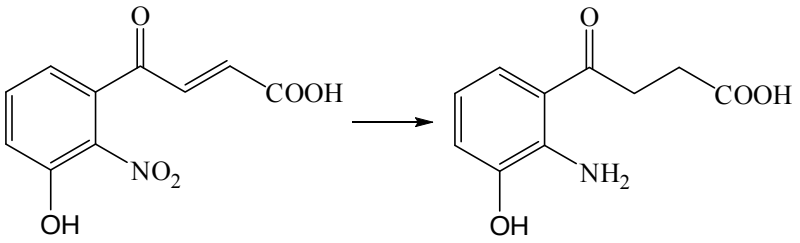

(7) AHB

4.4.9.1 Method 1

A solution of 4-(3-hydroxy-2-nitrophenyl)-4-oxobut-2-enoic acid (7) (143 mg, 0.60 mmol), EtOAc (185 mL) and AcOH (250 μL) was treated with H_2 gas (1 atm) in the presence of PtO_2 (15 mg, 0.06 mmol) at RT in the dark for 3 h. TLC analysis of normal (EtOAc/1% AcOH, v/v) and reversed phase (20% CH_3CN/H_2O, v/v) revealed AHB, visualising by UV light and ninhydrin. The yellow reaction mixture was worked up in a similar manner to AHA (Method 1), and purified by using a C18 reversed phase Sep-Pak column to yield AHB in ~80-85% purity. Subsequent purification by preparative RP-HPLC yielded AHB (59 mg, 47%, R_f 0.65 (EtOAc/1% AcOH, v/v), R_f 0.57 (20% CH_3CN/H_2O, v/v), mp 134-135°C) as a light brown solid and 8-hydroxy-4-oxo-1,4-dihydroquinoline-2-carboxylic acid (7.4 mg, 6%, R_f 0.75 (EtOAc/1% AcOH, v/v)) as a red solid.

4-(2-Amino-3-hydroxyphenyl)-4-oxobutanoic acid (AHB): $M+H^+$, 210.0779. Calculated for $C_{10}H_{12}NO_4$: $M+H^+$, 210.0766; ν_{max}(KBr disc) 3500-2300 (br, NH_2, OH, with C-H superimposed), 1709 (C=O), 1681 (C=O), 1652 (C=O), 1195 (C-O), 1149, 788 (out-of-plane aromatic C-H bend), 719 (out-of-plane aromatic C-H bend) cm^{-1}; ^1H NMR δ (CD_3OD) 7.82 (1H, dd, *J* 1.3, 8.3, ArH-6), 7.25 (1H, dd, *J* 1.3, 8.0, ArH-4), 6.57 (1H, dd, *J* 8.0, 8.3, ArH-5), 3.26 (2H, t, *J* 6.4, H-2), 2.66 (2H, t, *J* 6.4, H-3); ^{13}C NMR δ (CD_3OD) 202.0 (CO-4), 201.8 (CO-4), 176.9 (CO-1), 147.1 (ArC-3), 139.0 (ArC-2), 122.5 (ArC-6), 120.4 (ArC-1), 118.3 (ArC-4), 117.6 (ArC-5), 35.0 (C-2), 29.1 (C-3); ES-MS/MS *m/z* 210.08 ($M+H^+$, 100%), 192.1 ($M+H^+ - H_2O$, 28%), 164.1 ($M+H^+$ - HCOOH, 54%), 146.1 (33%), 122.1 (20%), 110.1 (15%). λ_{max} 267 and 369 nm and maximum fluorescence at λ_{ex} 346 / λ_{em} 435 nm.

8-Hydroxy-4-oxo-1,4-dihydroquinoline-2-carboxylic acid (57): ^1H NMR δ (CD_3OD) 7.07 (1H, d, *J* 7.7), 7.00 (1H, d, *J* 7.7), 6.82 (1H, dd, *J* 7.7, 7.7), 5.96 (1H, s); ES-MS/MS *m/z* 206.1 ($M+H^+$, 10%), 188.1 ($M+H^+ - H_2O$, 100%), 162.0 ($M+H^+ - CO_2$, 2%), 160.0 ($M+H^+$ -

HCOOH, 15%), 132.0 ($M+H^+$ - HCOOH - CO, 19%), 105.0 (5%). λ_{max} at 266 and 489 nm and maximum fluorescence at λ_{ex} 395 / λ_{em} 520 nm.

4.4.9.2 Method 2 (modified method of Moriya *et al.*[338])

A yellow solution of 4-(3-hydroxy-2-nitrophenyl)-4-oxobut-2-enoic acid (7) (21.5 mg, 0.10 mmol) and aqueous HCl (1.0 mL (2.2%, v/v), 0.71 mmol) was treated with H_2 gas (1 atm) in the presence of Pd/C (~10 mg) at RT in the dark for 50 min. TLC analysis of normal phase (EtOAc/1% AcOH, v/v), visualising by UV light and ninhydrin, revealed multiple spots including AHB. The reaction mixture was gravity filtered through a plug of celite and the pH adjusted to ~6 by dropwise addition of 1 M NaOH. The yellow solution was lyophilised and the yellow solid was purified by RP-HPLC to afford AHB (7.2 mg, 38%, R_f 0.65 (EtOAc/1% AcOH, v/v)) as an off-white solid. ^{1}H NMR, ^{13}C NMR, ES-MS/MS, mp, absorbance and fluorescence were consistent with above.

4.4.10 Synthesis of glutathionyl-kynurenine (GSH-Kyn) (modified method of Garner *et al.*[86])

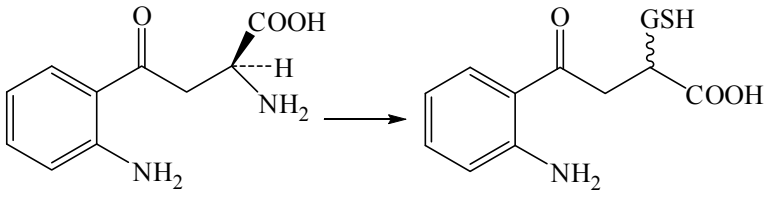

Kyn GSH-Kyn

DL-Kynurenine sulphate salt (100 mg, 0.32 mmol) was dissolved in argon-gassed (~20 min) Na_2CO_3-$NaHCO_3$ buffer (20 mL, 25 mM, pH 9.5). GSH (500 mg, 1.62 mmol) was added and the light yellow solution was gassed with argon for ~20 min, sealed with parafilm and incubated in the dark at 37°C with shaking. The progress of the reaction was monitored by normal phase TLC (BAW) and reversed phase TLC (20% CH_3CN/H_2O, v/v). After 24 h another portion of GSH (100 mg, 0.32 mmol) was added to the reaction mixture and the pH was readjusted to 9.5 by dropwise addition of 1 M NaOH. After 72 h the light yellow solution was acidified to pH 2 by dropwise addition of 25% aqueous HCl (v/v) and lyophilised. The crude solid was purified by preparative RP-HPLC to obtain GSH-Kyn (121 mg, 51%, R_f 0.25 (BAW), R_f 0.86 (20% CH_3CN/H_2O, v/v)) as a ~1:1 mixture of diastereomers.

Glutathionyl-kynurenine (GSH-Kyn): M+H$^+$, 499.1534 calculated for $C_{20}H_{27}N_4O_9S$: M+H$^+$, 499.1499; ν_{max}(KBr disc) 3500-2300 (br, zwitterionic NH_3^+, COO^-, NH_2, OH, with C-H superimposed), 1722 (br, C=O), 1652 (br, C=O), 1545, 1200 (br, C-O) cm^{-1}; ^{1}H NMR δ (CD_3OD) 7.77 (1H, br d, *J* 8.2, ArH-6), 7.24 (1H, ddd, *J* 1.0, 7.6, 8.3, ArH-4), 6.73 (1H, d, *J* 8.3, ArH-3), 6.60 (1H, dd, *J* 7.6, 8.2, ArH-5), 4.74 (~0.5H, dd, *J* 4.8, 9.2, SCH_2CH), 4.68 (~0.5H, dd, *J* 5.7, 7.9, SCH_2CH), 4.00 (1H, t, *J* 6.2, $CH_2CHCOOH$), 3.94 (2H, s, CH_2COOH), 3.87 (1H, dd, *J* 3.8, 9.9, H-2), 3.62 (1H, m, H-3), 3.34 (1H, m, H-3), 3.31 (~0.5H, dd, *J* 4.8, 14.0, SCH_2), 3.22 (~0.5H, dd, *J* 5.7, 13.9, SCH_2), 3.07 (~0.5H, dd, *J* 7.9, 13.9, SCH_2), 2.92 (~0.5H, dd, *J* 9.2, 14.0, SCH_2), 2.58 (2H, t, *J* 6.9, $COCH_2CH_2$), 2.20 (2H, m, $COCH_2CH_2$); ^{13}C NMR δ (CD_3OD) 200.1 (CO-4), 200.0 (CO-4), 175.9 (CO-1), 175.8 (CO-1), 174.5 ($NHCOCH_2$), 174.4 ($NHCOCH_2$), 172.8 ($CHCONH$), 172.8 ($CHCONH$), 172.6 (CH_2COOH), 171.7 ($CHCOOH$), 152.6 (ArC-2), 135.6 (ArC-4), 132.0 (ArC-6), 118.3 (ArC-3), 117.9 (ArC-1), 116.2 (ArC-5), 54.5 (SCH_2CH), 53.8 (SCH_2CH), 53.7 ($CH_2CHCOOH$), 43.3 (C-2), 42.6 (C-2), 42.6 (C-3), 42.2 (C-3), 41.8 (CH_2COOH), 34.5 (SCH_2), 34.4 (SCH_2), 32.4 ($COCH_2CH_2$), 27.1 ($COCH_2CH_2$), 27.0 ($COCH_2CH_2$); ES-MS/MS *m/z* 499.0 (M+H$^+$, 11%), 481.2 (M+H$^+$ - H_2O, 3%), 424.0 (M+H$^+$ - glycine, 30%), 370.0 (M+H$^+$ - glutamic acid, 21%), 352.0 (M+H$^+$ - glutamic acid - H_2O, 62%), 259.0 (100%), 192.0 (M+H$^+$ - GSH, 21%), 179.0 (76%), 174.0 (30%). λ_{max} 256 and 356 nm and maximum fluorescence at λ_{ex} 350 / λ_{em} 475 nm.

4.4.11 Synthesis of glutathionyl-3-hydroxykynurenine (GSH-3OHKyn) (modified method of Garner *et al.*[86])

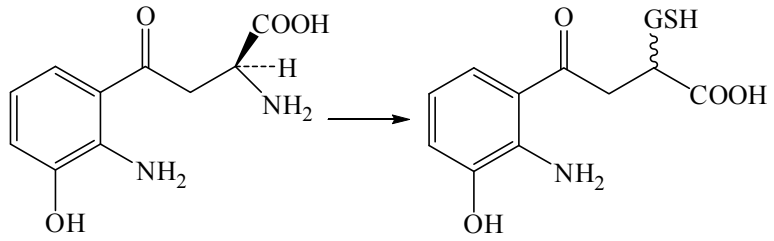

3OHKyn GSH-3OHKyn

3-Hydroxy-DL-kynurenine (100 mg, 0.44 mmol) was dissolved in argon-gassed (~20 min) Na_2CO_3-$NaHCO_3$ buffer (100 mL, 25 mM, pH 9.5). GSH (500 mg, 1.62 mmol) was added to the light yellow solution and the solution was gassed with argon (~20 min), sealed with parafilm and incubated in the dark at 37°C with shaking. The progress of the reaction was monitored as described above for GSH-Kyn. Another portion of GSH (100 mg, 0.32 mmol) was added after 24 h and the pH was readjusted to 9.5 by dropwise addition of 1 M NaOH.

After 72 h, the light yellow solution was worked up and purified, as described above for GSH-Kyn, to obtain GSH-3OHKyn (102 mg, 44%, R_f 0.28 (BAW), R_f 0.87 (20% CH_3CN/H_2O, v/v)) as a ~1:1 mixture of diastereomers.

Glutathionyl-3-hydroxykynurenine (GSH-3OHKyn): $M+H^+$, 515.1520. Calculated for $C_{20}H_{27}N_4O_{10}S$: $M+H^+$, 515.1448; ν_{max}(KBr disc) 3500-2300 (br, zwitterionic NH_3^+, COO^-, NH_2, OH, with C-H superimposed), 1721 (br, C=O), 1670 (br, C=O), 1545, 1200 (br, C-O) cm^{-1}; ^1H NMR δ (CD_3OD) 7.20 (~0.5H, dd, *J* 1.3, 8.4, ArH-6), 7.19 (~0.5H, dd, *J* 1.3, 8.4, ArH-6), 6.70 (1H, br d, *J* ~7.5, ArH-4), 6.40 (1H, br dd, *J* ~7.5, 8.4, ArH-5), 4.63 (~0.5H, dd, *J* 4.7, 9.2, $SCH_2C\underline{H}$), 4.57 (~0.5H, dd, *J* 5.9, 8.0 $SCH_2C\underline{H}$), 3.90 (1H, t, *J* 6.7, $CH_2C\underline{H}COOH$), 3.82 (1H, s, $C\underline{H_2}COOH$), 3.81 (1H, s, $C\underline{H_2}COOH$), 3.76 (1H, m, H-2), 3.50 (1H, m, H-3), 3.25 (1H, m, H-3), 3.20 (~0.5H, dd, *J* 4.7, 14.2, $SC\underline{H_2}$), 3.10 (~0.5H, dd, *J* 5.9, 14.1, $SC\underline{H_2}$), 2.97 (~0.5H, dd, *J* 8.0, 14.1, $SC\underline{H_2}$), 2.80 (~0.5H, dd, *J* 9.2, 14.2, $SC\underline{H_2}$), 2.47 (2H, t, *J* 7.0, $COC\underline{H_2}CH_2$), 2.10 (2H, m, $COCH_2C\underline{H_2}$); ^{13}C NMR δ (CD_3OD) 200.2 (CO-4), 200.1 (CO-4), 175.9 (CO-1), 175.9 (C-1), 174.5 ($NHCOCH_2$), 174.4 ($NHCOCH_2$), 172.9 ($CHCONH$), 172.8 ($CHCONH$), 172.6 (CH_2COOH), 171.7 ($CHCOOH$), 146.3 (ArC-3), 142.0 (ArC-2), 122.4 (ArC-6), 118.4 (ArC-1), 118.0 (ArC-4), 115.9 (ArC-5), 54.6 (SCH_2CH), 53.8 (SCH_2CH), 53.7 ($CH_2CHCOOH$), 43.3 (C-2), 42.8 (C-2), 42.6 (C-3), 42.4 (C-3), 41.8 (CH_2COOH), 34.5 (SCH_2), 34.5 (SCH_2), 32.4 ($COCH_2CH_2$), 27.1 ($COCH_2CH_2$), 27.0 ($COCH_2CH_2$); ES-MS/MS *m/z* 515.1 ($M+H^+$, 32%), 497.2 ($M+H^+ - H_2O$, 5%), 440.1 ($M+H^+$ - glycine, 45%), 386.1 ($M+H^+$ - glutamic acid, 32%), 368.1 ($M+H^+$ - glutamic acid - H_2O, 100%), 259.0 (97%), 208.1 ($M+H^+$ - GSH, 20%), 190.1 (18%), 179.1 (41%). λ_{max} 256 and 356 nm and maximum fluorescence at λ_{ex} 350 / λ_{em} 475 nm.

4.4.12 Synthesis of 4-oxo-1,2,3,4-tetrahydroquinoline-2-carboxylic acid (Kyn yellow)

(modified method of Tokuyama *et al.*[348])

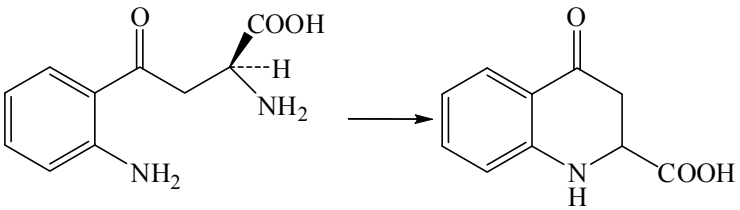

Kyn Kyn yellow

DL-Kynurenine sulphate salt (200 mg, 0.64 mmol) was heated to reflux in aqueous $NaHCO_3$ (50 mL, 0.49 M, pH ~9) under argon for 20 h. The progress of the reaction was monitored by TLC of normal (BAW) and reversed (20% CH_3CN/H_2O, v/v) phase. The orange solution was

cooled to RT, the pH adjusted to ~14 by dropwise addition of 1 M NaOH and extracted with diethyl ether (3 x 50 mL). The combined organic layers were discarded. The remaining basic aqueous layer was acidified to pH 2 by dropwise addition of aqueous HCl (10%, v/v) and extracted with diethyl ether (7 x 50 mL). The combined organic layers were washed with water (2 x 25 mL), dried with $MgSO_4$ and evaporated to dryness. The orange residue was purified by preparative RP-HPLC to afford Kyn yellow (32 mg, 26%, R_f 0.85 (BAW), R_f 0.61 (20% CH_3CN/H_2O, v/v)) as a yellow-orange solid. The spectral data were in agreement with the literature.[336,347]

4-Oxo-1,2,3,4-tetrahydroquinoline-2-carboxylic acid (Kyn yellow): $M+H^+$, 192.0651. Calculated for $C_{10}H_{10}NO_3$: $M+H^+$, 192.0661; ν_{max}(KBr disc) 3500-2300 (br, NH, OH, with C-H superimposed), 1695 (C=O), 1655 (C=O), 1618, 1283 (C-O), 760 (out-of-plane aromatic C-H bend) cm^{-1}; ^1H NMR δ (acetone-d_6) 7.66 (1H, dd, *J* 1.5, 7.9, H-5), 7.30 (1H, ddd, *J* 1.5, 7.4, 8.0, H-7), 6.96 (1H, br d, *J* ~8.0, H-8), 6.67 (1H, ddd, *J* 0.7, 7.4, 7.9, H-6), 6.20 (1H, s, N-H), 4.35 (1H, dd, *J* 5.5, 8.7, H-2), 2.90 (1H, dd, J 5.5, 16.2, H-3), 2.80 (1H, dd, *J* 8.7, 16.2, H-3), 1.40 (1H, s, COOH); ^{13}C NMR δ (acetone-d_6) 191.6 (CO-4), 173.0 (COOH), 152.1 (C-8a), 135.8 (C-7), 127.4 (C-5), 119.5 (C-4a), 118.1 (C-6), 117.1 (C-8), 55.1 (C-2), 40.58 (C-3); ES-MS/MS *m/z* 192.2 ($M+H^+$, 24%), 174.1 ($M+H^+$ - H_2O, 32%), 164.0 ($M+H^+$ - CO, 53%), 146.1 ($M+H^+$ - HCOOH, 100%), 132.1 (14%), 94.0 (22%). λ_{max} 260 and 378 nm and maximum fluorescence at λ_{ex} 310 / 392 and λ_{em} 400 / 513 nm.

4.4.13 Synthesis of 8-hydroxy-4-oxo-1,2,3,4-tetrahydroquinoline-2-carboxylic acid (3OHKyn yellow)

4.4.13.1 Method 1 (modified method of Tokuyama *et al.*[348])

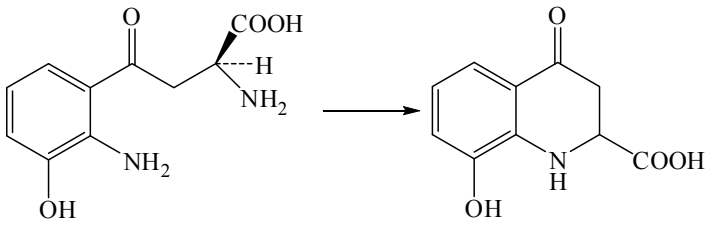

3OHKyn 3OHKyn yellow

3-Hydroxy-DL-kynurenine (20.4 mg, 0.09 mmol) was heated to reflux with aqueous $NaHCO_3$ (10 mL, 0.49 M) under argon for 20 h. The progress of the reaction was monitored by normal phase TLC (BAW). The orange reaction mixture was worked up and purified, as described

above for Kyn yellow, to afford 3OHKyn yellow (4.1 mg, 22%, R_f 0.78 (BAW)) as a yellow solid along with 4-(3-hydroxy-2-aminophenyl)-4-oxobut-2-enoic acid (52) (2.4 mg, 13%, R_f 0.81 (BAW)) and a trace amount of xanthurenic acid as yellow solids. The spectral data of 3OHKyn yellow were in agreement with the literature.[336]

8-Hydroxy-4-oxo-1,2,3,4-tetrahydroquinoline-2-carboxylic acid (3OHKyn yellow): $M+H^+$, 208.0466. Calculated for $C_{10}H_{10}NO_4$: $M+H^+$, 208.0610; ν_{max}(KBr disc) 3500–2400 (br, NH, OH, with C-H superimposed), 1635 (C=O), 1605 (C=O), 1510, 1400, 1269, 1223 (C-O), 787 (out-of-plane aromatic C-H bend), 732 (out-of-plane aromatic C-H bend) cm^{-1}; ^1H NMR δ (acetone-d_6) 7.21 (1H, dd, *J* 1.3, 7.9, H-5), 6.82 (1H, dd, *J* 1.3, 7.9, H-7), 6.50 (1H, dd, *J* 7.9, 7.9, H-6), 4.20 (1H, dd, *J* 5.0, 10.5, H-2), 2.93 (1H, dd, *J* 5.0, 16.5, H-3), 2.80 (1H, dd, *J* 10.5, 16.5, H-3), ^{13}C NMR δ (acetone-d_6) 193.4 (CO-4), 173.6 (COOH), 143.8 (C-8), 141.1 (C-8), 117.3 (C-4), 116.7 (C-7), 115.7 (C-5), 115.1 (C-6), 54.3 (C-2), 39.1 (C-3); ES-MS/MS *m/z* 208.2 ($M+H^+$, 15%), 190.2 ($M+H^+ - H_2O$, 21%), 180.2 ($M+H^+$ - CO, 8%), 166.1 (50%), 162.1 ($M+H^+$ - HCOOH, 100%), 148.1 (3%), 138.1 (2%), 120.0 (12%), 110.1 (22%), 99.0 (6%). λ_{max} 277 and 383 nm and maximum fluorescence at λ_{ex} 370 / 392 and λ_{em} 457 / 547 nm.

4-(3-Hydroxy-2-aminophenyl)-4-oxobut-2-enoic acid (52): ^1H NMR δ (CD_3OD) 7.91 (1H, d, *J* 15.5, H-3), 7.32 (1H, dd, *J* 1.2, 8.3, ArH-6), 6.83 (1H, dd, *J* 1.2, 7.5, ArH-4), 6.73 (1H, d, *J* 15.5, H-2), 6.50 (1H, dd, *J* 7.5, 8.3, ArH-5); ES-MS/MS *m/z* 208.1 ($M+H^+$, 35%), 190.1 ($M+H^+ - H_2O$, 32%), 180.1 ($M+H^+$ - CO, 7%), 166.1 (34%), 162.1 ($M+H^+$ - HCOOH, 100%), 148.1 (5%), 138.0 (5%), 120.0 (8%), 110.0 (28%), 99.0 (12%). λ_{max} 272 and 386 nm.

Xanthurenic acid: $M+H^+$, 206.0448. Calculated for $C_{10}H_8NO_4$: $M+H^+$, 206.0453; ^1H NMR δ (CD_3OD) 7.67 (1H, br d, *J* ~8.0, H-5), 7.22 (1H, dd, *J* 8.0, 8.0, ArH-6), 7.10 (1H, br d, *J* ~8.0, ArH-7), 6.95 (1H, s, H-2); ES-MS/MS *m/z* 206.1 ($M+H^+$, 2%), 178.1 ($M+H^+$ - CO, 65%), 160.1 ($M+H^+$ - HCOOH, 22%), 132.1 ($M+H^+$ - HCOOH - CO, 100%), 104.1 (12%), 77.1 (8%). λ_{max} 244 and 344 nm and maximum fluorescence at λ_{ex} 340 / λ_{em} 455 nm.

4.4.13.2 Method 2 (Bunce *et al.*[349])

A suspension of 4-(3-hydroxy-2-nitrophenyl)-4-oxobut-2-enoic acid (7) (20.0 mg, 0.084 mmol), AcOH (2 mL) and iron (20 mg, 0.36 mmol, > 100 mesh) was heated to 115°C under argon. TLC of normal (BAW) and reversed (20% CH_3CN/H_2O, v/v) phase revealed multiple

spots including AHB. After 1 h, the reaction mixture was cooled and filtered through a plug of celite. The yellow solution was made basic (pH ~12) by dropwise addition of NaOH (1 M) and extracted with EtOAc (4 x ~5 mL). The aqueous layer was made acidic by dropwise addition of aqueous HCl (10%) and extracted with EtOAc (4 x ~10 mL). The organic layers were evaporated under reduced pressure and the crude light brown solids were analysed by LC-MS. AHB (*m/z* 210 ($M+H^+$)) was seen as a major reaction product in the acidic extract, while the basic extract showed multiple unknown side products. ^1H NMR and ES-MS data of the crude AHB were consistent with an authentic sample of AHB. Further purification was not conducted.

4.4.13.3 Method 3

A mixture of 4-(3-hydroxy-2-nitrophenyl)-4-oxobut-2-enoic acid (7) (30 mg, 0.13 mmol), EtOAc (2 mL) and $SnCl_2 \cdot 2H_2O$ (50 mg, 0.22 mmol) was stirred under argon at RT in the dark. Normal phase TLC (BAW and EtOAc/1% AcOH, v/v) revealed multiple spots. Once all the starting material was consumed (12 h), the orange reaction mixture was mixed with $NaHCO_3$ (5 mL, 0.5 M), extracted with EtOAc (5 x ~5 mL) and filtered. The aqueous layer was acidified to pH 2 with aqueous HCl (10%, v/v) and extracted with EtOAc (5 x ~10 mL). The organic layers were combined, washed with cold water (2 x 5 mL) and the organic solvent removed under vacuum. LC-MS of the crude orange residue obtained upon extraction of the acidic aqueous layer revealed AHB (*m/z* 210 ($M+H^+$)) as a major product and trace quantities of 4-(3-hydroxy-2-aminophenyl)-4-oxobut-2-enoic acid (52) (*m/z* 208 ($M+H^+$), while the organic residue obtained upon extraction of the basic aqueous layer revealed multiple unknown products. Further purification and characterisation was not conducted.

4.4.14 Synthesis of cysteinyl-3-hydroxykynurenine-*O*-β-D-glucoside (Cys-3OHKG)

4.4.14.1 Method 1

4.4.14.1.1 Synthesis of methyl 2-cysteinyl-4-(2-nitro-3-((2,3,4,5-tetra-*O*-acetyl-β-D-glucopyranosyl)oxyphenyl)-4-oxobutanoate (59)

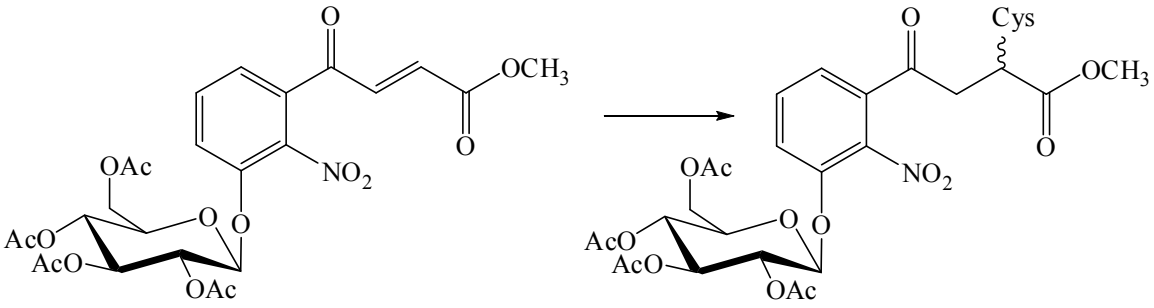

Methyl 4-(2-nitro-3-((2,3,4,5-tetra-*O*-acetyl-β-D-glucopyranosyl)oxyphenyl)-4-oxobut-2-enoate (11) (53 mg, 0.09 mmol) and Cys (14 mg, 0.12 mmol) were dissolved in aqueous CH_3CN (50%, v/v, 3 mL). The colourless reaction mixture was placed under argon and left to stir at RT. The reaction was monitored by TLC of normal phase (BAW). After 30 min the white suspension was evaporated to yield crude methyl 2-cysteinyl-4-(2-nitro-3-((2,3,4,5-tetra-*O*-acetyl-β-D-glucopyranosyl)oxyphenyl)-4-oxobutanoate (64 mg, R_f 0.43 (BAW)) as a white solid. Further purification was not conducted. ES-MS/MS *m/z* 703.0 ($M+H^+$, 80%), 582.3 ($M+H^+$ - Cys, 25%), 373.3 ($M+H^+$ - $Glu(OAc)_4$, 26%), 331.2 (47%), 271.2 (10%), 211.2 (8%), 169.0 (100%), 122.2 (10%), 109 (34%). Further characterisation was not conducted.

4.4.14.1.2 Synthesis of methyl 2-cysteinyl-4-(2-amino-3-((2,3,4,5-tetra-*O*-acetyl-β-D-glucopyranosyl)oxyphenyl)-4-oxobutanoate (60)

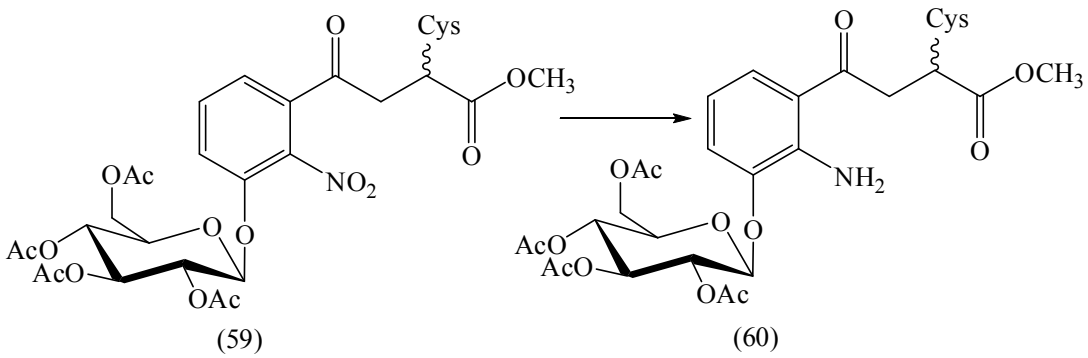

Methyl 2-cysteinyl-4-(2-nitro-3-((2,3,4,5-tetra-*O*-acetyl-β-D-glucopyranosyl)oxyphenyl)-4-oxobutanoate (59) (50 mg, 0.07 mmol) and Cys (9.0 mg, 0.07 mmol) were dissolved in aqueous MeOH (50%, v/v, 15 mL) under argon. $Na_2S_2O_4$ (124 mg, 0.71 mmol) was added in portions over 1 h. Additional Cys (4 mg, 0.03 mmol) was added after 30 and 60 min. The white suspension was monitored by TLC of normal phase (BAW). After 2 h, the white suspension was evaporated, dissolved in CH_3CN, filtered through a filter paper and evaporated to dryness. The pale yellow solid was purified by preparative RP-HPLC to obtain methyl 2-cysteinyl-4-(2-amino-3-((2,3,4,5-tetra-*O*-acetyl-β-D-glucopyranosyl)oxyphenyl)-4-oxobutanoate (18 mg, 38%, R_f 0.57 (BAW)) as a white solid. ES-MS/MS *m/z* 673.0 ($M+H^+$, 65%), 655.0 ($M+H^+$ - H_2O, 62%), 552.0 ($M+H^+$ - Cys, 7%), 331.0 (5%), 325.1 ($M+H^+$ - $OGlu(OAc)_4$, 8%), 211.0 (5%), 169.1 (100%), 109.0 (22%). Further characterisation was not conducted.

4.4.14.1.3 Synthesis of cysteinyl-3-hydroxykynurenine-*O*-β-D-glucoside (Cys-3OHKG)

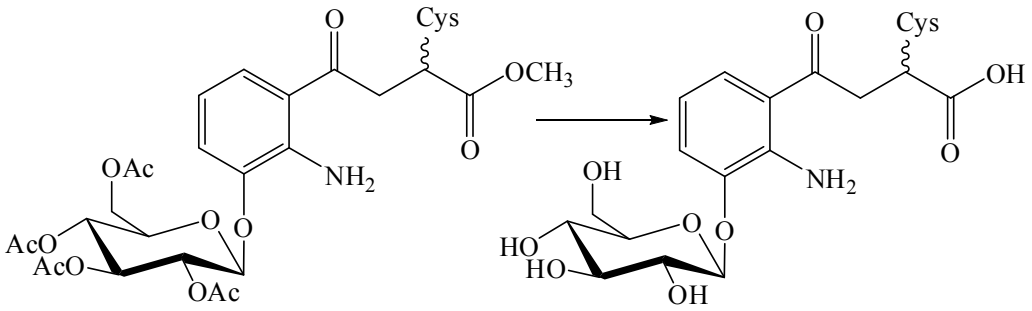

Methyl 2-cysteinyl-4-(2-amino-3-((2,3,4,5-tetra-*O*-acetyl-β-D-glucopyranosyl)oxyphenyl)-4-oxobutanoate (60) (10 mg, 0.02 mmol) was dissolved in argon-gassed (~20 min) aqueous NaOH (0.05 M, 1 mL). Cys (5.0 mg, 0.04 mmol) was added in portions over 1.5 h. Multiple spots (~ 6) were observed by normal (BAW) and reversed (H_2O) phase TLC. After 2 h, the pale yellow suspension was acidified to pH 6 using 1 M AcOH and analysed by LC-MS. Multiple peaks (~ 6) were observed by LC-MS, however none was the desired material. Hence the reaction mixture was discarded.

4.4.14.2 Method 2 (modified method of Garner *et al.*[86])

4.4.14.2.1 Synthesis of cysteinyl-3-hydroxykynurenine-*O*-β-D-glucoside (Cys-3OHKG)

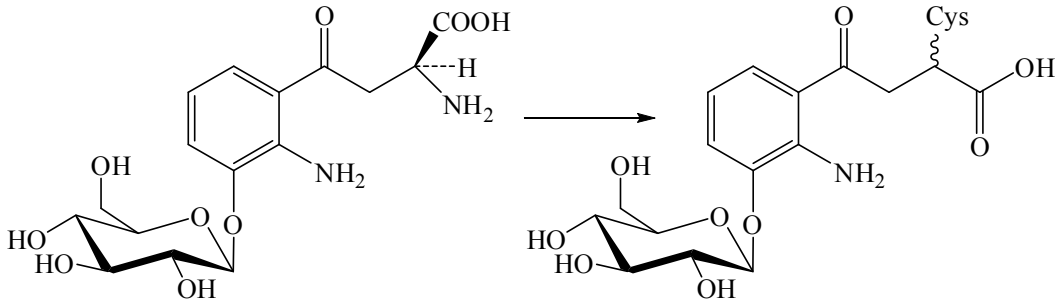

3-Hydroxykynurenine-*O*-β-D-glucoside (3OHKG) (20 mg, 0.06 mmol) was dissolved in argon-gassed (~20 min) Na_2CO_3-$NaHCO_3$ buffer (20 mL, 25 mM, pH 9.2). Cys (90 mg, 0.74 mmol) was added and the pH was readjusted to pH 9.2 by dropwise addition of 1 M NaOH. The light yellow solution was gassed with argon for ~20 min, sealed with parafilm and incubated in the dark at 37°C with shaking. The reaction was monitored by TLC (BAW). After 24 and 48 h another portion of Cys (90 mg, 0.74 mmol) was added to the yellow mixture and the pH was readjusted to 9.2 by the dropwise addition of 1 M NaOH. After 72 h, the light yellow reaction mixture was acidified to pH 6.5 by dropwise addition of 1 M AcOH and lyophilised. Purification by preparative RP-HPLC afforded Cys-3OHKG (9 mg, 36%, R_f 0.26 (BAW)) and 3OHKG (7 mg, 35%) as pale yellow solids.

Cysteinyl-3-hydroxykynurenine-*O*-β-D-glucoside (Cys-3OHKG): $M+H^+$, 491.1352. Calculated for $C_{19}H_{27}N_2O_{11}S$: $M+H^+$, 491.1335; ^1H NMR δ (D_2O) 7.55 (1H, d, *J*, 8.3, ArH-6), 7.24 (1H, d, *J* 7.9, ArH-4), 6.71 (1H, dd, *J* 7.9, 8.3, ArH-5), 4.94 (1H, d, *J* 7.4, H-1'), 3.93 (1H, m, $CH_2C\underline{H}$), 3.82 (1H, dd, *J* 1.1, 12.4, H-6'), 3.75 (1H, m, H-2), 3.60 (~0.5H, m, H-3), 3.57 (~0.5H, m, H-3), 3.49 (~0.5H, m, H-3), 3.45 (~0.5H, m, H-3), 3.67 (1H, dd, *J* 5.3, 12.4, H-6'), 3.53 (1H, m, H-3'), 3.52 (1H, m, H-2'), 3.48 (1H, m, H-5'), 3.42 (1H, m, H-4'), 3.32 (~0.5H, m, $C\underline{H_2}CH$), 3.25 (~0.5H, m, $C\underline{H_2}CH$), 3.18 (~0.5H, m, $C\underline{H_2}CH$), 3.08 (~0.5H, m, $C\underline{H_2}CH$); ^{13}C NMR δ (D_2O) 201.6 (CO-4), 201.4 (CO-4), 184.0 (CO-1), 172.5 (CO-Cys), 145.2 (ArC-3), 141.6 (ArC-2), 126.3 (ArC-6), 121.0 (ArC-4), 119.0 (ArC-1), 116.4 (ArC-5), 101.9 (C-1'), 76.5 (C-5'), 75.9 (C-2'), 73.2 (C-3'), 69.73 (C-4'), 60.8 (C-6'), 54.3 ($CH_2\underline{C}H$), 45.5 (C-2), 43.3 (C-2), 42.8 (C-3), 42.1 (C-3), 33.2 ($\underline{C}H_2CH$), 32.2 ($\underline{C}H_2CH$); ESI-MS/MS of *m/z* 491.1 ($M+H^+$, 8%), 473.1 ($M+H^+$ - H_2O, 52%), 370.1 ($M+H^+$ - Cys, 20%), 329.1 (8%),

311.1 ($M+H^+$ - OGlu, 88%), 272.1 (12%), 208.1 (67%), 202.0 (100%), 110.1 (28%). λ_{max} 262 and 365 nm and maximum fluorescence at λ_{ex} 337 / λ_{em} 438 nm.

4.4.15 Synthesis of cysteinyl-β-benzoylbutanoic acid (Cys-BAA)

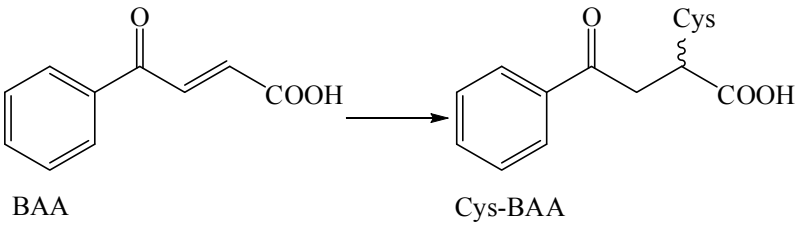

A mixture of β-benzoylacrylic acid (BAA) (307 mg, 1.74 mmol), Cys (268 mg, 2.2 mmol) and aqueous CH_3CN (50%, v/v, 27 mL) was placed under argon and left to stir at RT for 30 min. The reaction was monitored by TLC of normal (1:8.9:0.1 EtOAc/DCM/AcOH, v/v) and reversed phase (20% CH_3CN/H_2O, v/v). The white suspension was evaporated to dryness to yield crude Cys-BAA (565 mg, R_f 0.30 (1:9.9:0.1 EtOAc/DCM/AcOH, v/v), R_f 0.78 (20% CH_3CN/H_2O, v/v)) as a white solid. Further purification was not conducted.

Cysteinyl-β-benzoylbutanoic acid (Cys-BAA): ^{1}H NMR δ (D_2O) 8.02-7.97 (2H, m, ArH-6 and ArH-2), 7.68 (1H, ddd, *J* 1.0, 7.4, 7.4, ArH-4), 7.55 (2H, m, ArH-3 and ArH-5), 3.96 (1H, m, $SCH_2C\underline{H}$), 3.85 (1H, m, H-2), 3.70 (1H, m, H-3), 3.52 (1H, m, H-3), 3.37 (1H, m, $SC\underline{H_2}CH$), 3.16 (1H, m, $SC\underline{H_2}CH$); ES-MS/MS *m/z* 298.0 ($M+H^+$, 100%), 280.2 ($M+H^+$ - H_2O, 66%), 252.2 ($M+H^+$ - HCOOH, 16%), 209.2 ($M+H^+$ - 2 x CO_2H, 37%), 177.0 ($M+H^+$ - Cys, 50%), 159.1 (26%), 122.0 (95%), 105.0 (66%), 77.0 (45%).

4.4.16 Lens preparation and RP-HPLC purification

Eight normal human lenses of 24, 27, 42, 47, 65, 66, 83 and 88 years of age and two cataractous human lenses (60 and 70 years of age), assigned as Type III-IV according to the Pirie's classification system,[7] were analysed for all UV filters (Kyn, 3OHKyn, 3OHKG, AHBG, GSH-3OHKyn, AHBDG) and their metabolites (AHA, AHB, GSH-Kyn, GSH-3OHKyn, Kyn yellow, 3OHKyn yellow and Cys-3OHKG). In addition, known UV filters and Cys-3OHKG were extracted from a set of 10 dark cataractous lenses (assigned as Type III-IV according to the Pirie's classification system,[7] average age 66.6 years) and 15 individual cataractous lenses (assigned as Type I-IV). In all cases, lenses were separated into cortex and

nucleus using a 5 mm cork borer. The ends of each nuclear core were removed and added to the cortex. UV filters were extracted as described previously.[353] Briefly, the lens tissue was homogenised in 100% EtOH (v/v) (150 µL per nucleus, 350 µL per cortex). The homogenate was incubated at -20ºC for 60 min and centrifuged (13 000 g, 20 min, 4ºC). The supernatant was removed and stored at -20ºC while the pellet was reextracted in 80% aqueous EtOH (v/v). The supernatants were combined and lyophilised. The lens extracts were separated by RP-HPLC using a Microsorb (MV, 100 Å, 4.6 × 250 mm, C18) column. The following mobile phase system; buffer A (H_2O/0.1% TFA, v/v) and buffer B (80% CH_3CN/0.1% TFA, v/v), and the flow rate of 0.5 mL/min were kept constant. A mobile phase gradient was as follows: 0-5 min (0-50% buffer B), 5-50 min (50% buffer B), 50-55 min, (50-0% buffer B), 55-60 min (0% buffer B). The eluant was monitored at 360 nm. Fractions were collected at the known elution times of AHA (~37.5 min, ~26.5% CH_3CN/0.1% TFA), AHB (~36 min, ~20% CH_3CN/0.1% TFA), GSH-Kyn (~37.5 min, ~26.5% CH_3CN/0.1% TFA), GSH-3OHKyn (~36 min, ~20% CH_3CN/0.1% TFA), Kyn yellow (~40 min, ~32.5% CH_3CN/0.1% TFA), 3OHKyn yellow (~39 min, ~28% CH_3CN/0.1% TFA) and Cys-3OHKG (~31 min, ~17% CH_3CN/0.1% TFA).

4.4.17 Quantification of lens UV filters and their metabolites by LC-MS and RP-HPLC

The lens metabolites, AHA, AHB, GSH-Kyn, GSH-3OHKyn, Kyn yellow and 3OHKyn yellow, were analysed by LC-MS and detected in single-ion recording (SIR) mode on a Micromass Quattro micro in ESI positive mode. The settings were as follows LM1 16, HM1 15, cone 20 V, capillary 3.5 kV. Compounds were separated on a Phenomenex (Luna, 100 Å, 3 µm, 2.0 × 150 mm, C18(2)) column. The column was equilibrated in 95% buffer A (0.1% formic acid/H_2O, v/v) and 5% buffer B (80% CH_3CN/0.1% formic acid, v/v) at a flow rate of 0.1 mL/min. A mobile phase gradient was as follows: 0-5 min (5% buffer B), 5-50 min (5-50% buffer B), 50-55 min (50% buffer B), 55-60 min (50-5% buffer B), 60-75 min (5% buffer B). The following masses were used for SIR data acquisition: *m/z* 194.1 ($M+H^+$) (AHA), *m/z* 210.1 ($M+H^+$) (AHB), *m/z* 499.19 ($M+H^+$) (GSH-Kyn), *m/z* 515.19 ($M+H^+$) (GSH-3OHKyn), *m/z* 192.1 ($M+H^+$) (Kyn yellow) and *m/z* 208.1 ($M+H^+$) (3OHKyn yellow). These compounds were quantified using the standard addition method.[356]

3OHKG, AHBG, Kyn, GSH-3OHKG and Cys-3OHKG were quantified using RP-HPLC at 360 nm. They were separated on a Microsorb (MV, 100 Å, 4.6 × 250 mm, C18) column as described above. Standards were used as follows; synthetic 3OHKG for the quantification of

3OHKG and GSH-3OHKG, commercially available Kyn for Kyn, synthetic AHBG for AHBG and synthetic Cys-3OHKG for Cys-3OHKG.

4.4.18 Extraction efficiency of Kyn, 3OHKyn, 3OHKG, AHA, AHB, GSH-Kyn and GSH-3OHKyn from lens proteins

A known quantity (500 pmol/mg BLP) of 3OHKG, Kyn, 3OHKyn, GSH-Kyn, GSH-3OHKyn, AHA and AHB was separately homogenised with bovine lens tissue (10 mg) in 80% aqueous EtOH (150 μL, v/v) in duplicate. The homogenates were incubated at -20°C for 60 min and centrifuged (13 000 *g*, 20 min, 4°C). The supernatants were removed and stored at -20°C while the pellets were reextracted in 80% aqueous EtOH (150 μL, v/v). The supernatants were combined and lyophilised. The standard curves and extract analyses were performed by RP-HPLC on an Alltech (Prevail, 100 Å, 5 μm, 4.6 x 250 mm, C18) column fitted with a Phenomenex (Synergy Fusion, 100 Å, 4 μm, 2 x 4 mm, C18) guard column and the following mobile phase system; buffer A (water/0.05% TFA, v/v) and buffer B (80% acetonitrile/0.05% TFA, v/v). The flow rate of 1 mL/min was kept constant with a mobile phase gradient as follows: 0-5 min (5% buffer B), 5-18 min (5-70% buffer B), 18-23 min (70% buffer B), 23-28 min (70-5% buffer B), 28-35 min (5% buffer B). Detection was at 254 and 360 nm.

4.4.19 Stability of AHA, AHB, GSH-Kyn and GSH-3OHKyn under extraction, HPLC and pH 7.0 (aerobic) conditions

AHA was dissolved in 80% aqueous EtOH (v/v) to give a final concentration of 1.40 mM. The colourless solutions (3 × 4 mL) were sealed and incubated in the dark at 37°C with gentle shaking. Single aliquots were taken from each solution during 24 h and analysed by RP-HPLC. Separate incubations were repeated with AHB (0.25 mM), GSH-Kyn (0.40 mM) and GSH-3OHKyn (0.10 mM). Similar stability studies were carried out in H_2O/0.01% TFA (v/v) for 24 h (AHA, AHB, GSH-Kyn and GSH-3OHKyn) and chelex-treated PBS (pH 7.0) in the presence of atmospheric oxygen for 9 days (AHA, AHB, GSH-Kyn and GSH-3OHKyn).

4.4.20 Stability of AHB, GSH-Kyn and GSH-3OHKyn at pH 7.0 (anaerobic)

The colourless solution of AHB (0.25 mM), butylated hydroxytoluene (0.1 mM) and argon-degassed (5 cycles of freeze-thaw under argon and vacuum) chelex-treated PBS (3 x 4 mL) at pH 7.0 were incubated in the dark at 37°C with gentle shaking. From each solution single aliquots were taken during 208 h and analysed by RP-HPLC.

Separate solutions of AHB (0.25 mM), butylated hydroxytoluene (100 μM), ascorbic acid (2.0 mM) and argon degassed chelex-treated PBS (3 x 4 mL) at pH 7.0 were incubated in the dark at 37°C with gentle shaking. Single aliquots were taken during 9 days from each solution and analysed by RP-HPLC. Stability studies were repeated with GSH-Kyn and GSH-3OHKyn under similar conditions.

4.4.21 Stability of Cys-BAA

Cys-BAA was dissolved in argon-gassed (~20 min) ammonium acetate buffer (0.2 M, pH 4) to give a final concentration of 0.45 mM. The colourless solutions (2 × 4 mL) were sealed and incubated in the dark at 25°C. Single aliquots were taken from each solution after 0, 1, 2, 4, 6, 8, 20 and 25 h, and analysed by RP-HPLC. Separate incubations were repeated in AcOH (0.1 M, pH 2.5), NaH_2PO_4/Na_2HPO_4 buffer (0.2 M, pH 7.2), $NaHCO_3$/NaOH buffer (0.1 M, pH 9.5) and NaOH (0.1 M, pH 12.5). The aliquots taken from incubations at pH 9.5 and pH 12.5 were immediately acidified to pH 6 by 1 M AcOH. A separate incubation was repeated with Cys-BAA at pH 12.5 in the presence of excess of Cys (7.4 mg, 0.06 mmol).

4.4.22 Stability of Cys-3OHKG at pH 7.0

Cys-3OHKG was dissolved in chelex-treated PBS (pH 7.0) that was argon-gassed for ~20 min to give a final concentration of 0.20 mM. The colourless solutions (3 × 4 mL) were sealed under argon and incubated in the dark at 37°C with minimum shaking. Single aliquots (110 μL) were taken from each solution after 0, 1, 2, 3, 4, 6, 8, 11, 23, 32, 46, 57, 70, 94, 120, 134, 168, 192, 216 and 240 h, and analysed by RP-HPLC.

CHAPTER 5

MODIFICATION OF BOVINE LENS PROTEIN BY UV FILTERS AND RELATED METABOLITES

The overall aims of this chapter were to covalently modify bovine lens proteins with 3OHKG for subsequent UV light illumination studies, and determine the types of amino acids involved in those modifications. In addition, protein binding of AHB and AHA, as novel lens metabolites, was investigated.

5.1 Introduction

As explained in Chapter 1, the kynurenine-based human lens UV filters (*e.g.* Kyn, 3OHKyn and 3OHKG) are intrinsically unstable under physiological conditions and deaminate to α,β-unsaturated carbonyl compounds that can react with nucleophilic species, free or protein bound, in the human lens. These include amine and thiol nucleophiles such as His, Cys and Lys residues on human lens proteins (Scheme 5.1).[18,20]

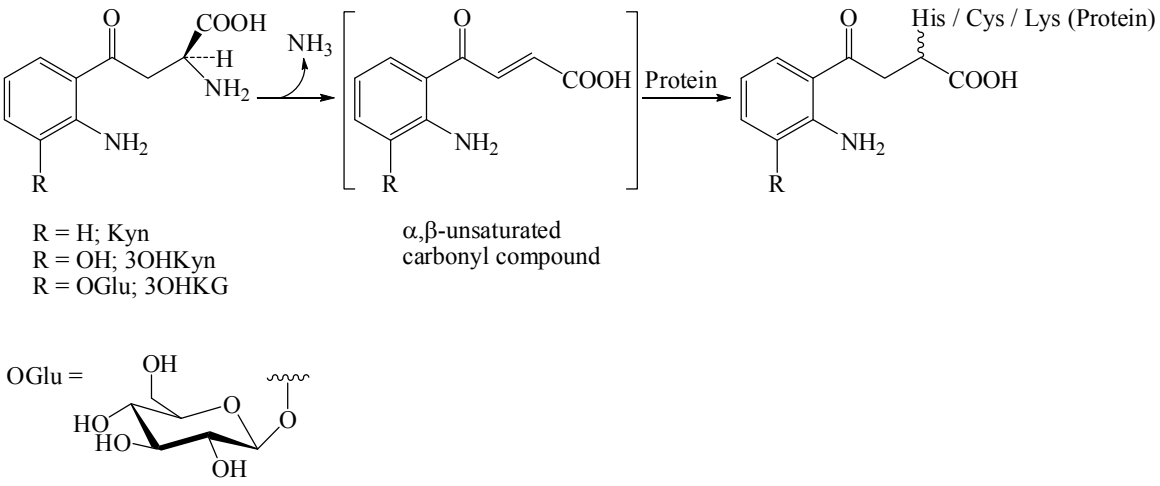

Scheme 5.1: Deamination of UV filters and binding to lens proteins.

In vivo studies suggest that Kyn and 3OHKyn react preferentially with Cys residues on human lens proteins.[20,176] The extent of protein modification by these compounds increases in an age dependent manner, with a significant increase after middle age in normal lenses.[18,20] A corresponding decrease in lenticular levels of free Kyn and 3OHKyn has also been observed, with these levels declining at a rate of approximately 12% per decade.[39] Additionally, recent

in vivo studies have revealed that 3OHKG binds to Cys residues of γS- and βB1-crystallins in older normal human lenses.[120]

Model studies with bovine lens proteins (BLP) have shown that Kyn and 3OHKyn bind preferentially with Cys residues at physiological pH.[20,175,383,384] At higher pH, binding to His and Lys becomes more significant.[20,175,383] The amino acid site(s) involved in 3OHKG binding to BLP *in vitro* have not been previously investigated.

The main aim of the studies reported here was to investigate the properties of 3OHKG-treated BLP and identify and quantify the types of amino acids (His, Cys and/or Lys) involved in covalent binding. For comparative purposes, and to undertake the study described in Chapter 6, BLP treated with Kyn, 3OHKyn and the novel lens metabolites, AHB and AHA, were also examined.

5.2 Results and Discussion

5.2.1 Modification of BLP with Kyn, 3OHKyn, 3OHKG, AHB and AHA

The modification of BLP with Kyn and 3OHKyn at pH 7.2 and 9.5 has been investigated previously.[175,247,383] pH 7.2 was chosen as it is physiologically relevant, and pH 9.5 was employed as these conditions are known to result in greater deamination of UV filters and increase the ease of nucleophilic attack by the amino or thiol groups compared to neutral pH.[100] BLP were used as a model for human lens proteins, since there is a large degree of sequence homology between bovine and human crystallins (~80%).[385] In addition, bovine lenses lack human UV filter compounds and are therefore an excellent model for examining the effects of exogenous UV filters.[80]

In this study, BLP were incubated with Kyn, 3OHKyn and 3OHKG. The Kyn- and 3OHKyn-modified lens proteins were used as positive controls and unmodified lens proteins as a negative control. In addition, lens proteins were incubated with AHB and AHA. As AHB and AHA lack the side chain amino group, it was of interest to determine if they could still bind to the proteins. This study would therefore ascertain the relative importance of the aromatic group and the α,β-unsaturated carbonyl moiety in protein binding.

Following the conditions of previous studies,[18,247] BLP (10 mg/mL) and each UV filter (2 mg/mL) were dissolved in argon-gassed Na_2HPO_4/NaH_2PO_4 buffer at pH 7.2 or $Na_2CO_3/NaHCO_3$ buffer at pH 9.5. As an antibacterial agent, chloroform was added and the reaction vials were sealed, wrapped in foil and incubated in the dark at 37°C. Reactions at pH 7.2 were conducted for 14 days for 3OHKG and 48 h for 3OHKyn, while the reactions at pH 9.5 were conducted for 48 h for Kyn, 3OHKyn and 3OHKG. The reaction with Kyn under physiological conditions was not investigated. The 3OHKyn reaction at physiological pH was carried out for 48 h due to the known instability of 3OHKyn on prolonged incubation.[20] Despite their lack of α-amino group on the side chain, for consistency, basic conditions were also used for AHB and AHA. AHB and AHA were incubated with BLP for 48 h under both conditions examined (pH 7.2 and 9.5).

Kyn, 3OHKyn, 3OHKG and AHB reaction mixtures changed in colour from colourless or pale yellow to intense yellow and red-brown upon incubation (Figure 5.1). Most of the colour diffused into the buffer during subsequent dialysis, while only 3OHKyn (pH 7.2 and 9.5) and AHB (pH 9.5) treated BLP stayed highly coloured (Figure 5.2).

Figure 5.1: The reaction mixtures of BLP treated with the UV filters before dialysis. 3OHKG at pH 9.5 and 7.2, 3OHKyn at pH 9.5 and 7.2, AHA at pH 9.5 and 7.2, and AHB at pH 9.5 and 7.2, from left to right.

Figure 5.2: Lyophilised UV filter-treated BLP after dialysis. 3OHKG at pH 9.5 and 7.2, 3OHKyn at pH 9.5 and 7.2, AHA at pH 9.5 and 7.2, and AHB at pH 9.5 and 7.2, from left to right.

5.2.2 Characterisation of UV filter-treated BLP by UV-vis absorbance and fluorescence

All of the BLP samples that had been treated with the UV filters were characterised by UV-vis and 3-D fluorescence spectroscopy after dialysis (Table 5.1). Unmodified BLP was analysed as a negative control. Unmodified and treated proteins were dissolved in 6 M guanidine hydrochloride at pH ~5.5. Guanidine hydrochloride has an absorption maximum at 245 nm and fluorescence maxima at λ_{ex} 315 / λ_{em} 366 nm (possibly due to impurities). This did not interfere with the absorbance and fluorescence measurements of the protein samples.

Table 5.1: Absorbance and fluorescence data for UV filter-treated BLP in 6 M guanidine hydrochloride (~2 mg/mL protein). N/D; not determined.

BLP modification	Absorbance (λ_{max}, nm)		Fluorescence ($\lambda_{ex}/\lambda_{em}$, nm)	
	pH 7.2	pH 9.5	pH 7.2	pH 9.5
Kyn	N/D	363	N/D	350/470, 390/472
3OHKyn	367, 440	367, 440	345/490, 392/505	350/515, 390/512
3OHKG	366	366	390/485	355/485, 390/485
AHA	364	364	385/480	385/485
AHB	328, 398, 440	328, 398, 440	382/475	390/490

The Kyn and 3OHKyn-treated BLP exhibited similar absorbance and fluorescence profiles to those reported previously.[18,20] The absorbance maxima of the modified BLP at 363, 367 and 366 nm were consistent with those of Kyn, 3OHKyn and 3OHKG, respectively (Table 5.1). An absorbance at 440 nm was also observed for 3OHKyn-treated lens proteins. Despite attempts to remove oxygen by gassing the solutions with argon, the species most likely to give rise to this peak are the oxidative products of 3OHKyn, which have absorption maxima at ~440 nm.[201,203,214] It is known that *o*-aminophenols are readily oxidised to quinone imines even in the presence of low levels of oxygen and that such oxidation occurs at a greater rate under basic conditions than at physiological pH.[205] BLP treated with Kyn and 3OHKG exhibited two similar fluorescence maxima with excitation at 350-355 and 390 nm, and emission at 470-485 nm. The characteristic fluorescence of Cys-Kyn (λ_{ex} 410 and λ_{em} 490 nm) and Cys-3OHKG (λ_{ex} 337 and λ_{em} 438 nm) were not seen in any of the samples at either pH examined. The fluorescence profile of 3OHKyn-treated BLP varied depending on the pH during the incubation. This may be due to the presence of fluorophores whose formation is

pH dependent. Some of the observed fluorophores may be 3OHKyn protein-bound adducts (*e.g.* Cys-3OHKyn, λ_{ex} 340 and 405, and λ_{em} 520 and 475 nm) and oxidised 3OHKyn protein-bound adducts (*e.g.* benzimidazole and benzoxazolone adducts, λ_{ex} 390 and λ_{em} 490 nm).[214,215] Similar fluorescence profiles are found in aged lenses, *i.e.* λ_{ex} 340-360 and λ_{em} 420-440 nm, and cataractous human lenses, *i.e.* λ_{ex} 420-435 and λ_{em} 500-520 nm.[103]

BLP treated with AHA showed AHA-like absorbance and fluorescence, which was surprising given the fact that AHA does not form an α,β-unsaturated carbonyl or reactive quinone imines that can bind to lens proteins. The UV-vis spectrum of lens proteins treated with AHB, at both pH values, showed three main wavelength maxima centered at 328, 398 and 440 nm. No distinct absorbance or fluorescence was observed for the free AHB (λ_{max} 369, λ_{ex} 346 and λ_{em} 435 nm). Similarly to 3OHKyn-treated BLP, the characteristic absorbance of higher wavelengths might be due to the presence of compounds arising from the oxidation of AHB (*e.g.* xanthommatin-like compounds, Section 4.2.7). The fluorescence profile of AHB-treated BLP seemed to be pH dependent, which resembles that of 3OHKyn-treated BLP.

5.2.3 RP-HPLC analysis of modified BLP

In previous studies the major sites of protein modification by Kyn and 3OHKyn at both physiological and basic pH were determined by acid hydrolysis and comparison to authentic standards of Kyn- and 3OHKyn-amino acid adducts, respectively.[18,20,177,384] Therefore, to quantify the amount of protein-bound 3OHKG and determine the amino acid residues it was bound to, acid hydrolysis of the 3OHKG-treated BLP was conducted. This resulted in the formation of 3OHKyn amino acids adducts, as the glucose moiety of 3OHKG is hydrolysed under acidic conditions (Scheme 5.2). In a similar manner, Kyn- and 3OHKyn-treated BLP were hydrolysed to free amino acid adducts of Kyn and 3OHKyn, respectively (Scheme 5.2). In order to quantify the extent of protein modification, authentic synthetic standards of the expected 3OHKyn amino acid adducts, His-3OHKyn, Lys-3OHKyn and Cys-3OHKyn, were synthesised. Quantification of the Kyn amino acid adducts in the modified lens proteins was conducted by the use of Kyn amino acid adducts.

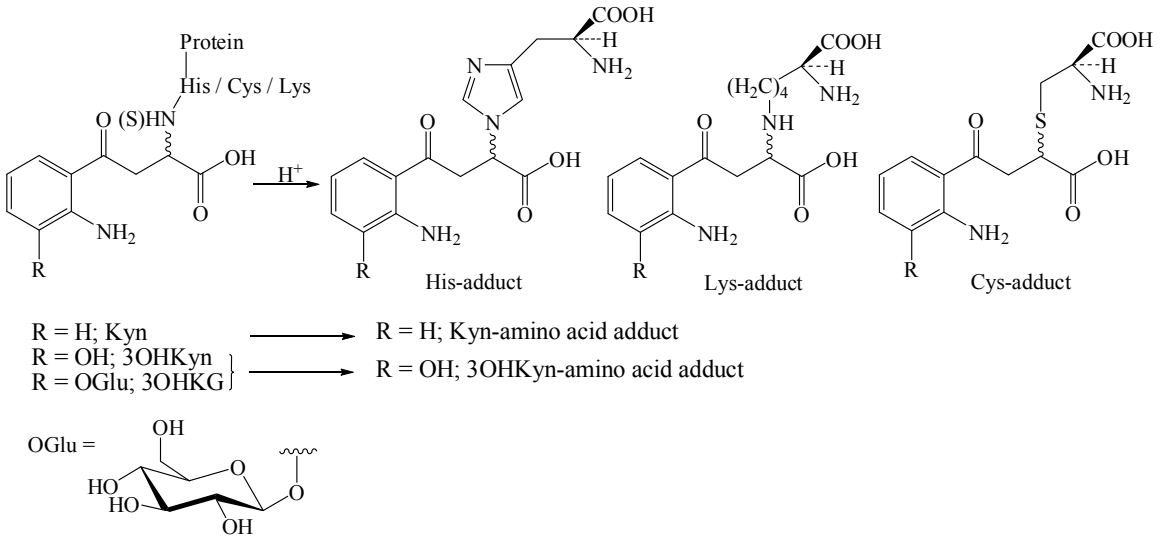

Scheme 5.2: Acid hydrolysis of Kyn-, 3OHKyn- and 3OHKG-treated BLP, and recovery of Kyn-and 3OHKyn-amino acid adducts.

5.2.4 Synthesis of 3OHKyn amino acid adducts

5.2.4.1 Synthesis of *t*-Boc-His-, *t*-Boc-Lys- and Cys-3OHKyn

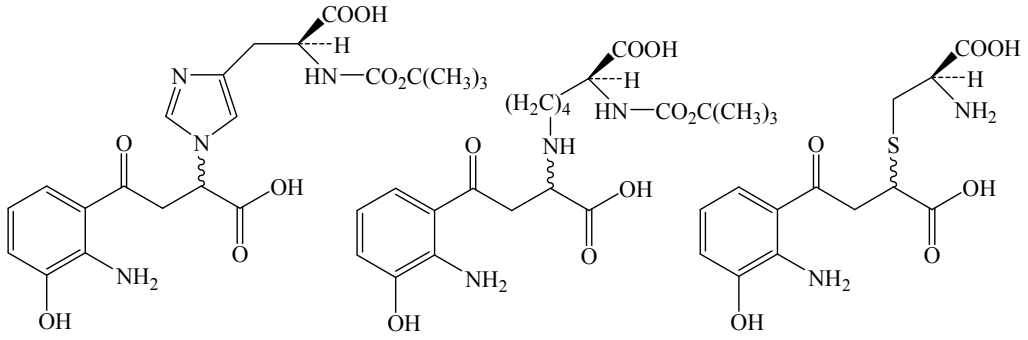

The 3OHKyn amino acid adducts were synthesised using the modified method of Vazquez *et al.*[18] for the synthesis of Kyn amino acid adducts. *N*-α-*t*-Boc protected His and Lys, and free Cys, in 10 mol equivalents were incubated with 3OHKyn at pH 9.5 under argon to limit auto-oxidation. The light yellow solutions were sealed and incubated at 37°C in the dark for 72 h. Basic conditions were used to promote deamination of the side chain and *t*-Boc protection was used to prevent reaction with the α-amino group of the amino acid.[18,20,100] No protection was needed for Cys as the thiol group is much more reactive than the α-amino group, resulting from a high energy non-bonding lone pair of electrons.[386] The reactions proceed *via* initial deamination of the amino acid side chain of 3OHKyn to give the α,β-unsaturated carbonyl compound, followed by the non-stereoselective Michael addition of the nucleophilic

amino or thiol group.[100,117] The reaction mechanism is summarised in Scheme 5.3, using formation of *t*-Boc-His adduct as an example.[18,117,177]

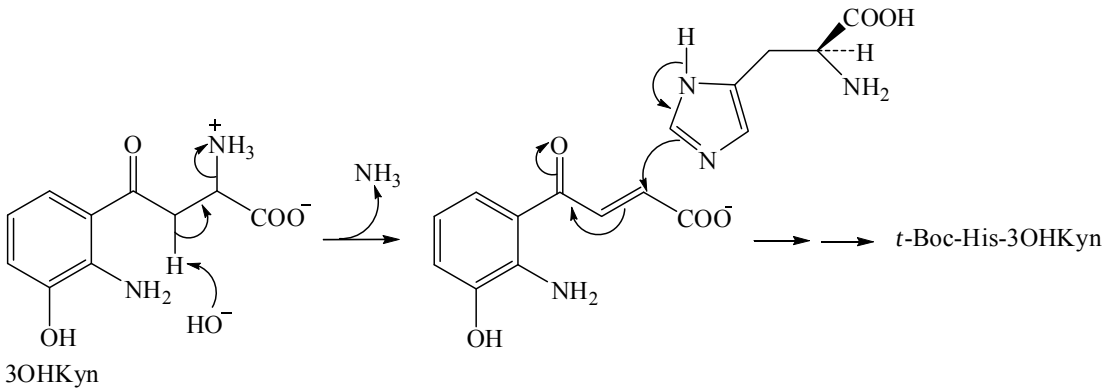

Scheme 5.3: Proposed mechanism for the formation of the *t*-Boc-His adduct of 3OHKyn.

As Cys can readily undergo oxidation, even in the presence of trace amounts of oxygen, ~10 mol equivalents of Cys were added after 24 and 48 h to the Cys containing reaction mixture and the pH was adjusted to pH 9.5 with 1 M NaOH. The progress of the reactions was monitored by TLC every 12 h, which revealed two major compounds, the amino acid adducts and the starting material. After 24 h of incubation each solution turned dark yellow. After 48 h, the His and Lys reaction solutions turned dark brown, whilst the Cys reaction solution stayed dark yellow in colour. As the reactions did not progress further towards the total usage of the starting material, after 72 h, the dark brown *t*-Boc-His and *t*-Boc-Lys reaction solutions and dark yellow Cys reaction solution were acidified to pH 6.5 by dropwise addition of 1 M AcOH and lyophilised. The crude solids were separately purified by RP-HPLC with the eluent monitored at 360 nm. *t*-Boc-His and *t*-Boc-Lys reaction mixtures showed 3 major peaks, while the Cys reaction mixture showed 2 major peaks with one of those peaks being the amino acid adduct in each case. The adducts eluted as double peaks (diastereomers), due to the addition of the chiral amino acids on either face of the double bond. The diastereomeric amino acid adducts were not resolved under the conditions employed and were therefore collected together. Yields of the *t*-Boc-His, *t*-Boc-Lys and Cys adducts were obtained in ~15%, 21% and 50%, respectively. In addition to the desired product, the *t*-Boc-His-3OHKyn reaction yielded unreacted *N*-α-*t*-Boc-L-His (12.3 mg, 2.2%, *m/z* 256 ($M+H^+$), λ_{max} 245 and 343 nm) and 3OHKyn (10 mg, 20%). In addition to *t*-Boc-Lys-3OHKyn, unreacted *N*-α-*t*-Boc-L-Lys (10.3 mg, 1.9%, *m/z* 247 ($M+H^+$), λ_{max} 245 and 345 nm) and 3OHKyn (4.3 mg, 8.6%) were recovered from the *t*-Boc-Lys-3OHKyn reaction mixture, while the Cys-3OHKyn reaction yielded the desired product and 3OHKyn (9 mg, 18%). The high recovery of 3OHKyn in each reaction is most likely due to its relatively low solubility under the reaction

conditions, which resulted in its partial precipitation and subsequent detection by RP-HPLC. In addition to some oxidation of 3OHKyn *via* the *o*-aminophenol moiety, this may contribute to low to moderate yields of amino acids adducts.

For all adducts, the aromatic region of the ^{1}H NMR spectra revealed three adjacent aromatic resonances with chemical shifts and coupling patterns consistent with 3OHKyn.[20] The aliphatic side chains contained characteristic signals for a CH_2-CH moiety with diastereotopic methylene protons at δ 3.4-3.9 and a methine proton at δ 3.9-5.5. Due to the overlap of diastereomers, the aliphatic side chain protons were seen as multiplets. The distinctive deshielded diastereotopic protons are indicative of covalent attachment of the amino acid residues at C-2.[20] The *t*-Boc protecting groups of His and Lys adducts were seen as isolated singlets at δ 1.36-1.42 with an integration of 9H for the methyl groups. The chemical shifts and coupling constants were consistent with the literature.[20,387]

The ES-MS/MS (positive mode) spectra of the *t*-Boc protected His- and Lys-3OHKyn, and the Cys-3OHKyn, revealed molecular ions at *m/z* 463 ($M+H^+$), *m/z* 454 ($M+H^+$) and *m/z* 329 ($M+H^+$), respectively, which indicated the formation of the desired amino acids adducts. The MS profile of both *t*-Boc-His- and *t*-Boc-Lys-3OHKyn exhibited a significant protonated molecular ion for His-3OHKyn (*m/z* 363) and Lys-3OHKyn (*m/z* 354), respectively, due to loss of the *t*-Boc group. In addition a protonated amino acid fragment ions at *m/z* 156, 147 and 122 were shown for His, Lys and Cys, respectively. All adducts showed characteristic fragment ions at *m/z* 208 (3OHKyn yellow), *m/z* 162 (decarboxylated 3OHKyn yellow) and *m/z* 110 (2-aminophenol) (Figure 5.3).[20] These data were consistent with a previous report.[20] These characteristic fragments can be used as markers for the detection of 3OHKyn and 3OHKG attachment *in vivo*.

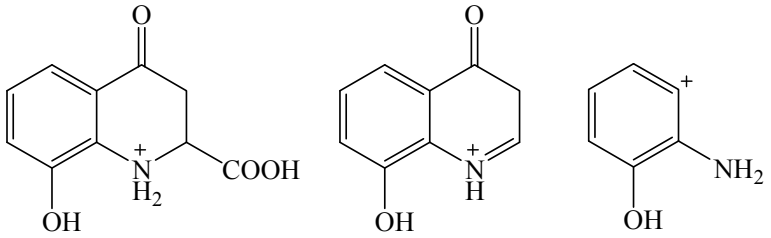

m/z 208 *m/z* 162 *m/z* 110

Figure 5.3: Characteristic fragments observed by ES-MS/MS analysis (positive mode) of 3OHKyn amino acid adducts.

The UV-vis spectra of the *t*-Boc protected amino acid adducts and Cys adduct were obtained in PBS at pH 7.0. All 3OHKyn-amino acid adducts displayed an absorbance at λ_{max} ~268-269 and 368-376 nm, which is similar to literature data and consistent with the increased absorbance at this wavelength in the aged and cataractous lenses.[20,103] A detailed fluorescence analysis of the *t*-Boc-3OHKyn amino acids adducts and Cys-3OHKyn has been reported previously.[20] In this study, Cys-3OHKyn exhibited maximum fluorescence intensities at excitation of 340 and 405 nm and emission of 520 and 475 nm, respectively. These data are consistent with a previous report.[20]

5.2.4.2 Synthesis of His- and Lys-3OHKyn

Hydrolysis of the *t*-Boc-His- and *t*-Boc-Lys-3OHKyn adducts was conducted in 6 M HCl at 37°C.[18] After 12 h, the pH was adjusted to ~6 and the yellow solutions were lyophilised. The crude products were separately purified by RP-HPLC to afford His- and Lys-3OHKyn in 97 and 98% yield, respectively (Figure 5.4).

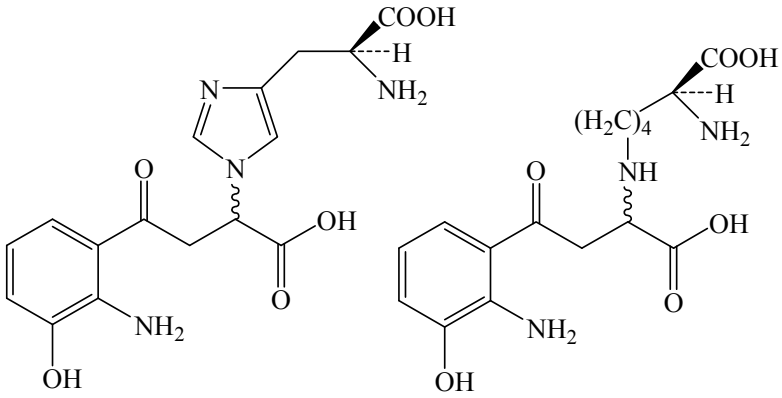

His-3OHKyn Lys-3OHKyn

Figure 5.4: Chemical structures of His- and Lys-3OHKyn.

The ^{1}H NMR spectra revealed three adjacent aromatic resonances consistent with the aromatic ring of 3OHKyn. Characteristic signals for a CH_2-CH moiety with diasterotopic methylene protons at δ 3.76-4.05 and a methine proton at δ 4.31-5.75 were seen. This was indicative of covalent attachment of the amino acid residues at C-2. Further analysis by COSY, HSQC and HMBC confirmed that the amino acid moieties were intact, with the chemical shifts and coupling constants consistent with the literature and those reported above.[20,387]

ES-MS/MS (positive mode) of His- and Lys-3OHKyn adducts revealed the molecular ions at *m/z* 363 ($M+H^+$) and *m/z* 354 ($M+H^+$), respectively, and protonated amino acid fragments at *m/z* 156 and *m/z* 147 for His and Lys amino acid moieties. These fragment ions are consistent with the formation of the desired amino acids adducts. Both adducts showed characteristic fragment ions at *m/z* 208 (3OHKyn yellow), *m/z* 162 (decarboxylated 3OHKyn yellow) and *m/z* 110 (2-aminophenol), consistent with the *t*-Boc protected amino acid adducts (Figure 5.3) and the literature.[20]

UV-vis spectra were obtained for the His- and Lys-3OHKyn adducts in PBS at pH 7.0. This information was important as it would assist in subsequent identification of 3OHKyn amino acid adducts from lens protein digests. The spectra had absorption maxima at 267-269 and 372 nm and were found to be essentially identical with the *t*-Boc protected amino acid adducts in this study and the literature.[20]

5.2.5 Acid hydrolysis of UV filter-treated and unmodified BLP

Samples of each of the UV filter-treated and unmodified BLP were separately subjected to acid hydrolysis in 6 M HCl under vacuum for 24 h at 110°C.[20] To minimise protein oxidation, proteins were hydrolysed in the presence of antioxidants (thioglycolic acid and phenol) and subsequently analysed by RP-HPLC with the eluent monitored at 360 nm.[20,256] The identity of amino acid adducts was confirmed by spiking the experimental samples with authentic synthetic samples and by ES-MS/MS. Kyn- and 3OHKyn-treated lens proteins, and unmodified lens proteins, were hydrolysed as the positive and negative controls, respectively. The acid hydrolysis detailed for each UV filter-treated BLP and unmodified BLP are discussed in detail below.

5.2.5.1 Untreated BLP

Unmodified BLP at both conditions examined (pH 7.2 and 9.5) were hydrolysed and chromatographed by RP-HPLC (Figure 5.5, A and B). Peaks of only low absorbance (< 5 absorbance units) were observed, which is consistent with the presence of only unmodified amino acids, as expected.

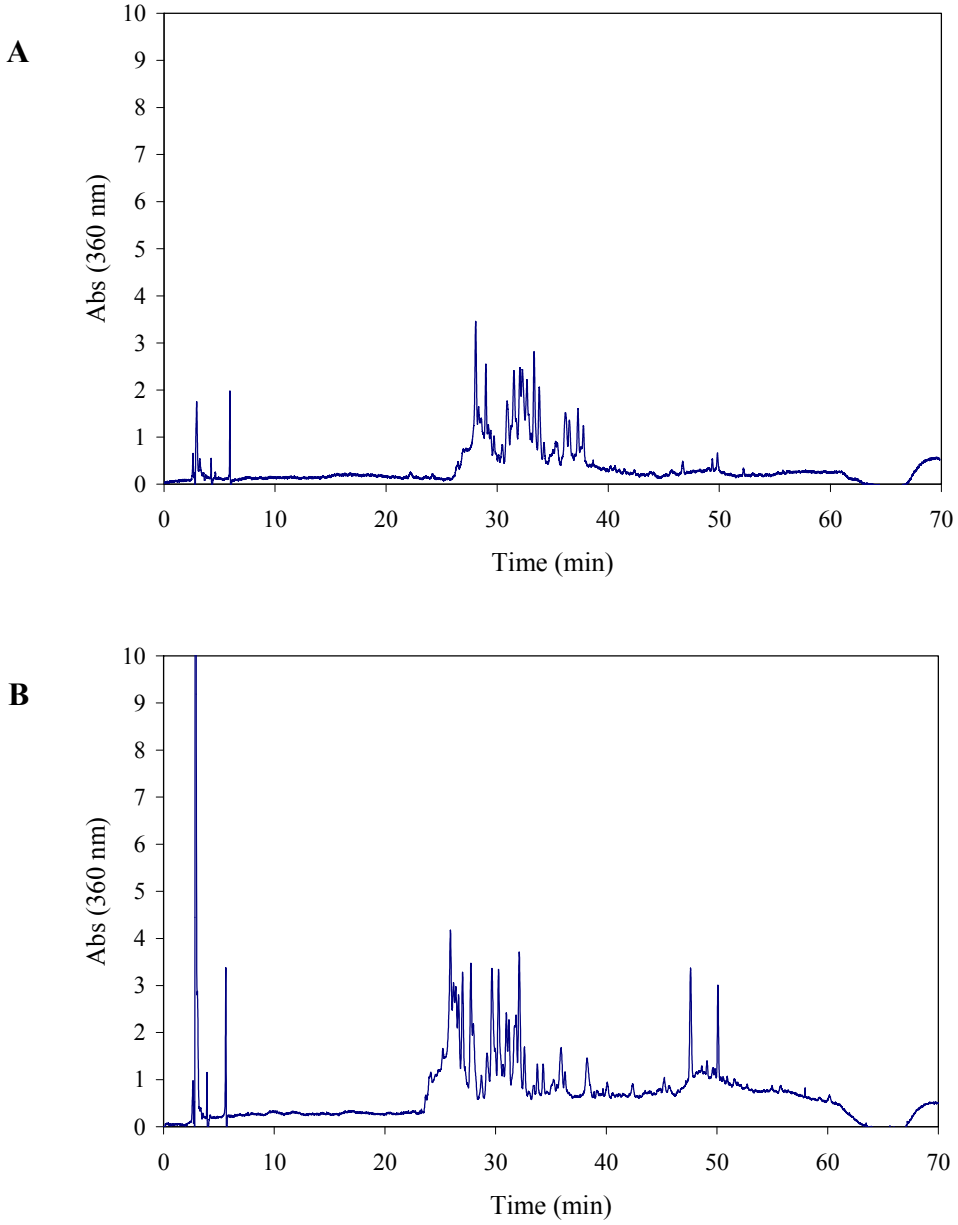

Figure 5.5: RP-HPLC profiles of acid-hydrolysed unmodified BLP. BLP incubated at pH 7.2 for 14 days (**A**); BLP incubated at pH 9.5 for 48 h (**B**).

5.2.5.2 Kyn-treated BLP

As Kyn-treated BLP were used only as a positive control for the 3OHKG-treated samples, BLP were only treated with Kyn at pH 9.5. RP-HPLC analysis of acid-hydrolysed Kyn-treated BLP showed 3 distinct peaks when monitored at 360 nm (Figure 5.6). This included a double peak at 30.1 min, which exhibited absorption maxima at 256 and 362 nm (Figure 5.6, peak 2). This is in agreement with data reported for Cys-Kyn.[18] The MS analysis (positive mode) of this peak revealed a prominent molecular ion at *m/z* 313 ($M+H^+$), corresponding to the mass of Cys-Kyn (312 Da). ES-MS/MS showed that this ion fragmented further to give

m/z 295 (loss of water), *m/z* 224 (loss of Cys side chain), *m/z* 192 (Kyn yellow), *m/z* 174 (loss of water from Kyn yellow), *m/z* 146 (decarboxylated Kyn yellow) and *m/z* 122 (Cys), which are all characteristic fragment ions of Cys-Kyn.[18] Quantification of this peak gave a value of 0.96 mol of Cys-Kyn/mol of protein, as determined from a Cys-Kyn standard. This is comparable to the data of Parker *et al*.[247] (0.86 mol of Cys-Kyn/mol of protein).

A small peak was also observed at a retention time of 18.3 min (Figure 5.6, peak 1). This peak had absorption maxima at 252 and 361 nm and a prominent molecular ion at *m/z* 338 ($M+H^+$), which further fragmented to *m/z* 203 (carboxylated Lys), *m/z* 192 (Kyn yellow), *m/z* 147 (Lys) and *m/z* 136 (2-aminoacetophenone). These fragment ions are all characteristics of Lys-Kyn.[18] As Lys-Kyn was only found in low amounts, it was not quantified in this study.

LC-MS analysis of the peak at 39.7 min (Figure 5.6, peak 3) showed absorption maxima at 252 and 362 nm and three distinct molecular ions at *m/z* 378 ($M+H^+$), *m/z* 306 ($M+H^+$) and *m/z* 284 ($M+H^+$). By ES-MS/MS analysis; the ion at *m/z* 378 ($M+H^+$) was further fragmented to *m/z* 247, *m/z* 219 and *m/z* 120; the ion at *m/z* 306 ($M+H^+$) was further fragmented to *m/z* 214, *m/z* 196 and *m/z* 115; and the ion at *m/z* 284 ($M+H^+$) was further fragmented to *m/z* 266, *m/z* 220, *m/z* 192, *m/z* 174, *m/z* 146, *m/z* 120 and *m/z* 94. Due to three molecular ions being present in this fraction, where some of them may account for oxidised amino acids and their derivatives or dipeptides, this fraction was not further investigated. No distinct peak corresponding to His-Kyn was detected by RP-HPLC with monitoring at 360 nm. Under similar conditions, Parker *et al*.[247] found His-Kyn to be present in the lowest concentration out of all three adducts observed (0.08 mol/mol of protein).

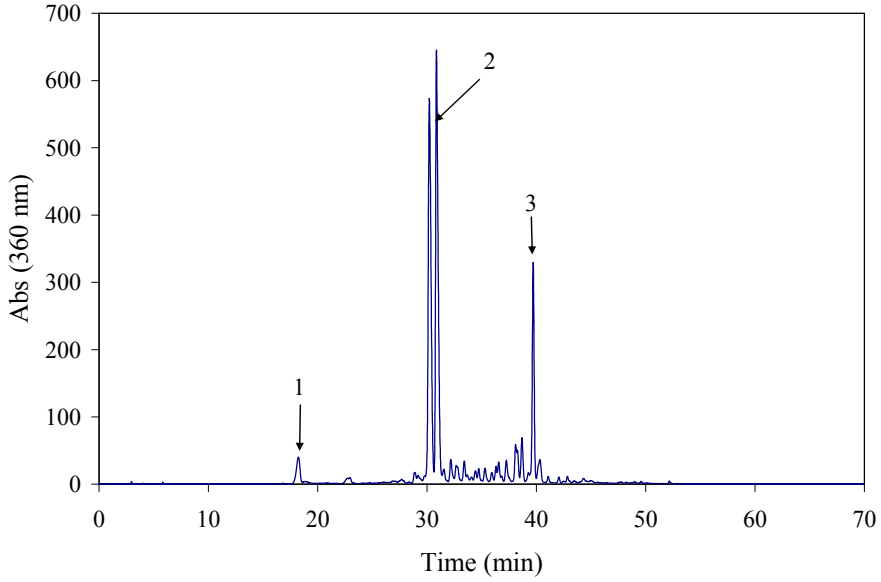

Figure 5.6: RP-HPLC profile of acid-hydrolysed Kyn-treated BLP at pH 9.5 for 48 h at 37°C. Lys-Kyn (1); diastereomers of Cys-Kyn (2, double peak); unidentified peak (3).

5.2.5.3 3OHKyn-treated BLP

Similarly to previous reports, RP-HPLC analysis of acid-hydrolysed 3OHKyn-treated BLP at pH 7.2 showed one distinct double peak, while acid-hydrolysed 3OHKyn-treated BLP at pH 9.5 showed 5 prominent peaks.[175] Both 3OHKyn-treated BLP at pH 7.2 and pH 9.5 showed a prominent double peak at ~26 min (Figure 5.7, peak 1 (A) and peak 2 (B)), that co-eluted with an authentic standard of Cys-3OHKyn. It showed absorption maxima at 268 and 368 nm, which is in agreement with authentic synthetic standards of Cys-3OHKyn.[20] ES-MS/MS of the prominent ion at *m/z* 329 ($M+H^+$) resulted in the detection of fragment ions with *m/z* 311 (loss of water), *m/z* 208 (3OHKyn yellow), *m/z* 190 (loss of water from 3OHKyn yellow), *m/z* 162 (decarboxylated 3OHKyn yellow), *m/z* 122 (Cys) and *m/z* 110 (2-aminophenol). This is in agreement with literature data reported on Cys-3OHKyn.[20] In comparison to pH 7.2, a greater extent of modification was observed at pH 9.5, suggesting that the initial deamination is a rate-limiting step in the BLP modification by 3OHKyn.[100] Cys-3OHKyn was found to be present at a level of 0.02 mol/mol protein at pH 7.2 and 0.05-0.64 (depending on the batch) mol/mol protein at pH 9.5 on the basis of a standard curve constructed using a synthetic standard of Cys-3OHKyn. Variations in the degree of 3OHKyn modification were observed between the batches of 3OHKyn-modified BLP at pH 9.5, possibly due to variations in the scale of the reactions (with either 100 or 300 mg of BLP).

The hydrolysate of BLP modified at pH 9.5 had a broad peak at 11.5 min that co-eluted with an authentic standard of Lys-3OHKyn and showed absorption maxima at 265 and 371 nm (Figure 5.7 (B), peak 1). ES-MS/MS showed a molecular ion at *m/z* 354 ($M+H^+$) that further fragmented to ions similar to those detected for Cys-3OHKyn (*i.e. m/z* 208 (3OHKyn yellow), *m/z* 162 (decarboxylated 3OHKyn yellow) and *m/z* 110 (2-aminophenol)) and an additional fragment ion at *m/z* 147 due to loss of the Lys moiety. These data are consistent with the presence of Lys-3OHKyn.[20] The concentration of this adduct was not determined as it coeluted with other compounds that absorbed at similar wavelengths. Under similar conditions, Lys-3OHKyn was identified by Korlimbinis *et al*.[175] as a major adduct.

No characteristic ions corresponding to the His adduct could be found at the known retention time of the authentic standard. This suggests that His modifications were either not present in the modified protein samples or were present at levels below the limits of instrument detection. Under similar conditions, Korlimbinis *et al*.[175] found His-3OHKyn to be present in the lowest abundance out of all three adducts observed.

Other distinct peaks in the RP-HPLC trace of 3OHKyn-treated protein at pH 9.5 were seen at 35.0 (peak 3) and 36.0 min (peak 4) (Figure 5.7, B). These exhibited absorption maxima at 249 and 323 nm, and 266 and 372 nm, respectively. ES-MS/MS analysis of peak 3 showed a molecular ion at *m/z* 378 ($M+H^+$), which fragmented to *m/z* 332, *m/z* 304, *m/z* 287, *m/z* 277, *m/z* 259 and *m/z* 187. Peak 4 displayed a molecular ion at *m/z* 300 ($M+H^+$), which fragmented to *m/z* 282 (loss of water), *m/z* 236 (loss of HCOOH), *m/z* 208 (3OHKyn yellow), *m/z* 190 (loss of water), *m/z* 162 (decarboxylated 3OHKyn yellow), *m/z* 136 and *m/z* 110 (2-aminophenol). Due to the low yields obtained, these compounds could not be identified further, even though, particularly for peak 4, a characteristic 3OHKyn fragmentation pattern on ES-MS/MS was observed. In this study no distinct oxidation products of 3OHKyn of molecular mass ≥ 400 Da were seen after hydrolysis. Perhaps prolonged incubations (> 48 h) would lead to protein binding of species formed upon oxidation of 3OHKyn. Oxidation could occur in the presence of trace amounts of oxygen that possibly remained in the reaction mixture after argon-degassing. The stability of 3OHKyn oxidation products is also questionable under the acidic conditions used for protein hydrolysis in this study. Recent studies, however, have shown that oxidation products of 3OHKyn can become bound to urinary and amniotic α-1-microglobulin extracellular proteins where, apart from the major Lys-3OHKyn adduct, Lys-hydroxanthommatin (*m/z* 555 ($M+H^+$)) was identified after acid hydrolysis in the absence of antioxidants.[388]

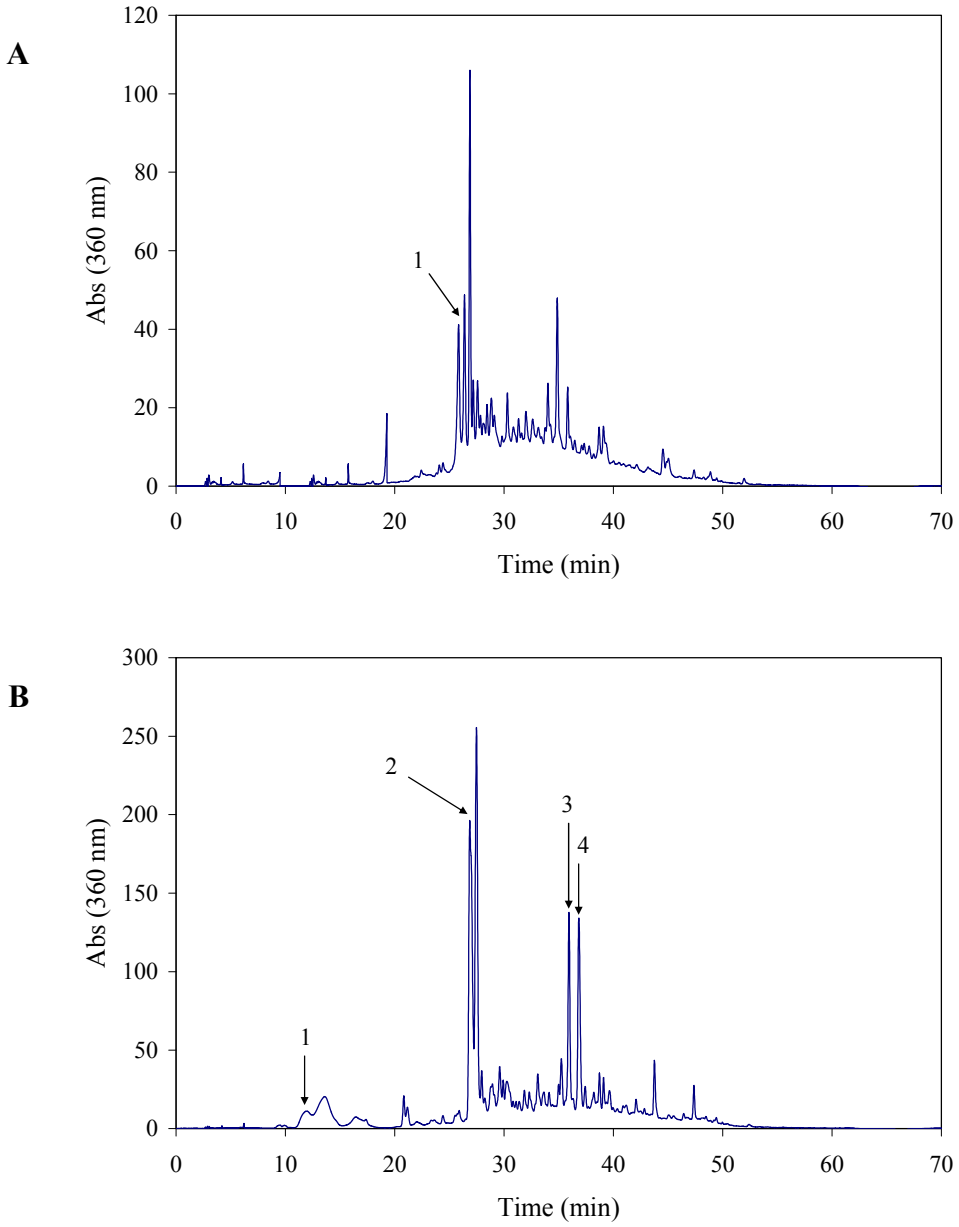

Figure 5.7: RP-HPLC profiles of acid-hydrolysed 3OHKyn-treated BLP at pH 7.2 (**A**) and pH 9.5 (**B**) for 48 h at 37°C. Lys-3OHKyn (1); diastereomers of Cys-3OHKyn (2); 35.0 min (3) and 36.0 min (4) peaks were unidentified.

5.2.5.4 3OHKG-treated BLP

RP-HPLC analysis of the hydrolysed 3OHKG-treated BLP with detection at 360 nm revealed that Cys residues were the main sites of protein modification at both pH 7.2 and 9.5 (Figure 5.8, A and B, peak 2). Peak 2 showed absorption maxima at 268 and 368 nm, which is in agreement with an authentic synthetic standard of Cys-3OHKyn.[20] ES-MS/MS analysis of the prominent ion at *m/z* 329 yielded data consistent with a previous report and data presented above.[20] Similarly to 3OHKyn modifications, this adduct was detected at higher concentration (as assessed by RP-HPLC) at pH 9.5 compared to pH 7.2, with this species being present at 0.26 mol/mol protein at pH 7.2 and 0.40-1.14 (depending on the batch) mol/mol protein at pH 9.5. Similarly to 3OHKyn modifications, variations in the degree of 3OHKG modification at pH 9.5 were possibly due to variations in the scale of the reactions (with either 100 or 300 mg of BLP).

RP-HPLC analysis of incubations carried out at both pH 7.2 and 9.5 revealed a broad peak at ~10 min that coeluted with an authentic standard of Lys-3OHKyn (Figure 5.8, A and B, peak 1). ES-MS/MS analysis showed a molecular ion at *m/z* 354 that further fragmented to ions similar to those detected for an authentic standard of Lys-3OHKyn (Section 5.2.4.2). Due to the coelution of this species with a number of other compounds that absorbed at similar wavelengths, this adduct was not quantified. Peaks 3 and 4 showed similar ES-MS/MS profiles to peaks 3 and 4 detected in hydrolysates of 3OHKyn-modified lens proteins (Section 5.2.5.3). These species were not characterised further, however their presence in both 3OHKyn- and 3OHKG-modified lens protein samples indicate that they are probably 3OHKyn derivatives.

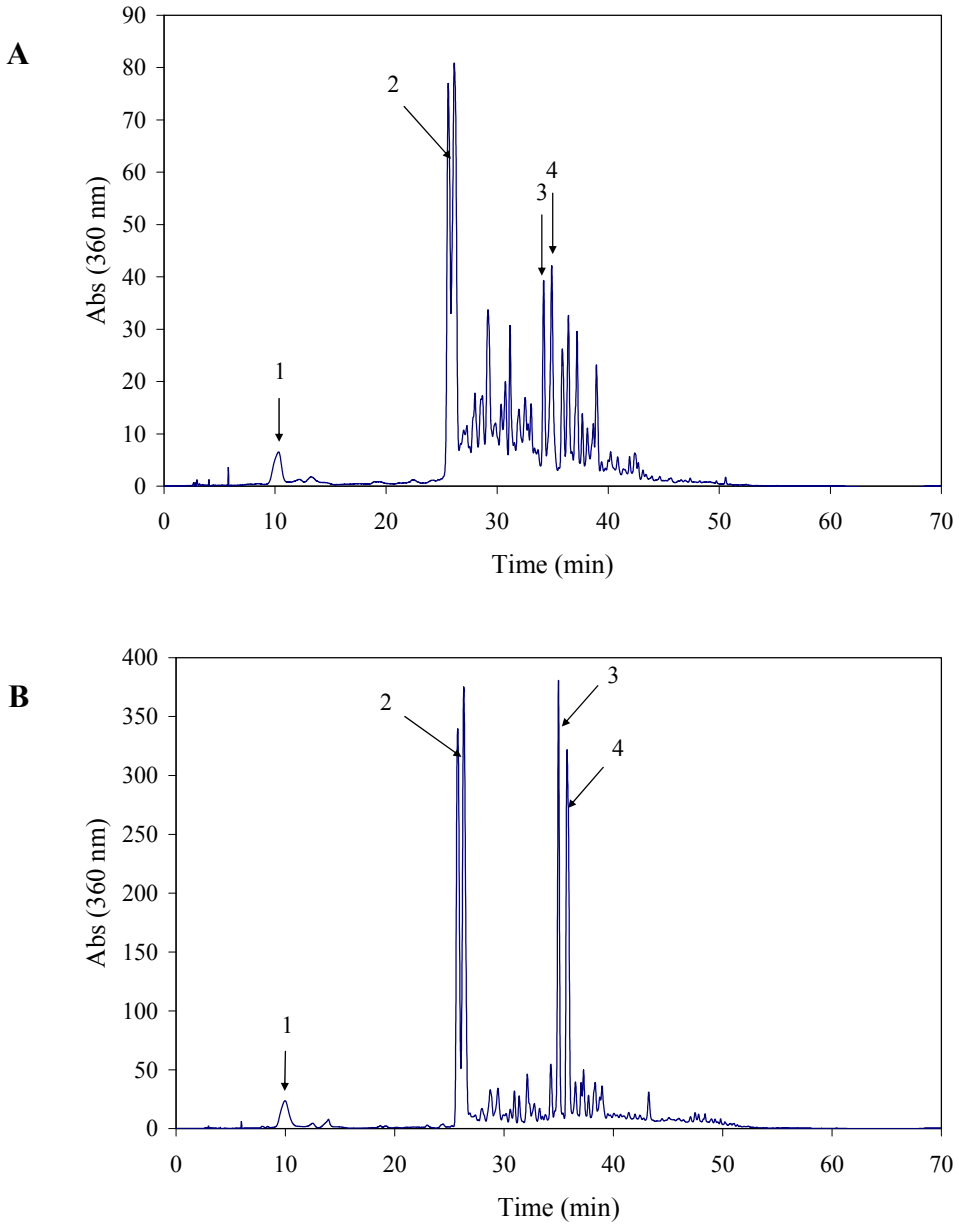

Figure 5.8: RP-HPLC profiles of acid-hydrolysed 3OHKG-treated BLP at pH 7.2 (**A**) for 14 days and pH 9.5 (**B**) for 48 h at 37°C. Lys-3OHKyn (1); diastereomers of Cys-3OHKyn (2); 35.0 min (3) and 36.0 min (4) peaks were unidentified.

5.2.5.5 AHB-treated BLP

RP-HPLC analysis of AHB-treated BLP after acid hydrolysis, with detection at 360 nm, revealed 4 prominent single peaks at both pH 7.2 and 9.5 (Figure 5.9, A and B). In contrast to pH 9.5 treatment, lower levels of these peaks were seen at pH 7.2.

A peak at ~31 min (Figure 5.9, peak 1) coeluted with an authentic standard of AHB. Spectral data (ES-MS/MS and absorbance) of peak 1 were identical to that of authentic AHB, as described in Chapter 4 (Section 4.2.3). On the basis of a standard curve constructed using a synthetic standard of AHB, AHB was found to be present at a level of 0.03 mol/mol protein at pH 7.2 and 0.09 mol/mol protein at pH 9.5. The peaks at 37.6 and 38.6 min (Figure 5.9, peaks 2 and 3), which exhibited absorbance at ~400 nm, were collected as highly coloured red-yellow solids. Upon drying both changed colour to brown, consistent with decomposition of this material on isolation and drying. The suggested decomposition of these products is supported by the ES-MS/MS data with more than one molecular ion identified for each peak. Peak 4 eluted at 39.5 min (Figure 5.9) with absorption maxima at 263 and 395 nm and a molecular ion at *m/z* 399, which fragmented to *m/z* 353, *m/z* 294, *m/z* 279 and *m/z* 240. This molecular ion was also observed as a decomposition product of AHB upon incubation at pH 7.0 (Section 4.2.7) and pH 9.5. The AHB stability at pH 9.5 is discussed later in this chapter (Section 5.2.8). Further identification of these peaks was not carried out.

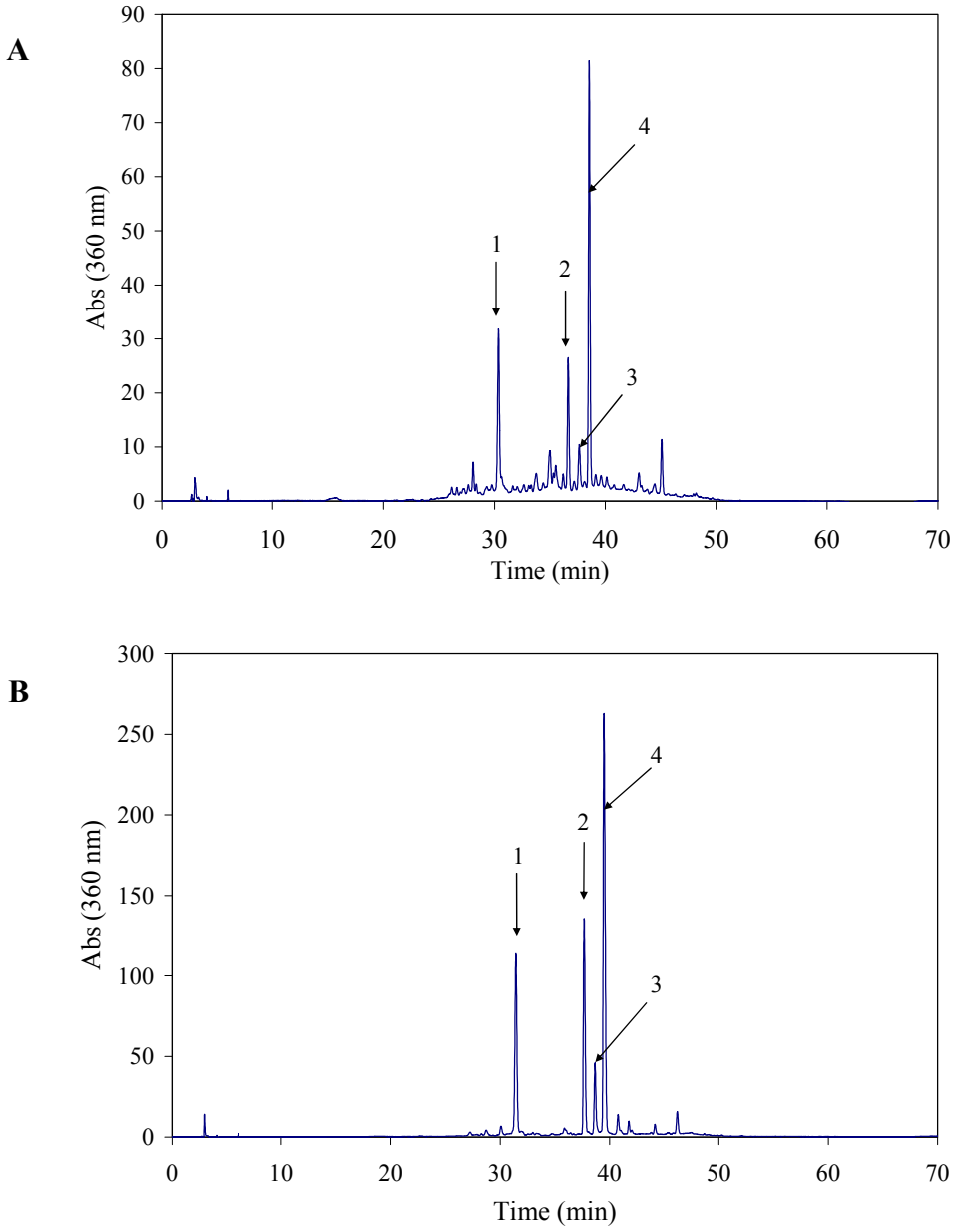

Figure 5.9: RP-HPLC profiles of acid-hydrolysed AHB-treated BLP at pH 7.2 (**A**) and pH 9.5 (**B**) for 48 h at 37°C. 31.4 min (1, AHB); 37.6 min (2); 38.6 min (3); 39.5 min (4).

5.2.5.6 AHA-treated BLP

A single peak with a retention time of 35.7 min was observed by RP-HPLC analysis of the hydrolysed AHA-treated BLP at both pH 7.2 and 9.5 with detection at 360 nm (Figure 5.10, A and B). This peak coeluted with an authentic standard of AHA. Spectral data (ES-MS/MS and absorbance) of this peak were identical to that of authentic AHA, as described in Chapter 4. On the basis of a standard curve constructed using a synthetic standard of AHA, AHA was found to be present at a level of 0.07 mol/mol protein at pH 7.2 and 0.11 mol/mol protein at pH 9.5.

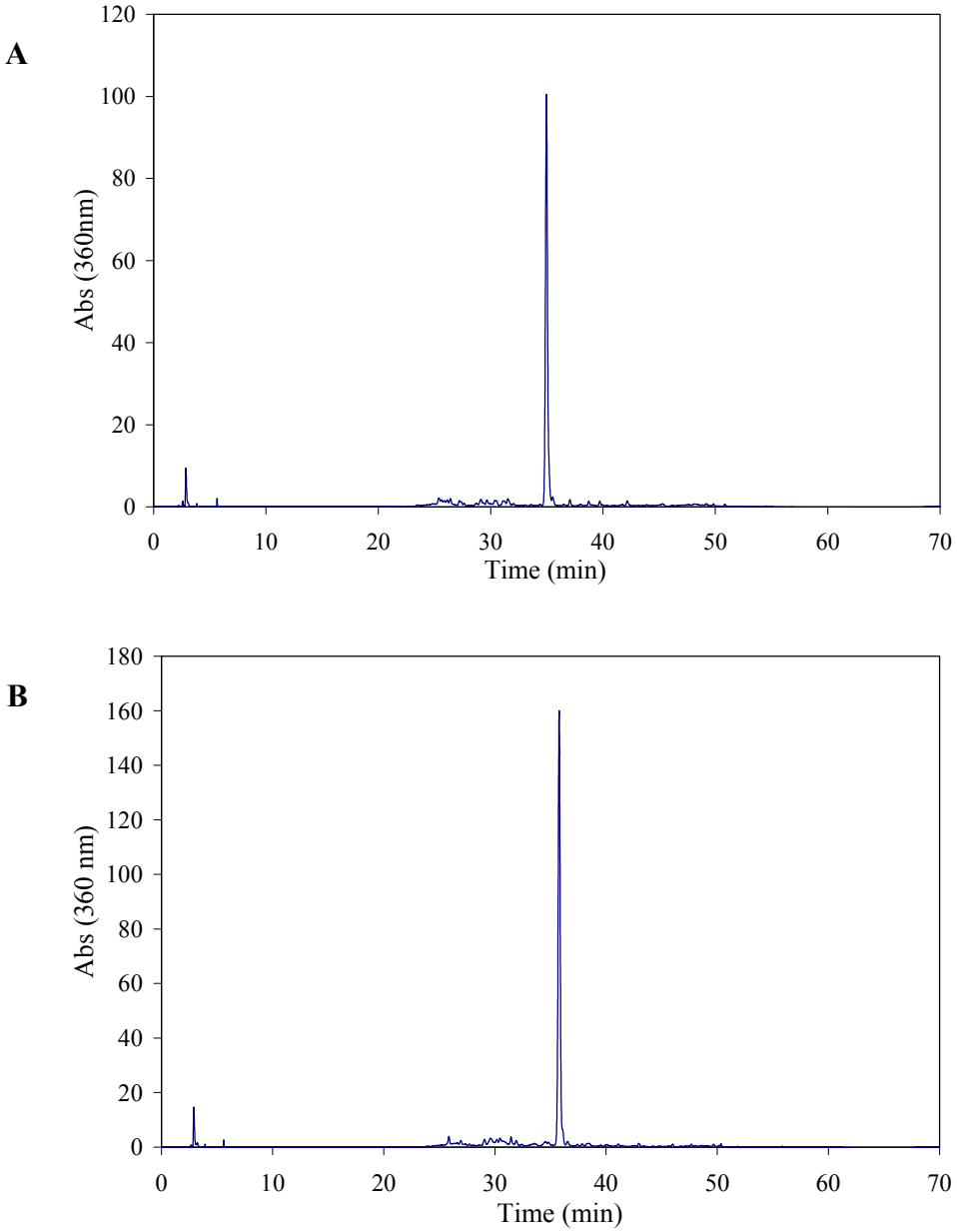

Figure 5.10: RP-HPLC profiles of acid-hydrolysed AHA-treated BLP at pH 7.2 (**A**) and pH 9.5 (**B**) for 48 h at 37°C.

5.2.6 Removal of non-covalently bound material from modified proteins

The apparent binding of AHA to BLP was not expected as AHA lacks the two main binding requirements; the *o*-aminophenol moiety and an ability to form an α,β-unsaturated carbonyl compound. Therefore, further experiments were carried out to investigate if the recovery of free AHB and AHA from AHB- and AHA-treated BLP, respectively, arose from insufficient dialysis leaving trapped unbound material within the protein or aromatic interactions with hydrophobic regions of the proteins.

BLP treated with 3OHKyn, 3OHKG, AHB and AHA at pH 9.5 for 48 h were dissolved in guanidine hydrochloride (6 M, pH 5.5), mixed thoroughly and filtered through a 10,000 Da molecular mass cut-off membrane (Centricon centrifugal device). Guanidine hydrochloride has chaotropic properties (unfolds protein by disrupting non-covalent bonds, *e.g.* hydrogen bonds) and is used to denature proteins.[389,390] The proteins were washed twice with guanidine hydrochloride to remove all unbound material. The concentrated protein was then hydrolysed and analysed by RP-HPLC for the presence of UV filters or amino acid adducts. Unmodified protein was used as a control. In addition, the guanidine hydrochloride filtrates from all protein washes were separately dried, extracted three times with CH_3CN, evaporated to dryness and analysed by RP-HPLC with detection at 360 nm.

The results confirmed that 3OHKyn and 3OHKG were covalently bound to lens proteins *via* Cys residues and that dialysis after the protein modification was sufficient to remove all unbound UV filters (Table 5.2). This was also supported by the remaining yellow-brown and pale yellow colour of the 3OHKyn- and 3OHKG-treated BLP, respectively, after guanidine hydrochloride treatment. The loss of Cys-3OHKyn after hydrolysis could be explained by the instability of the Cys adducts during the experimental conditions.

Table 5.2: Bound versus unbound UV filters following treatment of BLP with UV filters at pH 9.5 for 48 h. The percentage recovery was calculated from the initial amount of UV filters (*i.e.* AHA and AHB) or adducts (*i.e.* Cys-3OHKyn) found in the modified BLP upon acid hydrolysis (before guanidine hydrochloride extraction). GdHCl; guanidine hydrochloride. Quantification was conducted using the appropriate standard curves of Cys-3OHKyn, AHB and AHA.

Treated BLP	Recovery of free UV filters by CH_3CN extraction of GdHCl filtrate (%)	Recovery of protein-bound adducts from GdHCl washed BLP after acid hydrolysis (%)
3OHKyn	0	43
3OHKG	0	63
AHA	72	0
AHB	53	0

Furthermore, these results strongly support the hypothesis that AHA is non-covalently bound to lens proteins and that the original dialysis method had not been sufficient to remove all of the AHA. Extraction of the AHB-treated lens proteins by guanidine hydrochloride was followed by a reduction in protein colouration. In addition to AHB, a compound with absorption maxima at 236 and 441 nm and a molecular ion at *m/z* 413 ($M+H^+$) was recovered from the filtrate. A compound with similar characteristics was observed in the dialysis buffer recovered from AHB-treated proteins (Section 5.2.9) and from AHB stability studies

(Sections 4.2.7 and 5.2.8). This compound was not seen in the hydrolysates of AHB-treated proteins, so it may be a product of further oxidation of AHB.[201,204,207,209,211,391] A potential structure for this compound is discussed in Chapter 4.

Following the guanidine hydrochloride extraction, samples of the AHA- and AHB-treated BLP were acid hydrolysed and were found to contain no detectable amounts of AHA and AHB or any other compounds that have significant optical absorption at 360 nm. These data also suggest that oxidative products of AHB may not be involved in covalent protein modification, however this requires further investigation.

5.2.7 Stability of UV filters and their adducts during acid hydrolysis

The stability of Kyn and 3OHKyn amino acid adducts to acid hydrolysis has been determined previously.[18,20,383] The stability of each adduct was determined by hydrolysing Kyn and 3OHKyn amino acid adducts with 6 M HCl at 110°C for 24 h in the presence, or absence, of antioxidants (phenol and thioglycolic acid) and in the presence or absence of BLP (Table 5.3).

Table 5.3: Literature data on recovery of Kyn and 3OHKyn amino acid adducts after acid hydrolysis in the presence/absence of antioxidants and presence/absence of BLP. N/T, not tested; +, presence; -, absence.[18,20,383]

Amino acid adduct	Recovery (%) + antioxidants - BLP	Recovery (%) - antioxidants - BLP	Recovery (%) + antioxidants + BLP
Cys-Kyn	78	96 or 6.6	80
Lys-Kyn	N/T	96	N/T
His-Kyn	79	99	73
3OHKyn	58	N/T	N/T
Cys-3OHKyn	87	17	N/T
Lys-3OHKyn	95	24	N/T
His-3OHKyn	78	20	N/T

Greater recovery of 3OHKyn amino acid adducts was observed in the presence of antioxidants, suggesting that oxidation may play a major role in determining the recovery of these adducts. Variability was seen with the Kyn amino acid adducts in the absence of antioxidants, where Cys-Kyn was recovered in 6.6% yield by Parker *et al.*[383] compared to 96% yield by Vazquez *et al.*[18] In addition, Parker *et al.*[383] have shown that recovery of Cys-Kyn was dependent on the amount of protein present during hydrolysis in the absence of antioxidants. Recovery was highest with a larger amount of protein (10 mg) in comparison to a lower amount of protein (5 mg), 65% versus 50%.

As the stability of 3OHKG, Cys-3OHKG, AHB and AHA to acid hydrolysis were not investigated previously, further experiments were conducted following similar conditions to those reported above. A known quantity (< 1 mg) of 3OHKG, Cys-3OHKG, AHB or AHA was hydrolysed with 6 M HCl in the presence of antioxidants (phenol and thioglycolic acid) and in either the absence or presence of BLP (~10 mg). The identity of products was confirmed by spiking experiments with authentic standards and by ES-MS/MS of the collected peaks. The recovery of 3OHKG and Cys-3OHKG was determined by quantifying the levels of 3OHKyn and Cys-3OHKyn, respectively, as acid cleaves the glucose moiety. AHB and AHA were quantified using a standard curve constructed using synthetic standards of AHB and AHA, respectively.

The data obtained indicate that the recoveries of 3OHKG and AHB and particularly Cys-3OHKG are increased in the presence of BLP (Table 5.4). This may be due to the non-covalent binding of UV filters to hydrophobic sites on the amino acids thereby limiting UV filter oxidation. It is suggested that the sugars (*e.g.* glucose) undergo decomposition in acid to active compounds (*e.g.* aldehydes) that could possibly react with 3OHKyn. Protein may therefore spare the UV filters from these reactions.

Table 5.4: Recovery of 3OHKG (3OHKyn), Cys-3OHKG (Cys-3OHKyn), AHB and AHA after acid hydrolysis for 24 h at 110°C in the presence of antioxidants and presence/absence of BLP. The experiment was done in duplicate.

Compound		Recovery (%) + antioxidants - BLP	Recovery (%) + antioxidants + BLP
Pre- hydrolysis	Post-hydrolysis		
3OHKG	3OHKyn	18, 24	35, 39
Cys-3OHKG	Cys-3OHKyn	14, 16	85, 91
AHB	AHB	40, 48	66, 68
AHA	AHA	76, 84	71, 73

The low recoveries of 3OHKG, Cys-3OHKG and AHB after hydrolysis are consistent with the proposed generation of decomposition products detected by RP-HPLC. The majority of 3OHKG in the absence of BLP decomposed to a double peak with absorption maxima at 263 and 367 nm and a molecular ion at *m/z* 461 ($M+H^+$) that fragmented to *m/z* 444 (loss of NH_3) and other ions similar to those detected for 3OHKyn amino acid adducts, *i.e.* 208 (3OHKyn yellow), 162 (decarboxylated 3OHKyn yellow) and 110 (2-aminophenol) (Figure 5.11, A). The molecular mass of this compound is consistent with the quinone dimer (62) (460 Da). The quinone dimer is proposed to be formed *via* conjugate addition of 3OHKyn to quinone (63) (Scheme 5.4).[363,392] This dimeric compound of 3OHKyn was not seen in the presence of

BLP (Figure 5.11, B). In the absence of BLP, generation of other minor peaks with absorption maxima at ~230-250 nm was also observed (Figure 5.11, A inset).

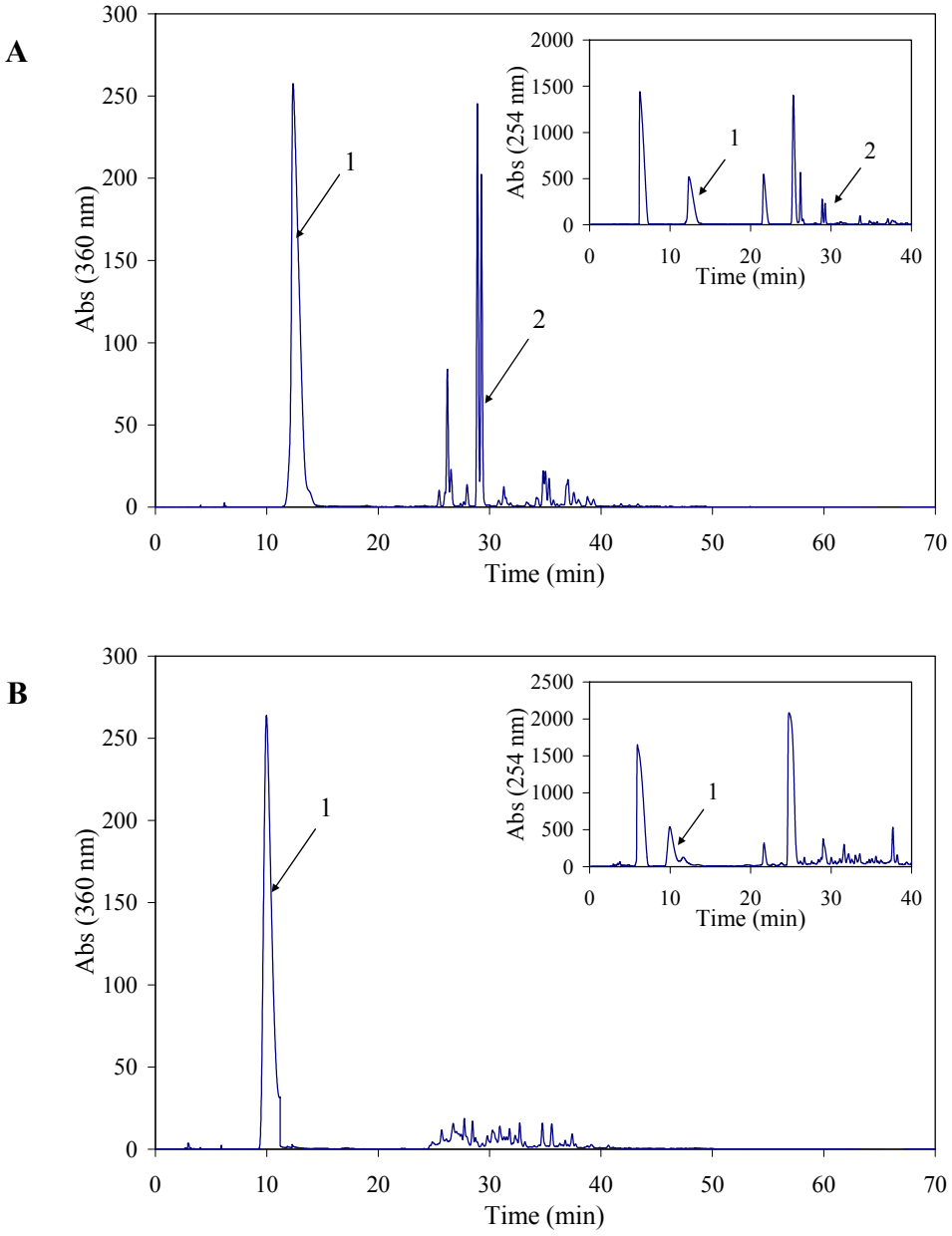

Figure 5.11: RP-HPLC profiles at 360 nm and 254 nm (inset) of acid-hydrolysed 3OHKG (0.6 mg) (**A**) and 3OHKG (0.4 mg) in the presence of BLP (13.2 mg) (**B**). 3OHKyn (1); decomposition product of *m/z* 461 ($M+H^+$) and λ_{max} 263/367 nm (2, double peak). RP-HPLC injection volumes were 50 µL for A and B.

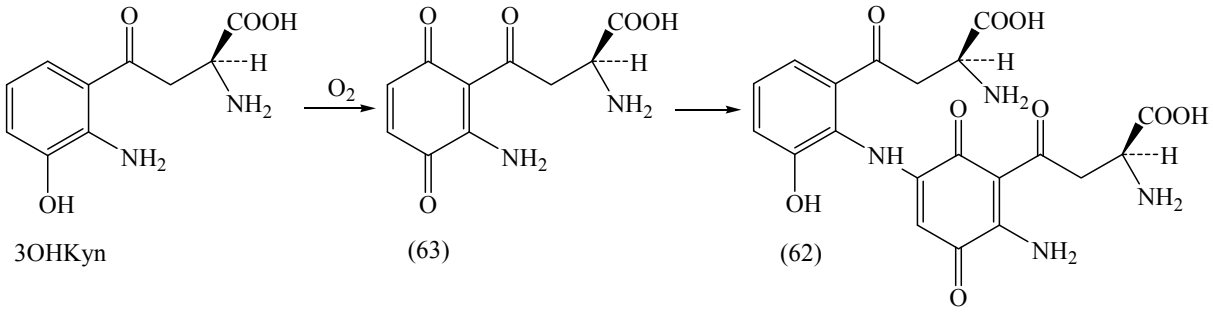

Scheme 5.4: Proposed formation of the quinone dimer (62).[392]

Decomposition of Cys-3OHKG in the absence of BLP resulted in the detection of multiple minor peaks and two major decomposition products with absorption maxima at 266 and 372 nm, and 252 and 340 nm, and with molecular ions at *m/z* 300 ($M+H^+$) and *m/z* 264 ($M+H^+$), respectively (Figure 5.12, A). The former compound was observed by RP-HPLC of 3OHKyn- and 3OHKG-modified BLP acid hydrolysates, suggesting that it possibly arises from the decomposition of the Cys adduct of 3OHKyn. In the presence of BLP this compound was observed in minimum quantities, while the compound which gave rise to a molecular ion at *m/z* 264 was not observed (Figure 5.12, B). Further identification of these compounds was not conducted.

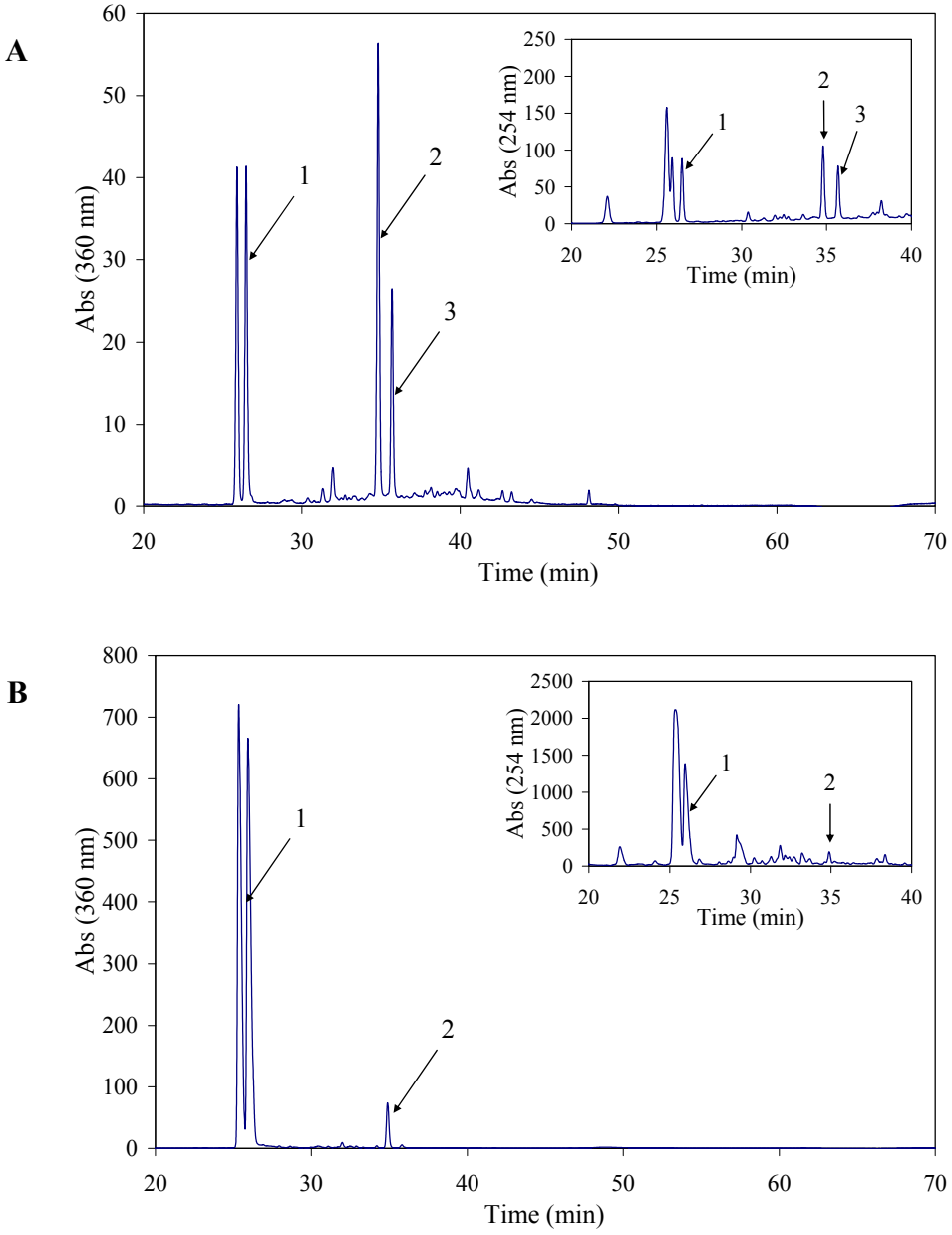

Figure 5.12: RP-HPLC profiles at 360 nm and 254 nm (inset) of acid-hydrolysed Cys-3OHKG (1.1 mg) (**A**) and Cys-3OHKG (0.5 mg) in the presence of BLP (10.5 mg) (**B**). Cys-3OHKyn (1, double peak); unknown decomposition product of *m/z* 300 ($M+H^+$) and λ_{max} 266/372 nm (2); unknown decomposition product of *m/z* 264 ($M+H^+$) and λ_{max} 252/340 nm (3). RP-HPLC injection volumes were 5 µL (A) and 50 µL (B).

Similarly, AHB proved to be relatively unstable to acid conditions in the absence of proteins. Three major peaks were observed by RP-HPLC with absorption maxima at ~230 nm (Figure 5.13, A). Greater stability of AHB was observed in the presence of proteins (Figure 5.13, B). The nature of these species was not examined further.

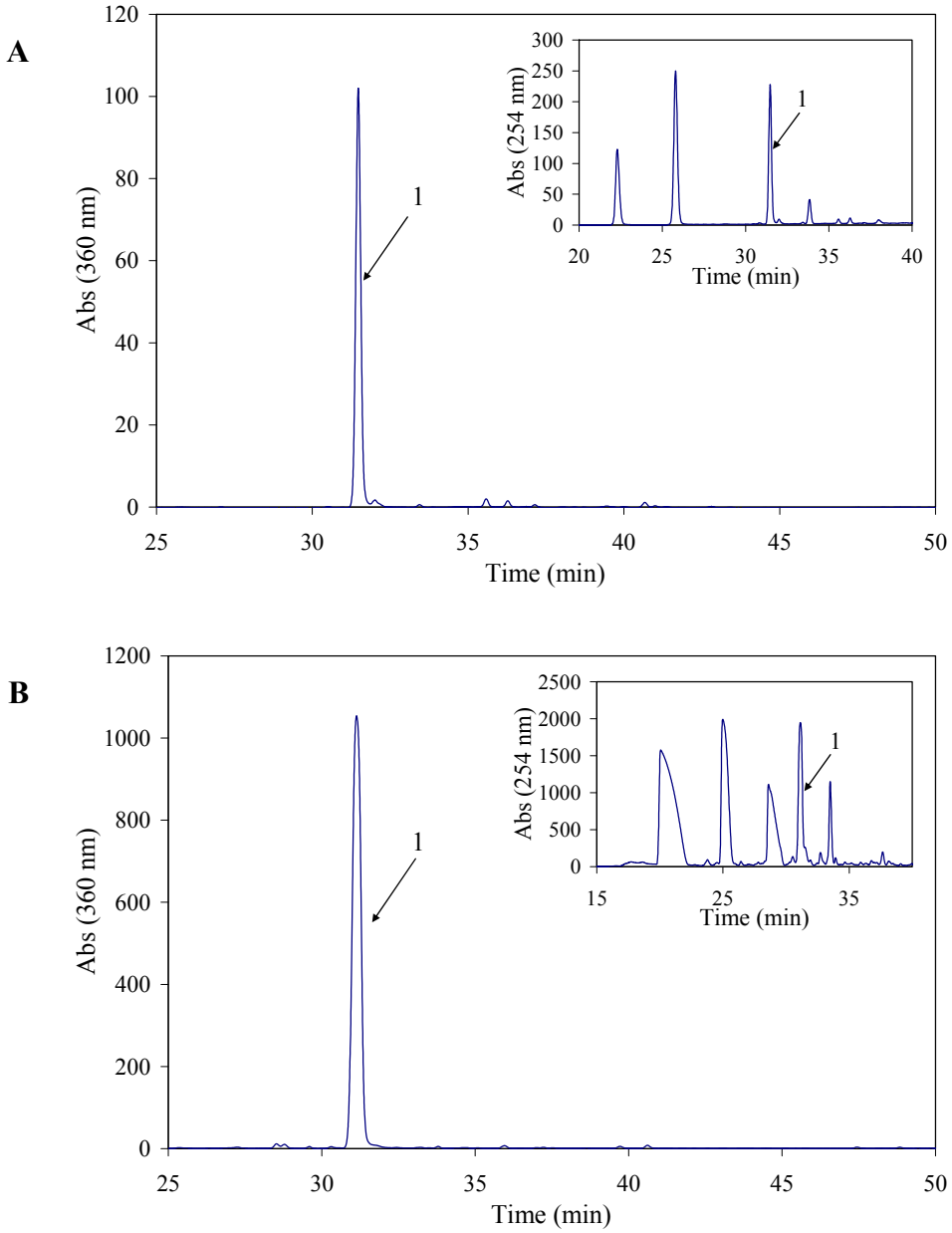

Figure 5.13: RP-HPLC profiles at 360 nm and 254 nm (inset) of acid-hydrolysed AHB (0.3 mg) (**A**) and AHB (0.2 mg) in the presence of BLP (13.1 mg) (**B**). AHB (1). RP-HPLC injection volumes were 5 µL (A) and 50 µL (B).

Relatively high recovery of AHA of ~75%, in either the presence (1.0 mg AHA and 13.0 mg BLP) or absence (0.9 mg AHA) of proteins, was observed. An additional peak of similar polarity compared to AHA was seen in the RP-HPLC and LC-MS traces, exhibiting absorption maxima at 258 and 340 nm (~14% peak area at 360 nm). By ES-MS/MS it showed a molecular ion at *m/z* 333 ($M+H^+$) and fragment ions at *m/z* 287 and *m/z* 231. This compound was not characterised further.

5.2.8 Stability of AHA and AHB at pH 9.5

The data presented earlier in this thesis (Chapter 4), is consistent with AHA being stable upon incubation at pH 7.2 for 48 h at 37°C in the presence of O_2. In contrast, ~50% of AHB decomposed under similar conditions, and ~18% in the absence of O_2 and in the presence of antioxidants. As the stability of AHA and AHB at pH 9.5 was not previously investigated, further experiments were conducted for 48 h at 37°C under argon. As expected, AHA was found to be stable at pH 9.5 for 48 h (2.7 mM AHA at 0 min and 48 h). In contrast to AHA, the solutions of AHB become highly coloured (yellow/tanned) after 48 h. Triplicate samples were removed at indicated time points during the incubation time for RP-HPLC analysis. One sample of each triplicate was acidified to pH ~5.5 with 1 M AcOH, to prevent possible decomposition of AHB during storage and RP-HPLC analysis. It is known that acidic conditions improve the stability of AHB by keeping the aromatic amine and hydroxyl groups in the protonated state. RP-HPLC analysis with optimal detection at 360 nm showed that AHB was unstable with increasing incubation time, with 96% decomposition after 24 h of incubation. This decomposition resulted in the formation of at least four detectable new species (Figure 5.14, A). Only a small improvement in AHB stability (~2%) was seen where aliquoted samples were acidified before storage or RP-HPLC (Figure 5.14, B). These data suggest that the majority of AHB had decomposed during the incubation period prior to RP-HPLC analysis. However, it can be seen that acidification delayed the formation of the 32.7 min decomposition product of AHB, as it appeared only after 48 h of incubation. Even though this experiment indicated that the majority of AHB decomposed after 24 h of incubation, this was not observed in the BLP modification experiments. It is possible that higher concentration (9.6 mM versus 0.45 mM) of AHB in the solution for the BLP modification experiment and possibly the presence of BLP may result in greater recovery of AHB.

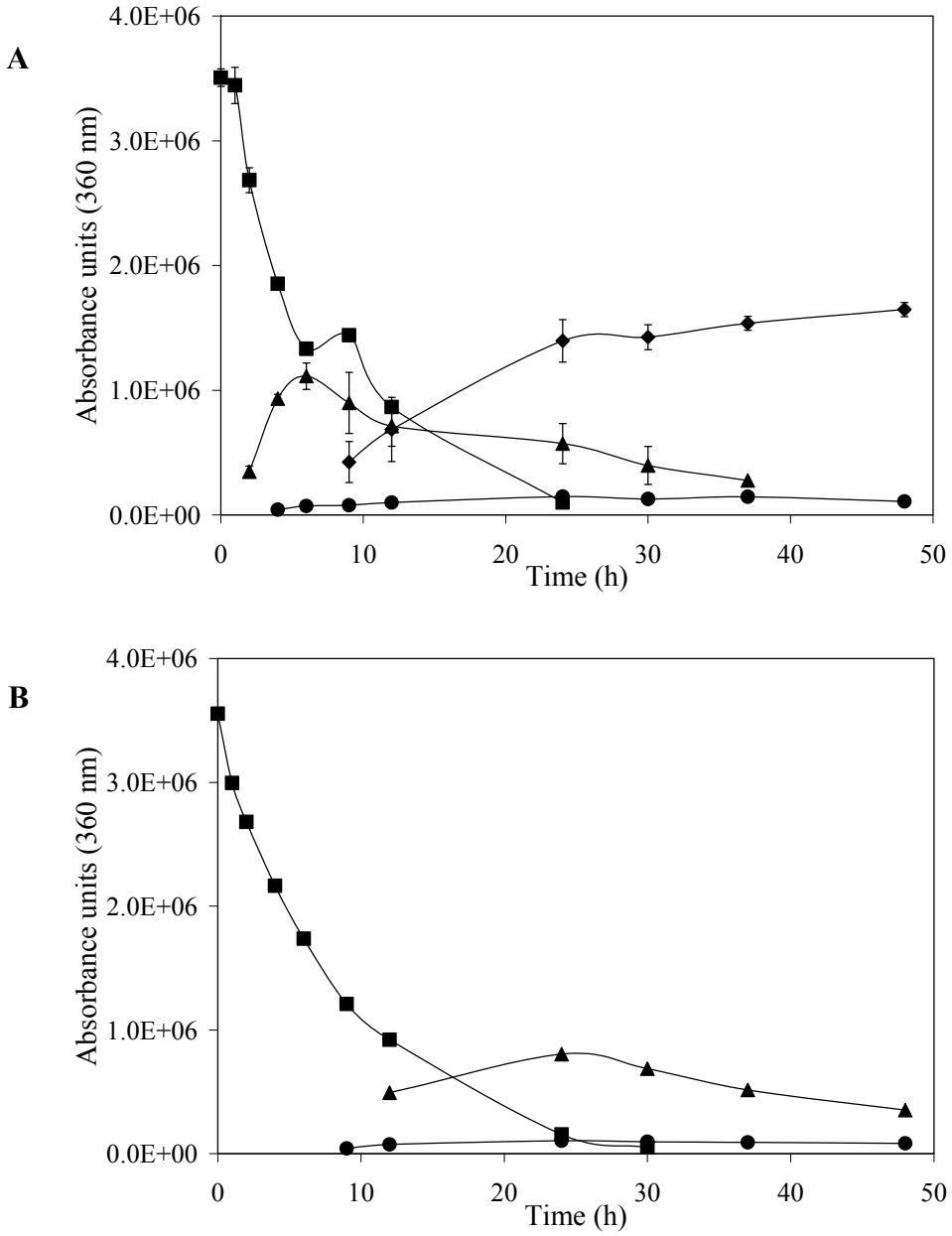

Figure 5.14: Stability of AHB over 48 h at pH 9.5 at 37°C. (**A**) Duplicate analysis and (**B**) single analysis of AHB stability with acidification of samples before storage or RP-HPLC analysis. AHB (■); 30.7 min (*m/z* 413 ($M+H^+$)) (▲); 31.7 min (*m/z* 399 ($M+H^+$)) (●); 32.7 (*m/z* 414 ($M+H^+$)) (♦).

The major decomposition products of AHB were characterised spectrally by LC-MS using samples removed after 6, 12, 30 and 48 h of incubation. As for the stability studies at pH 7.0 (Chapter 4), a series of molecular ions were detected by MS with *m/z* 399-414, indicative of the presence of dimeric species (Section 4.2.7). It is clear from these data that despite the degassing with argon, sufficient oxygen remained in the sample to support auto-oxidation of this compound.

The data outlined above support the hypothesis that AHB produces a range of products under the conditions used for protein modification at pH 9.5, and it was therefore suspected that some of these products might be involved in protein colouration. Hence, AHB was incubated at pH 9.5 for 24 h at 37°C and then BLP was added, and the incubation continued for a further 24 h. No obvious differences between this sample (0.16 mol AHB/mol protein) and the previously described AHB-treated BLP sample (pH 9.5 for 48 h) were observed spectrally and upon hydrolysis, suggesting that either the oxidised species are not involved in binding to BLP under the experimental conditions investigated, or due to their instability they can not be recovered upon acid hydrolysis.

5.2.9 Characterisation of low molecular mass compounds isolated upon dialysis

Lens proteins were covalently-modified by Kyn, 3OHKyn and 3OHKG and not by AHB and AHA. To help understand the species that might be involved in protein modification, the low molecular mass compounds present in the 3OHKyn-, 3OHKG-, AHB- and AHA-treated BLP reaction mixtures were analysed. After incubation with the lens proteins at pH 9.5, the reaction mixtures were dialysed against phosphate buffer at pH 5.5-6 for 48 h. Five buffer changes were made during this time. The buffer from the first change was kept for each sample for analysis.

Initially, these dialysis buffer samples were lyophilised, and analysed by UV-vis and fluorescence in PBS at pH 7.0. The results are summarised in Table 5.5. The absorbance spectra indicated the presence of the relevant UV filters, while fluorescence spectroscopy revealed the presence of additional fluorophores for 3OHKyn, 3OHKG and AHB samples compared to the equivalent modified BLP. The 3OHKyn buffer sample contained fluorophore at λ_{ex} 385 and λ_{em} 525 nm, which were similar to that found in the 3OHKyn-modified proteins (Section 5.2.2).

Table 5.5: Absorbance and fluorescence data of dialysis buffer samples collected after protein modification at pH 9.5.

Modified proteins	Absorbance (nm)	Fluorescence ($\lambda_{ex}/\lambda_{em}$, nm)
3OHKyn	267, 371	375/455, 385/525, 330/500
3OHKG	264, 369	370/440, 370/500
AHB	264, 366	360/445, 350/510
AHA	255, 362	345/485

Subsequent analysis of these species by LC-MS revealed that the major compounds present in each reaction mixture were the original UV filters, suggesting that not all the UV filters at a 2 mg/mL concentration had decomposed over 48 h in the argon-gassed reaction mixtures. The buffer sample from 3OHKG-modified lens proteins at pH 9.5 also exhibited a significant peak with absorption maxima at 282 and 410 nm and a molecular ion at *m/z* 370 ($M+H^+$) that on ES-MS/MS gave a fragment ion at *m/z* 208 due to loss of glucose. This is consistent with the direct deamination product of 3OHKG, which would be expected to have higher absorption maxima than its starting material, or a cyclised derivative due to greater conjugation. The 3OHKyn buffer sample showed three different dimerised/oxidised products with molecular ions at *m/z* 395-396 ($M+H^+$). These peaks accounted for ~20% of the peak area at 254 nm. Xanthurenic acid (*m/z* 208 ($M+H^+$), λ_{max} 242/340 nm) and deaminated 3OHKyn (*m/z* 208 ($M+H^+$), λ_{max} 293/420 nm) were also identified in 7 and 17%, respectively, of the peak area at 254 nm. The AHB buffer sample showed similar decomposition products to those observed on incubation of AHB at 9.5 (*i.e. m/z* 399 ($M+H^+$), *m/z* 413 ($M+H^+$) and *m/z* 414 ($M+H^+$)) (Section 5.2.8), while AHA showed no decomposition products.

5.3 Conclusions

The initial experiments in this chapter were aimed at studying the reactivity of 3OHKG, AHB and AHA towards BLP. Comparative experiments with Kyn and 3OHKyn as positive controls, and unmodified BLP as a negative control, were simultaneously conducted.

Kyn, 3OHKyn and 3OHKG were found to react with BLP, at both pH 7.2 and 9.5, to give coloured (λ_{max} ~360 nm for Kyn and 3OHKG, and ~360 and 440 nm for 3OHKyn) and fluorescent (λ_{ex} 345-390 and λ_{em} 470-515 nm) modified proteins. RP-HPLC and ES-MS/MS analysis of acid hydrolysed Kyn-, 3OHKyn- and 3OHKG-treated BLP showed that these UV filters are covalently bound to lens proteins predominantly *via* Cys amino acid residues under both investigated pH conditions. Consistently higher quantities of the Cys adducts were seen at pH 9.5, which is likely to be due to the greater rate of UV filter deamination under these conditions. As Kyn-, 3OHKyn- and 3OHKG-Cys adducts showed relatively good stability under the conditions used for acid hydrolysis of modified BLP, the quantities determined for these three adducts were representative of the concentrations in the modified proteins. Only minor quantities of Lys adducts were seen, while His binding was not observed in all three UV filter treatments. In comparison to levels of UV filter-modified proteins detected in older

human lenses,[176] the UV filter-modified BLP in this study were found to be more heavily modified at both pH 7.2 and 9.5 (Table 5.6).

Table 5.6: Average concentrations of protein bound UV filters from *in vitro* and *in vivo* studies.

	In vitro[a] (mol Cys adduct/mol protein)		*In vivo*[b] (mmol bound UV filter/mol protein)	
Kyn	pH 7.2	N/D	Nucleus	0.74 ± 0.06
	pH 9.5	0.96	Cortex	0.04 ± 0.02
3OHKyn	pH 7.2	0.02	Nucleus	0.18 ± 0.06
	pH 9.5	0.05 - 0.64	Cortex	N/D
3OHKG	pH 7.2	0.26	Nucleus	26.1 ± 1.78
	pH 9.5	0.40 - 1.14	Cortex	1.12 ± 0.20

[a] modified BLP investigated in this study. The average concentrations of the Cys adducts.
[b] older human lenses investigated by Korlimbinis *et al.*[176] The average concentrations of the Cys and Lys adducts. N/D, not determined

In bovine lens crystallins, Lys is the most abundant amino acid of the three binding residues (α, 7.8%; β, 5.6%; γ, 7.3%) followed by His (α, 4.6%; β, 3.5%; γ, 3.1%) and then by Cys (α, 0.3%; β, 1.9%; γ, 3.4%), indicating that the pattern of BLP modification observed is not simply a function of amino acid abundance.[385] Other amino acids may also be modified, but in significantly lower levels compared to the Cys and Lys modifications found in this study. For example, modification of Arg residues by 3OHKyn has been determined previously.[106]

The binding is likely to be influenced by the tertiary structure of the protein, the accessibility of residues for the reactions, the nucleophilicity of the amino acid residues and the stability of the amino acid adduct. The nucleophilicity of amino acids is closely related to their pK_a values.[393] If pK_a values are considered, the order of reactivity of His, Lys and Cys towards deaminated UV filters at physiological pH would be expected to be His (pK_a 6.0), followed by Cys (pK_a 8.33) and then Lys (pK_a 10.53), although pKa values, in particular for Cys residues on proteins, are know to vary and may depend on the local environment.[18]

Recent studies on BLP extracted in an identical manner to that employed in this study have indicated that there were 2.5 mol of protein sulfhydryl (PSH) groups per mol of protein.[175] These data are comparable to previous reports of BLP and normal human lens proteins.[394,395] PSH content, however, decreased rapidly to ~10% of the original value upon incubation of lens proteins under physiological conditions in the presence of 3OHKyn for 3 days.[175] This

coincided with the observed formation of Cys-3OHKyn. The prolonged incubation (> 6 days) of 3OHKyn with lens proteins resulted in the Cys adducts being replaced to some extent by Lys and His adducts possibly due to greater instability of the former species followed by the formation of disulfide bond linkages.[175] The short incubation time (48 h) used in this study may therefore be one of the reasons for the preferred modification at Cys residues. Overall, it is clear that the data obtained in this study is consistent with the Cys residues being better nucleophiles than His and Lys residues under the investigated experimental conditions, resulting in rapid reaction with the side chains of the deaminated UV filters.

Analysis of AHB- and AHA-treated BLP showed non-covalent binding of these species to proteins. This may be through protein hydrophobic sites, however this requires further investigation. These experiments support the previous statement in Chapter 4, that the reduction of the deaminated Kyn to AHA could act as a defense mechanism of the lens to reduce the amount of Kyn binding to lens proteins and in addition decrease the photosensitiser activity of oxidative damage on lens proteins (discussed in Chapter 6). The former was also demonstrated in the model experiments of Taylor *et al.*,[117] where inclusion of NADH in the mixture containing Kyn and BLP resulted in ~50% decrease in the amount of Kyn bound to the lens protein. These observations are consistent with the hypothesis that deamination of the Kyn side chain and formation of an α,β-unsaturated carbonyl compound is the key step in lens protein modification.

The same could not be concluded for AHB. Even though no binding *via* the side chain of AHB to lens proteins is possible, proteins did undergo changes in absorbance (λ_{max} 328, 398 and 440 nm) and fluorescence (λ_{ex} 382-390 and λ_{em} 475-490 nm) properties at both pH 7.2 and 9.5, compared to the unmodified proteins. Similar changes were seen for 3OHKyn-modified BLP (λ_{max} 367 and 440 nm; λ_{ex} ~350-390 and λ_{em} 490-515 nm) suggesting that some part of the change in absorbance and fluorescence properties of 3OHKyn-treated lens proteins is due to oxidation of the *o*-aminophenol moiety. RP-HPLC analysis of acid-hydrolysed AHB-treated BLP showed, in addition to AHB, three additional highly coloured compounds that exhibited long wavelength absorbance. These decomposition products of AHB appeared as dimeric species exhibiting molecular ions at *m/z* ~400, as characterised by LC-MS and ES-MS/MS. Compounds with similar characteristics were observed upon incubation of AHB at pH 9.5 and pH 7.2 in the absence of BLP and in the recovered dialysis buffer from the AHB-treated BLP. In contrast, no apparent free or protein bound oxidative products of 3OHKyn in 3OHKyn-modified BLP were seen upon acid hydrolysis, even though dialysis buffer samples

collected from 3OHKyn-modified BLP showed three different dimerised/oxidised products with molecular ions at *m/z* 395-396. This suggests possibly lower reactivity of the *o*-aminophenol moiety with BLP compared to the deaminated side chain or that protein bound oxidation species can not be recovered after acid hydrolysis due to their instability. Further experiments are needed to investigate the mode of binding of 3OHKyn and AHB oxidative products to lens proteins, and to find out the importance of the *o*-aminophenol moiety in protein modification and possibly ARN cataract formation.

5.4 Experimental

5.4.1 General experimental

All organic solvents and acids were of HPLC grade (Ajax, NSW, Australia). Milli-Q® H_2O (purified to 18.2 MΩ cm^{-2}) was used in preparation of all solutions. Dulbelcco's phosphate-buffered saline (PBS), without calcium and magnesium, consisted of KCl (2.7 mM), KH_2PO_4 (1.4 mM), NaCl (137 mM), Na_2HPO_4 (7.68 mM).[257] Pre-washed chelex resin was added to the PBS buffer (~2 g/L) and left for 24 h prior to use. The pH of PBS was adjusted to 7.0 with 1 M NaOH. DL-Kynurenine sulphate salt (Kyn, ≥ 95%), 3-hydroxy-DL-kynurenine (3OHKyn), Cys-Kyn (synthesised[18] and kindly provided by Dr N. R. Parker), amino acids (*N*-α-*t*-Boc-L-histidine (*t*-Boc-His), *N*-α-*t*-Boc-L-lysine (*t*-Boc-Lys) and L-cysteine (Cys)), trifluoroacetic acid (TFA, > 99%), formic acid (~98%), thioglycolic acid, phenol, sodium azide (NaN_3), guanidine hydrochloride, all buffer salts (*e.g.* 100 mM Na_2HPO_4/NaH_2PO_4 (NaH_2PO_4 [0.2 M, 14 mL] and Na_2HPO_4 [0.2 M, 36 mL] diluted to 100 mL with H_2O) and 50 mM $Na_2CO_3/NaHCO_3$ ($NaHCO_3$ [0.1 M, 50 mL] and NaOH [0.2 M, 6.2 mL] diluted to 100 mL with H_2O)) and dialysis tubing (molecular mass cut-off 20,000 Da) were from Sigma-Aldrich. Thin-layer chromatography (TLC) plates were of normal phase 60 F_{254} (Merck, Germany) and developed using the mobile phase of *n*-butanol/AcOH/H_2O (12:3:5 BAW, v/v). TLC plates were visualised under UV light (254 and 365 nm) and sprayed with ninhydrin (ninhydrin [0.2%, w/v] in *n*-butanol [94.8%, v/v] and AcOH [5%, v/v]),[288] where indicated. Vivaspin (6 mL) protein concentrators (molecular mass cut off 10,000 Da) were purchased from Crown Scientific. MeOD (99.8%) was purchased from Cambridge Isotope Laboratories. A Labconco FreeZone 12 plus freeze drier (0.04 mBa, -80°C) from Crown Scientific was used for lyophilisation of aqueous solutions. The reactions under vacuum and removal of

organic solvents during rotary evaporation were conducted using a vacuum pump at ~20 mBar.

5.4.2 UV-visible (UV-vis) absorbance and fluorescence spectrometric measurements

UV-vis absorbance spectra were obtained using a Varian DMS 90 UV-vis spectrometer with quartz cuvettes (0.75 mL). Fluorescence spectra were recorded on a PerkinElmer LS55 Luminescence spectrometer using SUPRASIL® PerkinElmer fluorescence cells (0.3 or 3mL). Slit widths were 10 nm for excitation and emission. Guanidine hydrochloride (6 M, pH 5.5, ~2 mg protein/mL) and PBS (pH 7.0, ~0.5 mg amino acid adduct/mL) were used as solvents. Samples were analysed against a blank solution of guanidine hydrochloride or PBS.

5.4.3 Reversed phase-high performance liquid chromatography (RP-HPLC)

RP-HPLC was performed on a Shimadzu HPLC equipped with LC-10ADvp pumps, a SIL-10Avp autoinjector and SPD-M10Avp diode array detector. The analytical analyses were performed on an Alltech (Prevail, 100 Å, 5 μm, 4.6 x 250 mm, C18) column fitted with a Phenomenex (Synergy Fusion, 100 Å, 4 μm, 2 x 4 mm, C18) guard column, while preparative purifications were performed on a Phenomenex (Luna, 100 Å, 10 μm, 15 x 250 mm, C18) column fitted with a Phenomenex (Synergy Fusion, 100 Å, 4 μm, 10 x 10 mm, C18) guard column. The following mobile phase system; buffer A (H_2O/0.05% TFA, v/v) and buffer B (80% CH_3CN/0.05% TFA, v/v) and the flow rate 1 mL/min for analytical and 5 mL/min for preparative separations were kept constant. The eluents were monitored at 254 and 360 nm. Preparative purification of *t*-Boc-His-3OHKyn (30.2 min) and *t*-Boc-Lys-3OHKyn (26.7 min) were purified with a mobile phase gradient as follows: 0-10 min (5% buffer B), 10-40 min (50% buffer B), 40-45 min (50% buffer B), 45-50 min (5% buffer B) and 50-60 min (5% buffer B). Preparative separation of His-3OHKyn (9.8 min), Lys-3OHKyn (6.7 min) and Cys-3OHKyn (21.1 min) was conducted with a mobile phase gradient as follows: 0-10 min (5% buffer B), 10-30 min (50% buffer B), 30-35 min (50% buffer B), 35-40 min (5% buffer B) and 40-50 min (5% buffer B). The analytical separation of protein acid hydrolysates was conducted with a mobile phase gradient as follows: 0-10 min (5% buffer B), 10-40 min (5-50% buffer B), 40-50 min (50-100% buffer B), 50-55 min (100% buffer B), 55-60 min (100-5% buffer B) and 60-70 min (5% buffer B). The analytical separation of AHB stability analyses was conducted with a mobile phase gradient as follows: 0-6 min (5% buffer B), 6-40

min (5-70% buffer B), 40-45 min (70% buffer B), 45-50 min (70-5% buffer B), 50-57 min (5% buffer B). The analytical separation of AHA stability analyses was conducted with a mobile phase gradient as follows: 0-4 min (5% buffer B), 4-18 min (5-100% buffer B), 18-21 min (100% buffer B), 21-23 min (100-5% buffer B), 23-29 min (5% buffer B).

5.4.4 Liquid chromatography-mass spectrometry (LC-MS)

See Section 2.4.4 for details.

5.4.5 Nuclear magnetic resonance (NMR) spectroscopy

See Section 2.4.5 for details.

5.4.6 Mass spectrometry (MS)

See Section 2.4.6 for details.

5.4.7 **Synthesis of 3OHKyn amino acid adduct** (modified method of Vazquez *et al.*[18])

3OHKyn (50 mg, 0.22 mmol) was dissolved in argon-gassed (~20 min) Na_2CO_3-$NaHCO_3$ buffer (30 mL, 50 mM, pH 9.5). *N*-α-*t*-Boc-L-histidine (0.57 g, 2.23 mmol), *N*-α-*t*-Boc-L-lysine (0.55 g, 2.23 mmol) or free base L-cysteine (0.27 g, 2.23 mmol) was added and the pH was adjusted to pH 9.5 by dropwise addition of 1 M NaOH. The light yellow solutions were bubbled with argon for ~20 min, sealed with parafilm and incubated in the dark at 37°C with shaking. The progress of the reactions was monitored by normal phase TLC (BAW). After 24 and 48 h, another 10 mol equivalents of L-cysteine (0.27 g, 2.23 mmol) were added to the L-cysteine reaction mixture and the pH was readjusted to 9.5 by dropwise addition of NaOH (1 M) for all reactions. After 72 h, the dark yellow (L-cysteine) and dark brown (*N*-α-*t*-Boc-His and *N*-α-*t*-Boc-Lys) reaction mixtures were acidified to pH 6.5 by dropwise addition of 1 M AcOH and lyophilised. RP-HPLC preparative purification afforded *N*-α-*t*-Boc-L-histidine-3OHKyn (15.7 mg, 15.2%, R_f 0.33), *N*-α-*t*-Boc-L-lysine-3OHKyn (21.6 mg, 21.4%, R_f 0.37) and Cys-3OHKyn (36.2 mg, 49.5%, R_f 0.22) as light yellow solids in ~1:1 diastereomeric ratios.

N-α-Butoxycarbonyl-L-histidyl-3-hydroxy-DL-kynurenine (*t*-Boc-His-3OHKyn): ^{1}H NMR δ (MeOD) 8.87 (1H, s, NC<u>H</u>N), 7.42 (1H, s, NC<u>H</u>C), 7.30 (1H, d, *J* 8.2, ArH-6), 6.80 (1H, d, *J* 7.4, ArH-4), 6.48 (1H, dd, *J* 7.4, 8.2, ArH-5), 5.49 (1H, m, H-2), 4.38 (1H, m, $CH_2C\underline{H}COOH$), 3.92 (2H, m, H-3), 3.18 (1H, br dd, *J* ~5.0, ~15.1, $C\underline{H_2}CHCOOH$), 3.03 (1H, m, $C\underline{H_2}CHCOOH$), 1.35 (9H, s, 3 x $C\underline{H_3}$); ES-MS/MS *m/z* 463.1 ($M+H^+$, 4%), 407.1 ($M+H^+$ - $C(CH_3)_3$) 55%), 363.1 ($M+H^+$ - *t*-Boc, 100%), 317.1 ($M+H^+$ - *t*-Boc - HCOOH, 20%), 208.1 ($M+H^+$ - *t*-Boc-Lys, 15%), 190.0 ($M+H^+$ - *t*-Boc-Lys - H_2O, 4%), 162.0 ($M+H^+$ - *t*-Boc-Lys - HCOOH, 4%), 156.1 ($M+H^+$ - *t*-Boc - 3OHKyn, 50%), 136.0 (2%), 110.0 ($M+H^+$ - *t*-Boc - His - $C(O)CH_2CH(NH_2)COOH$, 5%). λ_{max} 269 and 375 nm.

N-α-Butoxycarbonyl-L-lysyl-3-hydroxy-DL-kynurenine (*t*-Boc-Lys-3OHKyn): ^{1}H NMR δ (MeOD) 7.27 (1H, d, *J* 8.0, ArH-6), 6.81 (1H, d, *J* 7.9, ArH-4), 6.46 (1H, dd, *J* 7.9, 8.0, ArH-5), 4.08 (1H, m, H-2), 3.95 (1H, m, $C\underline{H}NH_2$), 3.70 (1H, m, H-3), 3.60 (1H, m, H-3), 3.15 (2H, m, $NHC\underline{H_2}$), 1.83 (2H, m, CH_2-CH_2-$C\underline{H_2}$), 1.70 (2H, m, $C\underline{H_2}$-CH_2-CH_2), 1.52 (2H, m, CH_2-$C\underline{H_2}$-CH_2), 1.42 (9H, s, 3 x $C\underline{H_3}$); ES-MS/MS *m/z* 454.1 ($M+H^+$, 30%), 354.1 ($M+H^+$ - *t*-Boc, 00%), 247.0 ($M+H^+$ - 3OHKyn, 8%), 208.0 ($M+H^+$ - *t*-Boc-Lys, 15%), 203.0 (80%), 162.0 ($M+H^+$ - *t*-Boc-Lys - HCOOH, 3%), 152.0 (31%), 147.0 ($M+H^+$ - *t*-Boc - 3OHKyn, 28%), 128.0 (12%), 110.0 ($M+H^+$ - *t*-Boc-Lys - $C(O)CH_2CH(NH_2)COOH$, 9%). λ_{max} 268 and 376 nm.

L-Cysteinyl-3-hydroxy-DL-kynurenine (Cys-3OHKyn): ^{1}H NMR δ (MeOD) 7.31 (1H, m, ArH-6), 6.82 (1H, br dd, *J* ~1.2, ~7.9, ArH-4), 6.47 (1H, dd, *J* 7.9, 7.9, ArH-5), 4.30 (~0.5H, m, $SCH_2C\underline{H}$), 4.18 (~0.5H, m, $SCH_2C\underline{H}$), 3.90 (1H, m, H-2), 3.62 (1H, m, H-3), 3.58 (~0.5H, m, $SC\underline{H_2}CH$), 3.43 (~0.5H, m, $SC\underline{H_2}CH$), 3.42 (1H, m, H-3), 3.24 (~0.5H, m, $SC\underline{H_2}CH$), 3.07 (~0.5H, m, $SC\underline{H_2}CH$); ^{13}C NMR δ (MeOD) 199.9 (CO-4), 199.8 (CO-4), 175.6 (CO-1), 170.7 ($NH_2CH\underline{C}OOH$), 146.3 (ArC-3), 142.3 (ArC-2), 122.3 (ArC-6), 118.1 (ArC-1), 118.0 (ArC-4), 115.8 (ArC-5), 54.4 ($SCH_2\underline{C}H$), 53.6 ($SCH_2\underline{C}H$), 44.3 (C-2), 42.7 (C-3), 42.2 (C-2), 41.8 (C-3), 34.1 ($S\underline{C}H_2$), 33.2 ($S\underline{C}H_2$); ES-MS/MS *m/z* 329.0 ($M+H^+$, 10%), 311.1 ($M+H^+$ - H_2O, 5%), 240.0 ($M+H^+$ - $CH_2CH(NH_2)COOH$, 7%), 208.1 ($M+H^+$ - Cys, 55%), 202.0 (100%), 190.0 ($M+H^+$ - Cys - H_2O, 28%), 162.1 ($M+H^+$ - Cys - HCOOH, 42%), 122.0 ($M+H^+$ - 3OHKyn, 7%), 110.0 ($M+H^+$ - Cys - $C(O)CH_2CH(NH_2)COOH$, 48%). λ_{max} 268 and 368 nm, and maximum fluorescence at λ_{ex} 340 / λ_{em} 520 nm and λ_{ex} 405 / λ_{em} 475 nm.

5.4.8 Acid hydrolysis of *N*-α-*t*-Boc protected 3OHKyn amino acid adducts (modified method of Vazquez *et al.*[18])

t-Boc-His-3OHKyn (13.2 mg, 28.5 μmol) and *t*-Boc-Lys-3OHKyn (19.1 mg, 42.1 μmol) were separately hydrolysed with HCl (6 M, 1 mL) at 37°C. After 12 h, the pH of the yellow solutions was adjusted to pH ~6.0 by dropwise addition of 1 M NaOH. The reaction mixtures were subsequently lyophilised and purified by RP-HPLC to afford His-3OHKyn (10.0 mg, 97.0%) and Lys-3OHKyn (14.5 mg, 98.0%) as light yellow solids.

L-Histidyl-3-hydroxy-DL-kynurenine (His-3OHKyn): $M+H^+$, 363.131253 Da. Calculated for $C_{16}H_{19}N_4O_6$: $M+H^+$, 363.130460 Da; ^{1}H NMR δ (MeOD) 8.92 (1H, s, NC<u>H</u>N), 7.60 (1H, s, NC<u>H</u>C), 7.39 (1H, d, *J* 8.3, ArH-6), 6.80 (1H, d, *J* 7.5, ArH-4), 6.48 (1H, dd, *J* 7.5, 8.3, ArH-5), 5.75 (1H, m, H-2), 4.24 (1H, m, CH_2-C<u>H</u>-COOH), 4.05 (1H, m, H-3), 3.95 (1H, m, H-3), 3.38 (1H, m, C<u>H</u>$_2$-CH-COOH), 3.24 (1H, m, C<u>H</u>$_2$-CH-COOH); ^{13}C NMR δ (MeOD) 198.1 (CO-4), 172.0 (CO-1), 171.0 (CH_2CH<u>C</u>OOH), 146.4 (ArC-3), 142.6 (ArC-2), 137.5 (N<u>C</u>HN), 122.2 (ArC-6), 121.8 (N<u>C</u>HC), 118.2 (ArC-4), 117.7 (ArC-1), 115.9 (ArC-5), 59.2 (C-2), 53.3 (CH_2<u>C</u>HCOOH), 42.4 (C-3), 27.2 (<u>C</u>H_2CHCOOH); ES-MS/MS *m/z* 363.0 ($M+H^+$, 80%), 317.1 ($M+H^+$ - HCOOH, 30%), 208.1 ($M+H^+$ - Lys, 25%), 190.0 ($M+H^+$ - Lys - H_2O, 11%), 162.0 ($M+H^+$ - Lys - HCOOH, 23%), 156.1 ($M+H^+$ - 3OHKyn, 100%), 136.0 (6%), 110.0 ($M+H^+$ - His - $C(O)CH_2CH(NH_2)COOH$, 68%). λ_{max} 267 and 372 nm.

L-Lysyl-3-hydroxy-DL-kynurenine (Lys-3OHKyn): $M+H^+$, 354.167364 Da. Calculated for $C_{16}H_{24}N_3O_6$: $M+H^+$, 354.166511 Da; ^{1}H NMR δ (MeOD) 7.26 (1H, dd, *J* 1.0, 8.1, ArH-6), 6.87 (1H, dd, *J* 1.0, 7.9, ArH-4), 6.49 (1H, dd, *J* 7.9, 8.1, ArH-5), 4.31 (1H, m, H-2), 3.94 (1H, m, C<u>H</u>NH_2), 3.76 (2H, m, H-3), 3.18 (2H, m, NH-C<u>H</u>$_2$), 1.95 (2H, m, CH_2CH_2C<u>H</u>$_2$), 1.84 (2H, m, C<u>H</u>$_2CH_2CH_2$), 1.57 (2H, m, CH_2C<u>H</u>$_2CH_2$); ^{13}C NMR δ (MeOD) 197.7 (CO-4), 170.8 (CO-1), 170.8 (NH_2CH<u>C</u>OOH), 145.3 (ArC-3), 142.0 (ArC-2), 121.2 (ArC-6), 117.3 (ArC-4), 116.2 (ArC-1), 114.8 (ArC-5), 56.6 (C-2), 52.7 (<u>C</u>HNH_2), 47.3 (NH<u>C</u>H_2), 38.5 (C-3), 30.0 (CH_2-CH_2-<u>C</u>H_2), 25.5 (<u>C</u>H_2-CH_2-CH_2), 22.2 (CH_2-<u>C</u>H_2-CH_2); ES-MS/MS *m/z* 354.1 ($M+H^+$, 28%), 208.1 ($M+H^+$ - Lys, 15%), 203.2 (100%), 162.0 ($M+H^+$ - Lys - HCOOH, 7%), 152.0 (50%), 147.1 ($M+H^+$ - 3OHKyn, 31%), 128.0 (80%), 110.0 ($M+H^+$ - Lys - $C(O)CH_2CH(NH_2)COOH$, 9%). λ_{max} 269 and 372 nm.

5.4.9 Preparation of BLP[117]

Fresh bovine eyes (≤ 2 years old) were obtained from Ziems Butcher (Corrimal, NSW, Australia). The lenses were immediately removed from each eyeball and lens capsule, and stored at -20°C until processed. Tris-HCl buffer (50 mM, pH 7.2) containing EDTA (5 mM), PMSF (1 mM), DTT (1 mM) and NaN_3 (0.04%, w/v) was homogenised with lenses (2 mL/lens). Insoluble material was pelleted by centrifugation at 12,000 rpm at 5°C for 15 min. The supernatant was removed and dialysed against Milli-Q water and lyophilised. BLP were stored at -20°C until used.

5.4.10 Modification of BLP with UV filters[18,247]

BLP (10 mg/mL) and UV filters (Kyn, 3OHKyn, 3OHKG, AHB and AHA, 2 mg/mL) were dissolved in argon-gassed (~20 min) Na_2CO_3/$NaHCO_3$ buffer (50 mM, pH 9.5) or in NaH_2PO_4/Na_2HPO_4 buffer (100 mM, pH 7.2). Chloroform was added (100 µL/10 mL) as an antibacterial agent and the reaction vial was sealed, wrapped in aluminium foil and incubated at 37°C for 48 h (pH 9.5; Kyn, 3OHKyn, 3OHKG, AHA, AHB and pH 7.2; 3OHKyn, AHA, AHB) or 14 days (pH 7.2; 3OHKG). The coloured (pale yellow and brown) mixtures were separately dialysed against NaH_2PO_4/Na_2HPO_4 buffer (1 mM, pH 5.5-6) for 48 h with 5 buffer changes. The buffer from the first dialysis step was collected, lyophilised and analysed by RP-HPLC. The collected protein samples were lyophilised and stored under argon at -20°C until used.

5.4.11 Acid hydrolysis of UV filter-treated proteins[20]

Unmodified BLP or UV filters-treated BLP (10 mg) at both pH 9.5 or 7.2 was hydrolysed in an evacuated hydrolysis tube with HCl (6 M, 0.95 mL), thioglycolic acid (5%, v/v) and phenol (1%, w/v) for 24 h at 110°C. The samples were lyophilised, dissolved in aqueous TFA (0.05%, v/v) and purified by RP-HPLC.

5.4.12 Stability of AHA at pH 9.5

AHA (2.7 mmol/L) was dissolved in argon-gassed (~20 min) Na_2CO_3/$NaHCO_3$ buffer (50 mM) and the pH adjusted to 9.5 by dropwise addition of 1 M NaOH. The resulting solution

was gassed with argon, sealed and incubated at 37°C in the dark for 48 h. Duplicate aliquots were taken at 0, 1, 2, 3, 4, 6, 9, 24, 32 and 48 h and examined by RP-HPLC.

5.4.13 Stability of AHB at pH 9.5

AHB (0.45 mmol/L) was prepared as described above for the AHA stability experiment. Triplicate aliquots were taken at 0, 1, 2, 4, 6, 9, 12, 24, 30, 37 and 48 h. One aliquot from each sampling was acidified to pH ~5.5 with 1 M AcOH and all samples were examined by RP-HPLC.

5.4.14 Extraction of unbound UV filters from modified proteins

BLP (10.0-10.5 mg) treated with 3OHKyn, 3OHKG, AHB or AHA were dissolved in cold and argon-gassed (~20 min) guanidine hydrochloride (6 M, pH 5.5, 2 mg protein/mL), and stirred at RT for 30-40 min in the dark. The mixture was poured into the protein concentrator and spun at 4700 G at 4°C. The concentrated BLP were washed twice with guanidine hydrochloride (6 M, pH 5.5). The concentrated proteins (~150 μL) and the combined filtrates were separately lyophilised. The protein samples were hydrolysed in 6 M HCl for 24 h (Section 5.4.11) and analysed by RP-HPLC. The dried guanidine hydrochloride filtrates were extracted with CH_3CN (3 x ~10 mL) and dried on a rotary evaporator. The collected solids were redissolved in buffer A and analysed by RP-HPLC, as previously described for protein acid hydrolysates. The extraction and acid hydrolysis procedure was repeated with unmodified protein used as a negative control.

5.4.15 Stability of UV filters and amino acid adducts under acid hydrolysis

A known quantity (0.2-1 mg) of UV filter (3OHKG, Cys-3OHKG, AHB and AHA) or a mixture of unmodified protein (~10 mg) and free UV filter (3OHKG, Cys-3OHKG, AHB and AHA, 0.2-1 mg) were hydrolysed in duplicate and analysed by RP-HPLC, as described previously for protein acid hydrolysates. The samples of hydrolysed free UV filters were additionally analysed by LC-MS.

CHAPTER 6

EFFECT OF UV LIGHT ON UV FILTER-TREATED LENS PROTEINS

The overall aims of this chapter were to investigate the responsiveness of UV filter-modified lens proteins upon exposure to UV light and determine whether protein bound UV filters act as photosensitisers of oxidative damage.

6.1 Introduction

The lens is chronically exposed to light of wavelengths > 300 nm during the lifetime of an individual.[396] The majority of the UV light (*i.e.* that with wavelengths between 300 and 400 nm) that reaches the lens is absorbed by UV filter compounds, such as Kyn, 3OHKyn and 3OHKG.[79,80] Even though these species have high extinction coefficients for light of these wavelengths, and hence are highly effective UV-absorbing compounds, they are poor sensitisers of the formation of excited state (*e.g.* $^1O_2$) or radical species. Therefore they have been proposed to prevent photo-oxidative damage.[79,246] After middle age the concentration of the free UV filters decreases markedly.[39,176] At the same time the levels of bound UV filters increase, which occurs *via* deamination and binding to nucleophilic sites on lens proteins.[18,176] The photochemical behaviour of these protein-bound species is much less well understood than that of the free species, and it has been postulated that these UV-absorbing protein-bound chromophores may initiate oxidative damage to lens proteins.

Photo-oxidation of proteins is known to occur either through Type I (direct) photo-oxidation or Type II (indirect) photo-oxidation.[90,234,397] In the former process UV light absorbed by protein side chains or protein-bound chromophores results in the formation of excited state species or radicals. In the latter process UV light energy absorbed by chromophores is transferred to ground state species (*e.g.* O_2) resulting in excited state species or radicals (*e.g.* $^1O_2$, $O_2^{\cdot-}$, $HO^{\cdot}$). These reactive oxygen species can undergo further reactions to yield H_2O_2, $ROO^{\cdot}$ and organic hydroperoxides (ROOH).[31] The majority of these species react rapidly with molecules, such as proteins, lipids and DNA, chemically modifying them.[31,396,398] As proteins are present in the human lens at a high concentration,[31,399] they are a major site of damage by reactive oxygen species. These reactions are known to result in protein aggregation, oxidation of amino acid side chains, denaturation, conformational change and loss of enzyme

activity.[11,397] The mechanisms and agents that bring about such oxidation in the human lenses are incompletely understood.

Recently, it has been demonstrated that exposure of protein-bound Kyn to wavelengths of light that penetrate the lens can initiate oxidative damage to lens proteins *via* $^1O_2$-mediated photo-oxidation. This covalent binding of Kyn to lens proteins resulted in the transformation of this compound, which in the free state is protective, to species that are capable, upon UV illumination, of generating H_2O_2, protein peroxides and oxidation of protein-bound tyrosine (Tyr) residues to di-tyrosine (di-Tyr) and 3,4-dihydroxyphenylalanine (DOPA).[247]

The aim of this study was therefore to examine whether the other major UV filters, 3OHKyn and 3OHKG, also induce oxidant formation and protein damage on exposure to UV light in either their protein-bound or free form. In particular, their role in the generation of protein-bound or free peroxides (**Part A**) and oxidation of amino acid side chains (Tyr and Phe; **Part B**) on lens proteins was examined. The role of Type I versus Type II photo-chemistry in protein damage was investigated. An additional aim was to investigate reactivity of the two related novel filter compounds, AHA and AHB, with UV light. As discussed in Chapter 5, these do not bind covalently to lens proteins. Furthermore, the role of UV light in the formation of protein aggregates from UV filter-modified lens proteins was investigated (**Part C**).

6.2 Results and Discussion

BLP were modified with Kyn, 3OHKyn and 3OHKG at pH 9.5, as described in Chapter 5. The Kyn-modified proteins were used as a positive control and for comparison with the data of Parker *et al*.[247] As detailed in Chapter 5, Kyn, 3OHKyn and 3OHKG were preferentially bound at the Cys residues with the levels of Cys-Kyn, Cys-3OHKG (Cys-3OHKyn after hydrolysis) and Cys-3OHKyn being 0.96 mol per mol of protein, 0.40-0.78 mol per mol of protein and 0.05-0.64 mol per mol of protein, respectively. The level of Cys-Kyn, in the Kyn-modified lens proteins, was similar to that reported by Parker *et al*.[247]

Part A

6.2.1 Determination of peroxides

Kyn-, 3OHKyn- and 3OHKG-modified lens proteins, together with non-modified samples, were dissolved in H_2O (pH ~7) and illuminated using a broad spectrum mercury arc UV lamp through a 305 nm cut-off filter, unless otherwise stated. The intensity of light passed through this filter was of particular interest, as shorter wavelengths are of greater energy and therefore have the potential to induce greater biological damage.[225] Although longer wavelengths are less energetic, they penetrate the eye more deeply, and hence are also of biological interest.[225]

In these experiments the light intensity emitted from the broad spectrum mercury arc UV lamp through a 305 nm cut-off filter was 0.19 $\mu W/cm^2$ (UVB) and 1.29 mW/cm^2 (UVA) (measured using a OL-754 Spectroradiometer; Optronic Laboratories, Inc.), which is 1.5% of UVB and 98.5% UVA. This UV light intensity is of a similar magnitude to ambient UV light exposure experienced in Sydney (NSW, Australia) at midday on a sunny day (September 2006), which has been measured as 32.6 $\mu W/cm^2$ (UVB) and 0.61 mW/cm^2 (UVA) (5.1% of UVB and 95.9% UVA) by Linda MacDonald (Dermatology Research Laboratories, University of Sydney, Sydney, NSW). These figures are known to vary with the latitude, time of day (solar zenith angle) and geometry of exposure.[226,245] These values are comparable to an average determined for the 48 states of USA taken over a period of one year of 0.16 mW/cm^2 (UVB) and 4.47 mW/cm^2 (UVA) or 3.4% of UVB and 96.6% of UVA.[400] The spectral irradiances and light intensities of UV light emitted from the broad spectrum mercury arc UV lamp through the 305, 345 and 385 nm cut-off filters used in this study are summarised in the Experimental section.

Aliquots from the illuminated samples, or control incubations kept in the dark, were taken at 0, 15, 30, 60 and 120 min and diluted to 1/10, 1/25 and 1/50 with water to obtain triplicate readings for each dilution. The prepared samples were subsequently assayed for peroxides by use of a modified ferrous oxidation-xylenol orange (FOX) assay.[401-403] This assay is a colourimetric method based upon the oxidation of ferrous (Fe^{2+}) to ferric (Fe^{3+}) ions by peroxides and subsequent binding of the Fe^{3+} ion to the dye xylenol orange. The Fe^{3+}-xylenol orange chromogen absorbs strongly at λ_{max} 560 nm.

6.2.1.1 Kyn-, 3OHKyn- and 3OHKG-modified bovine lens proteins

The samples were continuously gassed with air during the illumination to mimic the oxygenated environment present in cataractous lenses, albeit with higher O_2 levels. Higher yields of peroxides were detected in the illuminated samples compared to non-illuminated, with the levels of peroxides also dependent on the nature of the protein modification (Figure 6.1). Thus, the extent of peroxide formation from the modified proteins decreased in the order 3OHKyn (60 μM peroxides) > Kyn (29 μM peroxides) ≃ 3OHKG (22 μM peroxides). The data for 3OHKyn were statistically different from the latter two at all of the non-zero time points, as assessed by one-way ANOVA with Tukey's post hoc-test. The values for the Kyn- and 3OHKG-modified lens proteins were not statistically different to each other. Control samples of modified lens proteins that were not exposed to illumination gave peroxide values of ≤ 8 μM at all time points. Illuminated and non-illuminated unmodified lens proteins gave peroxide values of ≤ 6 μM.

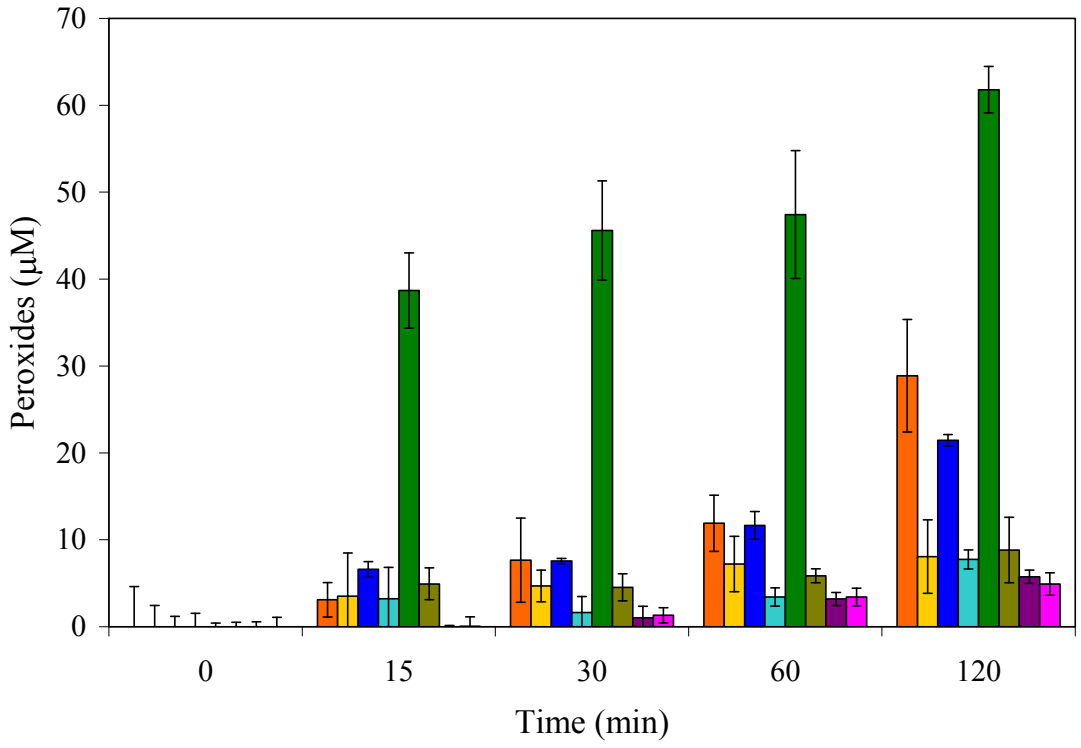

Figure 6.1: Concentration of peroxides generated following illumination of Kyn-modified lens protein (0.96 mol of Cys-Kyn per mol protein,) at 4°C and pH ~7 and corresponding non-illuminated control ( ); 3OHKG-modified lens protein (0.74 mol of Cys-3OHKyn per mol protein,) and corresponding non-illuminated control ( ); 3OHKyn-modified lens protein (0.05 mol of Cys-3OHKyn per mol protein,) and corresponding non-illuminated control ( ); and unmodified lens proteins ( ) and corresponding non-illuminated control ( ). Equal concentrations of protein (1 mg/mL) were used in each case. Data are means ± SD of triplicate measurements from a single experiment typical of several.

6.2.1.2 Determination of peroxide yield-dependency on the level of protein-bound 3OHKG and 3OHKyn

The effect of different concentrations of bound 3OHKG and 3OHKyn on the formation of peroxides was investigated using 3OHKG- and 3OHKyn-modified protein samples that had different levels of bound UV filters as determined by acid hydrolysis. Illumination of these modified BLP through a 305 nm UV filter and subsequent analysis for peroxides indicated that the yield of peroxides generated from 3OHKG-modified lens proteins was dependent on the concentration of bound 3OHKG, with a greater degree of 3OHKG modification producing a higher peroxide yield (Figure 6.2, A). Data for all three 3OHKG-modified lens protein samples were statistically different to each other at the 120 min time point by one-way ANOVA with Tukey's post hoc-test. A similar dependency was reported for Kyn-modified lens proteins.[247] In contrast, the yield of peroxides generated upon illumination of 3OHKyn-modified lens proteins showed no dependency on the concentration of bound 3OHKyn (Figure 6.2, B). This was not surprising as 3OHKyn is prone to oxidation and the formation of oxidation products, which although present were not determined by acid hydrolysis of 3OHKyn-modified lens proteins. These oxidation products may, therefore, also contribute towards peroxide production. Data for peroxides generated in the 3OHKyn-modified lens protein sample with the lowest amount of bound 3OHKyn (0.05 mol of Cys-3OHKyn per mol protein) were statistically different to the other two 3OHKyn-modified lens protein samples with higher amounts of bound 3OHKyn (0.08 and 0.64 mol of Cys-3OHKyn per mol protein) at the 120 min time point by one-way ANOVA with Tukey's post hoc-test.

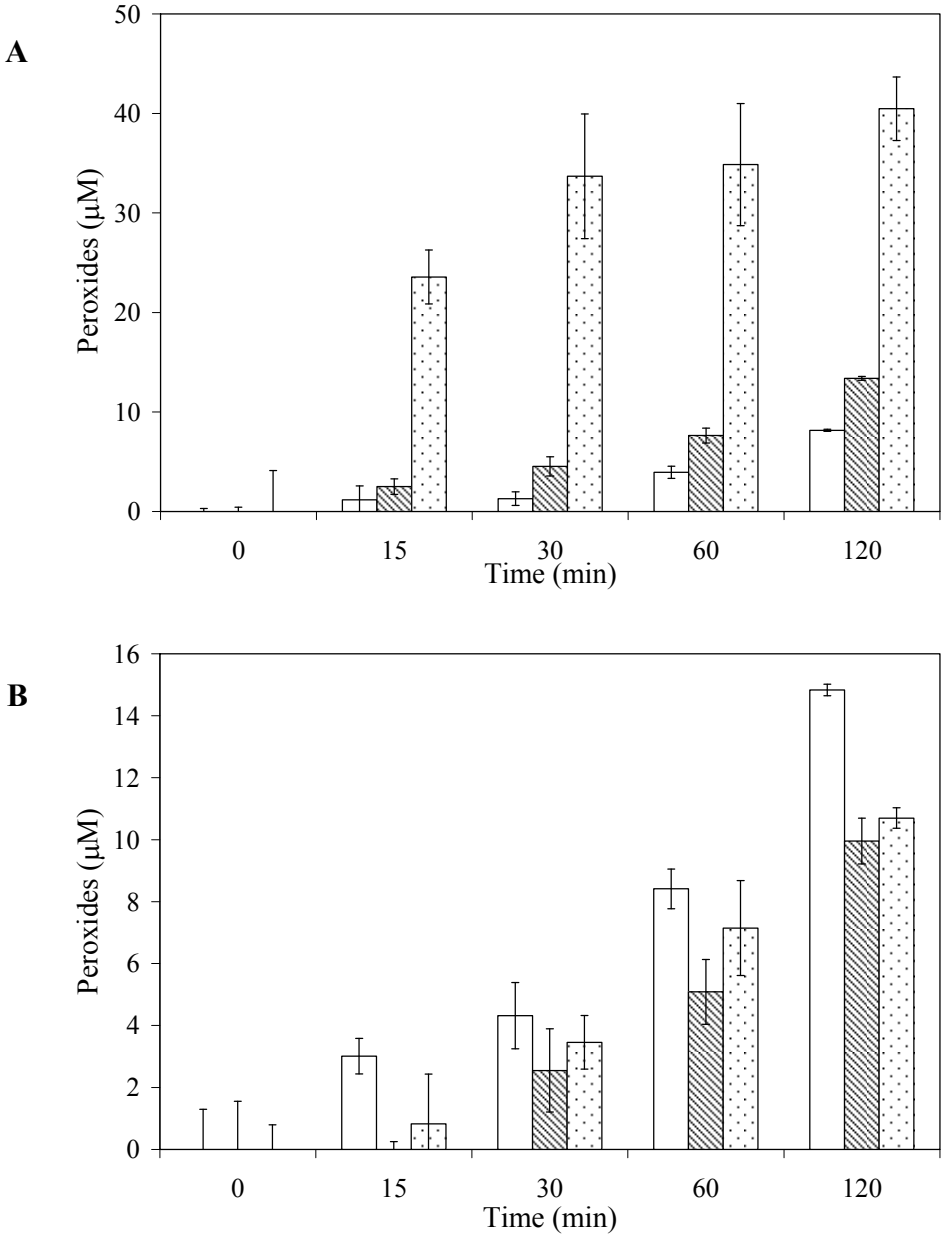

Figure 6.2: Effect of the level of UV filter modification on peroxide yield. Concentration of peroxides generated following illumination of **A**) 3OHKG-modified lens proteins (0.40 mol of Cys-3OHKyn per mol protein; white bar, 0.78 mol of Cys-3OHKyn per mol protein; striped bar, and 1.14 mol of Cys-3OHKyn per mol protein; dotted bar) and **B**) 3OHKyn-modified lens proteins (0.05 mol of Cys-3OHKyn per mol protein; white bar, 0.08 mol of Cys-3OHKyn per mol protein; striped bar, and 0.64 mol of Cys-3OHKyn per mol protein; dotted bar) at 4°C and pH ~7. Equal concentrations of protein (1 mg/mL) were used in each case. Data are means ± SD of triplicate measurements from a single experiment typical of several.

6.2.1.3 Determination of wavelength-dependency

The yield of peroxides detected from 3OHKG-modified lens proteins (0.74 mol of Cys-3OHKyn per mol protein) was found to be dependent on the wavelength of incident light, with the highest yields of peroxides detected with the shortest wavelengths of UV light

(Figure 6.3). Data for the 385 nm filter were statistically different to that for the 345 and 305 nm filters at the 120 min time point by one-way ANOVA with Tukey's post hoc-test.

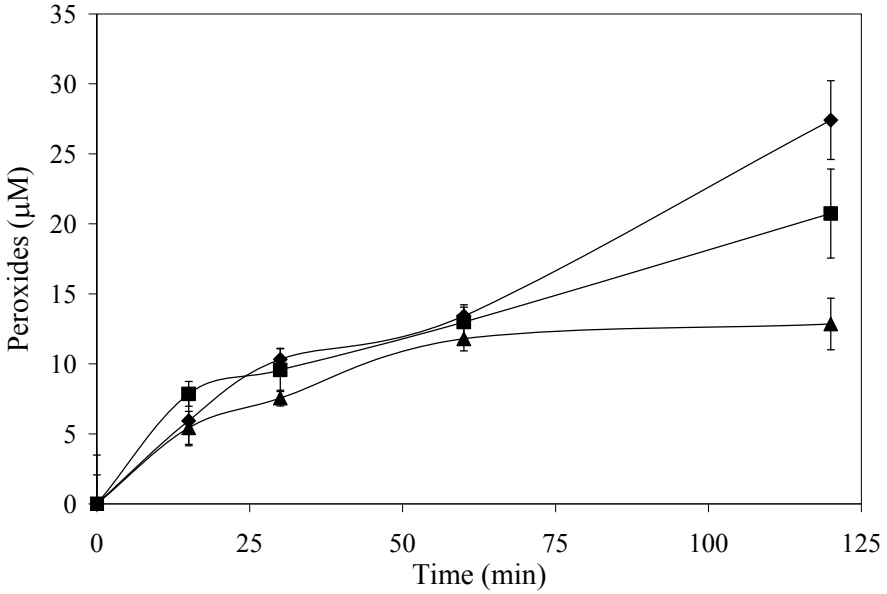

Figure 6.3: Effect of wavelength of illuminating light on peroxide production by 3OHKG-modified lens proteins (0.74 mol of Cys-3OHKyn per mol protein, 1 mg protein/mL) at 4°C and pH ~7. Illumination was carried out as described in the Experimental section using filters which cut-off the transmitted light at 305 (♦), 345 (■) and 385 (▲) nm. Data are means ± SD of triplicate measurements from a single experiment typical of several.

6.2.1.4 Determination of O_2-dependency

The effect of an oxygenated (air) versus N_2 atmosphere on peroxide production was examined by quantifying peroxide formation following illumination of protein samples modified by 3OHKG and 3OHKyn (Figure 6.4, A and B). Water at pH ~7 was gassed with N_2 for ~20 min prior to protein addition. In the absence of such a treatment an increase in peroxide production, similar to the control samples that had been gassed with air, was observed. The samples under N_2 atmosphere were continuously gassed with N_2 during the experiment. With both 3OHKG- and 3OHKyn-modified lens proteins there was a statistically greater yield of peroxides generated under an atmosphere of air compared to N_2 at all non-zero time points, as assessed by Student's *t*-test. This indicated as expected that peroxide formation is an O_2-dependent process.

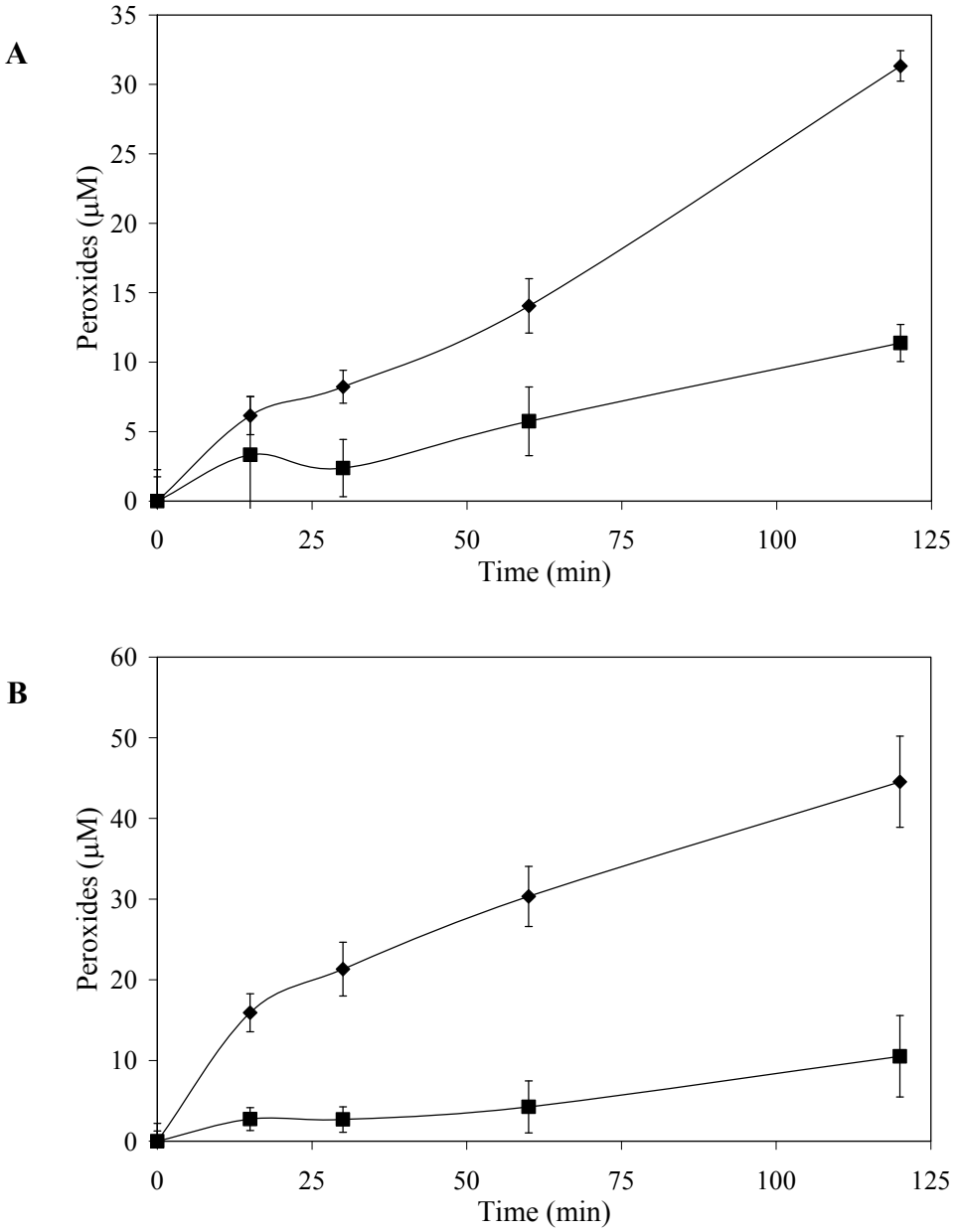

Figure 6.4: Effect of air (♦) and N_2 (■) atmospheres on the yield of peroxides formed at 4°C and pH ~7 during illumination of **A**) 3OHKG-modified lens proteins (1 mg protein/mL, 0.74 mol of Cys-3OHKyn per mol protein) and **B**) 3OHKyn-modified lens protein (1 mg protein/mL, 0.05 mol of Cys-3OHKyn per mol protein). Modified protein samples illuminated under an air atmosphere were statistically different to the samples illuminated under N_2 at the 60 and 120 min time points as assessed by Student's *t*-test. Data are means ± SD of triplicate measurements from a single experiment typical of several.

6.2.1.5 Determination of $^1O_2$ role

In order to examine the role of $^1O_2$ (formed by the transfer of energy to ground state molecular oxygen) in peroxide production, 3OHKG- and 3OHKyn-modified lens proteins were illuminated in buffers made up using D_2O. D_2O is known to extend the lifetime of $^1O_2$ by ~10-fold.[404-406] The presence of D_2O resulted in higher yields of peroxides compared to H_2O and was approximately twice that observed in H_2O at both the 60 and 120 min time points

examined (Figure 6.5, A and B). Addition of catalase, which removes H_2O_2 enzymatically ($H_2O_2 \rightarrow H_2O + ½O_2$),[407,408] to samples of 3OHKG- or 3OHKyn-modified lens proteins that had been illuminated for either 60 or 120 min resulted in a significant decrease in the peroxide yields by ~2.3-3.6 fold when compared to non-catalase-treated samples in both H_2O and D_2O buffers. It was therefore evident that peroxides detected upon illumination of modified lens proteins were primarily H_2O_2 and possibly minor amounts of protein-bound peroxides.

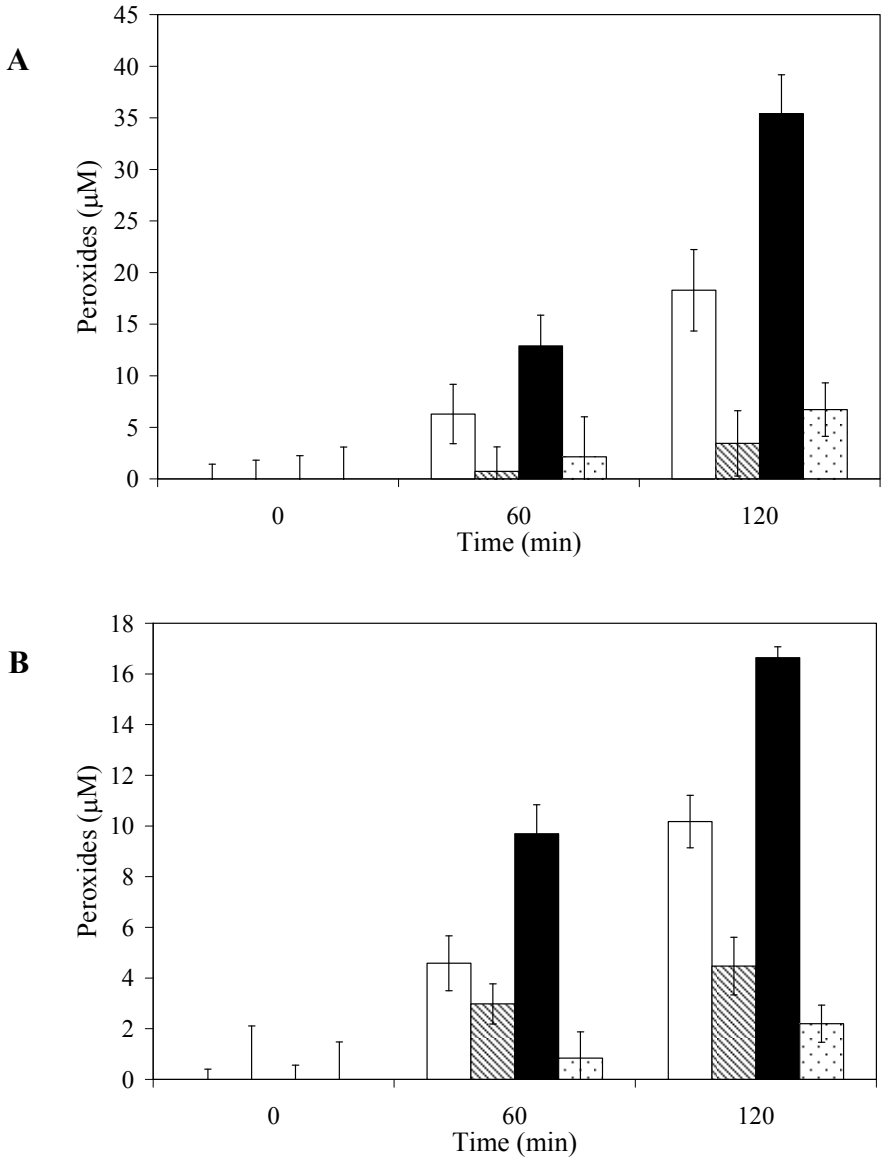

Figure 6.5: Effect of buffers made up using H_2O (white and striped bars) versus D_2O (black and dotted bars) on peroxide formation at 4°C and pH / pD 7, from **A**) 3OHKG-modified lens protein (0.40 mol of Cys-3OHKyn per mol protein) and **B**) 3OHKyn-modified lens protein (0.05 mol of Cys-3OHKyn per mol protein). Catalase was added to some of the samples immediately after the cessation of illumination (striped and dotted bars); controls (white and black bars) did not have catalase added. 3OHKG-modified lens proteins (2 mg/mL) and 3OHKyn-modified lens proteins (0.5 mg/mL) made up in D_2O were statistically different from the samples made up in H_2O at the 120 min time point as assessed by one-way ANOVA with Tukey's post hoc-test. The samples made up in D_2O and H_2O at the 0 min time point were not significantly different from the illuminated samples with added catalase at the 120 min time point. Data are means ± SD of triplicate measurements from a single experiment typical of several.

3OHKyn-modified lens proteins were then exposed to UV light in the presence of 10 mM sodium azide, which is a potent scavenger of $^1O_2$ ($N_3^- + {}^1O_2 \rightarrow N_3^{\cdot} + O_2^{\cdot -}$).[409,410] This resulted in a statistically-significant decrease (~2.4 fold) in peroxide formation compared to the samples illuminated in the absence of sodium azide at all time points examined (Figure 6.6). In the absence of light, sodium azide had no effect on the peroxide yield. These data for 3OHKyn-modified proteins are consistent with, but do not prove that, peroxide formation is being mediated by $^1O_2$. This suggests the major mechanism that occurs upon irradiation of the 3OHKyn-modified lens proteins is Type II photo-chemistry.[164,411] This is consistent with previous studies where the reaction of $^1O_2$ with proteins resulted in significant yields of free and protein-bound peroxides.[401,412] In contrast, illumination of 3OHKG-modified protein (0.74 mol of Cys-3OHKyn per mol protein at 1 mg/mL and 1.5 mg/mL) in the presence of sodium azide (5 mM or 10 mM) did not significantly affect the yield of peroxides detected over a 120 min illumination period when compared to the samples exposed in an identical manner except in the absence of azide (*e.g.* 17.52 ± 2.76 μM for illuminated sample (1 mg/mL) in the presence of 10 mM sodium azide, 21.45 ± 0.65 μM for illuminated sample (1 mg/mL) in the absence of sodium azide, 6.54 ± 2.09 μM for non-illuminated sample (1 mg/mL) in the presence of 10 mM sodium azide, 7.74 ± 1.10 μM for non-illuminated sample (1 mg/mL) in the absence of sodium azide, $p > 0.05$, after 120 min). This suggests that $^1O_2$ mediated reactions may be less important in peroxide formation from illuminated 3OHKG-modified lens proteins compared to 3OHKyn-modified lens proteins. In both cases, a contribution arising from superoxide radical ($O_2^{\cdot -}$) formation can not be eliminated. $O_2^{\cdot -}$arises from an electron transfer from a sensitiser to molecular oxygen. This process competes with the formation of $^1O_2$, however the latter reaction usually has a higher rate constant, k ~1-3 x 10^9 versus $k \leq 1 \times 10^7$ dm^3 mol^{-1} s^{-1}.[234] The involvement of the $O_2^{\cdot -}$ in peroxide formation has been postulated by Linetsky *et al.*,[162,258] where UVA (> 338 nm, 1.5 kJ/cm^2) dependent H_2O_2 formation was observed upon illumination of water-insoluble proteins from aged human lenses (55-75 years). The yield of H_2O_2 increased by 50% from 50 μM on addition of the superoxide dismutase and was abolished by catalase. Superoxide dismutase is an enzyme that catalyses the dismutation of $O_2^{\cdot -}$ to H_2O_2 and O_2 ($2O_2^{\cdot -} + 2H^+ \rightarrow H_2O_2 + O_2$).[64]

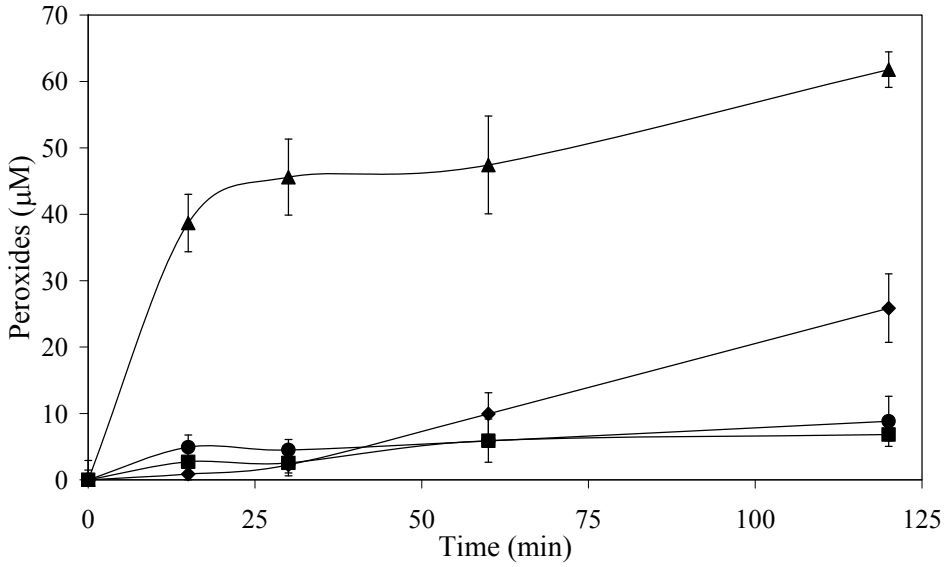

Figure 6.6: Effect of sodium azide (10 mM; ♦,■) on the formation of peroxides following illumination of 3OHKyn-modified lens protein (1 mg protein/mL, 0.05 mol of Cys-3OHKyn per mol protein) compared to samples with no added sodium azide (▲,●) at 4°C and pH ~7. Control samples, with (■) or without (●) azide were incubated in the dark for 120 min. Data in the presence of sodium azide were statistically different to the samples in the absence of sodium azide. Both illuminated samples were statistically different from the non-illuminated samples in either the presence or absence of sodium azide, as assessed by one-way ANOVA with Tukey's post hoc-test. Data are means ± SD of triplicate measurements from a single experiment typical of several.

6.2.1.6 Role of free 3OHKyn and 3OHKG and their Cys adducts in peroxide formation

The role of free UV filters and their Cys adducts in generating peroxides was examined by illuminating free 3OHKG and 3OHKyn, and their Cys adducts, in the presence of unmodified BLP (Figure 6.7, A and B). The amount of UV filters and their Cys adducts used in these experiments was based on the concentration of the Cys adducts recovered upon acid hydrolysis of 3OHKG- and 3OHKyn-modified lens proteins. 3OHKG and the Cys adducts of 3OHKG and 3OHKyn were synthesised and characterised, as described in Chapters 2, 4 and 5. 3OHKyn was commercially available. Unmodified protein samples illuminated in the absence of added compounds were used as a negative control and 3OHKG- or 3OHKyn-modified lens proteins as a positive control.

The presence of the Cys adducts or free 3OHKG and 3OHKyn did not result in a significant increase in peroxide production upon illumination when compared to the unmodified illuminated samples. In contrast, 3OHKG- and 3OHKyn-modified proteins showed a significant increase in peroxide production compared to the other samples, suggesting that 3OHKG and 3OHKyn, when bound to lens proteins, become more susceptible to photo-oxidation by UV light to which the lens is exposed.

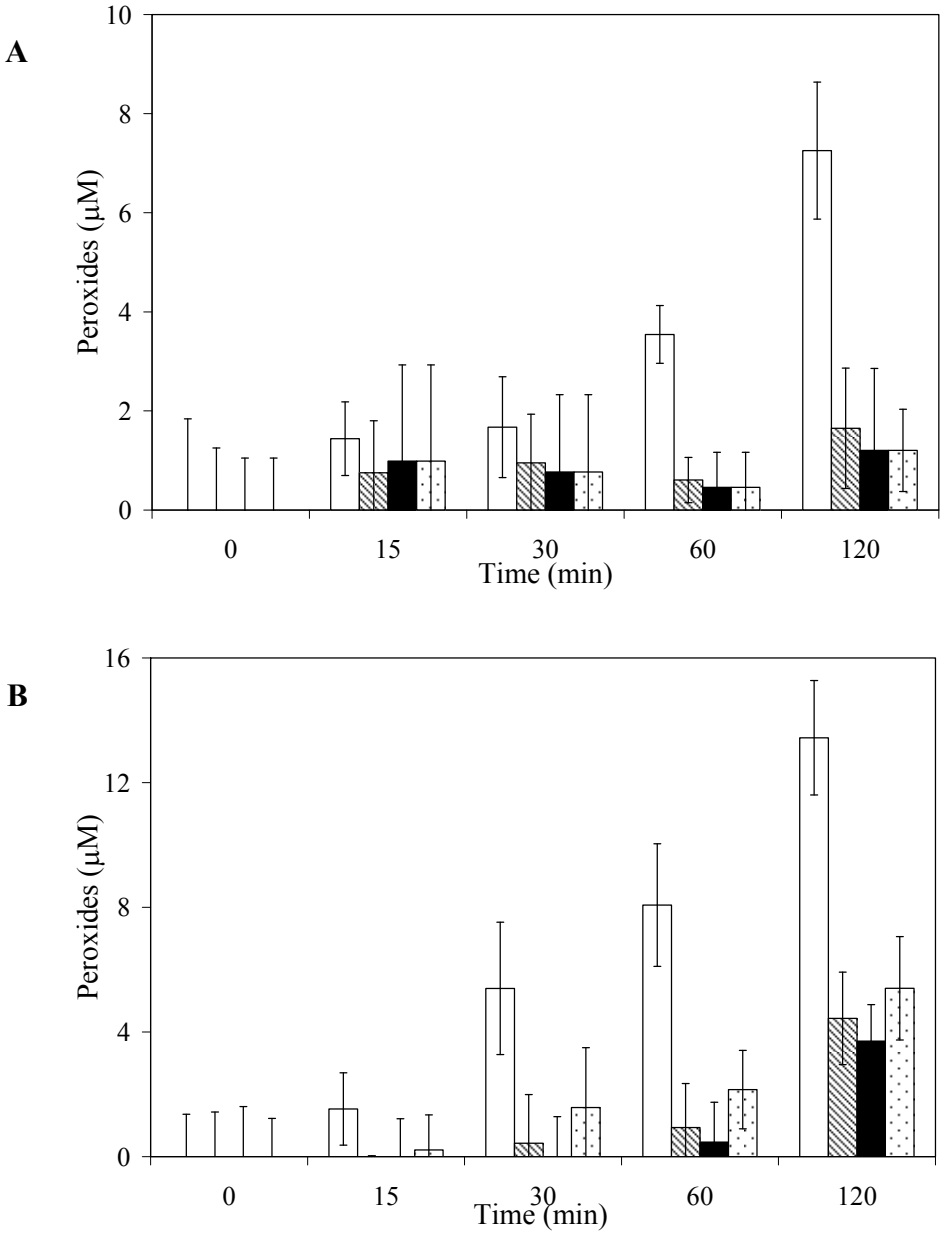

Figure 6.7: Effect of protein-bound versus protein-free UV filters on peroxide yield. Peroxide formation following illumination of **A**) 3OHKG-modified lens proteins (1 mg protein/mL, 0.78 mol of Cys-3OHKyn per mol protein; white bars) and **B**) 3OHKyn-modified lens proteins (1 mg protein/mL, 0.64 mol of Cys-3OHKyn per mol protein; white bars) compared to unmodified lens proteins with added free UV filters and free Cys amino acid adducts. Unmodified lens proteins (1 mg protein/mL, dotted bars) were illuminated in the presence of **A**) free 3OHKG (38.9 μM, striped bars) or free Cys-3OHKG adduct (38.9 μM, black bars), and **B**) free 3OHKyn (31.7 μM, striped bars) or free Cys-3OHKyn adduct (31.7 μM, black bars). Illuminated 3OHKG- and 3OHKyn-modified lens proteins samples were statistically different from the unmodified lens proteins in the presence or absence of free UV filters or free Cys-UV filter adducts as assessed by one-way ANOVA with Tukey's post hoc-test. Data are means ± SD of triplicate measurements from a single experiment typical of several.

In order to determine whether the results described above reflect a change in photochemical behaviour or are a concentration dependent phenomenon, analogous experiments were carried out with higher concentrations (1 mg/mL) of free 3OHKG and 3OHKyn in the absence of added proteins. Illumination of free 3OHKyn under these conditions resulted in the detection

of significantly elevated levels of peroxides when compared to non-illuminated samples (by ~2.2 fold) (Figure 6.8). This is consistent with the known cytotoxicity of 3OHKyn at concentrations as low as 1 μM, causing oxidative stress through the formation of H_2O_2.[413,414] It is believed that H_2O_2 is formed from reduction of O_2 by the radical anion of 3OHKyn to generate $O_2^{\cdot-}$, followed by dismutation of $O_2^{\cdot-}$ to H_2O_2 *via* the following reaction $2O_2^{\cdot-} + 2H^+ \rightarrow H_2O_2 + O_2$ (Scheme 6.1).[205,212] Since two $O_2^{\cdot-}$ molecules dismutate to produce one molecule of H_2O_2, approximately 1 mol of H_2O_2 is generated per 1 mol of 3OHKyn.[205] In contrast, much lower levels of peroxides were detected with free 3OHKG, and these levels were not significantly different from the levels detected with the non-illuminated material (Figure 6.8). This indicates that free 3OHKG in human lenses may not act as a source of H_2O_2 and that conjugation of the phenolic group with glucose acts to minimise oxidative stress in the lens.

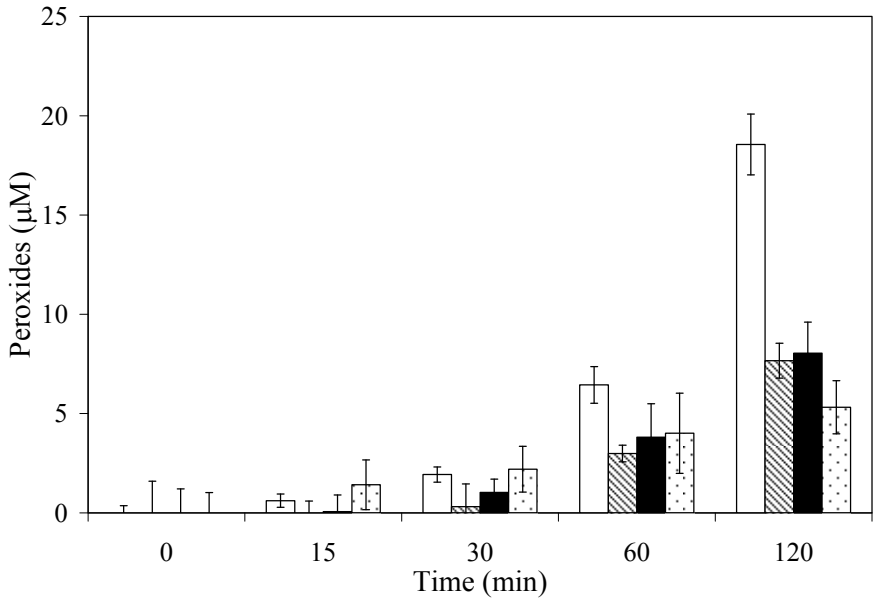

Figure 6.8: Peroxide formation from free 3OHKyn (white and striped bars) and free 3OHKG (black and dotted bars) (4.5 mM and 2.6 mM, respectively, in H_2O at 4°C and pH ~7), following illumination (white and black bars) or incubation in the dark (striped and dotted bars) for 120 min. The peroxide levels detected with illuminated 3OHKyn were statistically different from the non-illuminated control at 60 and 120 min time points as assessed by Student's *t*-test. The peroxide levels detected from the illuminated and control 3OHKG samples were not statistically different. Data are means ± SD of triplicate measurements from a single experiment typical of several.

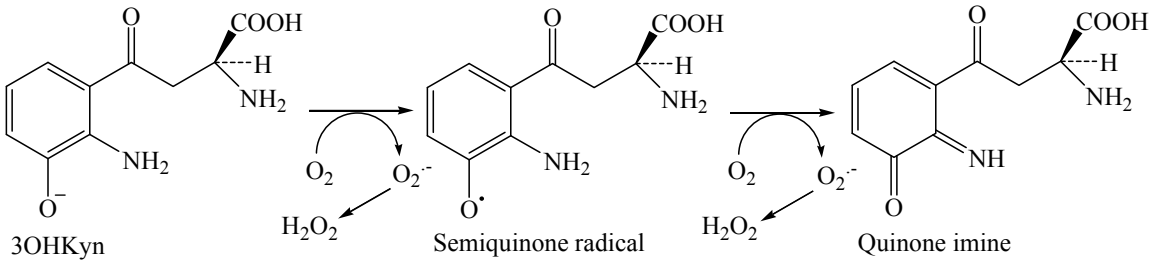

Scheme 6.1: Mechanism of H_2O_2 formation *via* 3OHKyn auto-oxidation.[205]

6.2.1.7 Role of AHB- and AHA-treated BLP and free AHB and AHA in peroxide formation

In Chapter 5, it was shown that the novel Trp-derived UV filter compounds, AHB and AHA, do not bind covalently to BLP, although they associate non-covalently with the polypeptides. Even though AHB and AHA do not appear to form covalent adducts with lens proteins, they may still act as efficient sensitisers for peroxide formation.

Therefore, lens proteins treated with AHB and AHA at pH 9.5 (as described in Chapter 5) were illuminated using a broad spectrum mercury arc UV lamp through a 305 nm cut-off filter and analysed using a FOX assay. The illuminated lens protein samples with (non-covalently) associated AHB (0.09 mol AHB/mol protein) contained peroxides, though these levels were not statistically greater than those detected with control samples that had been kept in the dark (Figure 6.9, A). The peroxide levels detected from these illuminated samples were however greater than those detected with unmodified BLP to which AHB (4.8 mM) had been freshly added and subsequently illuminated, or for control unmodified proteins subjected to illumination or kept in the dark in the absence of any added compound (Figure 6.9, A). The trend towards a higher level of peroxides in the samples with associated AHB, compared to those with freshly added AHB, or no AHB, was investigated in further experiments where higher concentrations of AHB (1 mg/mL) were exposed to light (or kept in the dark) at pH ~7 for up to 120 min in the absence of protein (Figure 6.9, B). Significantly higher levels of peroxides were detected in the illuminated, compared to dark samples, with these values increasing in a time-dependent manner. A time-dependent increase in peroxide level was also observed with the samples kept in the dark. This was most likely a result of the *o*-aminophenol moiety undergoing auto-oxidation with consequent formation of $O_2^{\cdot-}$ and hence H_2O_2 (Scheme 6.1).[205,212] This suggests that AHB, similarly to 3OHKyn, being an *o*-aminophenol may be involved in oxidative processes in the human lenses. However, peroxide production was significantly higher for 3OHKyn (~19 μM) compared to AHB (~10 μM) at concentrations of 4.5 mM and 4.8 mM, respectively.

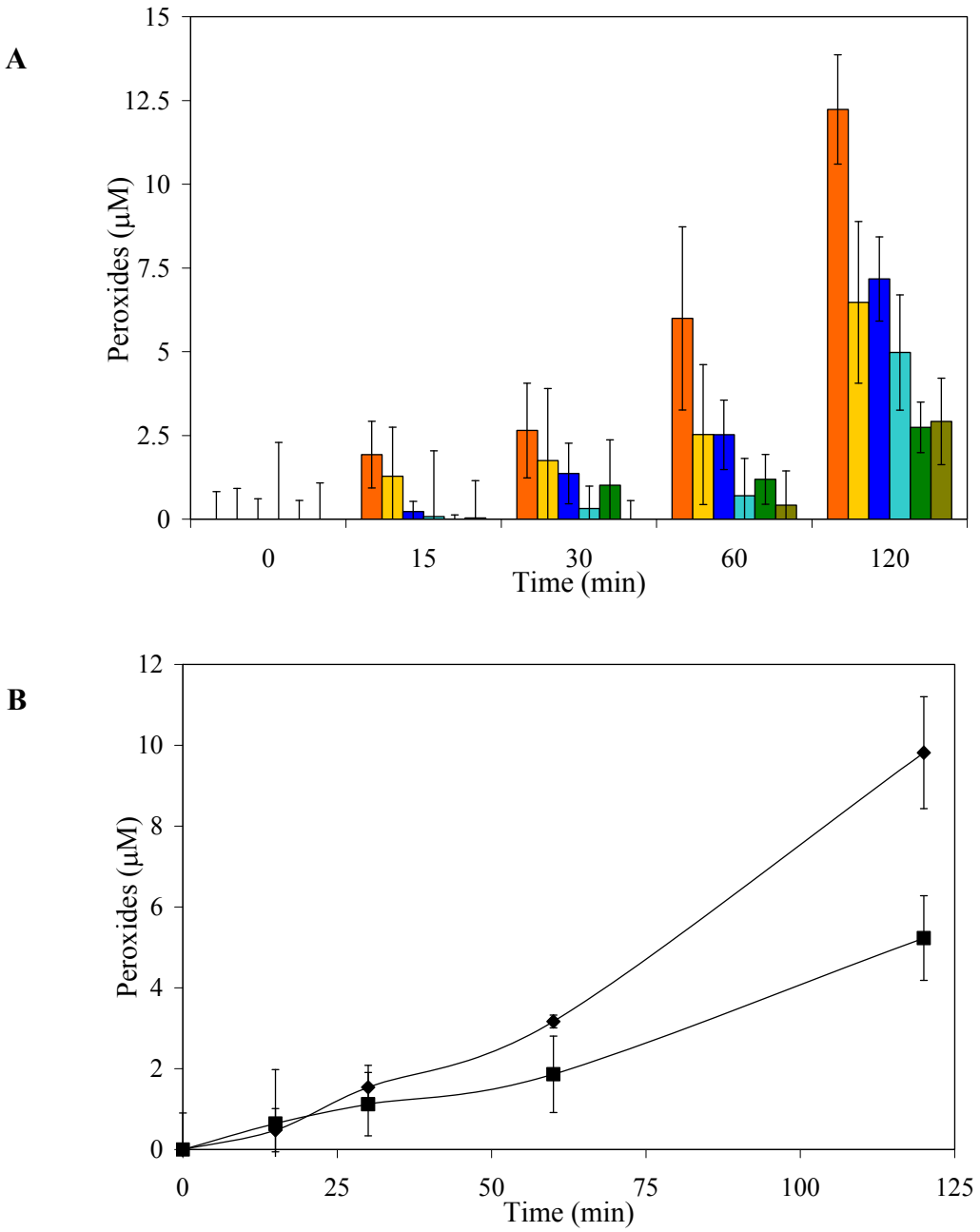

Figure 6.9: **A**) Peroxide formation following illumination of AHB-modified lens proteins (0.09 mol of AHB per mol protein;) and non-illuminated controls ( ) and illuminated unmodified lens proteins, with added free AHB (4.7 µM;) and corresponding non-illuminated control ( ), compared to illuminated unmodified lens proteins ( ) and non-illuminated unmodified lens protein ( ). The protein concentration in each case was 1 mg protein/mL. The peroxide levels detected from the illuminated AHB-modified lens protein samples were not statistically different from the corresponding non-illuminated controls as assessed by Student's *t*-test. **B**) Peroxide formation from free AHB (4.8 mM) over 120 min of illumination (♦) or incubation in the dark (■). The peroxide levels detected from the illuminated AHB samples were statistically different from the non-illuminated controls at the 120 min time point as assessed by Student's *t*-test. Data are means ± SD of triplicate measurements from a single experiment typical of several.

Analogous experiments using AHA (0.11 mol of AHA per mol protein), in place of AHB, did not give rise to a significant increase in peroxide levels over control values (4.73 ± 1.43 µM (illuminated sample) and 3.37 ± 1.81 µM (control), $p > 0.05$, after 120 min). Similar results

were obtained for the illuminated BLP with freshly added AHA (5.30 mM) compared to the control sample kept in the dark (5.44 ± 1.24 μM (illuminated sample) and 4.17 ± 1.88 μM (non-illuminated control), $p > 0.05$, after 120 min). Furthermore, illumination of higher levels of AHA (1 mg/mL) in the absence of protein did not give rise to significantly enhanced levels of peroxides compared to non-illuminated samples (10.50 ± 3.26 μM (illuminated sample) and 5.00 ± 2.42 μM (non-illuminated control), $p > 0.05$, after 120 min). The above results were not significantly different from the unmodified illuminated or control samples (2.74 ± 0.76 μM (illuminated sample) and 2.92 ± 1.29 μM (non-illuminated control), $p > 0.05$, after 120 min). These data suggest that the *o*-aminophenol moiety in AHB is of major importance for peroxide formation, as AHA lacks this moiety. These data also suggest that the deamination of Kyn and subsequent reduction to AHA may be a protective mechanism in human lenses as significantly higher levels of peroxides are produced from Kyn-modified proteins compared to non-covalently AHA-modified samples.

6.2.1.8 LC-MS investigation of illuminated UV filters

As the photochemical reactions described above may structurally alter the UV filter compounds, it was decided to investigate if illumination by the broad-spectrum 125 W mercury arc lamp filtered through a 305 nm cut-off filter induced any chemical changes to the UV filter compounds. 3OHKG, 3OHKyn, AHB and AHA were separately illuminated over a period of 120 min at 1 mg/mL and pH ~7. Control samples were prepared and kept in the dark at 4°C. Samples were collected at 0, 15, 30, 60 and 120 min and analysed by LC-MS. All four compounds proved to be chemically unchanged upon UV light illumination as determined by monitoring their molecular ions and absorbance values. This suggests that these UV filters lose the excess energy upon illumination *via* physical quenching (*e.g.* through loss of energy *via* energy transfer, emission of light or vibration) rather than being chemically altered themselves. However, as 3OHKyn and AHB samples resulted in peroxide formation upon UV light illumination, it is possible that the level of chemical change on these *o*-aminophenols induced by UV light under oxidative conditions may be too small to be detect by LC-MS but still sufficient to give significant levels of peroxides.

Part B

6.2.2 Oxidation products of Tyr (DOPA and di-Tyr) and Phe (*o*- and *m*-Tyr)

The amino acids Tyr and Phe are readily oxidised by reactive oxygen species. The ease of oxidation of these compounds makes them sensitive markers of oxidative damage.[415] It has been demonstrated that human nuclear cataract lenses contain elevated levels of oxidised amino acids, compared to healthy lenses, with particularly marked increases (up to 10-fold in Type IV cataracts) in the Tyr oxidation products, DOPA and di-Tyr.[256] Similar results were observed for the Phe oxidation products, *o*- and *m*-Tyr.[256,416]

DOPA can be formed by the addition of $HO^{\cdot}$ in both the presence and absence of O_2, however, it has been reported that the yields of DOPA are higher in the presence of O_2.[359] $HO^{\cdot}$ is a powerful oxidising agent formed by the action of high energy radiation on water, by UV-driven homolysis of H_2O_2 or by one electron reduction of H_2O_2.[396] The latter reaction occurs *via* Fenton chemistry ($H_2O_2 + M^{(n-1)+} \rightarrow HO^{\cdot} + HO^{-} + M^{n+}$), which is catalysed by Cu^{+}, Fe^{2+} and other redox-active metal ions that are present in low μg/g wet mass of lens proteins levels in normal human lenses and elevated in cataractous lenses.[35,37,71,417-419] This was supported by the finding that normal lenses were not as effective in catalysing $HO^{\cdot}$ production compared to cataractous lenses.[71]

DOPA formation can occur through formation of substituted cyclohexadienyl radicals (absence of O_2) or peroxyl radicals (presence of O_2) (Scheme 6.2, Path A and B).[359] In the presence of O_2, formation of the peroxyl radical is followed by rapid elimination of $HOO^{\cdot}$. DOPA, being a catechol, is prone to further oxidation reactions, resulting in quinone and cyclised products.[359,415]

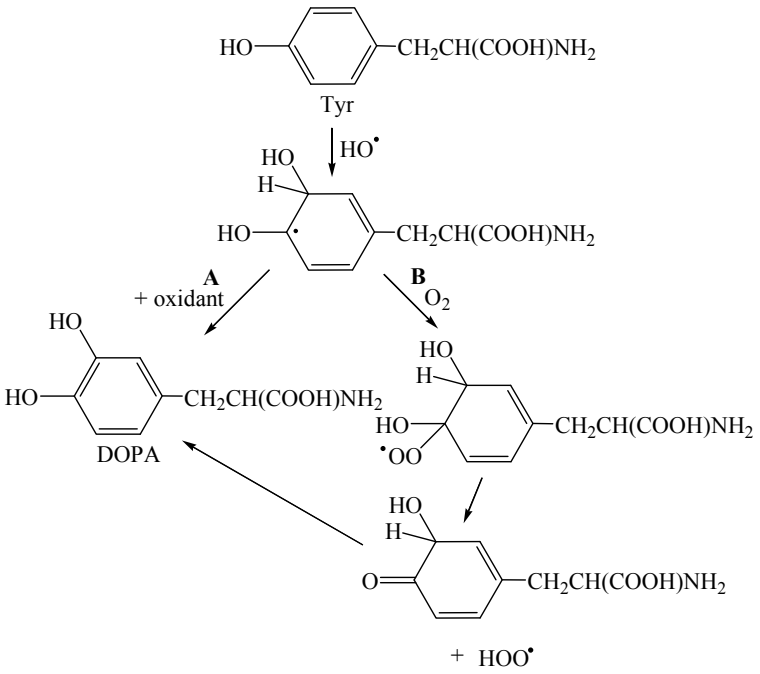

Scheme 6.2: Oxidation of Tyr by $HO^{\cdot}$ in the absence of O_2 (Path **A**) and presence of O_2 (Path **B**) to yield DOPA.[359]

Di-Tyr, which is a commonly used abbreviation for both carbon-carbon and carbon-oxygen linked dimers, arises *via* dimerisation of phenoxyl radicals, with the yield dependent on the radical flux.[359] Therefore, the yield of this product is dependent on both the extent of insult and the rate of radical formation. Dimerisation can occur through the *o*-positions to give dicyclohexadienone, which rapidly rearranges to give the phenolic tautomer ($\simeq$ 5 x 10^8 dm^3 mol^{-1} s^{-1}) or through the *o*-site and the oxygen (< 1 x 10^3 dm^3 mol^{-1} s^{-1}) (Scheme 6.3, Path A and B).[359] The yields are not affected by the presence of O_2.[359]

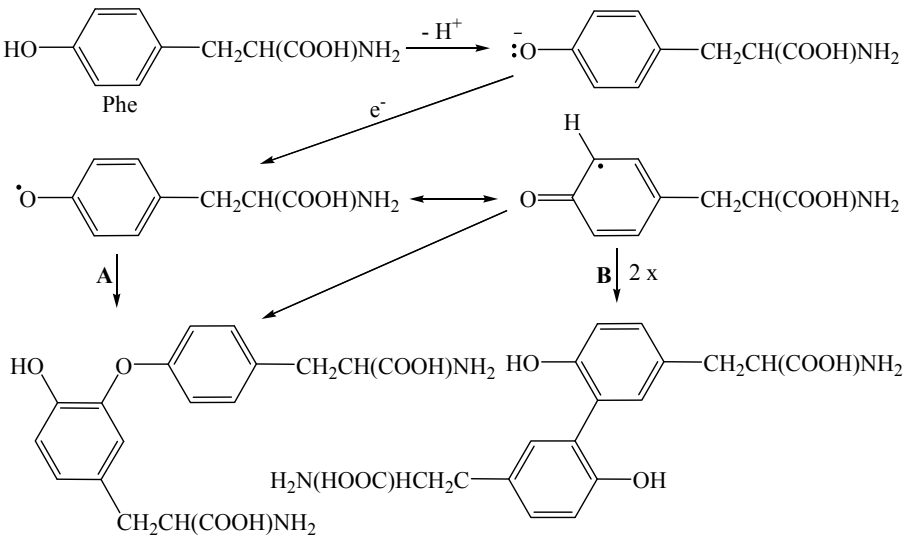

Scheme 6.3: Tyrosine oxidation involves one-electron oxidation to form phenoxyl (tyrosyl) radicals ($Tyr^{\cdot}$) that can dimerise to give both carbon-oxygen (Path **A**) and carbon-carbon (Path **B**) linked dimers.[359,420]

Similarly to DOPA, *o*- and *m*-Tyr can arise by direct addition of $HO^{\cdot}$ to the aromatic ring of Phe, or *via* oxidation of the aromatic ring to a radical-cation and subsequent reaction with water. The mechanism depends on whether O_2 is present or not. In the presence of O_2 these species are formed with the release of $HOO^{\cdot}$ (Scheme 6.4, Path A.). In the absence of O_2, the reaction proceeds as in Scheme 6.4 (Path B), however the yields can be low due to dimerisation of the hydroxycyclohexadienyl radicals to give bi-phenyls.[359]

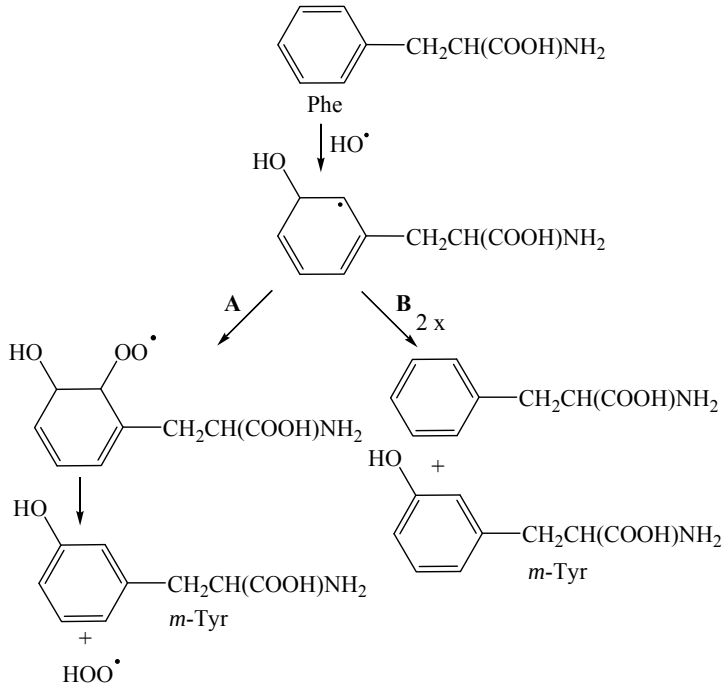

Scheme 6.4: Oxidation of Phe by $HO^{\cdot}$ in the presence of O_2 (Path **A**) and absence of O_2 (Path **B**). The position of the hydroxyl group on Phe can be at *o*-, *m*- and *p*- position.[359]

6.2.3 Determination of DOPA and di-Tyr

Statistically elevated levels of both DOPA and di-Tyr have been detected on BLP modified with Kyn upon exposure to UV light of wavelengths ≥ 345 nm.[247] In this study, experiments were designed to determine whether similar products were induced by 3OHKG, 3OHKyn, AHB and AHA, both free and associated with BLP, when subjected to UV light. Kyn-modified bovine lens protein was examined as a positive control and unmodified lens protein as a negative control.[247]

Kyn-, 3OHKyn- and 3OHKG-modified lens proteins, together with non-modified samples, were prepared and illuminated through a 305 nm UV filter, as described previously for the preparation of samples for the FOX assay. Triplicate or quadruplicate aliquots were taken

from illuminated or control samples at 0, 15, 30, 60 and 120 min. To minimise product formation as a result of further oxidation by hydroperoxides during storage and handling of samples, the reducing agent sodium borohydride was added to all aliquoted samples after each time point was taken for both illuminated samples and samples kept in the dark.[421,422] The samples were lyophilised and hydrolysed in nitrogen purged reaction vessels using HCl and thioglycolic acid for 16-18 h at 110°C. The hydrolysates were then lyophilised, redissolved in water and filtered to remove the unhydrolysed material. Within 5 days of their preparation, the samples were analysed by RP-HPLC. The elution profile was monitored in series with UV and fluorescence detectors. The measured levels of DOPA and di-Tyr are expressed per mol of parent amino acid (Tyr), assuming that both parent and oxidised material have not been lost during the sample preparation, or if lost are lost in equal amounts. There is no evidence to date that this assumption is incorrect. DOPA and di-Tyr were quantified using standard curves of the authentic materials. Quantitative analysis of *o*- and *m*-Tyr could not be achieved in this study due to the presence of co-eluting peaks under the conditions employed. Attempts to achieve better separation by modifying the mobile phase system were not successful. Typical RP-HPLC traces of protein samples after acid hydrolysis to free amino acids are shown in Figure 6.10 (A and B).

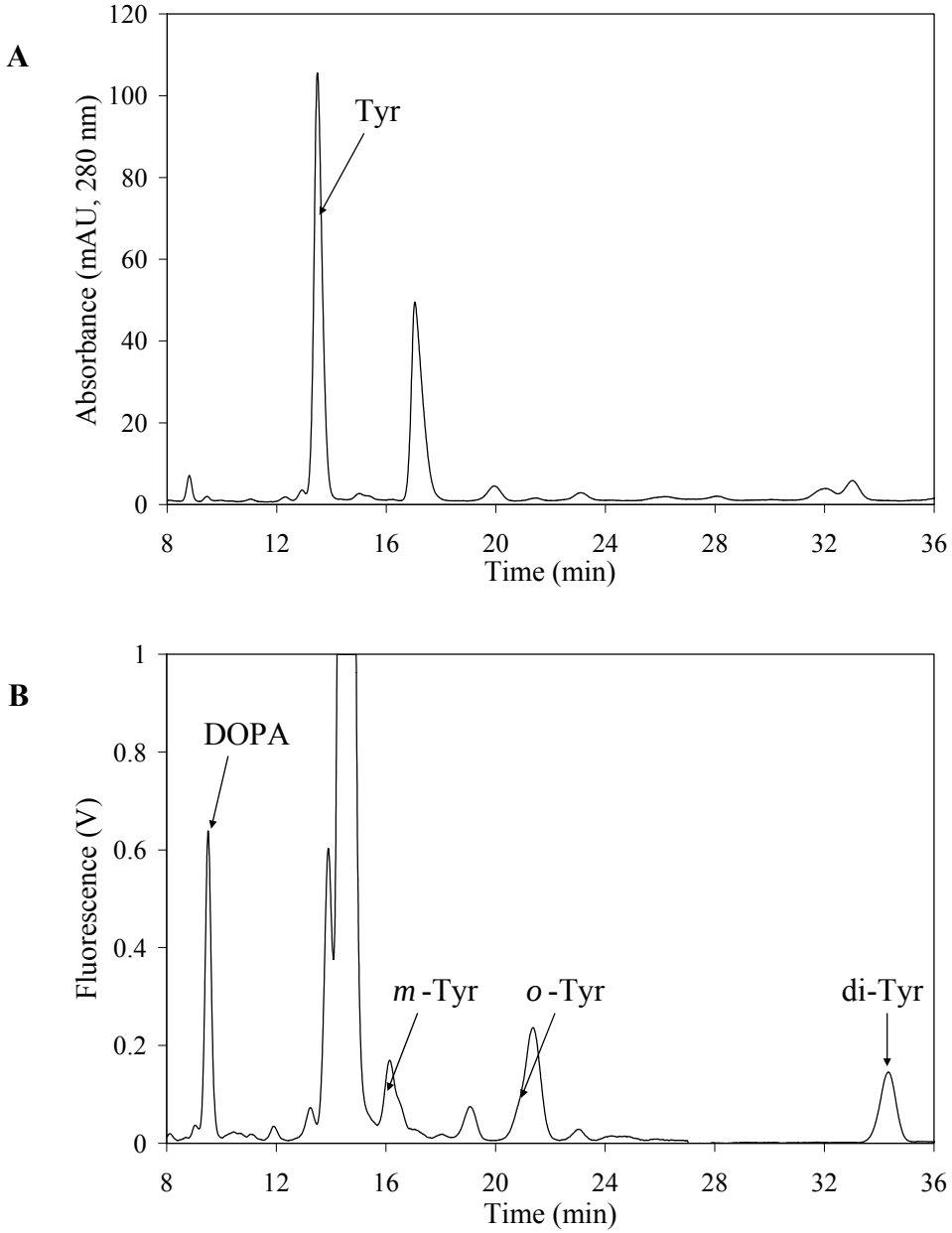

Figure 6.10: Typical RP-HPLC trace of acid hydrolysates of 3OHKG-modified proteins (0.78 mol of Cys-3OHKyn per mol protein) after 120 min of illumination. The level of parent Tyr (Rt 14.3 min) was quantified using UV detection (λ 280 nm) (**A**), and Tyr oxidation products were quantified by fluorescence detection ($\lambda_{ex/em}$ 280/320 nm for DOPA (Rt 9.5 min) and $\lambda_{ex/em}$ 280/410 nm for di-Tyr (Rt 34.3 min)) (**B**). *m*-Tyr (Rt 16.1 min) and *o*-Tyr (Rt 21.2 min) visibly coeluting with unknown peaks.

6.2.3.1 Kyn-modified BLP

Exposure of Kyn-modified lens proteins to UV light (305 filter) resulted in a time-dependent and statistically-significant elevation in the levels of protein-derived DOPA and di-Tyr, as compared to both control samples kept in the dark and to the unmodified protein samples (Figure 6.11, A and B). The absolute levels of these materials were of a similar magnitude to those reported previously.[247]

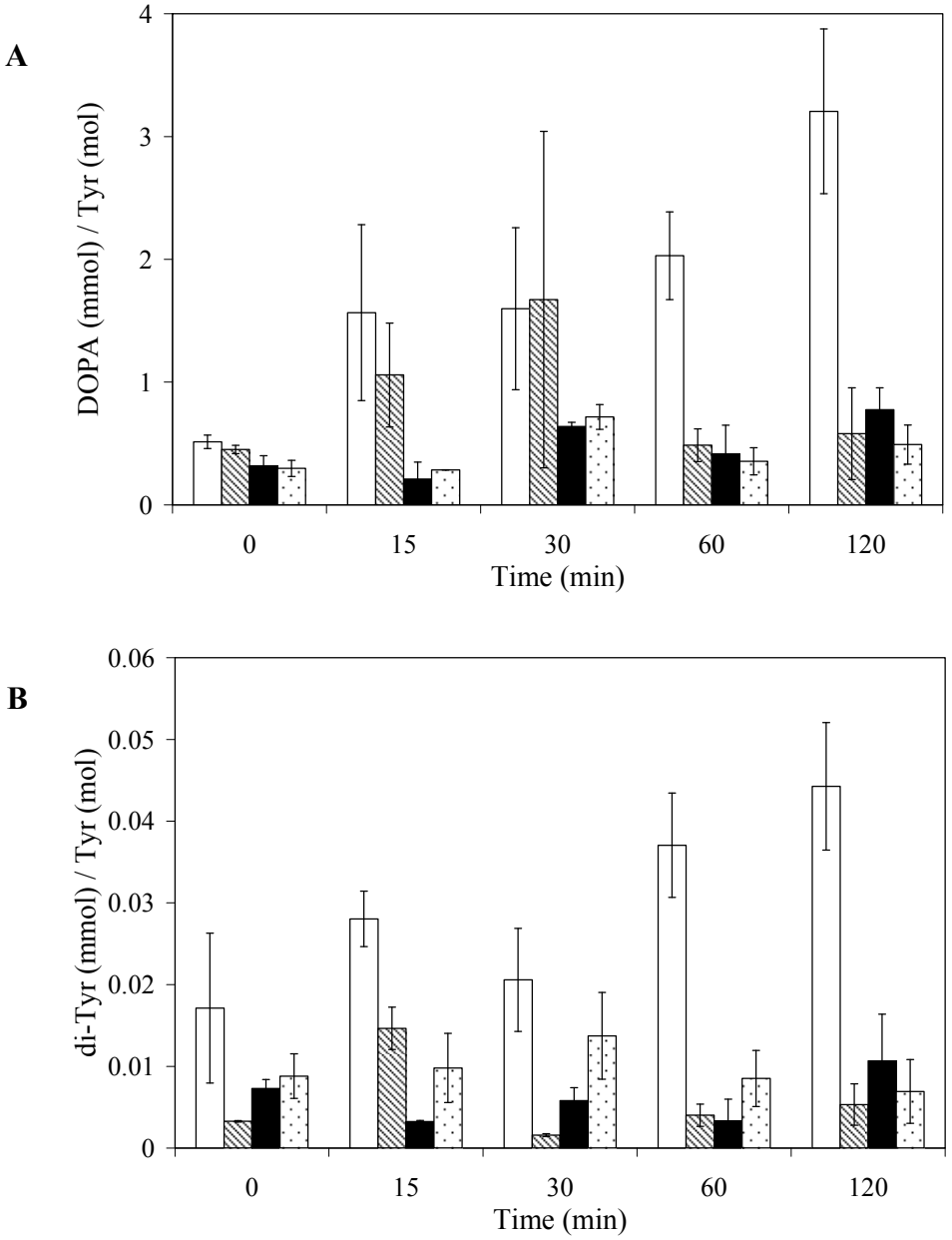

Figure 6.11: Time course of formation of DOPA (**A**) and di-Tyr (**B**) during illumination of Kyn-modified lens proteins (0.96 mol of Cys-Kyn per mol protein, white bars) and unmodified proteins (black bars). Samples of Kyn-modified (striped bars) and unmodified lens proteins (dotted bars) were kept in the dark as controls. Data (expressed as mM of modified amino acid per mol of parent Tyr) are means ± SD of triplicate (0, 15, 30 min time points) and quadruplicate (60 and 120 min time points) samples. For both measurements, DOPA (A) and di-Tyr (B) quantities were statistically elevated from those for the control samples kept in the dark, and unmodified proteins as assessed by one-way ANOVA with Tukey's post hoc-test.

6.2.3.2 3OHKG-modified BLP

Analogous experiments with lens proteins modified by 3OHKG resulted in a statistically-significant increase in di-Tyr levels compared to unmodified protein samples illuminated for the same time period (Figure 6.12). The maximum level of di-Tyr observed from the 3OHKG-modified lens proteins was ~0.20 mmol/mol Tyr, which is ~10-fold higher than that

detected in type IV cataract lenses.[256] In contrast, the levels of DOPA were not statistically elevated after 120 min of illumination (5.22 ± 0.60 mmol/mol Tyr for modified illuminated sample, 5.25 ± 0.15 mmol/mol Tyr for modified non-illuminated control, 3.36 ± 0.72 mmol/mol Tyr for unmodified illuminated sample and 3.40 ± 0.71 mmol/mol Tyr for unmodified non-illuminated control, $p > 0.05$).

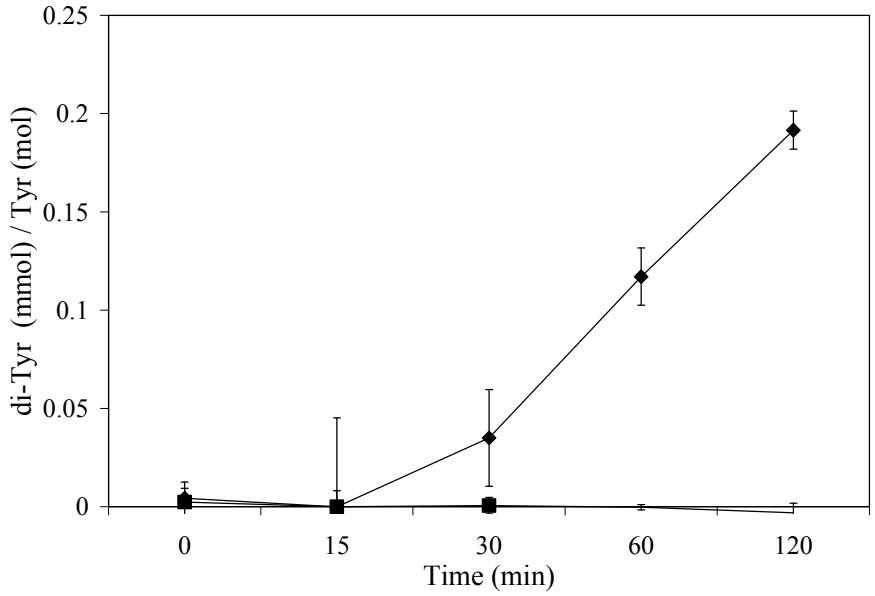

Figure 6.12: Time course of formation of di-Tyr during illumination of 3OHKG-modified lens proteins (0.78 mol of Cys-3OHKyn per mol protein, ♦) and unmodified lens proteins (■). Simultaneously, control samples that were kept in the dark, of modified and unmodified proteins were also analysed. Data (expressed as mM of modified amino acid per mol of parent Tyr) are means ± SD of triplicate (15 and 30 min time points) or quadruplicate (0, 60 and 120 min time points) experiments with the values from control samples subtracted (samples kept in the dark). Di-Tyr concentrations were statistically elevated from those of the control samples as assessed by Student's t-test.

6.2.3.3 3OHKyn-modified BLP

Illumination of 3OHKyn-modified lens proteins showed different behaviour to that detected with 3OHKG-modified protein, with unchanged levels of di-Tyr detected over a period of 120 min (0.01 ± 0.003 mmol/mol Tyr for modified illuminated sample, 0.008 ± 0.004 mmol/mol Tyr for modified non-illuminated sample, 0.003 ± 0.001 mmol/mol Tyr for unmodified illuminated samples, 0.001 ± 0.003 mmol/mol Tyr for unmodified non-illuminated sample, $p > 0.05$, after 120 min), whilst the levels of DOPA were significantly increased for the illuminated modified protein, compared to the illuminated unmodified protein samples (Figure 6.13). However, this increase was not dependent on the illumination time, and modified lens proteins incubated for the same time period in the dark also showed a significant elevation in DOPA levels, with the levels detected on illuminated versus non-illuminated modified proteins not being statistically different (Figure 6.13). This formation of

DOPA may be arising *via* auto-oxidation of the *o*-aminophenol moiety. The maximum levels of DOPA observed for 3OHKyn-modified lens proteins were ~8 mmol/mol Tyr, which is similar to that detected in type IV nigrescent cataract lenses.[256]

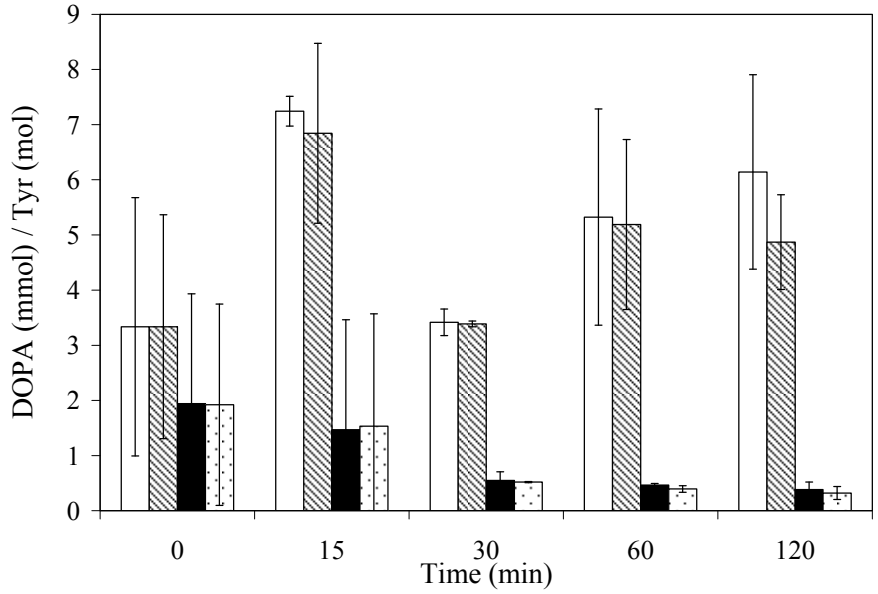

Figure 6.13: Time course of formation of DOPA during illumination of 3OHKyn-modified lens proteins (0.64 mol of Cys-3OHKyn per mol protein, white bars) and unmodified lens proteins (black bars). Control samples were kept in the dark, modified (striped bars) and unmodified (dotted bars) proteins were also analysed. Data (expressed as mM of modified amino acid per mol of parent Tyr) are means ± SD of triplicate (0, 15, 30 and 60 min time points) and quadruplicate (120 min time point) samples. DOPA quantities were statistically-elevated from those of the unmodified samples as assessed by one-way ANOVA with Tukey's post hoc-test. The levels of DOPA detected on illuminated 3OHKyn-modified samples were not statistically different from the non-illuminated control samples at any time point.

6.2.3.4 Determination of O_2-dependency

The formation of di-Tyr, upon illumination of 3OHKG-modified lens proteins, was found to be O_2-dependent, with significantly lower levels of this product detected under an atmosphere of N_2 (Figure 6.14, B). The small increase in di-Tyr levels over time detected under N_2 may be due to either non-O_2-dependent formation of this product, or incomplete removal of O_2 from the samples. Levels of di-Tyr and DOPA from illuminated 3OHKyn- and 3OHKG-modified lens proteins, respectively, were not significantly affected by the presence of an atmosphere of N_2 compared to air (Figure 6.14, A and B). DOPA levels from illuminated 3OHKyn-modified lens proteins, however, were higher at all time points compared to the DOPA levels in the 3OHKG-modified sample. This suggests that apart from not being UV light-dependent, DOPA produced by the 3OHKyn-modified lens protein sample is not O_2-dependent (Figure 6.14, A). In addition, this data suggest that DOPA, in the absence of O_2, might be formed *via* the disproportionation of two of the initial substituted cyclohexadienyl radicals (Scheme 6.2, Path A).[359] The yields of DOPA formed *via* the aerobic or anaerobic pathway were not

statistically different, even though it is known that the latter process only yields one DOPA molecule per two initial substituted cyclohexadienyl radials (Scheme 6.2, Path A).[359] It appears therefore that modification of lens proteins by 3OHKyn results in complex reaction mechanisms, which require further investigation.

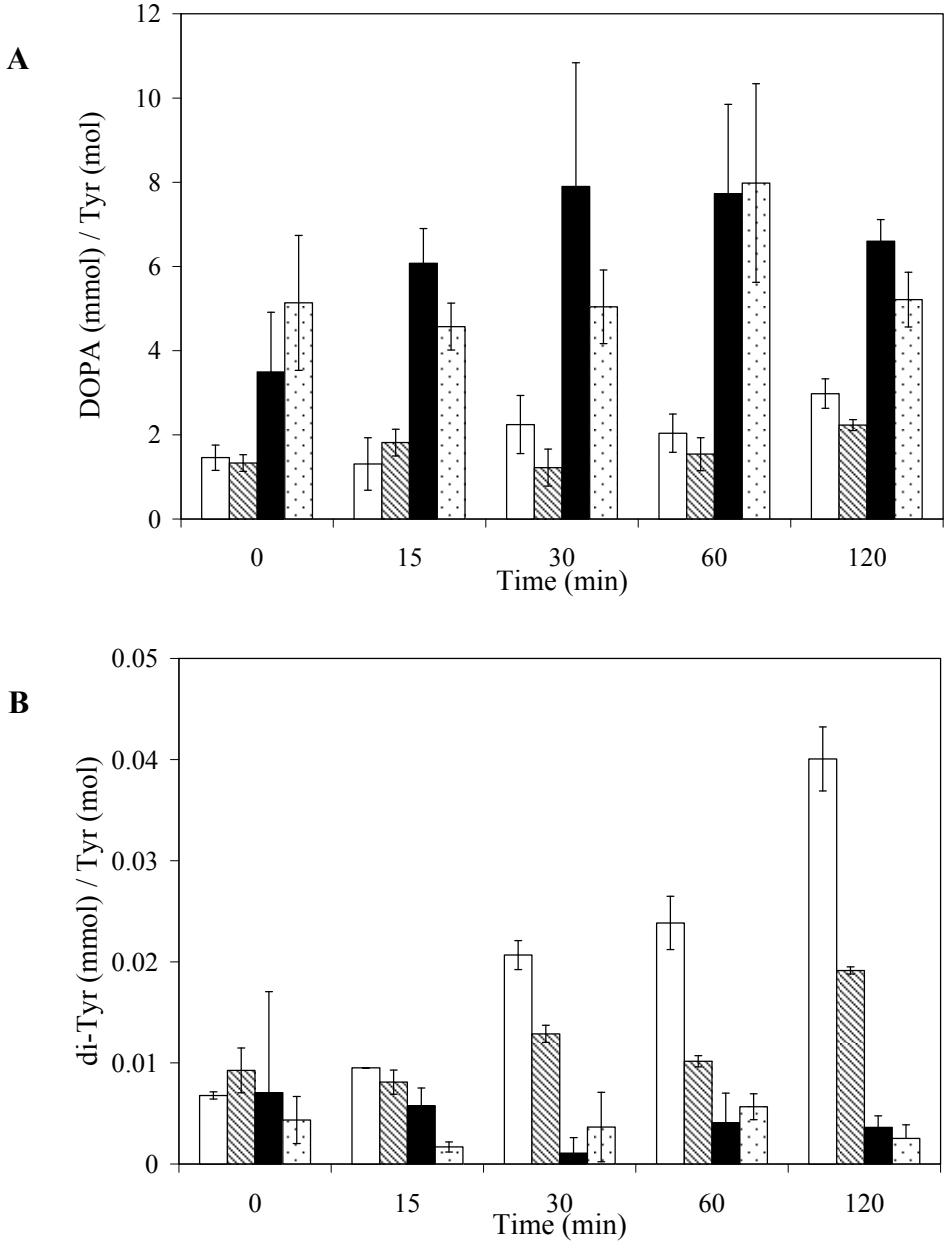

Figure 6.14: Time course of formation of protein-bound DOPA (**A**) and di-Tyr (**B**) on illumination of 3OHKG-modified lens proteins (1 mg protein/mL, 0.78 mol of Cys-3OHKyn per mol protein, white bars) and 3OHKyn-modified lens protein (1 mg protein/mL, 0.64 mol of Cys-3OHKyn per mol protein, black bars) under an atmosphere of air versus N_2. Control samples of 3OHKG-modified lens protein (striped bars) and 3OHKyn-modified lens protein (dotted bars) kept under N_2 were also analysed. Data (expressed as mM of modified amino acid per mol of parent Tyr) are means ± SD of triplicate (15 and 30 min time points) and quadruplicate (0, 60 and 120 min time points) samples. In (A), the levels of the oxidised products detected under air versus N_2 were not statistically different for all of the samples at any time point. In (B), the levels detected in the air versus N_2-gassed samples were statistically different at the 30, 60 and 120 min time points for the 3OHKG-modified lens protein samples, but not for 3OHKyn-modified lens protein samples as assessed by Student's *t*-test.

6.2.3.5 Determination of $^1O_2$ role

To determine the role of $^1O_2$ in Tyr oxidation, 3OHKG- and 3OHKyn-modified lens proteins in buffers made up using D_2O (extend the lifetime of $^1O_2$), in place of H_2O, were illuminated.[404,405] The presence of D_2O did not result in statistically-different data to that reported above. In contrast, use of buffers containing 10 mM sodium azide (a potent scavenger of $^1O_2$) resulted in a massive loss of parent Tyr in all samples (Figure 6.15, A and B). This is consistent with a previously reported interference of sodium azide in the acid hydrolysis of proteins where complete loss of Tyr and Phe was observed.[423] As a result of these observations no further experiments were carried out using this additive.

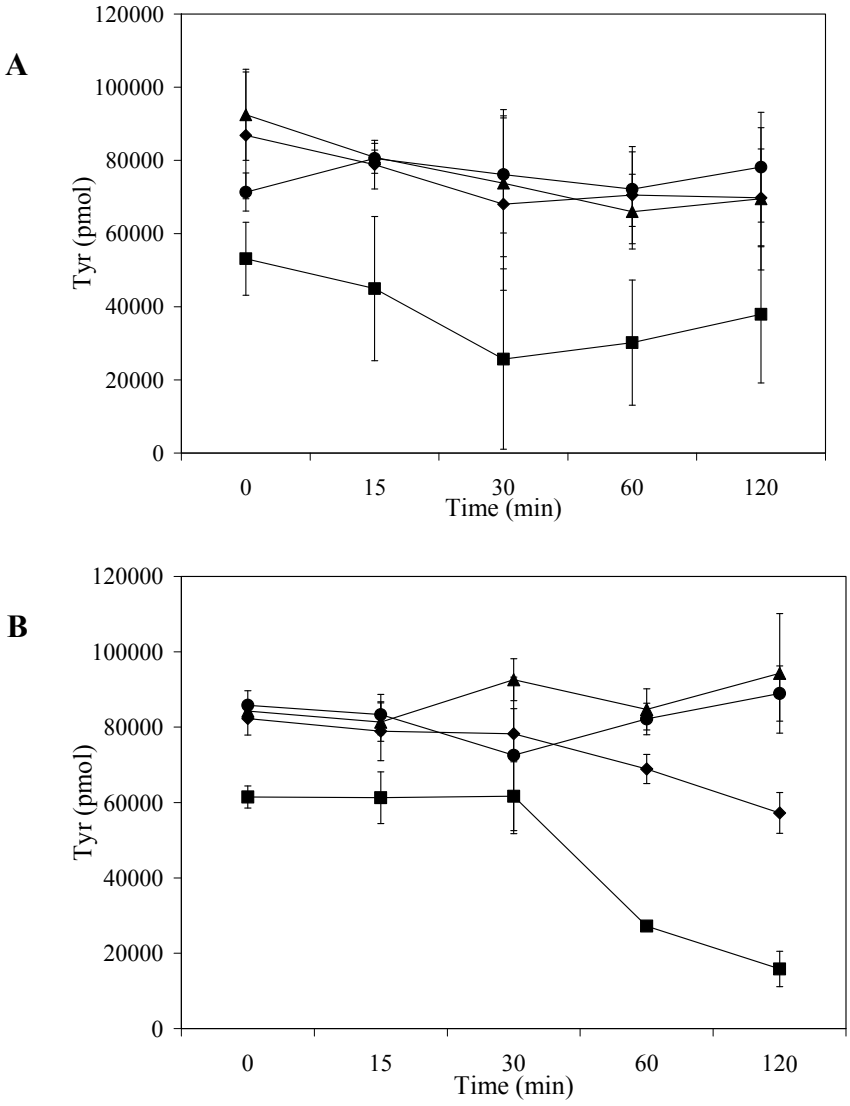

Figure 6.15: Time course of Tyr levels from 3OHKG (0.40 mol of Cys-3OHKyn per mol protein; **A**) and 3OHKyn (0.05 mol of Cys-3OHKyn per mol protein; **B**) modified lens protein samples upon illumination. Samples were prepared in H_2O (illuminated control, ♦) in the presence of sodium azide (■), or prepared in D_2O (▲). A control sample of unmodified lens protein prepared in H_2O was analysed simultaneously (●). Data (expressed as pmol of parent Tyr) are means ± SD of triplicate (0, 15 and 30 min time points) or quadruplicate (60 and 120 min time points) samples.

6.2.3.6 AHB- and AHA-treated BLP

Analogous behaviour was detected with AHB- versus AHA-treated BLP upon illuminated. No significant changes were detected in di-Tyr levels (0.013 ± 0.002 mmol/mol Tyr for AHB-treated illuminated sample, 0.010 ± 0.003 mmol/mol Tyr for AHB-treated non-illuminated sample, 0.013 ± 0.003 mmol/mol Tyr for AHA-treated illuminated sample and 0.014 ± 0.002 mmol/mol Tyr for AHA-treated non-illuminated sample, $p > 0.05$, after 120 min). A non-light dependent increase in DOPA levels was detected after incubation for 30 or 60 min (Figure 6.16). After 120 min this change was no longer statistically-significant (as assessed by Student's *t*-test), consistent with the known instability of DOPA residues on proteins.[424]

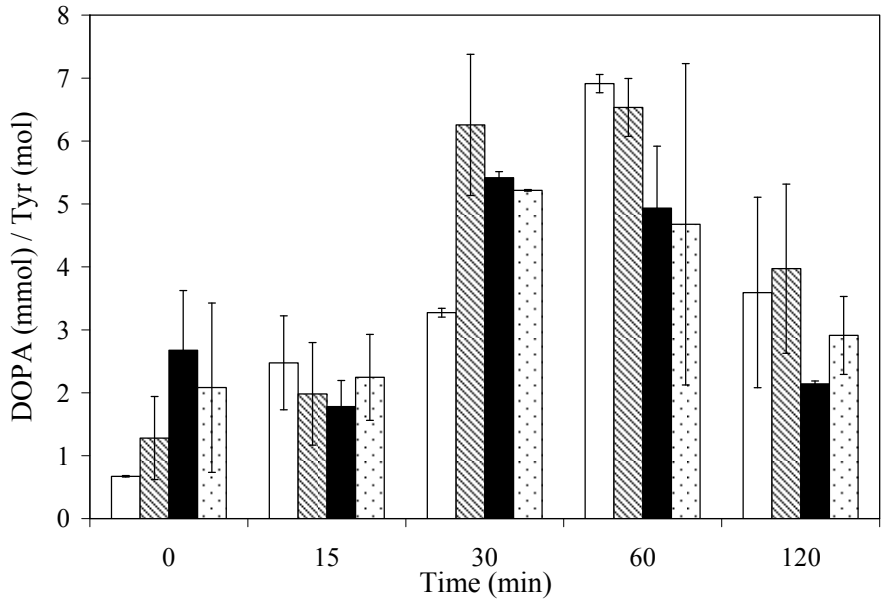

Figure 6.16: Time course of DOPA levels from AHB (0.09 mol of AHB per mol protein, white and striped bars) and AHA (0.11 mol of AHA per mol protein, black and dotted bars) modified lens protein samples upon illumination. Control samples for AHB (striped bars) and AHA (dotted bars) were kept in the dark and analysed simultaneously. Data (expressed as mM of modified amino acid per mol of parent Tyr) are means ± SD of triplicate (0, 15 and 30 min time points) and quadruplicate (60 and 120 min time points) samples. In both observations (AHB- and AHA-treated lens proteins) there was an UV light independent steady increase in DOPA levels.

Part C

6.2.4 Determination of protein cross-linking

Age-related cataractous lenses are characterised by insoluble and cross-linked protein aggregates.[9,395,425] These aggregates have been reported to have diameters of up to 350 nm and molecular masses of up to 10^6 kDa (*cf.* values of 12-15 nm and 8 x10^2 kDa for unmodified α-crystallins).[426,427] To examine whether cross-linking may be initiated by exposing protein-bound Kyn, 3OHKyn and 3OHKG and protein-associated AHB and AHA to wavelengths of light that are known to penetrate the lens, sodium dodecyl sulfate-polyacrylamide gel electrophoresis (SDS-PAGE) was carried out on illuminated and air-gassed (for 120 min) modified and unmodified protein samples compared to modified and unmodified protein samples not exposed to light and air (taken at time 0 min). Both reducing and non-reducing gels (*i.e.* in the presence and absence of β-mercaptoethanol, respectively), were used to examine the role of disulphide bonds, which would be disrupted under the former conditions. The electrophoretic separation of proteins was carried out by the method of Laemmli[428] with silver staining, as this is generally accepted to be one of the more sensitive staining techniques. The data presented in Figure 6.17 are consistent with the formation of both disulphide- and non-disulphide cross-linking in the modified proteins, with the extent of cross-linking being much greater in the illuminated samples compared to the non-illuminated modified samples. It is also clear that UV filter modification of lens proteins alone resulted in some aggregation, with this effect being particularly significant with 3OHKyn-modified protein and to a lesser extent with Kyn, 3OHKG, AHB and AHA. This is in contrast to previous studies that have not detected cross-linking of lens proteins modified under similar conditions with Kyn and 3OHKyn at both pH 7.2 and 9.5 and visualised by Coomassie staining.[175,383] This difference may be due to the use of the more sensitive silver staining technique in the current study. The extent of light-induced, non-reducible, aggregates decreased in the order Kyn $\simeq$ 3OHKyn $\simeq$ 3OHKG > AHB > AHA > unmodified protein, with a similar order detected for the reducible species.

The non-reducible cross-links may be associated with the generation of di-Tyr.[429] However, it is also clear that this compound can only be partly responsible, as the extent of cross-link formation observed with 3OHKyn- and 3OHKG-modified proteins by SDS-PAGE were similar, whereas the yields of di-Tyr detected by RP-HPLC were markedly different. Further reactions of both DOPA formed from Tyr residues, and reactions of the *o*-aminophenol

moiety of 3OHKyn and AHB, may contribute to the generation of cross-links in both the illuminated and non-illuminated modified proteins relative to the native protein. It has been shown that illumination can result in (intermolecular) cross-links involving 5-cysteinyl-DOPA generated from reaction of the DOPA oxidation product, DOPA quinone, with Cys residues.[430,431] Other photo-products (*e.g.* those formed by $^1O_2$) may also play a role in cross-linking of the illuminated proteins with evidence having been reported for cross-links involving other Tyr-derived products, His, Trp and Lys residues.[398,401,432-438]

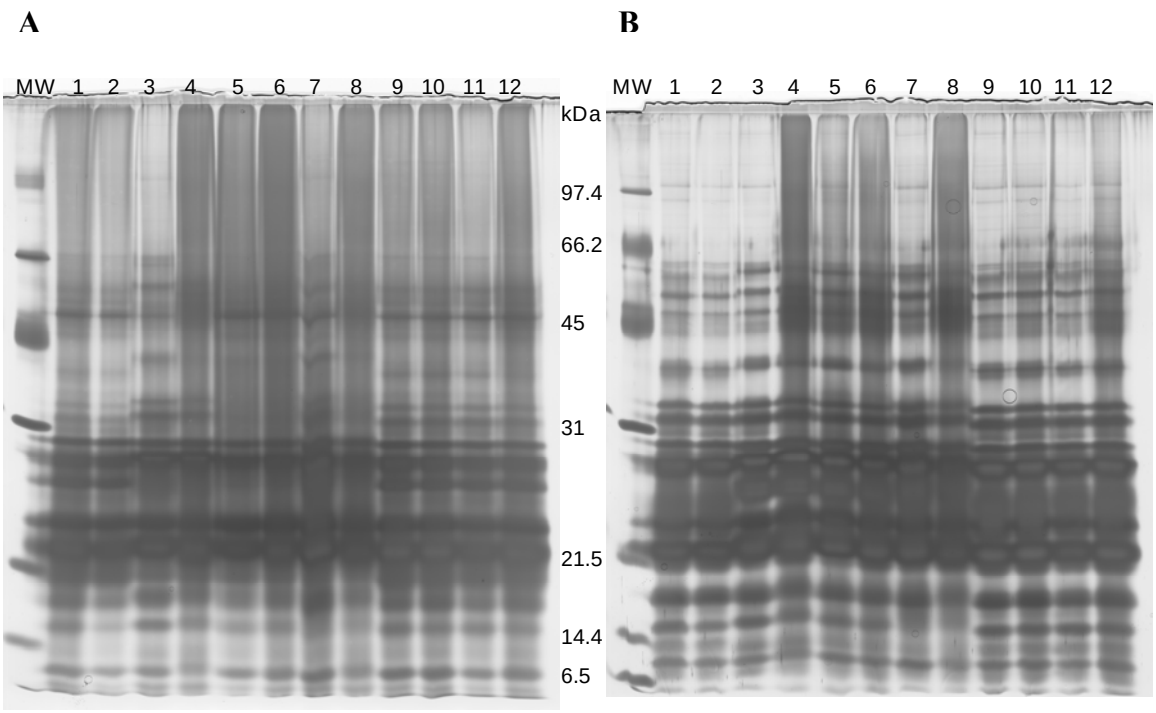

Figure 6.17: SDS-PAGE of lens proteins treated with Kyn (0.96 mol Cys-Kyn per mol protein), 3OHKyn (0.64 mol Cys-3OHKyn per mol protein), 3OHKG (0.78 mol Cys-3OHKyn per mol protein), AHA (0.11 mol AHA per mol protein) and AHB (0.09 mol AHB per mol protein) at pH 9.5 for 48 h, together with molecular mass markers, analysed on a 12% Tris-Glycine gels. Protein bands were detected by silver staining.
Lanes: 1 and 2 - unmodified lens protein
3 and 4 - Kyn-modified lens protein
5 and 6 - 3OHKyn-modified lens protein
7 and 8 - 3OHKG-modified lens protein
9 and 10 - AHA-treated lens protein
11 and 12 - AHB-treated lens protein
Samples run in odd-numbered lanes were non-illuminated samples taken at 0 min, whilst those run in even numbered lanes were illuminated and gassed with air for 120 min.
A) gel run under non-reducing conditions; **B**) gel run under reducing conditions.

6.3 Conclusions

Overall it is clear that the covalent binding of the Trp-derived UV filter compounds to lens proteins changes the photochemistry of these species and makes them more efficient sensitisers of damaging reactive species. Thus the increased level of these adducts, and the declining levels of the free UV filters with increasing age,[39,176] may exacerbate photo-oxidative damage to the lens and the retina. It has been shown that (at least) two major processes contribute to an enhanced level of peroxides and protein modification in this model system: one of these involves the generation of $^1O_2$, with 3OHKyn the most efficient sensitiser, and the second involves the auto-oxidation of the *o*-aminophenol moiety present in both this compound and AHB. The yield of peroxides (primarily H_2O_2) and protein oxidation products (DOPA and di-Tyr) do not parallel each other. This suggests that the formation of these materials occurs *via* different pathways. This conclusion is supported by the inverse correlation between peroxide formation and di-Tyr yield detected with 3OHKyn versus 3OHKG, and the effect of D_2O on these two processes, with only the peroxide yield markedly affected by the latter treatment. This may arise from competing energy transfer pathways from the initial chromophore excited state, with energy transfer to O_2 occurring in some cases (*e.g.* with the 3OHKyn adducts, to eventually generate H_2O_2) whereas with the 3OHKG adducts, formation of protein-derived phenoxyl radicals (and hence di-Tyr) is a major pathway. The generation of DOPA does not appear to involve oxygen-derived species directly, as the yield of this product does not appear to be diminished, unlike the other materials, by an atmosphere of N_2. This is in accord with previous studies that have shown that this compound can be generated by both O_2-dependent and independent pathways.[439] Irrespective of the contributions of these pathways, protein cross-linking appears to be a major consequence, with little protein fragmentation. This cross-linking appears to involve multiple pathways, for example di-Tyr generation and possibly reaction of nucleophiles (*e.g.* Lys and Cys residues) with oxidation products of DOPA and the *o*-aminophenol moiety (*e.g.* the *o*-quinone imine) present on 3OHKyn and AHB. Thus, multiple pathways may contribute to modification of lens proteins as a consequence of extended incubation with UV filter compounds, with some of these processes enhanced by exposure to UV light.

6.4 Experimental

6.4.1 General experimental

All organic solvents and acids were of HPLC grade (Ajax, NSW, Australia). Milli-Q® H_2O (purified to 18.2 MΩ cm^{-2}) was used in preparation of all solutions. DL-Kynurenine sulphate salt (≥ 95%), 3-hydroxy-DL-kynurenine, 3,4-dihydroxyphenylalanine (DOPA, > 99%), tyrosine (Tyr, > 99%), formic acid (> 99%), sodium azide (NaN_3), sodium perchlorate monohydrate (98%), catalase (from bovine liver, thymol free, 13,800 units/mg protein), xylenol orange sodium salt, β-mercaptoethanol, (> 98%), sodium borohydride ($NaBH_4$, 99%), deuterium oxide (D_2O, 99.9%) were from Sigma-Aldrich. Pico-Tag reaction vessels for protein hydrolysis were from Alltech (NSW, Australia). $FeSO_4 \cdot 7H_2O$ and hydrogen peroxide (H_2O_2, 30%, 9.881 M) were from Merck (Germany). *Ortho*-tyrosine (*o*-Tyr) and *meta*-tyrosine (*m*-Tyr) were from Biochemika (Fluka). Di-tyrosine (di-Tyr) was synthesised and kindly provided by Dr Catherine Luxford (The Heart Research Institute, Sydney, NSW).

6.4.2 Illumination procedures

Solutions of BLP (control or modified lens proteins at pH 9.5 for 48 h; 1 mg/mL, unless otherwise stated) were prepared in H_2O or D_2O at pH/pD ~7 and illuminated, at a distance of 10 cm, by a broad-spectrum 125 W mercury arc lamp filtered through a 305 nm cut-off filter, unless otherwise stated. Light intensity (W/cm^2) was measured using an IL 1700 Research Radiometer (International Light Pty Ltd) with appropriate detectors and spectral irradiance (W/cm^2) was measured by OL-754 Spectroradiometer (Optronic Laboratories, Inc.). The results of light intensities and spectral irradiances are presented in Table 6.1 and Figure 6.18, respectively.

Table 6.1: Light intensities of the broad spectrum 125 W mercury arc lamp, both filtered and not filtered, were measured by a IL 1700 Research Radiometer.

Filters	UVA (mW/cm^2)	UVB ($\mu W/cm^2$)
305 nm	3.03	5.92
345 nm	2.73	0.00
385 nm	1.84	0.00
no filter	4.16	14.02

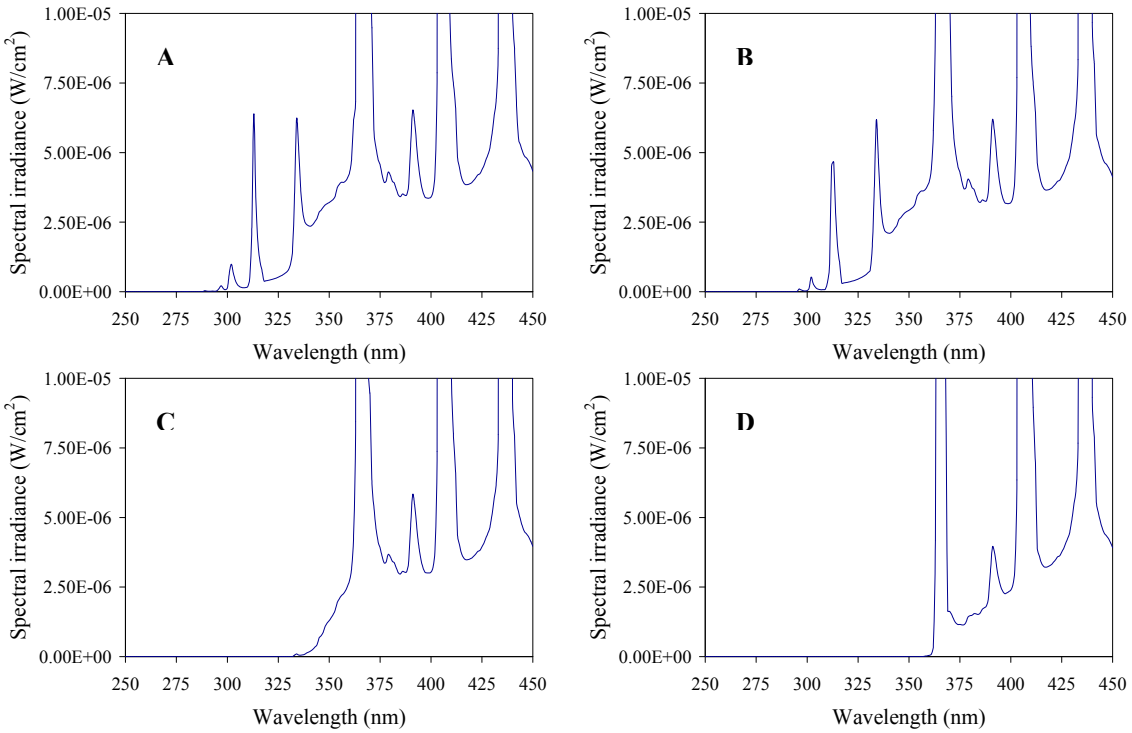

Figure 6.18: Spectral irradiance of light from 125 W mercury arc lamp. **A**) no filter; **B**) 305 nm filter; **C**) 345 nm filter; **D**) 385 nm filter.

The illuminated samples were continuously bubbled during illumination with compressed air, unless otherwise stated, and maintained at 4°C on ice. If an atmosphere of N_2 was used, H_2O was gassed with nitrogen for ~20 min before modified lens proteins were added and continued throughout the experiment. Sodium azide (5 mM or 10 mM) was added when indicated. Aliquots were removed at the stated times for analysis. Catalase (66.5 U/mL) was added immediately after the cessation of illumination, when stated, and the samples incubated in the dark at RT (~21°C) for 10 min before analysis. A diagram of the illumination set up is shown in Figure 6.19.

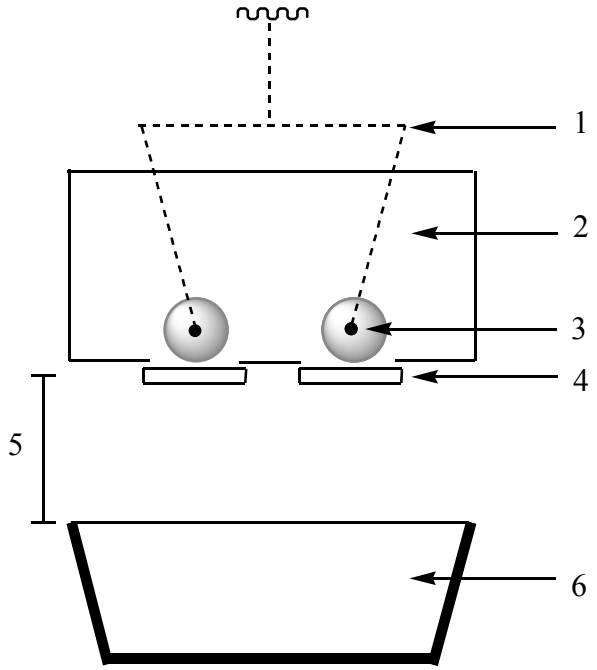

Figure 6.19: Solutions of BLP were illuminated using a system as shown in the diagram. The samples were prepared in 20 mL glass vials (**3**) and placed at 4°C (**2**) behind the 305, 345 or 385 nm cut-off filter (**4**). Samples were at a distance of 10 cm (**5**) from a broad spectrum 125 W mercury arc lamp (**6**). Samples were gassed continuously during the illumination using compressed air or nitrogen gas (**1**).

6.4.3 Peroxide quantification

Peroxide concentrations, expressed as H_2O_2 equivalents, were determined using an Fe(II)-xylenol orange (FOX) assay (in the absence of sorbitol) as previously described.[401-403] The aliquots were taken from illuminated or control samples at 0, 15, 30, 60 and 120 min and diluted to 1/10, 1/25 and 1/50 with Milli-Q water to obtain triplicate readings for each dilution. To the prepared samples (1 mL), FOX reagent (50 μL) was added and samples were vortexed before being incubated for 30 min at RT in the dark. The stock of FOX reagent consisted of $FeSO_4 \cdot 7H_2O$ (25 mM), xylenol orange (10 mM) and H_2SO_4 (2.5 M, 10 mL). The stock was kept at 4°C and used within 3-4 days. Prior to use, the stock solution (1 mL) was diluted with Milli-Q water (4 mL), vortexed and kept at 4°C. It was used within 12 h of preparation. The peroxide mediated oxidation of Fe^{2+} to Fe^{3+} was determined by measuring the λ_{max} 560 nm of the Fe^{3+}-xylenol orange complex using 1 mL cuvettes and PerkinElmer Lambda UV-visible spectrometer. A standard curve was constructed using commercial H_2O_2 on the day of sample analysis.

6.4.4 Liquid chromatography-mass spectrometry (LC-MS)

See Section 2.4.4 for details.

6.4.5 Amino acid analysis

Quantification of parent and modified amino acids in hydrolysates of BLP was performed as reported previously.[440,441] Triplicate or quadruplicate samples of illuminated or control samples (750 μL) were taken at 0, 15, 30, 60 and 120 min and placed in glass auto-sampler vials (1 mL) in the dark at 4°C. To each vial, freshly prepared $NaBH_4$ (10 mg/mL, 10 μL) was added. The samples were then lyophilised and hydrolysed, after purging with nitrogen and evacuation, in the Pico-Tag reaction vessels using HCl (6 M, 1 mL) and thioglycolic acid (50 μL) for 16-18 h at 110°C. The hydrolysates were then dried using a Speed Vac concentrator, redissolved in Milli-Q water (100 μL) and filtered through 0.45 μm Nanosep MF GHP centrifugal devices at 4°C. Analysis was performed either immediately or within 5 days with the samples kept at -80°C. RP-HPLC was performed using a Shimadzu RP-HPLC equipped with a column oven (Waters Corp., Milford, MA, USA) set at 30°C, UV and fluorescence detector (Shimadzu) and Class LC-10 software (Shimadzu). Separation of 50 μL samples was achieved at a flow rate of 1 ml/min using an Alltech (Prevail, 100 Å, 5 μm, 4.6 x 250 mm, C18) column preceded by a Phenomenex (Synergy Fusion, 100 Å, 4 μm, 4.0 x 3.0 mm, C18) guard column. Mobile phase consisted of buffer A (100 mM sodium perchlorate/10 mM orthophosphoric acid) and buffer B (80% MeOH/H_2O, v/v). A mobile phase gradient was as follows: 0-20 min (6% buffer B), 20-36 min (6-12% buffer B), 36-45 min (50% buffer B), 45-50 min (50% buffer B), 50-53 min (6% buffer B), 53-60 min (6% buffer B). Buffers were degassed before and during use. The elution profile was monitored in series with UV and fluorescence detectors, with the former set at 280 nm and the latter set as follows: λ_{ex} 280 nm / λ_{em} 320 nm for 0-27 min and λ_{ex} 280 nm / λ_{em} 410 nm for 27-60 min. Peaks were quantified using standard curves constructed using authentic standards. Parent Tyr (Rt 15.5 min) was quantified by UV absorbance. DOPA (Rt 9.5 min) was quantified by fluorescence detection at λ_{ex} 280 nm / λ_{em} 320 nm and di-Tyr (Rt 34.3 min) at λ_{ex} 280 nm / λ_{em} 410 nm. The oxidised amino acids were expressed relative to the Tyr levels to compensate for any losses during sample preparation and analysis.

6.4.6 Sodium dodecyl sulfate-polyacrylamide gel electrophoresis (SDS-PAGE)

Electrophoretic separation of UV filter-modified (prepared as described in Chapter 5) and unmodified proteins was carried out by the method of Laemmli.[428] Lyophilised illuminated (120 min at pH ~7) and control samples (taken at time 0 min) (0.4-0.5 mg) were dissolved in Milli-Q water and further diluted (1:1) with loading dye, containing Tris/HCl buffer (62.5 mM, pH 6.8), SDS (2%, w/v), glycerol (10%, v/v) and bromophenol blue (~1% w/v), to 10 μg protein in 50 μL. β-Mercaptoethanol (5%) was added for gels run under reducing conditions. The samples were then heated (95°C, 5 min), cooled and loaded (45 μL) onto the 12% polyacrylamide gels. Both, illuminated and non-illuminated unmodified BLP were used as controls. An aliquot of molecular weight markers (Bio-Rad broad range SDS-PAGE, 6,500-200,000 Da, Sigma) was loaded in lane 1. Bands were detected by silver staining and the resulting gels were digitised using a Bio-Rad Gel Doc 1000 system.

6.4.7 Statistical analysis

The statistical difference between mean values of control and treated samples were determined with the Student's *t*-test (two-sample assuming equal variance). Analysis was performed using Microsoft Office Excel (2003). Statistical significance between groups was determined by one-way ANOVA with Tukey's post hoc-test. Analysis was performed using GraphPad Prism version 4.0 for Windows software (GraphPad Software, San Diego, CA). $P \leq 0.05$ was taken as significant in both cases.

CHAPTER 7

CONCLUSIONS AND FUTURE DIRECTIONS

Human lens UV filter compounds are able to absorb UV light and consequently protect the lens and retina from photodamage. However, the kynurenine-based UV filters (Kyn, 3OHKyn and 3OHKG) are prone to deamination at physiological pH, resulting in the formation of reactive α,β-unsaturated carbonyl compounds. These compounds bind to nucleophilic sites on lens proteins (crystallins). This binding appears to be a significant factor in the changes that occur upon lens aging and in the formation of ARN cataract. The key amino acids involved in Kyn and 3OHKyn modifications in human lenses include Cys, Lys and His residues, however the specific binding sites on lens crystallins have not been determined.[18,20] In contrast, four specific Cys binding sites of 3OHKG have been determined for γS- and βB1-crystallins and from more recent studies it is clear that 3OHKG is by far the most abundant protein-bound UV filter in human lenses.[120,176] Being the major UV filter, an overall aim of this study was therefore to gain a greater insight into the role of 3OHKG in lens aging and ARN cataract. With the recent findings that protein-bound Kyn samples upon exposure to UV light generate reactive oxygen species and protein damage,[247] the investigation of the binding of 3OHKG to lens proteins, and the effect of UV light on 3OHKG- and 3OHKyn-modified lens proteins, were the major aims of this study. Given the importance of UV filters in human lens chemistry, and the likelihood of lenses containing additional unidentified UV filters, a further aim was to identify and quantify novel human lens metabolites and examine their reactivity.

As 3OHKG is not commercially available, an initial aim was to develop a synthetic strategy that would allow ready access to 3OHKG and a wide range of other UV filter compounds (Chapter 2). The procedure reported by Manthey *et al.*[262] for the synthesis of 3OHKG often gave irreproducible results and employed toxic reagents. Therefore, the goal was to synthesise 3OHKG by optimising Manthey *et al.'s* procedure using commercially available, inexpensive and benign reagents. As a result, 3OHKG was successfully synthesised from 3-hydroxyacetophenone (8) *via* successive nitration, aldol condensation, methylation, glucosylation, amination, hydrogenation and hydrolysis reactions. The best conditions and product yields are shown in Scheme 7.1. Application of microwave and solvent-free chemistry in the synthesis of the acrylic acid (7) resulted in a significant improvement in both the reaction time and product yield in comparison to the method reported by Butenandt *et al.*[263] and conventional heating under vacuum. The acrylic acid (7) was subsequently

methylated to afford the methyl ester (10), with the methylation in dry MeOH in the presence of a catalytic amount of H_2SO_4 the most favourable method. In order to reduce the number of synthetic steps towards 3OHKG, 3-hydroxy-2-nitroacetophene (9) was condensed with ethyl glyoxylate in the presence of an acid catalyst. Microwave conditions and heating under vacuum were both successful, with the microwave conditions preferred as a significant reduction in reaction time was observed, while retaining similar yields. The methyl ester (10) or ethyl ester (17) were then treated under anhydrous conditions with ABG in the presence of a phase transfer catalyst and base. This method gave the desired glucoside in comparable yields to that obtained by Manthey *et al.*,[262] without the use of a toxic catalyst. The methyl (11) and ethyl (18) ester glucosides were subsequently aminated and hydrogenated in a "one pot" reaction, and subsequently hydrolysed in aqueous NaOH to obtain 3OHKG. In addition, U-24, as a side product, was obtained in 18-20% yield. Through careful analysis, it was proposed that U-24 is an isoxazole derivative of 3OHKG. Hydrogenation of U-24 resulted in nearly quantitative recovery of 3OHKG. This resulted in 3OHKG in ~46% yield from the methyl (11) or ethyl (18) ester glucoside. This is comparable to the literature.[262]

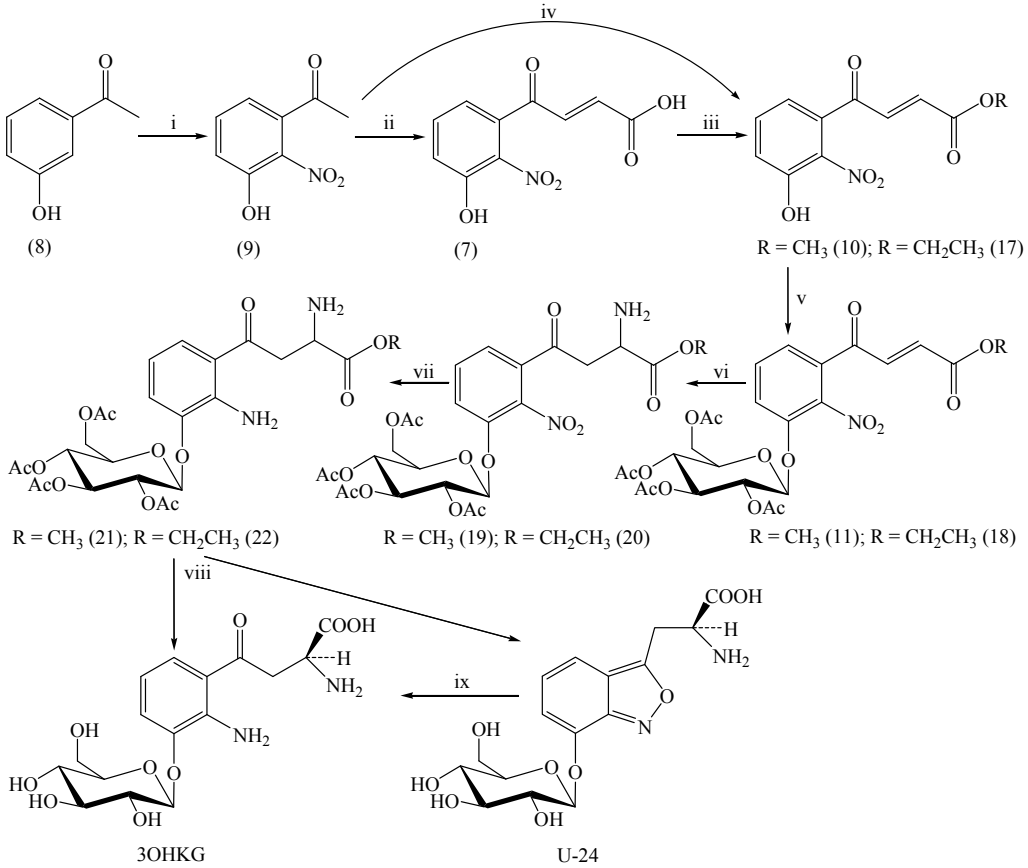

Scheme 7.1: The improved synthetic strategy towards 3OHKG. The preferred reaction conditions and product yields: i) $Cu(NO_3)_2 \cdot 2.5H_2O$, AcO_2, AcOH, 10-15ºC, 16 h, 25%; ii) HCOCOOH, MW, 110ºC, 17 min, 60%; iii) MeOH, H_2SO_4, reflux, 6 h, 90%; iv) HCOCOOEt (50% sol. in toluene), PPA/SiO_2, MW, 110ºC, 130 min, 58%; v) ABG, DCM, K_2CO_3, tetra-*n*-butyl ammonium bromide, 2.5 days, 70-78%; vi) EtOAc, aqueous NH_3, 3 h, not isolated; vii) EtOAc, H_2, Pd/C, 3 h, not isolated; viii) aqueous NaOH, NH_3, 8.5 h, 27% 3OHKG and 18-20% U-24; ix) H_2O, H_2, Pd/C, 10 min, 92%.

By expanding the optimised synthetic strategy for the synthesis of 3OHKG, the synthesis of 3OHKyn and AHBG was conducted (Chapter 3). The key precursors for their synthesis were the acrylic acid (7) and the methyl ester glucoside (11), respectively. 3OHKyn was synthesised using modified conditions of Butenandt *et al*.[263] The acrylic acid (7) was aminated and hydrogenated *via* a "one pot" reaction to obtain 3OHKyn in 72% yield (Scheme 7.2, A). This synthetic procedure resulted in an improvement in the reaction yield of 3OHKyn, cost, time and benignness of the reaction conditions compared to the literature,[263] allowing ready access to the commercially available but very expensive 3OHKyn (AU$103/25 mg). Following the literature hydrogenation procedures[262,335] and optimised deprotection conditions used for the synthesis of 3OHKG, AHBG was synthesised *via* hydrogenation and deprotection of the methyl ester glucoside (11) in 41% overall yield, without intermediate purification (Scheme 7.2, B). The yields were similar to the literature.[262] Following similar conditions, it is proposed that future studies could be focused on AHBG being obtained *via* the ethyl ester glucoside (18), given that this would eliminate one step in the synthesis. The synthesis of 3OHKyn and AHBG were conducted on small (mg) scale to explore their feasibility and to obtain sufficient AHBG for use as a standard in Chapter 4. Further investigation on a larger scale is required in future studies.

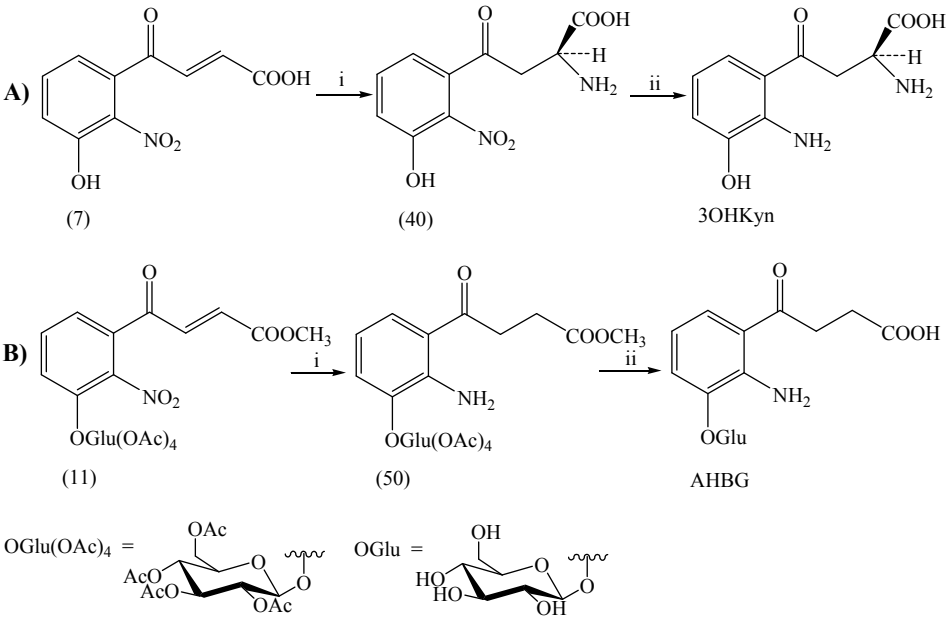

Scheme 7.2: The improved synthetic strategy towards 3OHKyn (**A**) and AHBG (**B**). The preferred reaction conditions and product yields: A, i) aqueous NH_3, 1.5 h, not isolated; ii) aqueous NH_3, H_2, Pd/C, 2 h, 72%; B, i) H_2, Pd/C, EtOAc/EtOH (4:1, v/v), 2 h, not isolated; ii) aqueous NaOH, 5 h, 41%.

Based on known lens chemistry, AHA, AHB, GSH-Kyn, GSH-3OHKyn, Kyn yellow and 3OHKyn yellow were synthesised and examined for their presence in human lenses (Chapter 4). These were proposed to be human lens metabolites due to their similarities to AHBG, GSH-3OHKG and 3OHKG yellow derived from deamination of 3OHKG. AHA was synthesised from 2-nitroacetophenone (55) (Scheme 7.3). 2-Nitroacetophenone was condensed with glyoxylic acid monohydrate under similar conditions to that for the synthesis of the acrylic acid (7). Several hydrogenation conditions of the acrylic acid (56) were trialled. It was found that hydrogenation over Pd/C and under slightly acidic conditions was favourable for this reaction. AHB was synthesised from the acrylic acid (7) under the conditions optimised for the synthesis of AHA (Scheme 7.3).

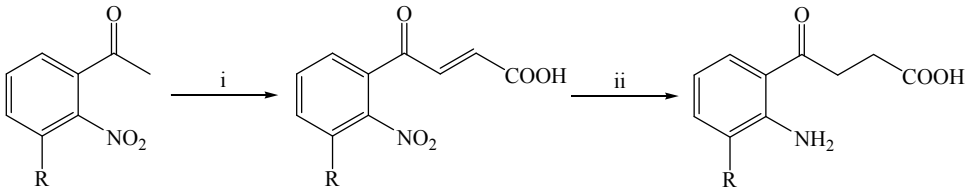

Scheme 7.3: The synthetic strategy towards AHA and AHB. The preferred reaction conditions and product yields: i) HCOCOOH, MW, 110ºC, 60 min, 54% (55) and 17 min, 60% (7); ii) H_2, Pd/C, EtOAc, AcOH (~0.2%), 22 h, 41% (AHA) and 3 h, 47% (AHB).

The GSH adducts of Kyn and 3OHKyn were synthesised *via* base-induced deamination of Kyn and 3OHKyn in the presence of GSH (Scheme 7.4). This resulted in GSH-Kyn and GSH-3OHKyn in moderate to good yields. Several procedures were investigated for the synthesis of Kyn yellow and 3OHKyn yellow. It was found that Tokuyama *et al.'s* original conditions,[348] which involved base-induced deamination and intramolecular cyclisation of Kyn and 3OHKyn to Kyn yellow and 3OHKyn yellow, respectively, were optimal (Scheme 7.4).

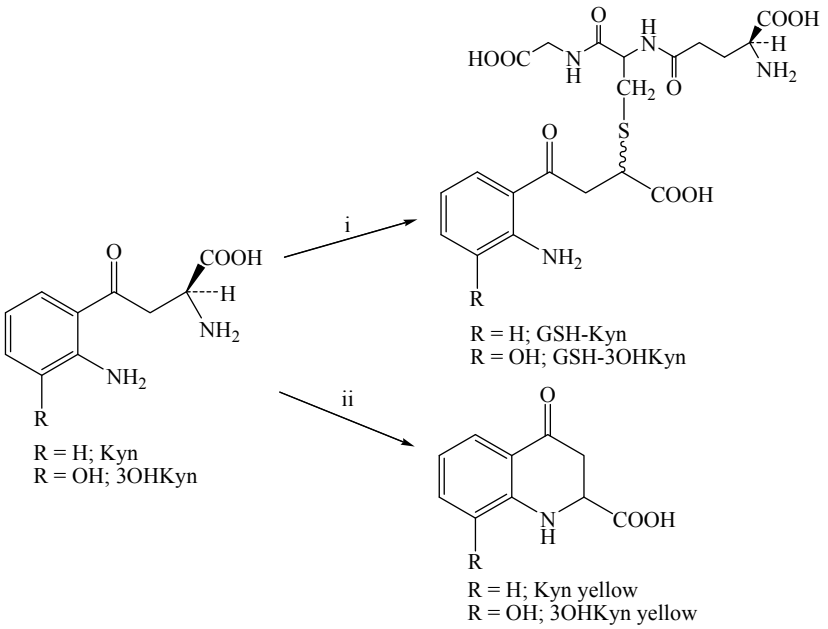

Scheme 7.4: The synthetic strategy towards GSH-Kyn, GSH-3OHKyn, Kyn yellow and 3OHKyn yellow from Kyn and 3OHKyn. The preferred reaction conditions and product yields: i) aqueous Na_2CO_3-$NaHCO_3$ (25 mM, pH 9.5), GSH, 37°C, 72 h, 51% (GSH-Kyn) and 44% (GSH-3OHKyn); ii) aqueous $NaHCO_3$ (0.49 M, pH ~9), reflux, 20 h, 26% (Kyn yellow) and 22% (3OHKyn yellow).

To determine the presence of the proposed metabolites and, for comparative purposes, known UV filters, normal and cataractous human lenses were extracted and analysed by RP-HPLC by Dr Peter Hains (Save Sight Institute, Sydney, NSW) (Chapter 4). A marked decline in the levels of 3OHKG, Kyn, AHBG and AHBDG was noted after the seventh decade of life, whilst the levels of GSH-3OHKG were generally higher after middle age. These findings are consistent with previous studies of human lens extracts.[39] ES-MS/MS analyses of human lens extracts and spiking experiments with the synthetic standards confirmed the presence of AHA, AHB and GSH-Kyn in low pmol/mg lens (dry mass) levels in normal and cataractous human lenses. Kyn yellow, 3OHKyn yellow and GSH-3OHKyn were not detected in any of the lenses. Stability studies of AHA, AHB, GSH-Kyn and GSH-3OHKyn under experimental conditions showed no decomposition, suggesting that the low concentrations measured for AHA, AHB and GSH-Kyn, and the lack of detection of GSH-3OHKyn, were representative of the concentrations in the investigated lenses. AHA was found to be very stable under physiological conditions, indicating that formation of AHA may protect the lens from modifications due to its greater stability compared to its precursor (Kyn). In contrast, AHB, GSH-Kyn and GSH-3OHKyn showed instability under physiological conditions, with the former resulting in yellowing/tanning of the incubation solutions and formation of dimeric species that showed similar spectral properties to those observed in aged and cataractous lenses. This study was performed on a limited number of available human lenses, therefore further studies are needed to determine the trend of deamination and reduction of Kyn and

3OHKyn with aging and development of ARN cataract. Also, further investigations are needed to examine human lenses for the presence of 3OHKG yellow. Previous attempts by other group members gave negative results. However, due to use of a very sensitive LC-MS detection technique in this study, it would be worthwhile repeating the experiment.

Following the isolation of an unknown compound in human lens extracts by RP-HPLC, and structural elucidation *via* total synthesis and spectral analysis, a new UV filter Cys-3OHKG was identified in human lenses (Chapter 4). Cys-3OHKG was synthesised *via* Michael addition of Cys to the deaminated 3OHKG under basic conditions (Scheme 7.5). Cys-3OHKG showed instability under physiological conditions, consistent with the observation that it was found in low pmol/mg lens (dry mass) levels in the normal lenses after the 5th decade of life and absent in cataractous lenses. The discovery of Cys-3OHKG appears to complete the identification of the major free UV filter compounds present in the human lenses. Future studies are required to isolate and identify other minor peaks seen by RP-HPLC of human lens extracts.

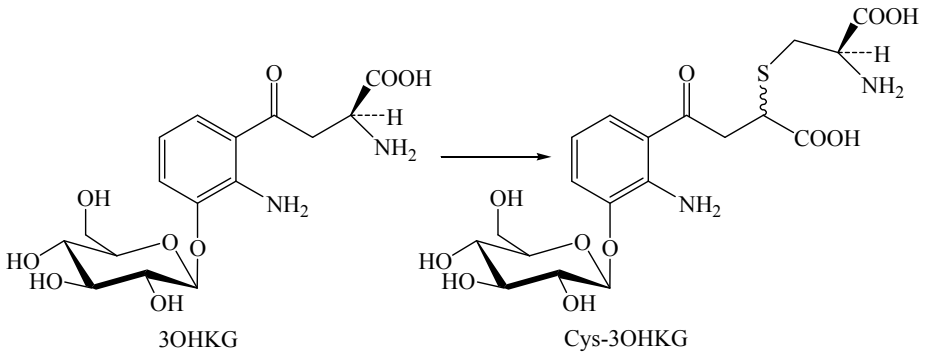

Scheme 7.5: The synthetic strategy towards Cys-3OHKG from 3OHKG. The preferred reaction conditions: aqueous Na_2CO_3-$NaHCO_3$ (25 mM, pH 9.2), Cys, 37°C, 72 h, 35%.

Model studies with bovine lens proteins and 3OHKG at pH 7.2 and 9.5, followed by identification of the amino acids involved in covalent binding by comparison to the synthetic standards, showed that 3OHKG reacts with lens proteins predominantly at Cys residues with a small amount of modification detected at Lys residues (Chapter 5). His adducts were not identified. This is consistent with Cys residues being better nucleophiles than Lys and His residues under the conditions investigated. Similar binding properties were observed for Kyn and 3OHKyn. The extent of all modifications investigated in this study was found to be significantly higher at pH 9.5, possibly due to a greater rate of deamination of the side chain of UV filters and greater nucleophilicity of the amino acid residues. 3OHKG-, Kyn- and 3OHKyn-modified lens proteins were found to be coloured and fluorescent, resembling those

of aged and ARN cataractous lenses.

In contrast, AHB and AHA resulted in non-covalent modification of lens proteins. This is due to lack of the side chain amino group. This suggests a greater importance of the α,β-unsaturated carbonyl moiety in protein binding. AHB and 3OHKyn were found to result in similar lens protein colouration and fluorescence properties, possibly due to oxidation of the *o*-aminophenol moiety. However, covalent binding through the *o*-aminophenol moiety was not examined in detail in this study. Further experiments are needed to investigate if binding to lens proteins *via* the *o*-aminophenol moiety occurs with prolonged incubation time and substituting the acid hydrolysis approach with an enzymatic digestion, *e.g.* trypsin, may assist in isolation of additional adducts. Furthermore, the importance of the *o*-aminophenol versus α,β-unsaturated carbonyl moiety in protein modifications needs to be investigated further. This could be determined through comparative protein binding experiments between a compound having both the *o*-aminophenol and α,β-unsaturated carbonyl moieties and a compound lacking one of these moieties, such as in the case of 3OHKyn versus AHB and Kyn versus AHA.

The final aim of this study was to investigate the ability of protein-bound 3OHKG and 3OHKyn to act as photosensitisers of oxidative damage upon exposure to UV light (> 305 nm). A protein-bound Kyn sample was used as a positive control, while unmodified lens protein was a negative control. The levels of UV light used in this study were comparable to levels of illumination experienced from ambient UV exposure. Protein-bound 3OHKG, Kyn and 3OHKyn were found to be better photosensitisers than in the unbound state. Free and protein-bound peroxides were found to accumulate in a time-dependent manner upon exposure to UV light (λ 305-385 nm), with shorter wavelengths generating more peroxides, and with H_2O_2 predominating over protein-bound peroxides. The extent of peroxide formation from the modified lens proteins decreased in the order 3OHKyn > Kyn > 3OHKG. Studies using D_2O and sodium azide gave higher and lower peroxide yields respectively, consistent with a role of $^1O_2$. AHB-treated lens proteins resulted in formation of low but statistically significant levels of peroxides, while AHA-treated lens proteins resulted in insignificant peroxide formation compared to the unmodified lens proteins. Unmodified proteins and non-illuminated modified proteins gave low peroxide yields. The consequences of these photochemical reactions have been examined by quantifying protein-bound Tyr oxidation products (DOPA and di-Tyr), and determining protein cross-linking. Peroxide formation was accompanied in some cases by an increase in the levels of protein-bound di-Tyr (for 3OHKG-

and Kyn-modified lens proteins) and DOPA (for Kyn- and 3OHKyn-modified lens proteins). DOPA formation by 3OHKyn-modified lens proteins was independent of illumination, with this believed to arise *via o*-aminophenol auto-oxidation. AHB- and AHA-treated lens proteins resulted in statistically insignificant di-Tyr formation, while a light independent increase in DOPA was observed for both samples. Di-Tyr formation and reaction of protein nucleophiles with the oxidation products of DOPA and the *o*-aminophenol moiety present on 3OHKyn and AHB may be potentially involved in the colouration and cross-linking observed in this study. Both reducible (disulfide) and non-reducible cross-links were detected on illuminated modified proteins. A lower level of these cross-links was observed for the equivalent non-illuminated modified samples. Unmodified protein samples showed no cross-linking. This suggests the importance of both UV filter modification and UV light in the observed protein damage.

Together these findings suggest that the final patterns of UV filter protein modification in human lenses is likely to be dependent on many factors, such as amino acid nucleophilicity, adduct stability and accessibility of the residues for the reactions. This covalent binding of UV filters to lens proteins yields efficient photosensitisers that may exacerbate UV-induced photodamage to the lens and retina *via* the reaction of multiple reactive species including H_2O_2 and other peroxides. Multiple processes appear to contribute to the enhanced level of peroxides and the protein modification detected in this system, with $^1O_2$ being a key intermediate. While the exact mechanism and processes involved are still unclear, this study has provided a basis for further investigations to define the role of Kyn, 3OHKyn and 3OHKG and their lens metabolites in the changes that occur in the human lenses with age and in the onset of ARN cataract. Further examination of the importance of the α,β-unsaturated carbonyl versus *o*-aminophenol moiety in lens protein modification and determining the contribution of *o*-aminophenol auto-oxidation versus protein-bound photosensitation upon exposure to UV light in the formation of reactive oxygen species and protein damage are potential topics for future studies.